

RC
1042
.N87
1985
v.1

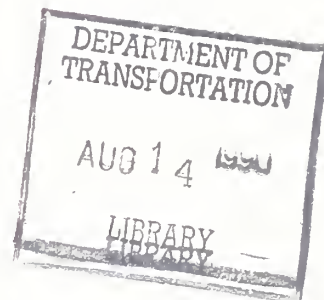
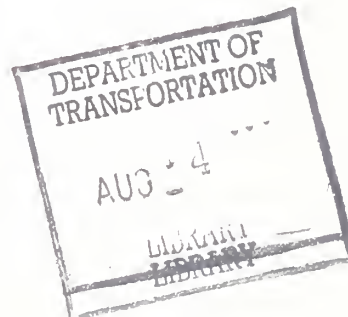


U.S. Department
of Transportation
**National Highway
Traffic Safety
Administration**

DOT HS 807 429
Final Technical Report

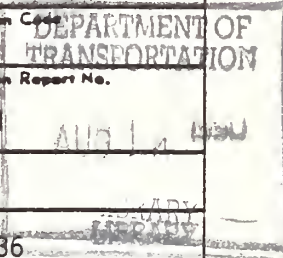

December 1985

Experimental Data for Development of Finite Element Models: Head/Thoraco-Abdomen/Pelvis Volume I: HEAD



- The United States Government does not endorse products or manufacturers. Trade or manufacturers' names appear only because they are considered essential to the object of this report.

RC
1042
.N87
1985
v.1

1. Report No. DOT HS 807 429		2. Government Accession No.		3. Recipient's Catalog No.	
4. Title and Subtitle Experimental Data for Development of Finite Element Models, v.1 Head/Thoraco-Abdomen/Pelvis: Vol.I: Head		5. Report Date December 31, 1985			
		6. Performing Organization Code			
7. Author(s) Guy S. Nusholtz, and Patricia S. Kaiker		8. Performing Organization Report No. UMTRI-85-55-1			
9. Performing Organization Name and Address Biosciences Division, Transportation Research Institute, The University of Michigan, 2901 Baxter Road, Ann Arbor, MI 48109		10. Work Unit No.		11. Contract or Grant No. DOT-HS-7-01636	
		13. Type of Report and Period Covered July 1977-Dec. 1983		14. Sponsoring Agency Code	
12. Sponsoring Agency Name and Address National Highway Traffic Safety Administration Department of Transportation, Seventh and E Streets, S.W., Washington, DC 20590					
15. Supplementary Notes Experimental data.					
16. Abstract Validation of biomechanical computer models of impact biodynamics cannot be accomplished without descriptive experimental data. The research program, therefore, involved data gathering on the kinematics and damage response of three human cadaver subsystems: the head, the thoraco-abdomen, and the pelvis. 14 unembalmed human cadavers were utilized in 68 dynamic impact tests. The research program entailed 14 head impacts (6 subjects), 41 thoraco-abdominal impacts (11 subjects), and 13 pelvis impacts (10 subjects). In addition, the thoraco-abdominal tests were supplemented with static three-point bending tests conducted on rib specimens from 5 of the dynamically tested cadavers.					
17. Key Words Impact Biomechanics, Head, Thoraco-Abdomen, Pelvis, Experimental Data			18. Distribution Statement Document is available to the public from the National Technical Information Service, Springfield, VA 22161		
19. Security Classif. (of this report)		20. Security Classif. (of this page)		21. No. of Pages 353	22. Price

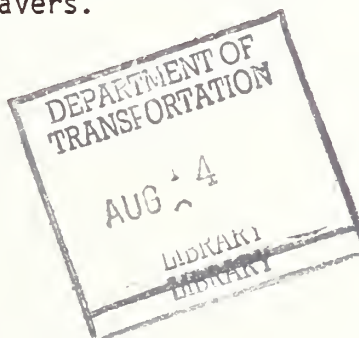


TABLE OF CONTENTS - HEAD SERIES

	Page
TECHNICAL REPORT DOCUMENTATION PAGE.....	i
TABLE OF CONTENTS.....	iii
LIST OF FIGURES.....	v
LIST OF TABLES.....	vi
OVERVIEW OF RESEARCH PROGRAM.....	1
1.0 BACKGROUND.....	3
1.1 Head Trauma Incidence.....	3
1.2 Mechanisms of Injury.....	3
Selecting Kinematic Parameters.....	4
Injury Response.....	5
Tissue Damage.....	5
Analysis.....	5
Concussion Injury.....	6
Validating Mechanisms of Injury.....	7
Head Geometry and Boundaries.....	7
Biomaterials Tolerances.....	8
Injury Severity Indices.....	8
Model Constraints.....	11
Technical Constraints.....	13
2.0 HISTORY OF THE LITERATURE.....	14
Proposed Mechanisms of Head Trauma...14	14
3.0 GOAL OF HEAD SERIES IMPACT TESTING.....	17
4.0 METHODOLOGY.....	18
4.1 Methods and Procedures of Impact Testing.....	18
4.11 Subjects.....	18
4.12 Pre-test Preparation.....	19
Morgue.....	19
Anatomy Lab.....	19
Radiology Lab.....	19
Dark Room.....	20
Physiology Lab.....	20
Impact Lab.....	20
Impact Lab and Instrumentation Room Electronics.....	20
4.13 Surgery.....	21
Nine-Accelerometer Head Plate.....	21
Thoracic Vertebral Mounts.....	22
Cerebrospinal Fluid Pressure Transducer Fittings.....	22
Cerebrospinal Repressurization.....	22
Vascular Repressurization.....	26
4.14 Trial Test and Impact Testing.....	26

Trial Test.....	29
Timing.....	30
Equipment.....	31
Linear Pendulum Impact Device.....	31
Ballistic Pendulum Impact Device.....	31
Data Handling.....	34
Epidural Pressure Transducers.....	34
Photokinematics System.....	34
Cineradiograph.....	36
Radiopaque Target Gel.....	36
Test Subject Preparation.....	37
Initial Test Conditions.....	37
4.15 Post-Test Autopsy.....	38
4.2 Method of Analysis.....	38
4.21 X-Ray Motion Descriptors.....	38
4.22 Frame Fields.....	40
Frenet-Serret Frame.....	41
Principle Direction Triad.....	42
4.23 Transfer Function Analysis.....	43
4.24 Statistical Measures.....	44
Auto-Correlation Function.....	44
Cross-Correlation Function.....	45
Coherence Function.....	46
4.25 Pressure Time Duration Determination.....	46
4.26 Force Time-History Determination.....	47
4.27 Impact Response Definition.....	48
5.0 RESULTS.....	49
6.0 DISCUSSION.....	50
6.1 Force Time-Histories.....	50
6.2 Tangential Acceleration Time-Histories.....	50
6.3 Comparison of Impacts: Cadaver Variability.....	51
6.4 Impact Response.....	51
6.5 The Effects of Skull Deformation on Linear and Angular Acceleration.....	54
6.6 Kinematic Response After Impact: Effect of Soft Tissue.....	58
6.7 Pressure Time History Response.....	60
6.8 Injury/Damage Response.....	64
7.0 CONCLUSIONS.....	65
8.0 REFERENCES.....	67
9.0 APPENDIX A: ANATOMY OF THE HEAD.....	A1
10.0 APPENDIX B: TEST PROTOCOL.....	B1
11.0 APPENDIX C: HEAD IMPACT SERIES - SELECTED TIME-HISTORIES.....	C1
12.0 APPENDIX D: ANTHROPOMETRY.....	D1

LIST OF FIGURES - HEAD SERIES

Figures

1A	Nine-Accelerometer Head Plate Orientation.....	23
1B	Radiopaque Target Gel in Situ.....	23
2	Acrylic for Securing Mounts.....	24
3	Cerebrospinal Fluid Pressure Transducer Fittings and Bit.....	25
4	Cerebrospinal Lumbar Catheter.....	27
5	Vascular Repressurization.....	28
6	Linear Pendulum Impact Device.....	32
7	UMTRI Pneumatic Ballistic Impact Device.....	33
8	Initial Test Conditions.....	39
9	Cross- and Auto-Correlations.....	52
10	Effect of Skull Deformation on Angular Acceleration.....	57
11	Mechanical Impedance Corridor for Tangential Acceleration Skull Deformation and No Skull Fracture.....	59
12	Cross- and Auto-Correlation for Epidural 1 and Epidural 4 Pressures.....	62
13	Transfer Functions between Force and Epidural 1 and Epidural 2 Pressures.....	63

LIST OF TABLES - HEAD SERIES

Tables

1	Initial Test Conditions.....	49-1
2	Impact Test Summary.....	49-2
3	Test Pressure Summary.....	49-3
4	Damages.....	49-4

FINAL REPORT:
EXPERIMENTAL DATA FOR
DEVELOPMENT OF FINITE ELEMENT MODELS
Contract No. DOT-NHTSA-C-HS-7-01636 UM Acct. No. 015651

OVERVIEW

The research program involved data gathering on the kinematic response of three human cadaver subsystems: 1) the head, 2) the thoraco-abdomen, and 3) the pelvis. Information on injury response as well as the relationship between impact parameters and the resulting injury are presented. Each impact target investigation subsystem is presented as a self-contained chapter in this final report: Chapter 1 presents the head series, Chapter 2 the thoraco-abdomen series, and Chapter 3 presents the pelvis series.

The research program utilized 14 cadavers¹ in 68 dynamic impact tests. For the head subsystem experiments, 6 subjects received a total of 14 impacts; for the thoraco-abdomen, 11 subjects received a total of 41 impacts; and for the pelvis, 10 subjects received a total of 13 impacts. Supplementing some dynamic thoraco-abdominal experiments were static three-point bending tests on rib specimens from 5 of the same dynamically-tested cadavers.

The research program utilized procedures for obtaining kinematic parameters that are still considered the most optimum. Although some procedures were developed prior to these series of experiments, in many instances major improvements in the procedures have been made. In addition, unique methods of analysis using moving frame fields, such as

¹The protocol for the use of cadavers in this experimental series was approved by the Committee to Review Grants for Clinical Research of the University of Michigan Medical Center and follows guidelines established by the U.S. Public Health Service and recommended by the National Academy of Sciences, National Research Council.

the Principal Direction Triad and Frenet-Serret frames, auto- and cross-correlations, and information in the frequency domain, are presented. The program also required the development of a new impact device which increased the magnitude of input force and lengthened the stroke compared to what was previously possible at the University of Michigan Transportation Research Institute's Biomechanics Laboratories.

ACKNOWLEDGEMENTS

The three test series in the Experimental Data for Development of Finite Element Models: Head/Thoraco-Abdomen/Pelvis research program were funded by the United States Department of Transportation, National Highway Traffic Safety Administration, Contract No. DOT-HS-7-01636. The authors wish to acknowledge the technical assistance of Donald F. Huelke, Nabih Alem, John Melvin, Bryan Suggitt, Gail Muscott, Paula Lux, Marvin Dunlap, Don Erb, and Jean Brindamour. The authors also acknowledge the contributions of Jeff Pinsky, Allen C. Bosio, Zheng Lou, Valerie Moses, Wendy Gould, Steven Richter, Peter Schuetz, Shawn Cowper, Tim Jordan, Patrice Muscott, and Reza Salehi. A special thank you goes to Jeff Marcus.

CHAPTER 1

EXPERIMENTAL DATA FOR DEVELOPMENT OF FINITE ELEMENT MODELS - HEAD
Contract No. DOT-NHTSA-C-HS-7-01636 UM Acct. No. 015651

1.0 BACKGROUND

1.1 Head Trauma Incidence

In 1980 U.S. citizens spent four billion dollars to treat acute head injury of over one million individuals [1-10]. Precise figures are not available so it is estimated that 49% of head injuries can be attributed to motor vehicle accidents, 28% to falls and 23% to other causes such as suicide attempts, firearms injury, recreational and occupational accidents [1-10]. Investigation of mechanisms of blunt head impact trauma is invaluable for allocating resources, and for formulating policy to reduce head impact trauma incidence, morbidity and mortality.

1.2 Mechanisms of Injury

Because motor vehicle field accident data do not provide the level of detail necessary to ascertain mechanisms of injury resulting from the interactions of the occupants with the vehicle interior during an accident, biomechanists use trauma experiments to document kinematic parameters so that mechanisms of injury can be better hypothesized, modeled, verified, and simulated.

Determining mechanisms of injury associated with blunt impact to the head can be viewed as determining the forces and the pathways in which those forces act to cause mechanical and physiological disruption. Biomechanists commonly use three approaches in assessing head impact and inertial loading phenomena to determine mechanisms of injury: 1) investigating the material properties and mechanical aspects of the skull-brain-neck system, and then deriving from fundamental laws of

physics the biomaterial failure levels or mechanism(s) of injury; 2) performing experiments so that kinematic variables and injury are correlated to deduce or validate injury tolerance levels as well as hypotheses concerning mechanism(s) of injury based on the results; and 3) combining these approaches to modelling mechanism(s) of head injury.

Selecting Kinematic Parameters: A major difficulty in the investigation of head trauma is designing impact experiments which interfere minimally with the biological and physical systems being tested, yet produce results that correspond well with clinically observed trauma and generate useful kinematic data. Some understanding of head injury mechanisms as a result of blunt impact has resulted from relating kinematic parameters to the injury/damage modes produced in experiments with human surrogates. With the possibility of several injury mechanisms and the effects of differences in human surrogates, correlations of this type do not always imply a causal relationship (a mechanism of head injury) for live humans.

The kinematic parameters commonly used for describing head mechanical response during direct blunt impact have been angular and translational accelerations, velocities, displacements of the head as a rigid body, skull bone deformations, and internal pressures in the brain. Many investigators have chosen to investigate a single parameter, such as "resultant head acceleration" for Head Injury Criterion (HIC) calculation, and later use it as an index of severity or tolerance threshold. Because of the complex response of the head to blunt impact, it may be necessary to use several kinematic parameters and relate these to the subject's injury/damage response in order to

accurately characterize and predict the response of the living human head to blunt impact.

Injury Response: For biomedical and biomechanical purposes "head injury" is defined as physiologic dysfunction or anatomical alteration of cerebral blood vessels, nerves, brain, skull and scalp. Injury can be classified as "tissue damage" or "concussion".

Tissue Damage - "Linear fractures" may be a complete break through the skull bone, or limited to only one layer. Linear fractures of the cranial vault may extend to the skull base. "Depressed fractures" are inward displacements of bone, with fragments of the skull being displaced into the dura mater and brain.

"Epidural hematomas" are usually due to a tear of the middle meningeal vessels. When cerebral arteries or veins are lacerated, the resulting "subdural hematoma(s)" produce masses which can compress brain tissue and vessels. A "subarachnoid hematoma" is one located on the pia mater which directly covers the brain. "Petechia" are small hemorrhagic spots on or in the brain tissue. "Intracranial hematomas" are located within the brain. A "contusion" is a laceration of tissue.

Analysis - Measurements obtained from accelerometers, strain gauges, and pressure transducers affixed to a human surrogate subject define the kinematic responses to blunt impact to the head used in experimental analysis. Although there are other human surrogates for modelling the kinematic-injury/damage response of live humans, two are frequently chosen for blunt head impact research. They are the non-human primate and the human cadaver. The geometry and soft tissue distribution of the unembalmed repressurized cadaver is similar to that of a live human. Damages to repressurized cadavers that correlate well

with clinically-observed injuries are those that can be documented by gross autopsy. They are tissue damage injuries that include scalp lacerations (linear, flap, stellate), fractures of the cranial vault or base (linear, depressed), lesions which are visible to the naked eye (contusions), and hemorrhage (petechia, subdural-, subarachnoid-, and intracranial hematomas). Because diagnosis of concussion requires the observation of physiologic and behavioral responses, the cadaver model is inappropriate. Instead, a non-human primate or other animal model is used to assess abnormal behavioral responses and neurologic deficits when studying concussion injuries.

Concussion Injury - Trauma to the brain may cause neurologic dysfunctions termed "concussion". These dysfunctions can be transient so that normal neurologic functioning returns and impairment is negligible, or they can be long-term and entail permanent disability. Symptoms can include dizziness, shock, weakness, paralysis, vomiting, rapid pulse, flushed face, headache, unequal pupils, and unconsciousness. "Neurologic deficit" can include sensory loss, lessened sensitivity to touch, visual field defects, fixed or non-reactive pupils, deviation of both eyes to the same side, the inability to use connected phrases when speaking, paralysis affecting one side of the body, and seizures.

"Mild concussion" can be considered a temporary disturbance of neurologic functioning without loss of consciousness. "Cerebral concussion" can be a resumption of normal neurologic functioning after disruption and loss of consciousness of less than 24 hours. Coma can be a deep stupor from which the patient cannot be aroused by external stimuli. These definitions evolved from non-invasive assessment of

motor, verbal, and ocular behavioral responses. Where diagnostic information has been available from more invasive technological (CAT-scan, PET, NMR, X-Ray) or pathologic (biopsy, autopsy) sources, the brains of some of those suffering concussion have failed to show discernible gross structural injury; the brains of others have shown microscopic disruptions of white matter fibers throughout both cerebral hemispheres. Perhaps some diffuse injuries such as extracerebral hematomas may be treatable so that disability is negligible, while others involving extensive microscopic disruption of nerve fibers may prove to be causes of long-term permanent disability. [11-32]

Validating Mechanisms of Injury - There are at least four classes of difficulties which limit understanding the mechanism(s) of injury. These are: 1)- complex head geometry and boundary conditions between different head components, as well as dissimilar biomaterial tolerances for different head/brain structures, 2) difficulty of relating injury to a numerical value on an index, 3) human surrogate model limitations, and 4) technical instrumentation and experimental limitations.

- 1) Head Geometry and Boundaries - The human head is a complex geometric structure. The structural characteristics of the skull contribute to its physical response so that blunt impact to the head is mediated by several protective features. For example, the scalp covering the skull absorbs and redistributes energy resulting from a direct blunt blow to the head. When hit, the bones and sutures in the skull tend to produce a transmission of energy through the skull along complex paths. The different skull thicknesses function like ribs and buttresses enhancing the skull's strength. The domelike shape

of the skull deflects blows. The mobility of the head upon the neck permits energy absorption. Furthermore, the gelatinous brain is bathed in pressurized fluid within interconnecting meningeal membranes. Energy transmission through such a system is complex. Appendix A briefly describes the common gross functional and structural components of the head. [33-36]

Biomaterial Tolerances - In general, the tissues of the head can be viewed as inhomogeneous, anisotropic, viscoelastic, strain rate dependent, and non-linear in response. Biomaterial parameters for head component solids, gels, fluids, and gases include density, hardness, fracture toughness, compressibility, elasticity, viscosity and turgidity [37-110]. Simplifying assumptions are commonly made for biomaterial properties so that an analytical understanding of the mechanism of injury can be assessed by nonbiological material means, that is, in terms of classic mechanics structures such as rigid body materials.

- 2) Injury Severity Indices - Although much tolerance data comes from materials testing of isolated head biomaterials, injury severity indices which establish "safe" levels for the head may be based on limited experimental test series which have oversimplified the basic dynamic and injury problem. [111-137] In such instances there is a danger of accepting one mechanism of injury, when several may more accurately characterize the dynamic possibilities.

Injury severity indices have been developed for a variety of purposes. The four most common types of indices are: 1)

medical injury severity, 2) field accident assessment of tissue damage, 3) laboratory assessment of relationships between kinematic parameters and biomaterial failure levels, and 4) regulative assessment of performance standards of safety equipment.

Medical injury severity scoring systems were designed to provide a standardized format for management of head injury cases to expedite emergency trauma care and to assess the patient's chances for recovery. The aim was to have a system which gave equal ranking to levels of severity for all types of injury. Risk to life evolved into the main medical trauma severity criterion. Perhaps, the most widely used injury severity indices developed by medical personnel pertinent to transportation-related trauma investigation are: 1) The Abbreviated Injury Scale (AIS-80) [111] and 2) The Glasgow Coma Scale (GSC) [134].

The AIS-80 is a tissue damage scale developed by the American Medical Association and refined by the American Association of Automotive Medicine. It is used by accident investigators to score tissue damage for a uniform national data base. The data base is useful to engineers, physicians, and legislators for assessing vehicular trauma for their specific needs.

In biomechanics laboratories scientists have formulated kinematic indices related to head injury severity as a by-product of their primary investigation into mechanism(s) of head injury and biomaterial tolerances. Some laboratory

indices are the J Tolerance Index (JTI), the Revised Brain Model (RBM), the Effective Displacement Index (EDI), and the Maximum Strain Criterion (MSC) [132].

In regulative settings, laboratory severity indices have been used to define safety test procedures [138-152]. Currently head trauma is assessed by the Head Injury Criterion (HIC) index. This index evolved from the Severity Index (SI) to the Wayne State Tolerance Curve (WSTC) to the HIC. Because indices can become part of protective regulations, it is important to have a clear idea of what any particular severity index is measuring and how well this relates to mechanism of head injury or to clinical outcome, so that preventive measures become indeed pertinent to eliminating or reducing causes of head injury. Because laboratory severity indices often correlate one parameter with one outcome, performance standards are meaningful only in a particular context. One parameter relates to the one outcome in that circumstance and may not accurately represent a parameter level that can be tolerated by live humans in another. Injury severity indices should be validated by correlating them with laboratory observations and medical outcomes. As vehicle interiors and safety devices change, laboratory tests should reflect these new designs. Multiple kinematic parameters need to be correlated with various mechanisms of injury and experimental contexts before head injury tolerance thresholds become truly predictive of head injury and of a patient's prognosis for recovery.

Injury severity indices may inhibit characterization of mechanisms of head injury. By reducing pathologic injury/damage to a numerical value on an injury severity tolerance scale, valuable descriptive information for understanding mechanisms of head injury is lost. The scales may not include type of injury, location of injury, the number of injuries, the relationship of each injury to the other or of one mechanism of injury to the others.

A weakness of most injury severity scoring schemes is that multiple injuries are scored as one injury. Injuries of varying severity can be misinterpreted as injuries of different types. The result seems to be that such scales may not really characterize injury sufficiently for induction of mechanism(s) of injury. The logic of some injury severity scoring schemes under-characterizes injury. The AIS-80 codes for lesions. Although a similar size lesion of the frontal lobe is not the same as one of the brain stem because the brain is disrupted functionally in different ways by each, the AIS-80 does not reflect this. The Glasgow Coma Score is another example: it codes for eye opening, verbal and motor function, but other aspects which may diagnostically be equally meaningful, such as whether the brain stem reflexes are intact or whether the pupils react, are ignored [134-135].

- 3) Model Constraints - Cadaver subjects have some disadvantages as experimental models. Biological material degrades differentially with time. The changes in the brain material

over time as well as problems with repressurization instrumentation may lead to misinterpretation of head damage response in the cadaver model. [153-160]

Using non-human primates as experimental subjects to determine mechanism(s) of injury entails several disadvantages [161-176].

The use of anesthetics and tranquilizers may severely limit muscular response and its accurate assessment. Difference in outcome may more reflect variability in specimens than a contrast between the test subjects and living humans.

Translating and scaling such data is constrained not only by statistical, mathematical and experimental techniques but also by what is still unknown about quantifying differences between and among these test subjects as surrogates for living humans.

Other models such as anthropomorphic test devices ("dummies") and finite element simulations also present empirical problems for validating mechanisms of head damage. The particular dummy may not be repeatable or may be accurate for anterior-to-posterior direction impact but not for lateral or other direction impacts [177-182]. Although finite element models can be very worthwhile for illustrating the mechanical significance of such structures as the foramen magnum, tentorium cerebelli, and falx cerebelli in mechanism of head damage, such models require components which are not true characterizations of biologic reality. Currently because of cost and model limitations, linearity of response and homogeneity of biomaterials must be assumed. Plus, the model may have to be

manipulated by pre-selecting biomaterial values which match laboratory observations [183-189].

To maintain an effective research design, it is important to judiciously select the human surrogate which is most appropriate for the aspect of the head trauma problem being investigated and for the type of response data being gathered. The model selected should be one that can best answer the questions being posed in the test design.

- 4) Technical Constraints - Data collection may be hampered by mechanical conditions in the laboratory setting.

Accelerometers may register outcomes that have been mediated by the accelerometers' response to temperature, cross-axis sensitivity, or high/low frequency noise. Instrumenting the skull for attachment of pressure transducers is an invasive technique that requires coring a small hole in the skull. Tracking anatomical movement through space and time relies on the movement of phototargets, which is recorded on film and then digitized. Error can be introduced by both the targeting and digitizing procedures. Accelerometers may not be properly aligned before impact. The response of the test subject is almost invariably determined in part by the instrumentation procedures. The testing apparatus may not be able to produce the type of impact conditions that are seen in the automobile environment.

2.0 HISTORY OF THE LITERATURE

The history of head trauma investigation has been complicated by the number of biologic and dynamic variables involved. Preconceptions about mechanisms of head injury/damage influence how laboratory investigations are designed and interpreted [190-323]. Both legislation and product safety testing reflect the development of contrasting philosophical preconceptions about blunt impact head trauma and mechanism(s) of head injury. Since there are too few experimental series to permit statistical manipulation of the thousands of parameters involved in biomechanics testing, researchers of head trauma must carefully design their experiments and be well informed of the conclusions drawn by other researchers and of the preconceptions and biases entailed in designs in order to be economical as well as successful. Severity indices are an alternative to laboratory investigation of mechanisms of head injury. They can be used to set tolerance limits even when an understanding of the mechanism(s) of head injury is absent. Their usefulness is due to statistical correlation of parameters. Understanding of mechanisms of injury results from laboratory investigation and analysis of parameters.

Proposed Mechanisms of Head Trauma - Within the context of rigid-body mechanics, the head rotates, moving forward, backward and sideways. Mechanisms of head injury can include non-impact mobility mechanisms such as inertial forces [324-333] which produce translational and rotational accelerations [334-351], causing differential movement of head components and injury/damage. During blunt impact both contact force [352-387] and inertial forces can be applied to the head. Impact phenomena are complex sequences of mechanical events. Injury can vary

with the magnitudes of the forces, the duration of the impact, and the size of the impacting surface. Impact phenomena can produce deformation [388-402], local injuries/damages, and secondary forces such as stress waves that cause skull oscillations and perhaps injuries/damages remote from the contact point of the blunt impact.

The fit between the analysis of experimental investigation of blunt impact trauma and predicting mechanism(s) of injury for live humans in a similar context is limited by the effectiveness of the selected human surrogate for answering the questions posed by the test, by simplifying assumptions made about complex head geometry and complex head biomaterial properties, and by the selection of kinematic parameters. The scientific literature [1-509] reflects the complexities of the problems inherent in analysis of mechanisms of head injury/damage as well as the evolution of ideas about the geometry of the head and the nature of its biomaterials [37-110,403-407]. Laboratory experiments have investigated stress waves through classic shapes such as spheres [403-407] and through classic materials that were viscous, elastic or viscoelastic [69, 85, 107, 394].

Deformation has been examined in the laboratory as a problem related to biomaterial failure levels [388-402, 408-426]. Injury severity indices have been used to attempt to code injuries/damages into equivalent levels of severity [111, 118-120, 134].

The location of the injury/damage and the location of the center of applied force has produced a body of literature on coup forces, counter coup forces [242-249, 286-288], and on rotational versus translational forces [334-351] are purported to cause certain types of injury/damage

or secondary parameters such as change in intracranial pressure [427-433].

In the literature "secondary forces" refer to transmission of energy along complex paths. Structural features such as the sphenoid bone wings, the foramen magnum, or the tentorium cerebelli play significant roles in differential movement of head components and in mechanism(s) of head injury/damage [434]. Elevated intracranial pressure or cavitation bubbles [427-433] and deformation become structural features which must be considered in the analysis of dynamic blunt head impact.

Some literature pertains to the predictability of one parameter for head injury/damage. Resultant angular acceleration is used to calculate the Head Injury Criterion (HIC), an injury severity index which has evolved into a regulatory device [435-440].

EXPERIMENTAL DATA FOR
DEVELOPMENT OF FINITE ELEMENT MODELS- HEAD SERIES

3.0 GOAL OF HEAD SERIES IMPACT TESTING

The goal of this test series was to investigate the relationship between selected kinematic parameters and resultant tissue damage caused by blunt impact to the head of the unembalmed, repressurized human cadaver as a surrogate model for living humans. The kinematic parameters selected were force, velocities, angular and translational accelerations, intracranial pressures, skull bone strain, displacements of brain tissue, displacements of the head as a rigid body, and skull bone deformations. A series of laboratory techniques precisely define the selected kinematic and injury parameters. Laboratory techniques and instrumentation procedures were both refined and created for this test series. Specifically, vascular repressurization techniques were refined and new techniques for cerebrospinal repressurization were created. New techniques which allowed high-speed angiographic radiology were created so that viewing in vitro motion of the brain with respect to the skull as well as differential motion of the brain was possible. Analytical procedures were upgraded during this project for obtaining a transfer function between any two transducer time-histories. Time domain procedures using moving frames, Principal Direction Triad, Frenet-Serret, and auto- and cross-correlation were improved. Frequency domain procedures were also refined (power spectra, mechanical impedance, spectral coherence, specialized transfer functions). Assessment of tissue damage was obtained by gross autopsy observations.

4.0 METHODOLOGY:

4.1 Methods and Procedures of Impact Testing:

4.1.1 Subjects - Six unembalmed repressurized cadavers were tested. The cadaver subjects were obtained by UMTRI from the University of Michigan Medical School Department of Anatomy.

There were two cadaver test series. In the first series, four cadavers were each subjected to a series of up to three head impacts using the UMTRI linear pendulum impacting device with either a 25 or 56 kg impactor. The remaining two cadavers were subjected to two head impacts each using the UMTRI pendulum impacting device with a 25 kg impactor. The cadavers were instrumented with a nine-accelerometer array on the head to measure three-dimensional motion. Both the cerebrospinal and vascular systems of the cadaver head-brain complex were repressurized. Epidural pressure transducers were used to monitor pressure changes of the skull-brain interface during impact. High-speed photokinematics were obtained using normal photographic or cineradiographic techniques. For some cadaver subjects, a radiopaque brain gel was used as a motion descriptor aid.

The execution and coordination of the testing sequence is guided by the use of a detailed protocol which is included in Appendix B [441-496]. The testing sequence is outlined below and additional information about application of specific techniques to analogous biomechanics problems can be found elsewhere [497-509]. Four groups of procedures are associated with the impact testing-data gathering activities. They are:

1) pre-test preparation, 2) instrumentation surgery, 3) trial test and impact testing, and 4) post-test autopsy and injury reporting in DOT format.

4.12 Pre-test Preparation - The arrival of a test subject cannot be predicted more than a half a day in advance. Generally, preparation for a test sequence begins the day a subject is received. The subject requires a day and a half of preparation, which is sufficient time to set up the impact lab and run equipment checks which include a trial test. The areas requiring special preparation are outlined below.

Morgue - Following transfer to UMTRI, cadaver subjects are stored at 4°C in coolers until subsequent use.

Anatomy Lab - Sanitary preparation, anthropometry, and surgical instrumentation of the test subject is done in the Anatomy Lab. All tools, materials, and instrumentation equipment necessary to prepare the subject are constructed or laid out in advance. Included in the setup are surgical instruments, measuring equipment, gauze and toweling, accelerometer mounting hardware, modified French Foley catheters and other pressurization hardware, and clothing for the cadaver subjects.

Radiology Lab - The table and X-Ray head are positioned and a sufficient supply of film is loaded into the X-Ray cassettes. Adequate film is loaded so that the test sequence can be completed without interruption. A subject may be X-rayed here on three occasions: when it is received to check for structural integrity and surgical implants, after instrumentation to check

that equipment is positioned properly and pressurization fluid can flow correctly, and when the impact testing is over, orthogonal X-Rays of the head are taken.

Dark Room - Chemicals are mixed for X-Ray developing. Labels for X-Rays are prepared. Courier forms and packaging for the 16 mm high-speed films are readied.

Physiology Lab - 16 mm high-speed films are chemically hypersensitized in an oven at 30-35°C with forming gas for 24 hours in order to obtain better image clarity. The saline-dye pressurization fluid is prepared here. Dental acrylic to be used as an instrumentation mounting medium is mixed here under a hood. In addition, the radiopaque brain gel target is manufactured in the Physiology Lab.

Impact Lab - Test facilities, recording equipment, accelerometers and transducers must be assembled, wired, and trial-tested. In addition, a portable cart containing surgical equipment for wiring the subject with accelerometers and transducers is prepared. Impact padding (styrofoam and ensolite) and support materials for the subject (balsa wood, foam, rope) are assembled near the impact pendulum. The cineradiograph system is readied, the Polaroid and high-speed cameras are tested and loaded with film. All electrical equipment is connected to a power source.

Impact Lab and Instrumentation Room Electronics - The input/output voltage characteristics of all analog tape channels are checked by calibration at predetermined voltage levels. The

tape channel calibrations are determined when the test pulses are played back off tape through a computer routine.

All accelerometers and pressure transducers are labeled and wired through a patch panel into the Instrumentation Room. From there, the signals are passed through amplifiers if necessary and connected to their designated channels as input to the analog tape recorders. Amplifiers are adjusted for the proper gain. The accelerometer and pressure transducers must have their excitation voltages set on the amplifiers, while their piezoresistive nature requires balancing to be performed on the amplifiers. Instrumentation Room wiring cannot be completed until the timer box and the devices it operates, such as lights, high-speed cameras and cineradiograph, and ropcutters, are wired and set for the proper control, delay and run times. Final wiring is completed in the Instrumentation Room and the pendulum is prepared for a trial test.

4.13 Surgery - In the Anatomy Lab the test subject is surgically instrumented with the required test hardware. The hardware includes accelerometer mounts, pressure transducer fittings, vascular and cerebrospinal catheters, and a nine-accelerometer head plate.

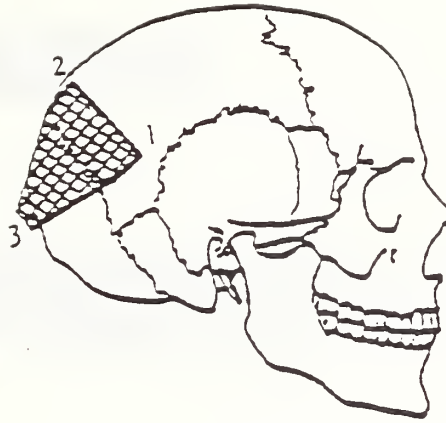
Nine-Accelerometer Head Plate - The nine-accelerometer plate is installed in the following manner. A two-by-two inch section of scalp is removed from the right occipital-parietal area. Four small screws are then placed in a trapezoidal pattern in the skull within the dimensions of the accelerometer plate mount. Quick setting dental acrylic is

molded around the screws to form a securing medium. The plate mount is then placed in the acrylic base. See Figure 1A for the orientation of the plate mount.

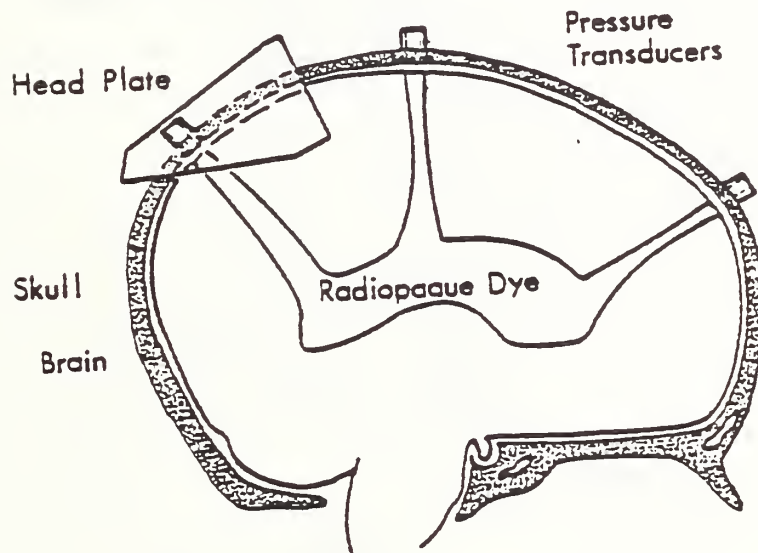
Thoracic Vertebral Mounts - Incisions are made over the T1 and T12 thoracic vertebrae. Supports for the accelerometer mounts are anchored on the lamina for each bilaterally, such that they would flank the spinous process. The accelerometer mount itself is fitted over these supports and screwed directly into the spinous process. Acrylic is applied under and around the mounts to insure structural rigidity (See Figure 2).

Cerebrospinal Fluid Pressure Transducer Fittings - Four 1 cm diameter circles of scalp are removed over the frontal, right and left parietal and occipital bones. A bone coring tool is used to tap and thread four holes in the skull (Figure 3). The brass pressure transducer couplings are twisted into place.

Cerebrospinal Repressurization - The subdural region surrounding the brain and spinal cord is instrumented for repressurization by coring a small hole into the second lumbar vertebra and inserting a Foley catheter under the dura of the spinal cord such that the balloon of the catheter reaches mid-thorax level. To check fluid flow through the ventricles, saline is injected through the Foley catheter until fluid rises to the top of the pressure transducer couplings. The couplings are capped until the radiopaque sodium iodide gel target has been slowly injected through the couplings into the brain cortex and a setup radiograph has been made of the head. The

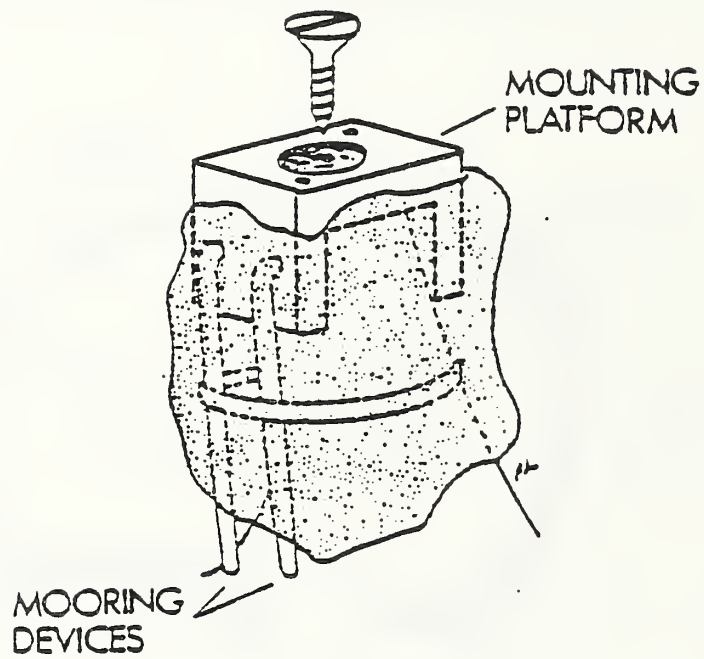


A. Nine-Accelerometer Head Plate Orientation



B. Radiopaque Target Gel in situ

Figure 1



SCHEMATIC REPRESENTATION OF
SPINAL MOUNTING PLATFORM

Figure 2

Acrylic for Securing Mounts

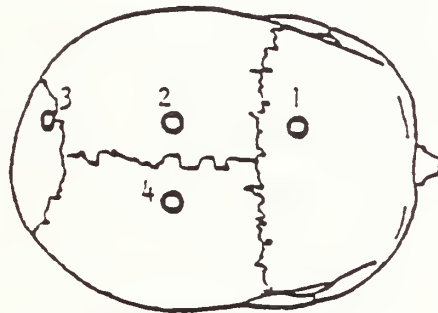
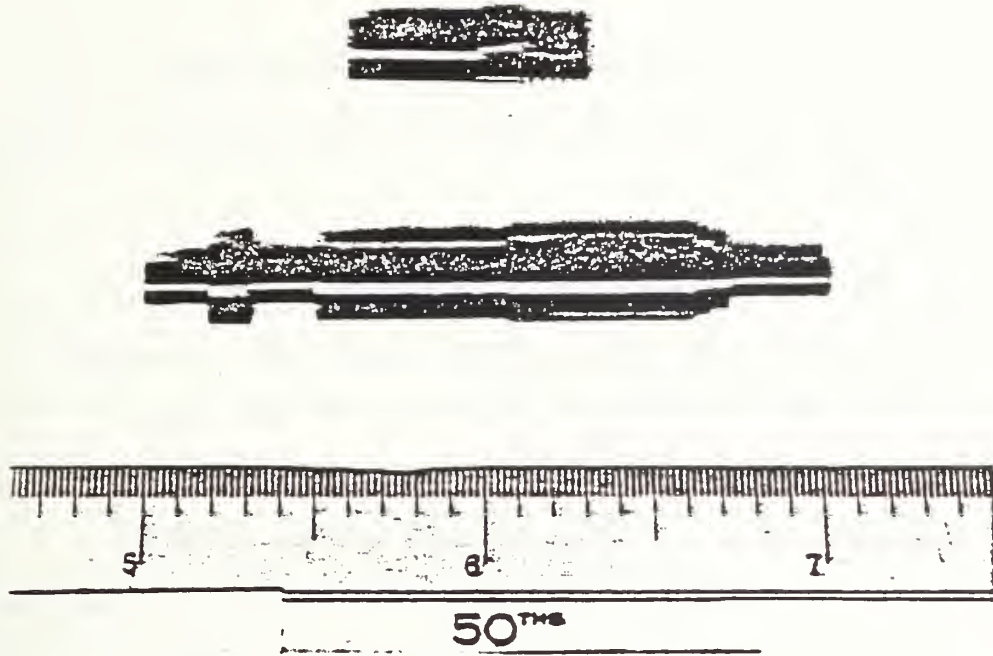


Figure 3
Cerebrospinal Fluid Pressure Transducer Fittings
and Bit

point at which the catheter passes through the lamina of the second lumbar vertebra is sealed with plastic acrylic. (Figure 4).

Vascular Repressurization - To instrument the subject for repressurizing the vascular system of the head, the common carotid artery is located at a point in the neck and an incision is made. (See Figure 5.) A balloon catheter is inserted and positioned such that the balloon is in the internal carotid artery just above the point where the external carotid artery branches. A narrow polyethylene tube is inserted at the same point and passes into the internal carotid artery just past the balloon. A Kulite pressure transducer is then fed through this tube so that vascular pressure may be monitored. Finally, the vertebral arteries are tied off above the clavicle such that fluid pressure in the head may be maintained. Just prior to testing, a solution of India ink and salt is released from a tank into the vascular system of the head. A pressure transducer monitors the flow so that the system is brought to normal physiological pressure immediately prior to impact.

4.14 Trial Test and Impact Testing - To insure that all mechanical and electronic equipment is functioning and wired appropriately for the test design, trial tests of the equipment are performed on the day before the test, allowing sufficient time to locate and correct system defects.

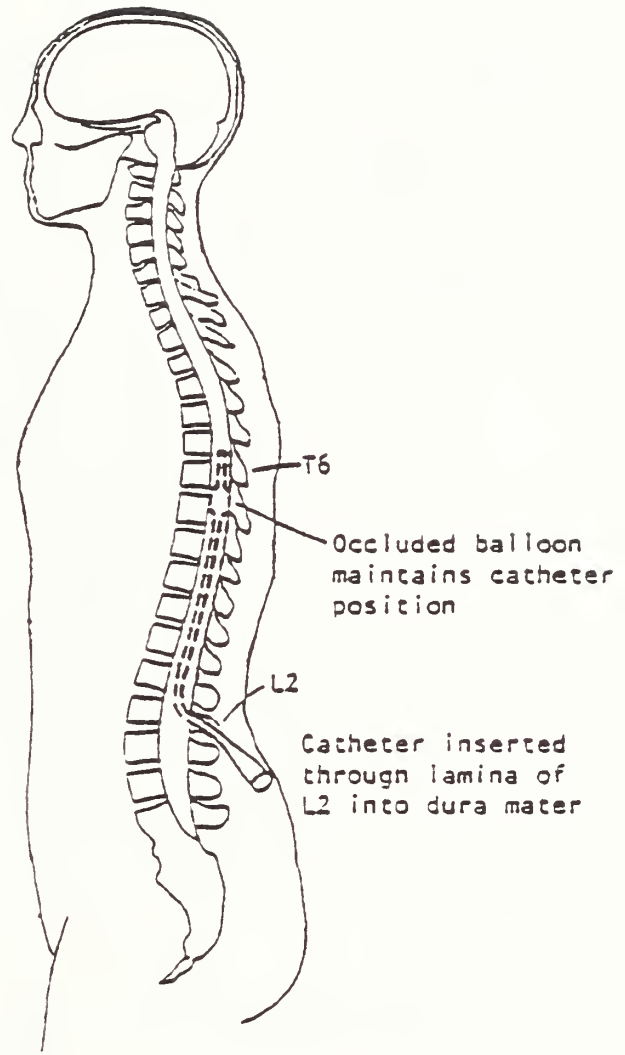


Figure 4
Cerebrospinal Lumbar Catheter

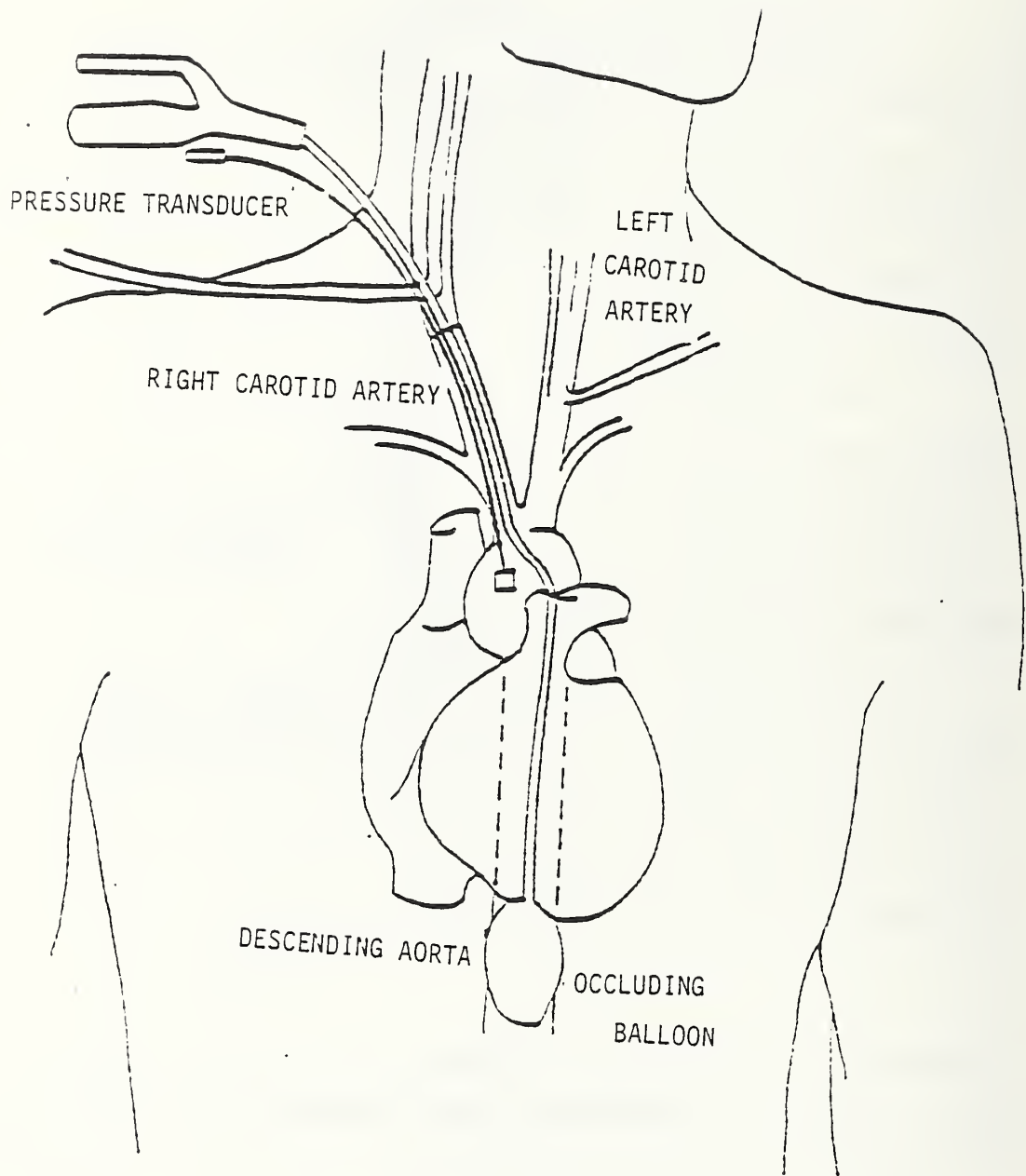


Figure 5
Vascular Repressurization

Trial Test - Accelerometers, amplifiers, umbilical cables, and recorders are tested by suspending a rubber cylinder weighing approximately 20 pounds in front of the pendulum impactor with all of the accelerometers taped to it. A preliminary check of the accelerometers and amplifiers is made to insure proper balancing and noise levels. The pendulum is then manually released via the impactor piston and the rubber cylinder is impacted. The signals from all accelerometers are recorded on the analog tape recorders. All channels are played back immediately on the brush chart for inspection purposes. The pendulum accelerometer is also tested in this procedure. Pressure transducers are tested individually by sending a signal directly to the brush chart recorder. The timer box, cameras, lights, ropecutter, cineradiograph, electroencephalograph, electrocardiograph, and velocity are tested individually. Triaxial clusters, uniax accelerometers and pressure transducers are then labeled for their specific point of attachment to the subject and placed in protective sleeves.

Three classes of operations take place before and during impact that are necessary for the documentation of the impact event: events associated with recording of electromechanical accelerometer and transducer output, events associated with cineradiographic and photometrics documentation, and events associated with the pendulum impactor.

Timing - The impact test event sequence is initiated by an operator-controlled manual switch and is thereafter controlled by signals generated by a specially constructed timer box. The timing requirements of the events associated with these signals are such that the cineradiograph is powered and ready when the high-speed X-ray camera begins to record the test, and that the lights, HyCam and Photosonics 1B cameras are synchronized so that both cameras are running at the correct speed and the test subject is fully illuminated at the time of impact. In addition, the cameras are sequenced to be operational for the minimum amount of time. This economizes the amount of effort associated with photokinematic documentation (changing film, etc.) and allows for a smoother running test sequence.

The recording equipment must be at operational speed before the pendulum is released. Additional events which must occur just prior to impact are the release of the subject from the restrained position and the activation of the sequencing gate. During the impact event, the output of the piston accelerometer must be fit into a "corridor" or window so that the pre-impact acceleration from rest and the post-impact acceleration from end-of-stroke are not recorded. The pendulum must be released so that impact will occur within the assigned time corridor. A synchronizing contact strobe, which places simultaneous electrical and photographic signals on the analog tape and high-speed film, must occur near the beginning of impact.

Equipment - The basic test equipment includes the timer box control, a signal conditioning unit for the force signal, the accelerometer-transducer patch panels, the impactor, the cineradiograph, the X-ray standby, the high-voltage power supplies, cameras, the photographic lights, and the restraints (hoists, ropeclutter). Each piece that plays a significant role in the data acquisition is described below.

Linear Pendulum Impact Device - The UMTRI linear pendulum impact device, using a free-falling pendulum as an energy source, strikes either a 25 or 56 kg impact piston. The piston is guided by a set of Thomson linear ball bushings. Axial loads were calculated from data recorded using a Setra Model 111 accelerometer (Figure 6).

Impact conditions between tests were controlled by varying impact velocity and the type and depth of padding on the impactor surface. Piston velocity was measured by timing the pulses from a magnetic probe which sensed the motion of the targets on the piston.

Ballistic Impact Device - The UMTRI ballistic impact device (Figure 7), consists of an air reservoir, a ground and honed cylinder, and a carefully fitted piston mechanically coupled to a ballistic pendulum. The piston, propelled by compressed air through the cylinder from the air reservoir chamber, serves to accelerate the ballistic pendulum. The mass of the ballistic pendulum can be varied from 10 to 150 kg. The piston is arrested at the end of its travel, allowing the ballistic

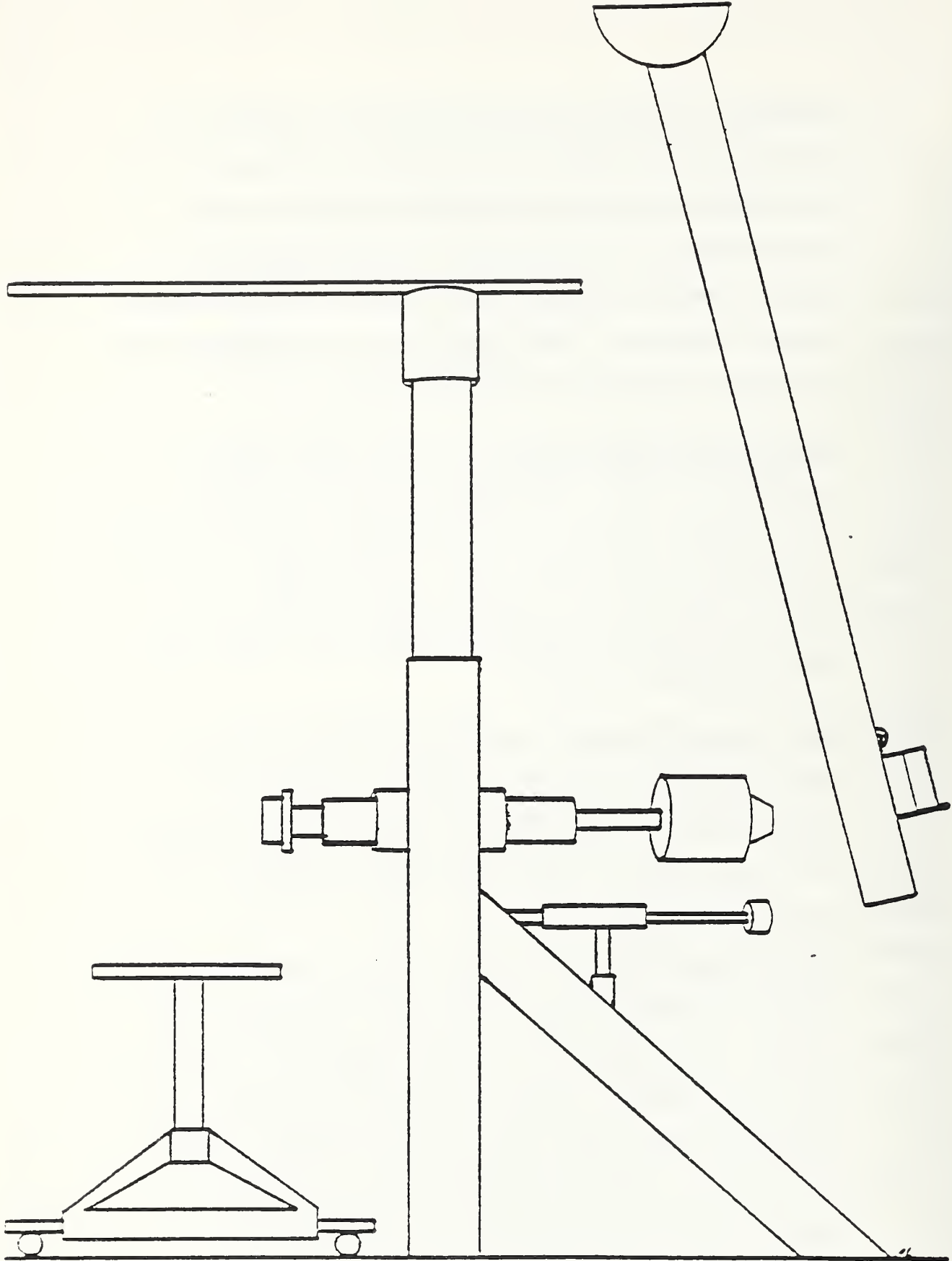


Figure 6

Linear Pendulum Impact Device

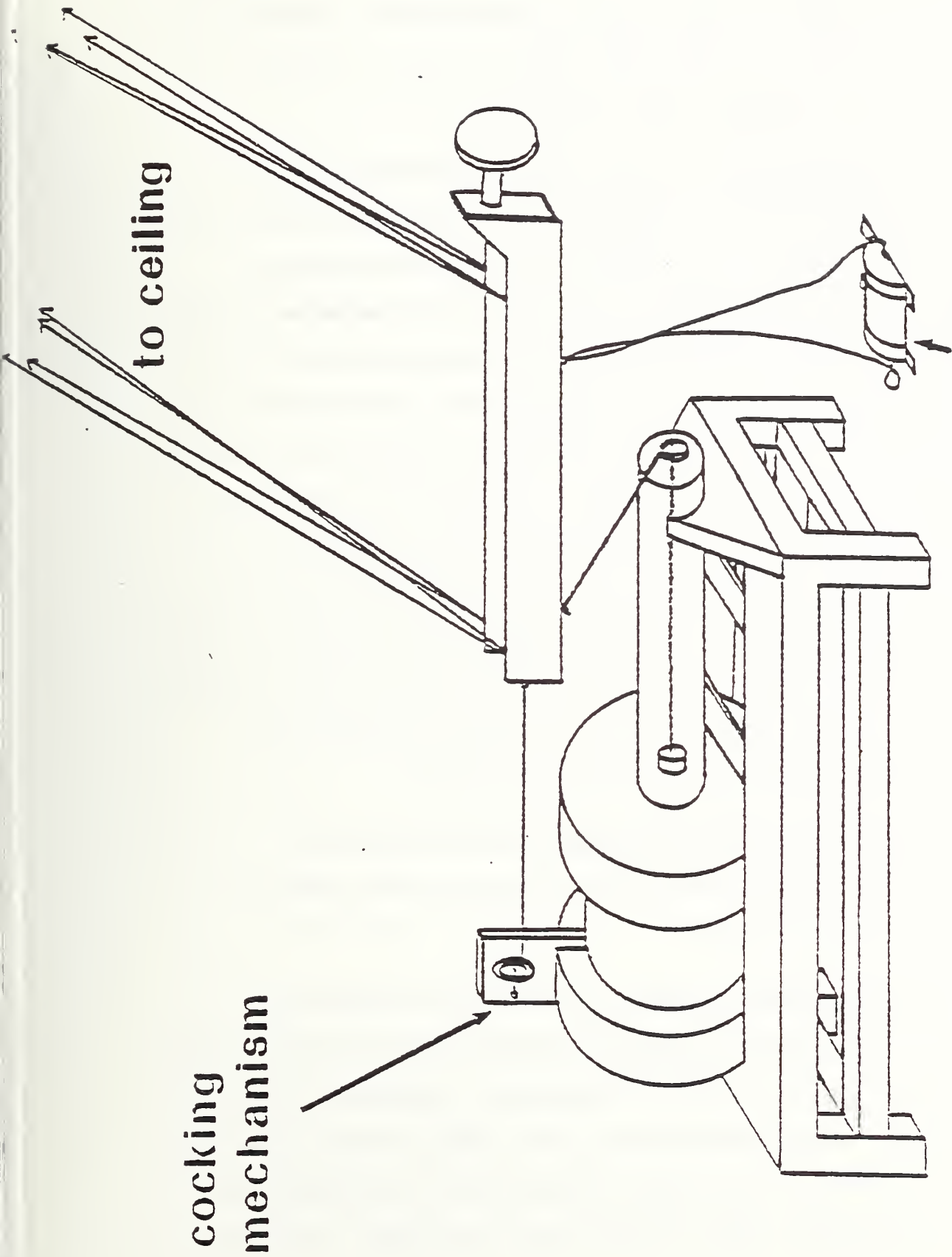


Figure 7

pendulum to become a free-traveling impactor. The ballistic pendulum is fitted with an inertia-compensated load cell for determination of impact force

Data Handling - All accelerometer and transducer time histories (pendulum force, impact acceleration, epidural pressures, nine head-accelerations) were recorded unfiltered on either a Honeywell 7600 FM Tape Recorder or a Bell and Howell CEC 3300/FM Tape Recorder. A synchronizing gate was recorded on all tapes. All data was recorded at 30 ips. The analog data on the FM tapes was played back for digitizing through the proper anti-aliasing analog filters. The analog-to-digital process for all data, results in a digital signal sampled at 6400 Hz equivalent sampling rate. It has been reported that skull vibrations above 1300 Hz could cause very local motion in the accelerometer mountings [308]. To reduce this effect, the raw transducer time histories were digitally filtered with a Butterworth filter at 1000 Hz, 6th order.

Epidural Pressure Transducers - Endevco series 8510 piezoresistive pressure transducers were used to measure epidural pressure.

Photokinematics System - The motion of the subject was determined from the high-speed (1000 frames per second) film by following the motion of single-point phototargets on the head and on the impactor piston. For selected cadaver frontal head impacts, a Hycam camera operating at 3000 frames per second provided a close-up lateral view of the impact. For these

cadaver frontal impacts, the Photosonics provided a overall lateral view at 1000 frames per second.

Analytical photogrammetry is used in these experiments to describe the geometry of anatomical structures and their motion in the laboratory reference frame. The objective space coordinates of points of interest are obtained once the coordinates of well-defined points in an image space and the calibration translation and rotations are specified. The points in an image space are obtained with camera and radiographic equipment and are preserved on film.

Motion of an anatomical structure in space is obtained by measuring the time-history of the position of a photographic target which has a well-defined position and orientation, relative to a predefined anatomical landmark. Defined descriptors of translations and rotations (position, velocity, acceleration) are associated with rigid body motion in object space. Once these descriptors are obtained and digitized, they can then be used to characterize the dynamic response of the subject under study and assist in understanding injury mechanism(s).

In these tests the descriptors chosen are based upon anatomical structures in a two-dimensional image space produced by a point source of X-Rays. The descriptors are two-dimensional and do not take into account rotations and translations which move objects in and out of a plane of gross whole body motion. In addition, changes in the X-Ray cross section of objects can

lead to changes in the descriptors which do not have a direct relation to rigid body motion.

Cineradiograph - The UMTRI cineradiograph allows non-invasive viewing of internal anatomical structures in situ. For rigid structures such as bones, the radiopaque targets can be placed on or near anatomical landmarks and motion can be similarly described to that of standard photometric techniques. For soft tissues and some bony structures, descriptors are chosen based upon the shadows of objects associated with anatomical structures.

Radiopaque Target Gel - A neutral density radiopaque gel is used to determine motion of the brain during impact. The gel is injected into the brain through the holes used for insertion of the pressure transducers. The injection technique produces lines of radio-contrast in the brain that show up in high-speed cineradiographic movies. See Figure 1B.

For selected subjects, high-speed cineradiographs were taken. The cineradiographs were taken of the impact events at 1000 or 400 frames per second. The UMTRI high-speed cineradiographic system [497-498] consisted of either a Photosonics 1B or Miliken high-speed 16 mm motion-picture camera which views a 5 cm diameter output phosphor of a high-gain, four-stage, magnetically focused image intensifier tube, gated on and off synchronously with shutter pulses from the motion-picture camera. A lens optically coupled the input photocathode of the image intensifier tube to X-Ray images produced on a

fluorescent screen by a smoothed direct-current X-Ray generator. Smoothing of the full-wave rectified X-Ray output was accomplished by placing a pair of high-voltage capacitors in parallel with the X-Ray tube. The viewing field for these experiments was between 20 and 40 cm.

Test Subject Preparation - The unembalmed cadavers were stored at 4°C prior to testing. The cadaver was X-Rayed as part of the structural damage evaluation and anthropomorphic measurements are registered. Next, the cadaver was instrumented, sanitarily dressed and transported to the testing room where the accelerometers and pressure transducers are attached. The subject was positioned. Next, the radiopaque gel target was inserted, and pretest X-Rays and photographs were taken. Pressurization was checked. The subject was then impacted. Each cadaver received either two duplicate head impacts or three triplicate head impacts. Various paddings and padding thicknesses were used.

Initial Test Conditions - Tests 82E001 thru 82E062 used the UMTRI 25 kg linear pendulum impacting device with a 15 cm diameter impacting surface padded with 2.5 cm Ensolite. Tests 83E081 thru 83E103 used the UMTRI 25 kg ballistic impacting device fitted with a 15 cm diameter impacting surface padded with 2.5 cm Ensolite, or a sandwich of 2.5 cm styrofoam, 5 cm Dow Ethafoam plus 2.5 cm Ensolite, or one of 0.5 cm Ensolite, 5 cm seating foam plus 0.5 cm Ensolite. The target area for all of these impacts was the center of the forehead above the

orbits (frontal bone). Impact occurred in the anterior to posterior direction. All cadavers were seated and positioned with paper tape so that the subject and the impact target were stable (Figure 8).

4.15 Post-Test Autopsy - After impact testing, the test subject was brought to the Anatomy Lab for autopsy. A gross autopsy was performed. All injuries were recorded in the test protocol on charts and brief descriptions were also written in the protocol. 35 mm still photographs in color and in black and white were taken of all significant tissue damages. These were later coded according to the AIS-80 scheme and reported in DOT format. Occasionally, knowledgeable medical professionals were consulted when more descriptive information might better characterize the observed tissue damages than the AIS-80 coding permits. All of this information was used in the analysis and reconstruction of mechanism(s) of injury and is included in the written reports to the sponsor.

4.2 METHOD OF ANALYSIS - The techniques used to analyze the results are outlined below. Additional information can be found in [311-312, 505-507].

4.21 X-Ray Motion Descriptors - The procedures used for defining X-Ray motion descriptors are explained in [504] and briefly outlined below. Body dynamics no longer offer a good approximation. Several methods have been suggested to produce analytical information describing the soft tissue of the brain. For this project the motion descriptors chosen are based upon

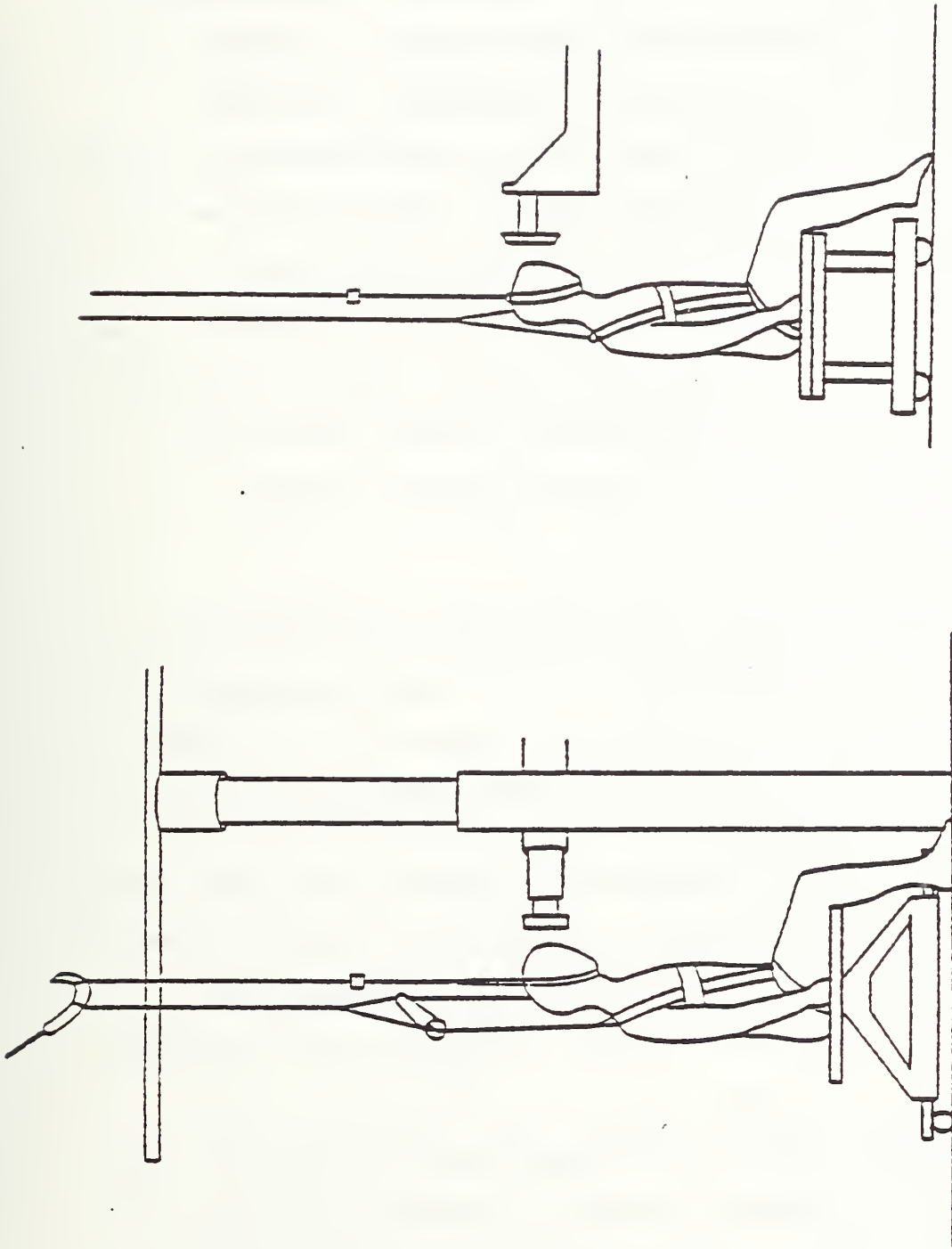


Figure 8
Initial Test Conditions

the shadows of objects in a two-dimensional image space produced by a point source of X-Rays which are associated with the anatomical structures or the radiopaque dye injected into the brain. In the impact tests presented in this report, radiopaque gel was injected into the head producing four curved lines in the brain and outlining the ventricles in some tests. Differential motion between the brain and the skull was obtained by comparing the motion of points on the curve closest to the center of the epidural pressure transducer. General characteristics of the motion of the brain were obtained through the changes in shape of the curved lines and ventricles.

4.22 Frame Fields - As the head moves through space, every point on the head generates a path in space. In head injury research we are interested in the description of the path of the anatomical center and in events which occur as it moves.

It is necessary to determine the instrumentation frame's exact location and orientation in relation to the anatomical frame. A three-dimensional X-Ray technique was developed which requires taking two orthogonal radiographs of the instrumented head. The procedure requires the identification of four anatomical landmarks (two superior edges of the auditory meati and two infraorbital notches) with four distinguishable lead pellets, plus the identification of four lead pellets inlaid in the plate to define the instrumentation frame.

A very effective tool for analyzing the motion of the anatomical center as it moves along a path in space, is the concept of a moving frame [499-500, 508-509]. The path generated as the point travels through space is a function of time and velocity. A vector field is a function which assigns a uniquely defined vector to each point along a path. Thus, any collection of three mutually orthogonal unit vectors defined on a path is a frame field. Therefore, any vector defined on the path (for example, acceleration) may be resolved into three orthogonal components of any well-defined frame field, such as the laboratory or anatomical reference frames. Changes in a frame field with time (for example, angular acceleration of the frame field) are interpreted as vectors defined on the curve and are also resolved into three components.

In biomechanics research frame fields are defined based on anatomical reference frames. Other frame fields such as the Frenet-Serret frame or the Principal Direction Triad [503, 505], which contain information about the motion embedded in the frame field, have also been used to describe motion resulting from impact.

The Frenet-Serret Frame [508-509] consists of three mutually orthogonal vectors T, N and B. At any point in time a unit vector can be constructed that is co-directional with the velocity vector. This normalized velocity vector defines the tangent direction T. A second unit vector N is constructed by

forming a unit vector co-directional with the time derivative of the tangent vector T (the derivative of a unit vector is normal to the vector). To complete the orthogonal frame, a third unit vector B (the unit binormal) can be defined as the cross product $T \times N$. This procedure defines a frame at each point along the path of the anatomical center. Within the frame field, the linear acceleration is resolved into two distinct types. The tangent acceleration [$Tan(T)$] is always the rate of change of speed (absolute velocity) and the normal acceleration [$Nor(N)$] gives information about the change in direction of the velocity vector. The binormal [$Bin(B)$] direction contains no acceleration information.

Our method of determining the principal direction of motion and constructing the Principal Direction Triad is to determine the direction of the acceleration vector in the moving frame of the triaxial accelerometer cluster and then assign the transformation necessary to obtain a new moving frame that would have one of its axes in the principal direction. A single point in time at which the acceleration is a maximum was chosen to define the directional cosines for transforming from the triax frame to a new frame in such a way that the resultant acceleration vector (AR) and the "principal" unit vector ($A1$) were co-directional. This then can be used to construct a new frame rigidly fixed to the triax but differing from the original one by an initial rotation. After completing the necessary transformation, a comparison between the magnitude of

the principal direction and the resultant acceleration is performed.

4.23 Transfer Function Analysis - The relationship between an accelerometer/transducer time-history at a given point and the accelerometer/transducer time-history of another given point of a biomechanical system (human surrogate) can be expressed in the frequency domain through the use of a frequency-response transfer function. This input output function is a complex-valued function in the frequency domain and can be expressed by a magnitude and a phase at a given frequency. Transfer functions can be determined from the Fourier transforms of the input-output response time-histories or from the spectral densities of the input and output response signals. In the case of a force and a pressure, such as impact force and epidural pressure, a transformation of the form:

$$(X)(iw) = (F)[F(t)]/(F)[P(t)]$$

can be calculated from the transformed quantities, where w is the given frequency, and $F[F(t)]$ and $F[P(t)]$ are the Fourier transforms of the impact force time-history and the epidural pressure time-history, respectively.

A transformation of simultaneously monitored accelerometer/transducer time-histories can be used to obtain the frequency-response functions of impact force and accelerations of remote points. Once the frequency-response functions are obtained, a transfer function of the form:

$$(Z)(iw) = (w) (F)[F(t)]/(F)[A(t)]$$

can be calculated from the transformed quantities. w is the given frequency and $F[F(t)]$ and $F[A(t)]$ are the Fourier transforms of the impact forces and accelerations of the point of interest at the given frequency.

This particular transfer function is the mechanical transfer impedance which can be defined as the ratio between simple harmonic driving force and corresponding velocity of the point of interest. More information about how mechanical impedance procedures are applied can be found in [501].

4.24 Statistical Measures - To describe some of the fundamental properties of a time-history, such as acceleration or force, three types of statistical measures are used. They are the Auto-correlation Function, the Cross-Correlation Function, and the Coherence Function.

The Auto-correlation Function is the correlation between two points on a time-history, and is a measure of the dependence of the amplitude at time t_1 , on the amplitude at time t_2 where t_1 and t_2 are two points on a time-history separated by a given lag ($t_1 - t_2$). The auto-correlation function is formally defined as the average over the ensemble of the product of two amplitudes:

$$R_x(t_1, t_2) = \int x_1, x_2, p(x_1, x_2, t_1, t_2) dx_1, dx_2$$

where x_1, x_2 are the amplitudes of the time-history and $p(x_1, x_2, t_1, t_2)$ is the joint probability density. Through the

use of a Fourier transform, a discrete time-history of a finite duration is transformed into an auto-correlation function which illustrates the continuous function. For example, the Power Spectral Density Function is a quantity that describes the frequency or spectral properties of a single time-history. It is the Fourier transform of an auto-correlation function and is sometimes called the "Auto Spectral Density" function. Since it is devoid of phase information, only transfer function magnitude can be obtained from the Power Spectral Density Function.

The Cross-Correlation Function is a measure of how predictable, on the average, a time-history at any particular moment in time is from another time-history at any other particular moment in time. The cross-correlation of the time-histories of two signals begins by taking the Fourier transform of both time-histories (Y_1, Y_2). The cross-spectral density describes the joint spectral properties of two time-histories. Phase information is retained in cross-spectral density so that both the magnitude and phase of the transfer function are obtained. The cross-spectral density is the complex-valued function ($Y_1 \bullet Y_2^*$). The cross-correlation is then the Fourier transform of the cross-spectral density.

Cross-correlation between acceleration measurements at two different points of a material body may be determined to study the propagation of differential motion through the material body. Cross-correlation functions are also not restricted to

correlation of parameters with the same physical units; for example, the cross-correlation between the applied force and the acceleration response to that force can be determined.

The Coherence Function $c_{xy}^2(\omega)$, is a measure of the quality of a given transfer function at a given frequency:

$$c_{xy}^2(\omega) = \frac{|G_{xy}(\omega)|^2}{G_{xx}(\omega)G_{yy}(\omega)}$$

where $G_{xx}(\omega)$ and $G_{yy}(\omega)$ are the power spectral densities of the two signals, respectively. (Power Spectral Density is a Fourier transform of each signal's auto-correlation.) $|G_{xy}(\omega)|^2$ is the Cross-Spectral Density function squared. (Cross-Spectral Density is the Fourier transform of the cross-correlation of the two signals at ω , the given frequency.) In general, $0 \leq c_{xy}^2(\omega) \leq 1$. Values of $c_{xy}^2(\omega)$ near 1 indicate that the two signals can be considered causally connected at that frequency. Values significantly below 1 at a given frequency indicate that the transfer function at that frequency cannot accurately be determined. In the case of an input-output relationship, values of $c_{xy}^2(\omega)$ less than 1 indicate that the output is not attributable to the input and is perhaps due to extraneous noise. The coherence function in the frequency domain is analogous to the correlation coefficient in the time domain. For more information on this measure see [501].

4.25 Pressure Time Duration Determination - Two different types of pressure-time histories were observed, unimodal and bimodal. The unimodal waveform was characterized by one maximum and the bimodal waveform by two local maxima. In order to define the

pressure duration, a standard procedure was adopted which determined the beginning and end of a pulse. This procedure began by determining the peak, or the first peak in the case of a bimodal waveform. Next, the left half of the pulse, defined from the point where the pulse started to rise until the time of peak, was least-squares fitted with a straight line. This rise line intersected the time axis at a point which was taken as the formal beginning of the pulse. A similar procedure was followed for the right half of this pulse, i.e., a least-squares straight line was fitted to the fall section of the pulse, which was defined from the peak to the point where the pulse minimum occurred. The point where this line intersected the time axis was the formal end of the pulse in the unimodal case, and the formal end of the first peak in the bimodal case. The pressure duration for a unimodal waveform was defined by these points. For a bimodal waveform, these two points were used to determine the first pressure duration. Another least-squares straight line was fitted to the fall section of the second pulse. The point at which this line intersected the time axis was the formal end of the waveform, and the total pressure duration was then defined from this point and the beginning point.

4.26 Force Time-History Determination - In general the force-time histories were unimodal with a single maximum, smoothly rising, peaking and then falling. Various padding configurations on the striker surface effected different force time-history durations. Force duration was determined using

the same techniques for determining pressure duration, that is similar boundary defining and least-squares straight-line fitting techniques were employed.

4.27 Impact Response Definition - With the use of the UMTRI nine-accelerometer array it is possible to record three-dimensional six-degrees-of-freedom motion of the area of the the skull in which the accelerometers are located. Therefore, head impact response can be defined as a continuum of "events" characterized by the path traced by the motion of the "estimated anatomical center," by all the vectors defined on that path, and by changes of the associated frame fields. Physically this implies that head impact response is interpreted as the response of a material body (the nine-accelerometer array and area of the skull local to it) in contact with other material bodies. The curve and the vectors generated as the "estimated anatomical center" moves in time are, thus, a result of the interactions of the skull-mount area with other material bodies.

Examples of events which are used to characterize head impact are: the initiation of head impact response (denoted by Q_1 on the tangential acceleration time histories in the appendix), the positive maximum of the tangential acceleration time history (denoted by Q_2 in the accompanying data), and the negative maximum of the tangential acceleration time-history (denoted by Q_3 in the accompanying data). In research reported earlier in which similar Q_1 , Q_2 and Q_3 events were defined

[302], the tangential acceleration rose smoothly to a single maximum and fell smoothly until crossing zero. In some of the tests being reported here, the time interval near Q_2 contained several local maxima, therefore direct comparison is complex. Nevertheless, these defined events can be used to compare different types of impacts for the same human surrogate and to compare the response of one human surrogate to another.

5.0 RESULTS

Table 1 lists the initial test conditions. Table 2 summarizes the impacts. Table 3 characterizes impact pressures. Table 4 reports the tissue damages. Selected time histories in Appendix C are examples of important kinematic factors associated with the research performed in this test series. The variables these examples illustrate are tangential and normal acceleration, resultant acceleration, rate of change of the tangential vector (T-rate) and rate of change of the binormal vector (B-rate). In addition, impact force, resultant angular acceleration and velocity, linear velocity, and pressures are shown.

The effect of different filtering levels is illustrated in Appendix C by Test 82E041 which is presented at no-filtering, 100 hz, 200 hz, 400 hz, 800 hz, and 1600 hz levels.

Table 1. Initial Test Conditions

Test No.	Subject Condition	Impact Surface Padding Thickness+	Velocity m/s
82E001++	repressurized	2.5 cm Ensolite	5
82E021++	repressurized	2.5 cm Ensolite	5.2
82E022++	repressurized	2.5 cm Ensolite	5.7
82E041++	repressurized	2.5 cm Ensolite	5.5
82E042++	repressurized	2.5 cm Ensolite	5.5
82E061++	repressurized	2.5 cm Ensolite	5.5
82E062++	repressurized	2.5 cm Ensolite	5.5
83E081+++	repressurized	2.5 cm Ensolite	3.8
83E082+++	repressurized	2.5 cm Ensolite	3.8
83E101+++	repressurized	2.5 cm Ensolite 5.0 cm Dow Ethafoam 2.5 cm Ensolite	4.5
83E102+++	repressurized		4.5
83E103+++	repressurized		4.5

++25 kg linear pendulum
+++25 kg ballistic pendulum

Table 2. Impact Test Summary

Test No.	Linear Acceleration Tangent m/s/s	Resultant Acceleration m/s/s	Resultant Angular Acceleration r/s/s	Resultant Angular Velocity r/s	Linear Velocity m/s	Force N	Force Duration ms
82E001	3600	4500	42000	52	5	9100	10
82E021	1400	1440	7500	20	5.2	8400	11
82E022	1900	1900	7250	28	7.0	9600	10
82E041	1800	1800	7000	19	6.4	9600	12
82E042	1600	1800	8000	20	7.5	10200	12
82E061	1600	1700	6000	25	6.5	9000	10
82E062	1500	1600	7500	30	6.5	9600	12
83E081	1350	1350	7500	22	3.8	9600	12
83E082	1250	1000	7000	24	3.5	4100	8
83E101	-	-	-	-	-	-	-
83E102						1800	64
83E103							

Table 3. Test Pressure Summary

Test No.	Location	Type	Maximum Kpa	Time at Maximum ms	Duration ms
82E001	Epidural 1	Unimodal	75	5	10
	Epidural 2	Bimodal	11,3	5/25	10/120+
	Epidural 3	Unimodal	-36	5	15
	Epidural 4	Unimodal	11	5	5
82E021	Epidural 1	Unimodal	161	5	12
	Epidural 2	Bimodal	48,7	5/40	5/80
	Epidural 3	Bimodal	-61,8	5/45	10/80
	Epidural 4	Bimodal	34,6	5/25	5/70
82E022	Epidural 1	Unimodal	180	5	10
	Epidural 2	Bimodal	47,6	5/35	10/80
	Epidural 3	Bimodal	-43,6	5/50	15/100
	Epidural 4	Bimodal	12,51	5/13	5/5
82E041	Epidural 1	Bimodal	22,2	5/40	15/20
	Epidural 2	Bimodal	-20,11	5/45	10/15
	Epidural 3	Bimodal	-55,28	5/50	10/40
	Epidural 4	Bimodal	39,31	5/50	10/70
82E042	Epidural 1	Unimodal	58	5	140+
	Epidural 2	Bimodal	-20.9	5/45	5/20
	Epidural 3	Bimodal	-53,13	5/45	10/40
	Epidural 4	Bimodal	/38,42	5/60	5/25
*82E061	Epidural 1	Unimodal	97	5	8
	Epidural 2	Unimodal	24	5	5
	Epidural 3	Unimodal	-31	5	8
	Epidural 4	Bimodal	15/40,7	5	10/150
**82E062	Epidural 1	Unimodal	55	5	12
	Epidural 2	Bimodal	27,12	5/40	10/35
	Epidural 3	Bimodal	31,14	5/42	10/40
	Epidural 4	Bimodal	37,12	5/45	10/40
83E081	Epidural 1	Unimodal	52	5	150+
	Epidural 2	Bimodal	20,14	5/20	10/135+
	Epidural 3	Bimodal	-18,14	5/20	7/125+
	Epidural 4	Unimodal	25	5	75
83E082	Epidural 1	Unimodal	46	5	15
	Epidural 2	Bimodal	10,5	5/20	10/125+
	Epidural 3	Bimodal	-13,3	5/50	10/100+
	Epidural 4	Bimodal	7,4	5/25	5/50

Table 3. Test Pressure Summary (continued)

Test No.	Location	Type	Maximum Kpa	Time at Maximum ms	Duration ms
83E101	Epidural 1	Unimodal	1		
	Epidural 2	Unimodal	1		
	Epidural 3				
	Epidural 4	Unimodal	17		
83E102	Epidural 1	Unimodal	-6	5	
	Epidural 2	Unimodal	-1	5	
	Epidural 3	Unimodal	5	5	
	Epidural 4	Unimodal	2	5	
83E103	Epidural 1	Unimodal	18		
	Epidural 2	Bimodal	18		
	Epidural 3	Unimodal	7		
	Epidural 4	Bimodal	4		

*Epidural 1 = Frontal Bone
 Epidural 2 = Left Parietal Bone
 Epidural 3 = Occipital Bone
 Epidural 4 = Right Parietal Bone

**Epidural 3 = Right Parietal Bone
 Epidural 4 = Occipital Bone

Table 4. Damages

Test No.	Gross Skull	Gross Brain	Gross Other
82E001	No abnormality. Parietal fracture. Basilar fracture.	No abnormality. Sub-arachnoid hematoma frontal lobes (cerebrum) and on base of occipital lobe (cerebrum).	No abnormality or injury.
82E021 82E022	No abnormality or injury.	No abnormality. Sub-arachnoid hematoma right frontal lobe (cerebrum), hemorrhage central area left frontal lobe (cerebrum).	No abnormality or injury.
82E041	No abnormality or injury.	No abnormality. Sub-arachnoid hematoma frontal lobes (cerebrum) and subarachnoid.	No abnormality or injury.
82E061 82E062	No abnormality or injury.	No abnormality or injury.	No abnormality or injury.
83E081 83E082	No abnormality or injury.	No abnormality or injury.	No abnormality or injury.
83E101 83E102 83E103	No abnormality or injury.	No abnormality or injury. [Mechanical abnormality of incomplete repressurization].	No abnormality or injury.

6.0 DISCUSSION

Since the head impact tests entail different initial conditions, impact directions, and locations for the recording instruments, frame-independent variables and Frenet-Serret vectors were used for examination and analysis. Frame-independent variables include resultant angular and linear velocities and accelerations. Vectors expressed in the Frenet-Serret frame field include tangential acceleration, normal acceleration, T-rate and B-rate. The features of the data discussed briefly in this section represent trends that may be important factors in head impact response. In particular, the potential effect of skull deformation on head angular acceleration as well as on impact and injury response appears significant.

6.1 Force Time-Histories - Force time-histories of the head impact tests were divided into two types which correlate well with fracture and non-fracture tests. In non-fracture tests, the force rises smoothly to a maximum and drops smoothly to zero. In fracture tests, although the force rises smoothly to a maximum, the drop to zero has a greater number of inflections or local maxima and is of longer duration. Test 82E001 is an example of a fracture test.

Non-fracture head impacts can be broken into two groups consisting of long- and short-duration impacts. Short-duration impacts are those which last less than 15 ms; long-duration impacts are defined as lasting 15 ms or longer. In some cases, such as Test 83E102, durations as long as 60 ms were recorded. Test 82E041 illustrates a short-duration impact and Test 83E102 a long-duration impact.

6.2 Tangential Acceleration Time-Histories - The tangential acceleration time-histories separate into two groups, correlating well

with the presence or absence of subarachnoid hemorrhage. For those tests in which no subarachnoid hemorrhage was observed, the tangential acceleration had a single local maximum in the area of maximum acceleration. However, for those tests in which subarachnoid hemorrhage was observed, there were several local maxima in the area of maximum acceleration.

6.3 Comparison of Impacts: Cadaver Variability - To examine variability within the cadaver subjects, some subjects received two similar impacts (Tests 82E001 through 83E082). Figure 9 is an example of cross- and auto-correlations for Tests 82E021 x 82E022 and 82E061 x 82E062 and 82E021 x 82E061. The figure represents the general trend observed in relating the force time-histories of similar tests with different subjects to similar tests with the same subject. In general, it appears that force time-histories as well as acceleration time-histories vary more between subjects than between tests on the same subject. An analogous comparison for epidural pressures showed equivalent variance between different subjects undergoing similar impacts as between the same subject having similar impacts. This implies that experimental techniques associated with repressurization or with the effects of the postmortem state may produce as much variance in the pressure time-history response as do variations due to the population of test subjects.

6.4 Impact Response - The motion of a rigid body in space is the result of generalized forces: the total force and the total torque about a suitable axis. The dynamic problem of the motion of the area of the skull local to the nine-accelerometer array can be interpreted in the same way. However, due to the complex interactions of the area of

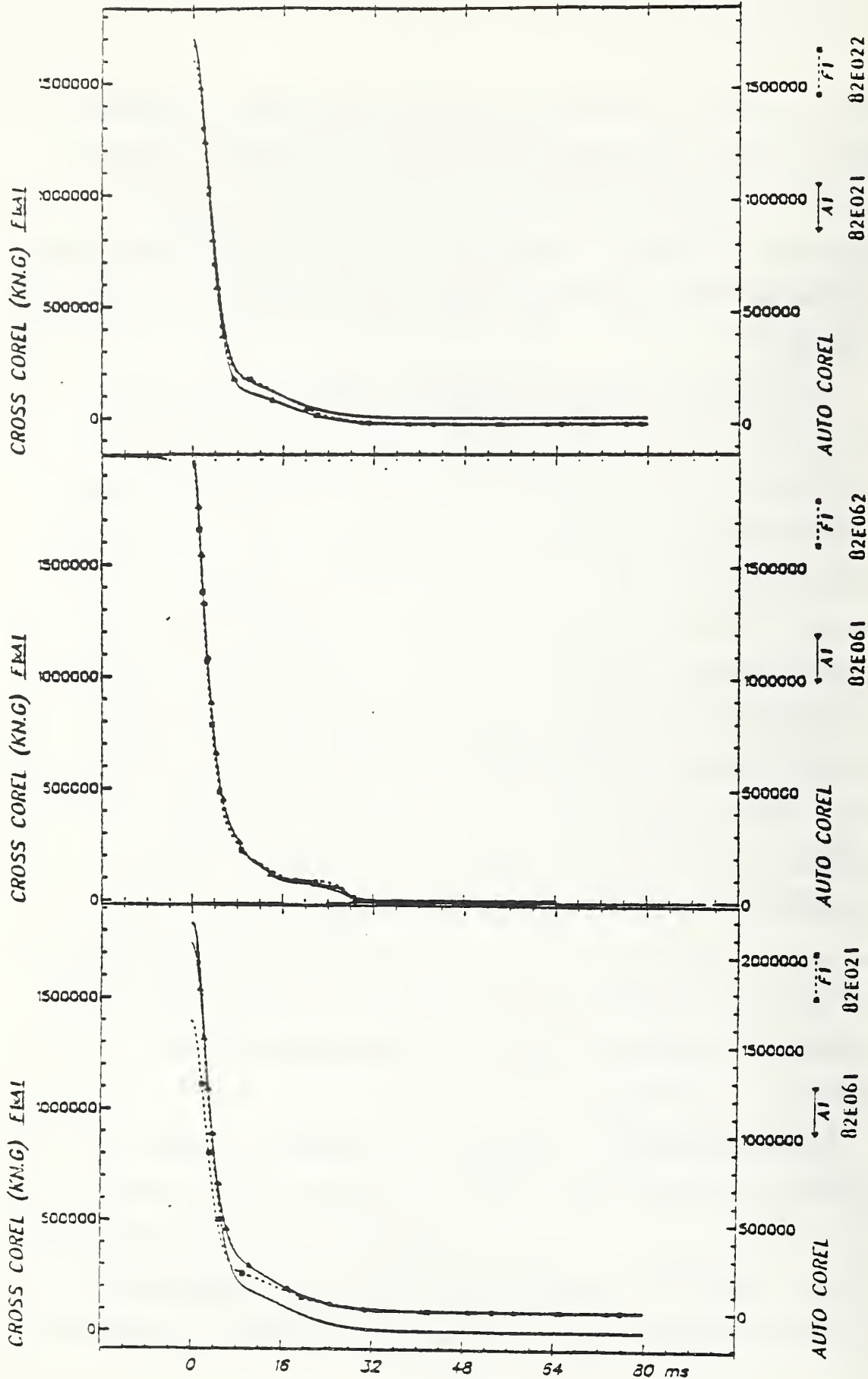


Figure 9

the skull local to the nine-accelerometer array with other material bodies, (for example, the muscle soft tissues of the neck, the rest of the skull, the brain, or the impactor), serious problems can arise in determining which of the bodies is producing these generalized forces.

When the head receives an impact, several events occur: 1) stress waves are propagated from the impact site, 2) the skull starts to deform, and 3) the skull begins to move due to the impact, transmitting impact energy to the brain via the dura mater. Eventually, the waves are dissipated, the deformation of the skull recovers partially or fully upon removal of the impact loads, and the acceleration of the skull occurs primarily due to forces generated through the brain and neck. If differential skull motion is severe, essentially due to either sufficient energy in the high frequency components of the force time-history or a sufficient peak force, the stresses at some point in the skull may exceed the failure strength of the bone, thereby producing fracture. The loads producing this type of impact are generally of shorter duration or contain a rise time sufficient to generate the high frequency components necessary to fracture the skull. The motion of the entire skull as a rigid body, as estimated by the nine-accelerometer array, depends on the degree of skull deformation as well as on the degree of precision being used in the investigation. If the skull deformations are small during and after impact, and the accelerometers are far enough from the impact contact point, then valid rigid body motion can be assumed. However, if skull deformations are significant, then three-dimensional motion of the nine-accelerometer array and of the skull local to its instrumentation mount can only be used to estimate the motion of the rest of the skull through the use of an "estimated

anatomical center." Interpretation of the results from the nine-accelerometer array must, therefore, take into account the non-rigid body motion taking place during "significant skull deformation" impacts. Using translations obtained from X-rays, three-dimensional approximate motion of an "estimated anatomical center" can be determined.

6.5 Effects of Skull Deformation on Linear and Angular Acceleration

Inspection of the three-dimensional motion of the skull local to the accelerometers, epidural pressure transducer response, and contact forces showed that skull deformation may have important implications for injury produced in blunt head impact.

For tests with force time-histories having unimodal peaks of the anatomical center, "the time interval between the events Q_1-Q_2 is probably primarily a result of the interaction of the impactor with the skull. During the Q_1-Q_2 interval, the "estimated anatomical center" does not move more than 1 cm and the motion is to some extent three-dimensional. This is indicated by the rate of change of the tangent vector (T-rate) and binormal vector (B-rate). A positive T-rate implies a curvature of the path or two-dimensional motion; significant T- and B-rate imply a torsion of the path or three-dimensional motion. However, the angular acceleration is principally in the binormal direction. The normal acceleration of the point on the skull of closest approach to the impactor was found to be less than that of the "estimated anatomical center." Reduced normal acceleration implies a "straighter" path for that point. These measurements of angular and normal acceleration imply that the skull may be rotating about the point of closest approach to the impactor centerline.

For the tests with time-histories displaying multimodal peaks of the tangential acceleration of the "estimated anatomical center" in the vicinity of the Q_2 event, the time interval between the events Q_1-Q_2 is probably a result of the interaction between impactor and skull. However, in these tests skull deformations seem to have significant effect on the angular, tangential, and normal acceleration responses. Comparison of this multimodal impact response (Test 82E041 for example) to the unimodal tangential acceleration response (Test 82E061 for example), shows that the following variables are greater during the Q_1-Q_2 interval of the multimodal impact: angular acceleration, normal acceleration, T-rate and B-rate. This implies that for the multimodal type of impact, the path of the "estimated anatomical center" is moving in a three-dimensional manner to a greater extent than the same path for the unimodal pattern impacts. This increased level of three-dimensional motion correlates well with the angular acceleration.

Comparison of the ratios of peak angular acceleration and velocity during the Q_1-Q_2 interval to the respective peak angular acceleration and velocity during the Q_2-Q_3 interval indicates that for a given multimodal impact, there is greater angular acceleration response during the Q_1-Q_2 interval. In addition, the local maxima of the angular velocities in the multimodal impact as well as the rapid rotation of the binormal and normal vectors of between $\pi/2$ and π radians indicates that the path of the "estimated anatomical center" has passed an inflection point near the Q_2 event. This is most evident when the skull fractured. In a skull fracture test, the head is loaded very rapidly (e.g., Test 82E001, while the force drops, the tangential acceleration drops below zero). This is accompanied by a short-lived rotation of the

skull which produces a local maximum in the angular velocity. Subsequent to fracture, the skull is in more complete contact with the impactor. The tangential acceleration increases, the angular velocity decreases, and the angular acceleration reverses direction.

The head is generally modeled as a rigid body when interpreting angular acceleration from nine-accelerometers. However, the complex nature of the skull geometry [262, 494-495] causes asymmetric loading during blunt impact, which leads to an interpretation of an angular acceleration by the nine-accelerometer array that is not directly related to rigid body motion. Therefore, in addition to local skull bending in the area of the nine-accelerometer array, a second mechanism of skull deformation which causes the accelerometers to interpret angular acceleration can be hypothesized.

A schematic display of this type of response is presented in Figure 10 to illustrate the effect of skull deformation on angular acceleration (a rotation is produced). This figure demonstrates the type of motion that might occur and is not necessarily representative of motion actually observed. Also, motion of the skull is not necessarily in the anterior-posterior, inferior-superior plane. Since angular displacement is small, movements are best detected through evaluation of angular acceleration.

Angular acceleration is an acceleration gradient over displacement at a given instant in time, so the results of the linear acceleration are influenced by the angular acceleration. Thus, the differences in the vicinity of the Q_2 event between the multimodal aspect and the unimodal aspect of the tangential acceleration of the "estimated

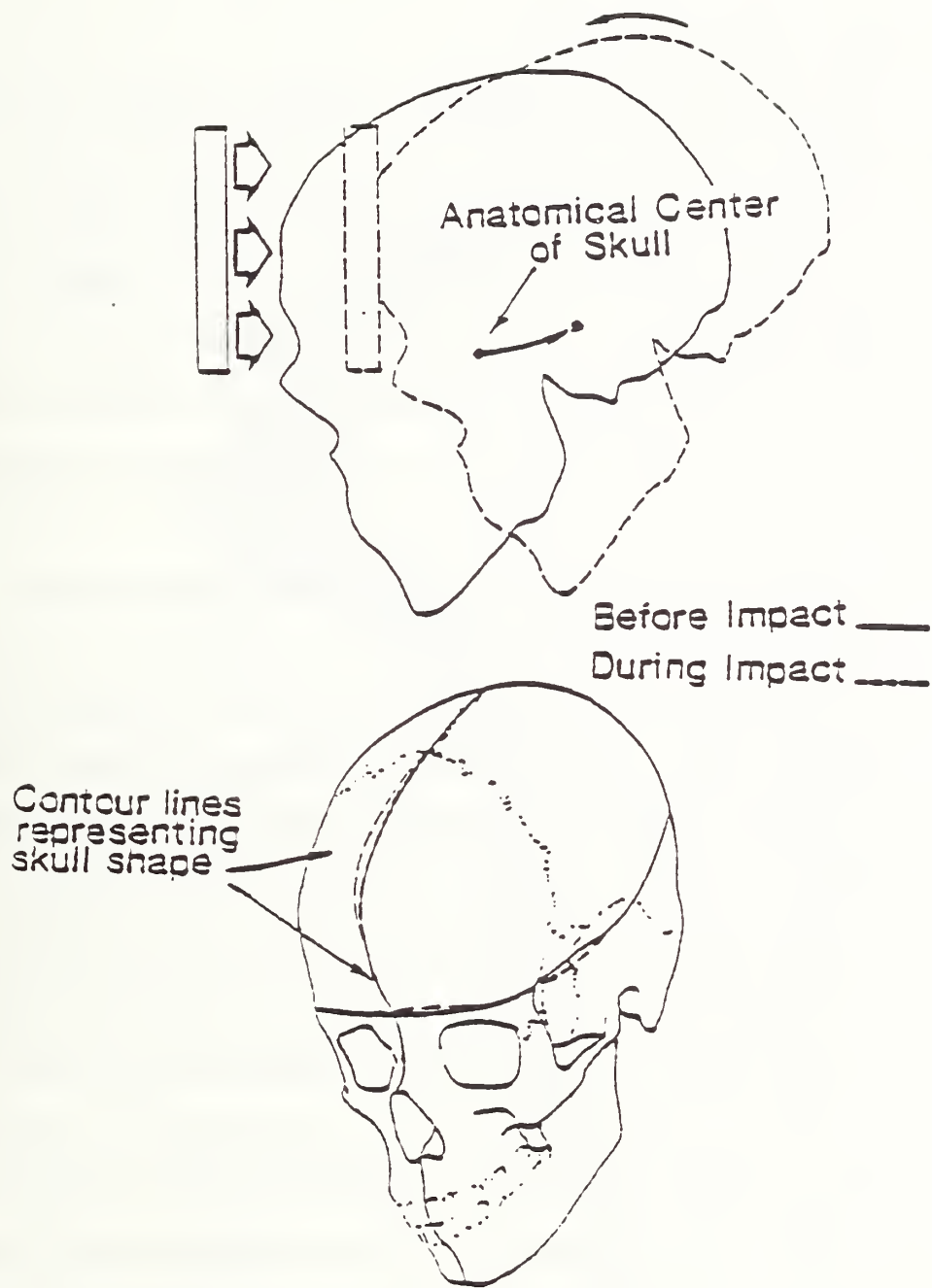


Figure 10

Effect of Skull Deformation on Angular Acceleration

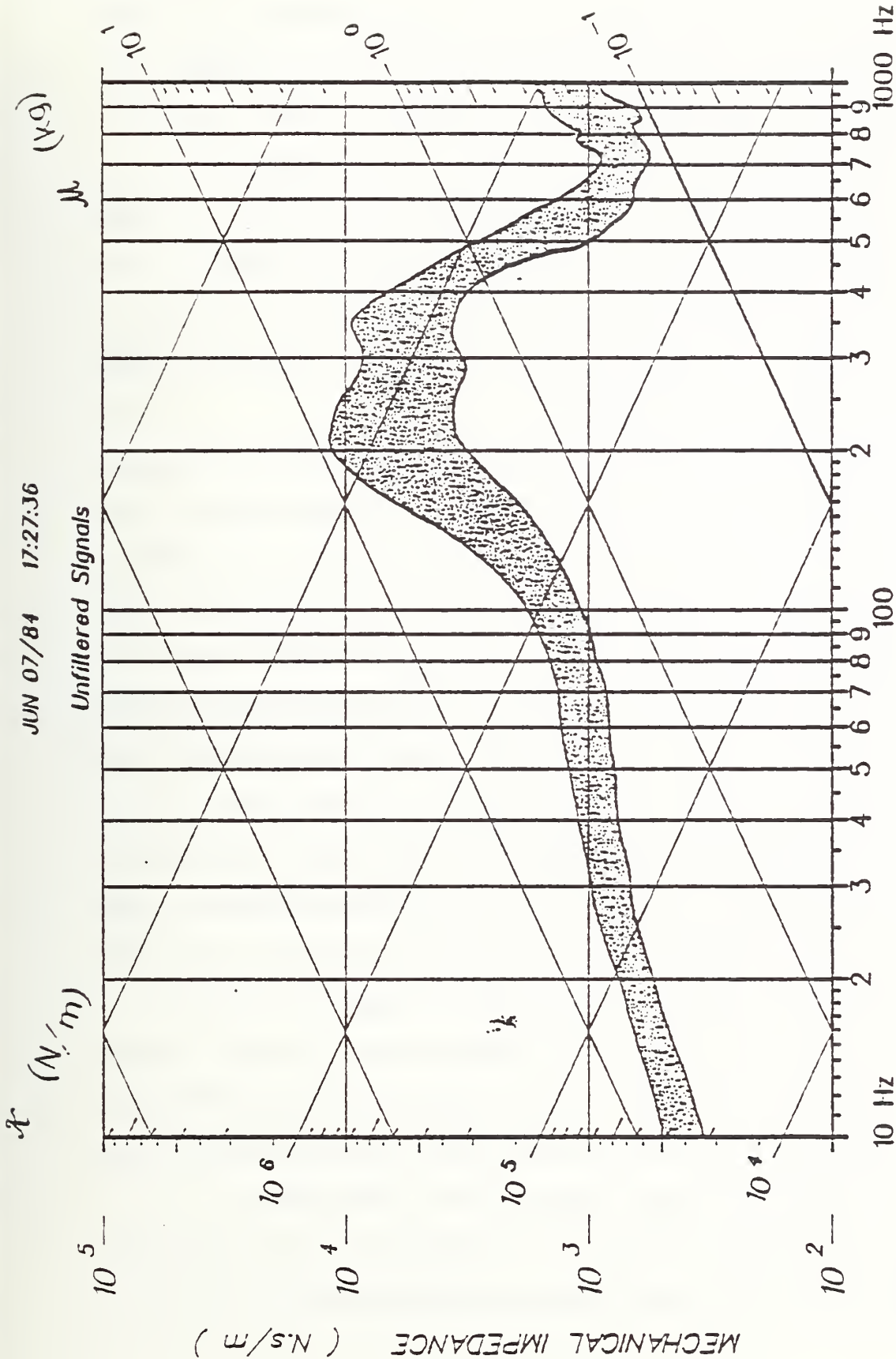
anatomical center" are a result of the acceleration gradient caused by the angular acceleration.

Figure 11 represents the mechanical impedance corridor of force and tangential acceleration for a test in which skull deformation was observed and no skull fracture occurred (82E021, 82E022, 82E041, 82E042, and 84E141). The impedance values for these impacts are similar to driving point impedance tests reported by other researchers [28, 64-65, 271, 308]. The skull deformation observed could be related to the same type of skull deformation obtained from the driving point impedance tests.

6.6 Kinematic Response After Impact: Effect of Soft Tissue -

Transmission of energy during intervals Q_1-Q_2 and Q_2-Q_3 was analyzed by comparing the acceleration response of the skull to the force time-history of the impactor. The following observations were made. During the Q_1-Q_2 interval, energy was transferred from the impactor to the skull and from the skull to the brain and neck. During the Q_2-Q_3 interval, significant energy was transferred from the brain and neck to the skull. Examination of all the tests show that during the Q_2-Q_3 interval, unless there were rapid changes in the binormal vector direction (large torsion and large B-rate), the normal acceleration was established by angular acceleration. In addition, the normal and binormal vectors were established first by the angular acceleration during the Q_2-Q_3 interval and then by the angular acceleration direction changes near the Q_3 event. In general, for those tests with multimodal/unimodal peaks, the angular acceleration direction changed near the Q_2 event. The extent and amount of rotation varied from test to test. This is probably a result of the complex three-dimensional motion of the

JUN 07/84 17:27:36



$Z=F1/V1$ for

Figure 11

Mechanical Impedance Corridor for Tangential Acceleration
Skull Deformation and No Skull Fracture

head during the Q_1-Q_2 interval as well as of the geometry of the head. The rotation tends to be between $\pi/2$ and π radians. The motion past the Q_3 event for multimodal tangential acceleration tests is similar to the unimodal tangential acceleration test. In other words, the trajectory traced by the "estimated anatomical center" and its attached frame field during multimodal tangential acceleration impacts is different from that traced during unimodal tangential acceleration impacts. However, the motion after impact is similar when the driving force is obviously not the impactor.

In past research [308] it has been determined that in the unpressurized or partially repressurized cadaver the response of the skull after impact is influenced by differential motion of the brain. In a similar manner, with the data presented here it appears that the brain was driving the skull and that this was manifested in both a linear and rotational manner. Potentially, energy had been transferred from the skull to the brain during impact, was stored as energy and then was released as the impact force dropped below a given level.

6.7 Pressure Time-History Response - The pressure time histories were separated into two significant types, unimodal and bimodal. The unimodal pressure pulses correlate well with short-duration (less than 15ms) large-valued (1500 m/s/s and greater) tangential accelerations. Bimodal pressure pulses were more commonly observed in longer duration and lower acceleration impacts. This result seems to be a consequence of the superposition of two different types of mechanisms for producing pressure changes in the head during and after blunt impact.

The first pressure mechanism is associated with impact force time-histories which contain short-duration loading of the skull on the

brain, and probably is primarily a result of inertial loading. When a blunt impact blow is delivered to the head, the skull is initially accelerated. Shortly afterwards, the brain compresses on the side closest to impact and is in tension on the side polarly distal to impact. The result is a pressure gradient in the brain encompassing the point of impact and including an area opposite from impact. Test 82E021 illustrates such pressures for selected impacts and shows that the highest magnitudes and positive pressures occur in the frontal lobe (epidural 1) and that negative pressures develop in the occipital lobe (epidural 3). Pressures in the parietal areas (epidural 2, epidural 4) are between the coup and counter coup areas. For most of these tests, the pressures in epidural 2 and epidural 4, correlated well, indicating that the pressure gradients were generally symmetric. However, some differences do exist which may be the result of three-dimensional motion of the head or of some asymmetry associated with the test subject. Figure 12 illustrates a cross- and auto-correlation between epidural 2 and epidural 4 for Tests 82E021 and 82E061 and shows that the auto-correlation for each pressure is similar to the cross-correlation, implying three-dimensional motion of the head or asymmetry of the subject. This is similar to results reported by others [312-317].

Figure 13 represents transfer functions between the force and the epidural 1 and epidural 2 pressures for Tests 82E021, 82E022, 82E041 and 82E042 in which skull deformation occurred without skull fracture. These transfer functions display a resonance in the area for which a resonance was predicted from the impedance transfer function for force and acceleration. This indicates that although the exact amount of the effect of skull deformation on the pressure response is not completely

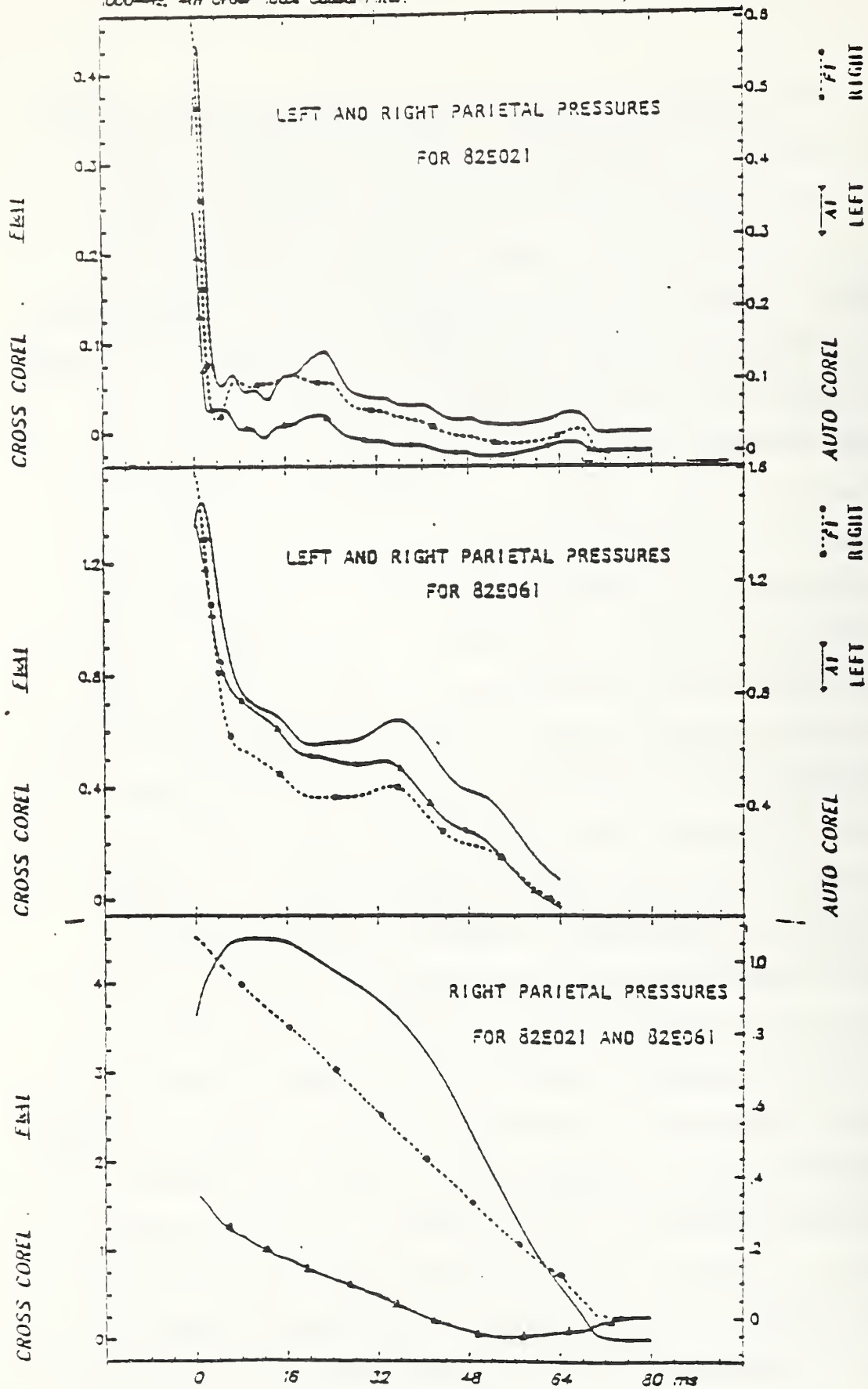
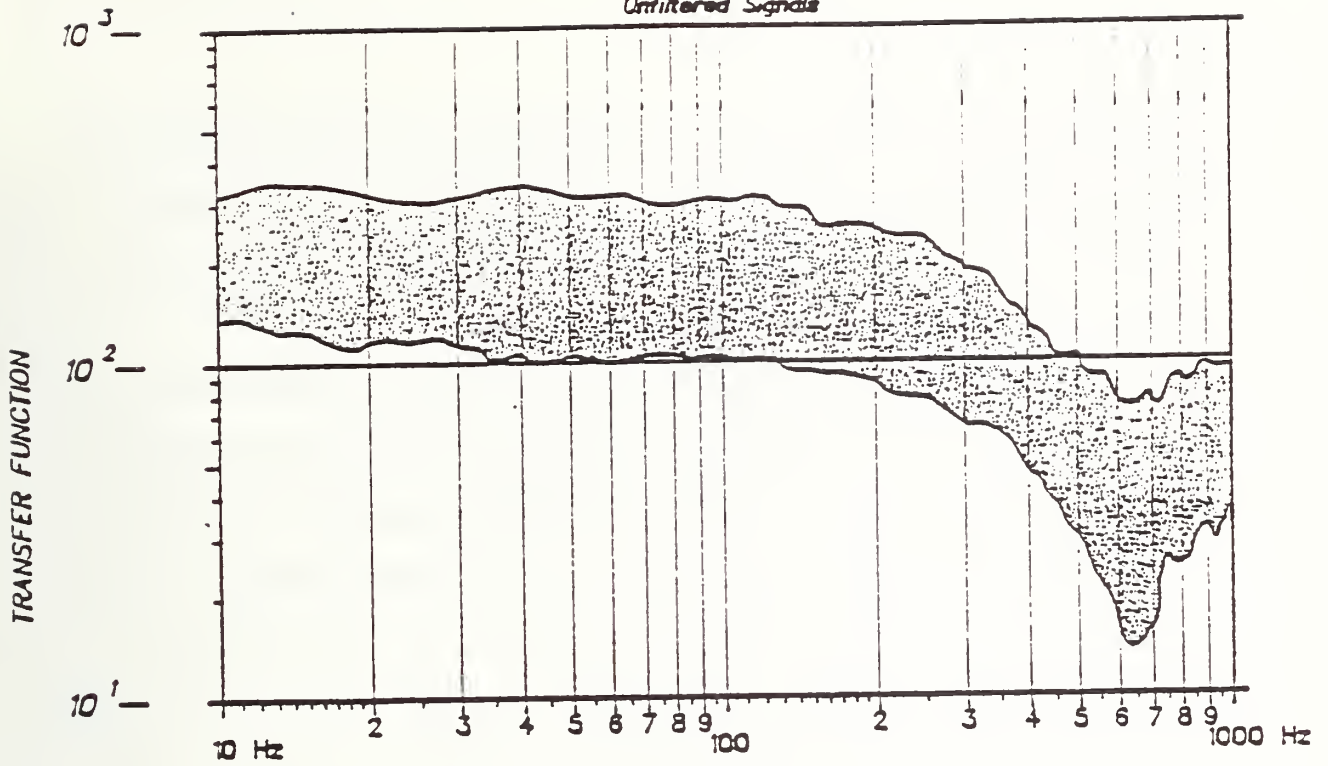
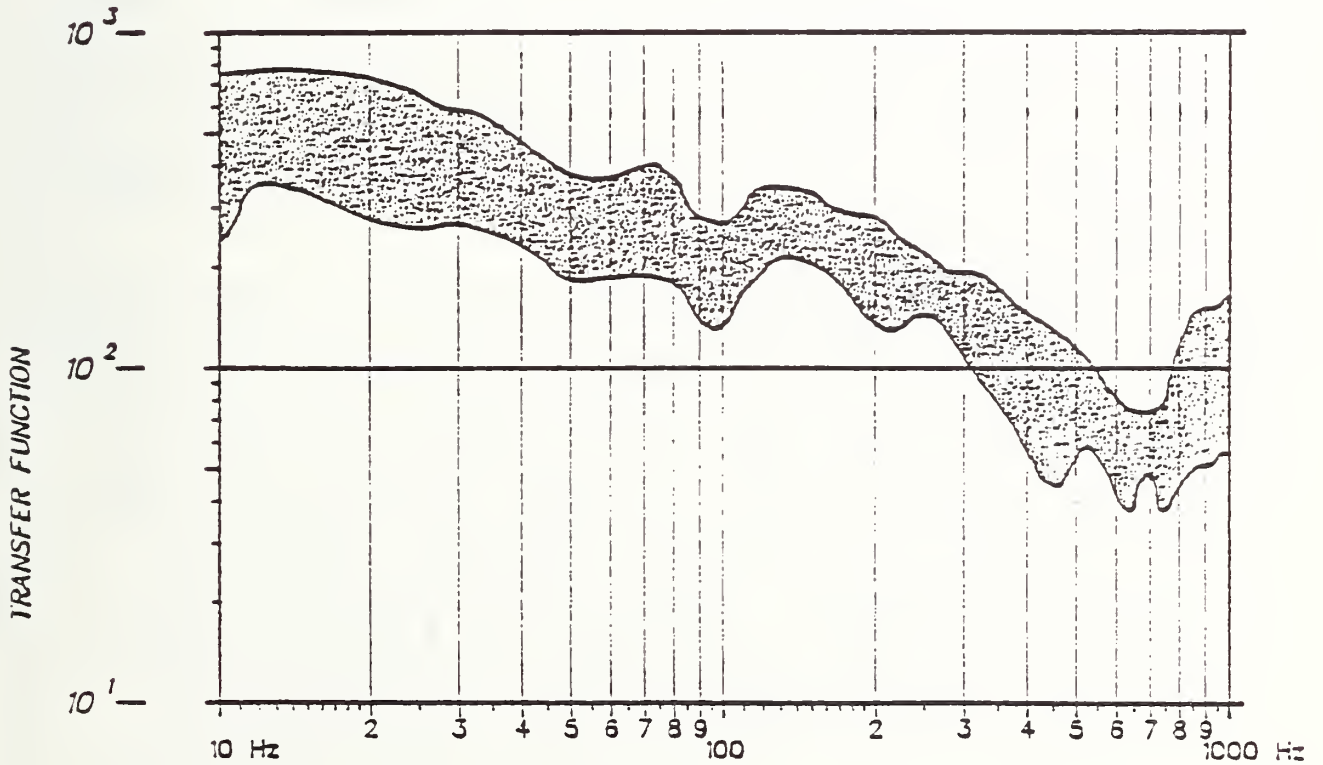


Figure 12

Unfiltered Signals



$X=F1/P1$ for EPI 1



$X=F1/P1$ for EPI 2

Figure 13

Transfer Functions between Force and Epidural 1 and Epidural 2 Pressures

determined, it has some effect which is observable in the pressure time-history. Therefore, a reasonable correlation might be found between pressure and acceleration, although such a correlation would depend on where the accelerometers are placed on the skull.

The second pressure mechanism is associated with impact force time-histories which contain low-frequency components of motion of the head after blunt impact. Unlike the first pressure mechanism which rarely produces pressure pulses longer than 15 ms, the second pressure mechanism produces pressure pulses that can last as long as 200 ms. Possibly, the second pressure mechanism is a result of the brain driving the skull as discussed earlier. Since the pressure is positive in all transducers regardless of location, the brain may be transferring energy to the skull; thus accelerating the skull. This is consistent with the results discussed earlier where the brain stores energy and releases it shortly afterwards in a manner that is manifested by skull angular acceleration. The results obtained from the high-speed cineradiograph support this hypothesis.

6.8 Injury/Damage Response - The results presented in Table 4 show that the most common brain injury/damage in the repressurized cadaver is subarachnoid hemorrhage. Damage occurs for repressurized cadavers in the frontal or parietal lobes of the cerebrum. Subarachnoid hemorrhage did not occur unless "significant skull deformation" had occurred.

Identifying mechanisms of head injury poses a formidable problem. In head impact response a number of potential injury mechanisms have been proposed [190-387]. It is believed that different mechanisms occur for direct head impact than for non-impact (inertial conditions). It is also possible that several mechanisms could be responsible for producing

the same injury/damage. The complex nature of the head/skull system under loading implies that during any given impact, several mechanisms could be occurring and that they may complement each other to produce injury/damage.

One possible mechanism for production of subarachnoid hemorrhage in the repressurized cadaver is induced differential motion between the skull-brain interface. Potentially, there are two types of differential motion of the skull with respect to the brain. One is associated with "local" movement of the skull differentially with respect to the brain. The second requires rotational differential motion of a "significantly large" section of the skull with respect to the brain. "Significant local acceleration" of any part of the skull may initiate differential motion of the brain surface with respect to the skull. However, because only a limited number of tests have been performed using techniques which make such observations possible, more work needs to be done before this hypothesis can be verified.

In repressurized cadaver tests, comparatively large pressure peaks were observed. It is possible that in those tests, high stress in the brain as well as skull deformations and angular accelerations were needed to produce the observed damage. In several tests, duplicate impacts were made to each subject. It is possible that this enhanced the damage response; and therefore the results presented here should not be used to set tolerance levels. However, it is believed that this did not affect the general trend of damage and/or injury response observed.

7.0 CONCLUSIONS - This was a limited study of some important kinematic factors and injury/damage modes associated with direct blunt head impact. Because of the complex nature of the skull-brain

interaction during an impact event, more work is necessary before these kinematic factors can be generalized to describe head impact response. However, the following conclusions can be made:

1. "Severe impacts" to the heads of repressurized cadavers can cause local motions in the skull with or without skull fracture. The motions are interpreted as angular acceleration by nine accelerometers mounted in a single array used to determine three-dimensional motion.

2. Skull deformation may cause direct and/or indirect subarachnoid hemorrhage.

3. Three-dimensional rigid body motion is not well defined in a "severe head impact" when using accelerometers located on the skull. The acceleration time histories, including the resultant acceleration used to calculate the Head Injury Criterion (HIC), of the anatomical center, depend not only on where the accelerometers have been placed on the skull but also on the biovariability of the test subject's skull.

4. Short duration impacts (less than 15 ms) in the anterior to posterior direction appear to involve two skull-brain interactions. One occurs during impact and is characterized by a transfer of energy from the skull to the brain, and a pressure gradient in the brain positive at the frontal bone and negative at the occipital bone. The second interaction occurs during and after impact and is characterized by energy transmission from the brain to the skull and positive pressure in the brain at the frontal, parietal, and occipital bones.

8.0 REFERENCES

INCIDENCE

1. Anderson, D.W.; Miller, J.D.; Kalsbeek, W.D. 1983. Findings from a Major Survey of Persons Hospitalized with Head Injuries. Public Health Reports 98(5):475-478.
2. Annegers, J.F.; Kurland, L.T. 1979. The Epidemiology of Central Nervous System Trauma. In: Guy L. Odom, ed., Central Nervous System Trauma Research Status Report, National Institute of Neurological and Communicative Disorders and Stroke, National Institutes of Health, U.S. Public Health Service, pp. 1-9.
3. Cooper, P.R. 1982. Epidemiology of Head Injury. In: Paul R. Cooper, ed., Head Injury, Baltimore: Williams and Wilkins, pp. 1-14.
4. Ewing, C.L. 1983. Preface. In: Channing L. Ewing, et al., eds. Impact Injury of the Head and Spine, Springfield, IL: Charles C. Thomas.
5. Gurdjian, S.; Gurdjian, E. 1980. Acute Head Injury: A Review. Surgery Annual 12:223-241.
6. Harris, B.S.H.; Kalsbeek, W.D.; McLaurin, R.L. 1981. The National Head and Spinal Cord Injury Survey: An Overview of the Study and Selected Findings Relative to Head Injury. In: DOT, NHTSA, Head and Neck Injury Criteria, Washington, D.C.
7. Newcombe, F. 1982. The Psychological Consequences of Closed Head Injury Assessment and Rehabilitation. Injury 14(2):111-136. September.
8. Insurance Institute for Highway Safety, 1982. The Year's Work 1981-1982. Washington, D.C.
9. Jones, J.J.; Jeffreys, R.V. 1983. Head Injury Patients Admitted to General Hospital in Murseyside. Injury 14(6):483-488.
10. Kraus, J.F., et al. 1984. The Incidence of Acute Brain Injury and Serious Impairment in a Defined Population. American Journal of Epidemiology 119(2):186-201.

CONCUSSION

11. Ashman, R.; Hull, E. 1941. Essentials of Electrocardiography. New York: The Macmillan Co.
12. Becker, W.H., et al. 1979. Head Injuries. Archives of Neurology 36:750-758.
13. Fernando, O.V.; Mariano, G.T., Gurdjian, E.S.; Hodgson, V.R. 1969. Electrocardiographic Patterns in Experimental Cerebral Concussion. Journal of Neurosurgery 31:34-40.

14. Gennarelli, T.A. 1983. Head Injury Lesion Analysis by CT Scan: Correlations to Neurological Variables and to Outcome. Final Report Contract No. DOT-HS-9-02088.
15. Gross, A.G. 1978. A New Theory on the Dynamics of Brain Concussion and Brain Injury. Journal of Neurosurgery, 15:548-561.
16. Gross, A.G. 1978. A New Theory on the Dynamics of Brain Concussion and Brain Injury. Journal of Neurosurgery 15:548-561.
- 16.6 Gross, A.G. 1958. Impact Thresholds of Brain Concussion. Journal of Aviation Medicine 29:275.
17. Gurdjian, E.S.; Webster, J.E.; Lissner, H.R. 1955. Observations on the Mechanism of Brain Concussion, Contusion and Laceration. Surgery, Gynecology and Obstetrics, 101:680-690.
18. Hersch, C. 1961. Electrocardiographic Changes in Head Injuries. Circulation 23:853, January-June .
19. Hodgson, V.R.; Thomas, L.M.; Khalil, T.B. 1983. The Role of Impact Location in Reversible Cerebral Concussion. In: 27th Stapp Car Crash Conference Proceedings, pp. 225-240.
20. Hodgson, V.R., et al. 1969. Advances in Understanding of Experimental Concussion Mechanisms. In: 13th Stapp Car Crash Conference Proceedings, pp. 18-37.
21. Jacobson, S.A.; Danufsky, P. 1954. Marked Electrocardiographic Changes Produced by Experimental Head Trauma. Journal of Neuropathology and Experimental Neurology 13:462.
22. Malinow, M.P. 1966. An Electrocardiographic Study of Macaca mulatta. Folia Primatologia 4:51.
23. Ommaya, A.K.; Gennarelli, T.A. 1974. Cerebral Concussion and Traumatic Unconsciousness. Brain 97:633-654.
24. Ommaya, A.K.; Hirsch, A.E.; Martinez, J.L. 1966. The Role of Whiplash in Cerebral Concussion. In: 10th Stapp Car Crash Conference Proceedings, pp. 314-324. SAE Paper No. 660804.
25. Ommaya, A.K., et al., 1970. Comparative Tolerances for Cerebral Concussion by Head Impact and Whiplash Injury in Primates. International Automobile Safety Conference Compendium, Society of Automotive Engineers, Detroit, May 13-15, pp. 808-817.
26. Plum, F.; Posner, J.B. 1980. The Diagnosis of Stupor and Coma, 2nd ed., Philadelphia: F. A. Davis.

27. Ommaya, A.K. 1966. Experimental Head Injury in the Monkey. In: William F. Caveness and A. Earl Walker, eds., Head Injury, Philadelphia: J.B. Lippincott, Co.
28. Ommaya, A.K.; Yarnell, P.; Hirsch, A.E.; Harris, E.H. 1967. Scaling of Experimental Data on Cerebral concussion in Subhuman Primates to Concussion Threshold in Man. In: 11th Stapp Car Crash Conference Proceedings, pp. 47-52.
29. Singh, R.; Chakravartii, R.N.; Chituttani, P.N.; Wahr, P.L. 1970. Electrocardiographic Studies in Rhesus Monkeys. Journal of Applied Physiology 28(3):346-349, March.
30. Walker, A.E.; Kollres, J.J.; Case, T.J. 1944. The Physiological Basis of Concussion. Journal of Neurosurgery 1:103.
31. Hubbard, R.P. 1971. Flexure of Cranial Sutures. Journal of Biomechanics 4(6):491-496, December.
32. Jones, R.M. 1975. Mechanics of Composite Materials, Scripta Book Co.

ANATOMY

33. Dean, M.R.E. 1975. Basic Anatomy and Physiology for Radiographers, 2nd ed., London: Blackwell Scientific Publications.
34. Heimer, L. 1983. The Human Brain and Spinal Cord Functional Neuroanatomy and Dissection Guide, New York: Springer-Verlag.
35. Schaeffer, D.P., ed., 1953. Morris' Human Anatomy, 11th ed., New York: McGraw-Hill.
36. Sinclair, D. 1975. An Introduction to Functional Anatomy, 5th ed., London: Blackwell Scientific Publications.

BIOMATERIAL PROPERTIES OF COMPONENTS OF THE HUMAN HEAD

37. Anderson, H.C. 1973. Calcium-Accumulating Vesicles in the Intercellular Matrix of Bone. Hard Tissue Growth, Repair and Remineralization.
38. Anderson, H.C.; Johnson, T.F. 1980. Matrix Vesicles and Mineralization. 4th International Workshop on Calcified Tissues, Kyriat, Anavim, Israel, 9-13 March.
39. Anderson, H.C.; Johnson, T.F. 1980. Matrix Vesicles in Osteomalacic Bone. Bone Third International Workshop on Bone Histomorphometry, 28 May to 2 June, Sun Valley, Idaho.
40. Barker, L.M. 1981. Compliance Calibration of a Family of Short Rod and Short Bar Fracture Toughness Specimens. TarraTek TR 81-07, Salt Lake City, February.

41. Barer, A.S., et al. 1982. Biomechanics of the Integumentary Tissues of the Human Head Upon In Vivo Dynamic Loading. 2. The Dynamics of Local Deformations of the Head upon Impact. Mechanics of Composite Materials 17(6):721-727, May.
42. Becker, E.B. 1972. Measurement of Mass Distribution Parameters of Anatomical Segments. In: 16th Stapp Car Crash Conference Proceedings. SAE Paper No. 720964.
43. Bergman, I.; Loxley, R. 1963. Two Improved and Simplified Methods for the Spectrophotometric Determination of Hydroxyproline. Anal. Chem. 35:1961-1965.
44. Cerquiglini, S., et al., editors, 1973. Biomechanics Proceedings, Krager Pub.
45. Cohnerty, H.; Briggs, A. 1966. A Determination of Serum Calcium by Means of Orthocresolphthalein Completion. Am. J. Clin. Pathol., 45:290.
46. Currey, J.D. 1969. The Mechanical Consequences of Variation in the Mineral Content of Bone. Journal of Biomechanics 2:1-11, January.
47. Engin, A.E. and Akkas, N. Application of a Fluid-Filled Spherical Sandwich Shell as a Biodynamic Head Injury Model for Primates. Aviation, Space and Env. Med., pp. 120-124, January.
48. Evans, F.G. 1973. Mechanical Properties of Bone. Springfield, IL: Charles C. Thomas.
49. Evans, F.G. 1961. Biomechanical Studies of the Musculo-Skeletal Systems. Springfield, IL: Charles C. Thomas.
50. Evans, F.G.; Lissner, H.R. 1957. Tensile and Comprehensive Strength of Human Parietal Bone. Journal of Applied Physiology 10:493-497.
51. Ewing, C.L., et al. 1976. The Effect of Duration, Rate of Onset and Peak Acceleration on the Dynamic Response of the Human Head and Neck. In: 20th Stapp Car Crash Conference Proceedings.
52. Fallenstein, G.T.; Hulce, V.D.; Melvin, J.W. 1969. Dynamic Mechanical Properties of Human Brain Tissue. Journal of Biomechanics 2(3):217-226.
53. Fan, W.R.S. 1971. Internal Head Injury Assessment. In: 15th Stapp Car Crash Conference Proceedings, 17-19 November, Coronado, Calif., pp. 645-665. New York: SAE Paper No. 710870.
54. Frankel, V.H.; Nordin, M., editors, 1980. Basic Biomechanics of the Skeletal System. Lea and Febiger, Pub.

55. Frankel, V.H.; Burstein, A.H. 1970. Orthopaedic Biomechanics, Lea and Febiger Publ.
56. Frost, H.M. 1979. Orthopaedic Biomechanics, Springfield, IL: Charles C. Thomas.
57. Frost, H.M. 1967. An Introduction to Biomechanics, Springfield, IL: Charles C. Thomas.
58. Fung, Y.C. 1980. Biomechanical Properties of Living Tissues, Springer-Verlag.
59. Fung, Y.C.; Perrone, N.; Aniliker, M. 1972 Biomechanics - Its Foundations and Objectives, Prentice-Hall.
60. Fung, Y.C. 1966. Biomechanics, Proceedings Symposium, ASME, NY.
61. Galford, J.E; McElhaney, J.H. 1970. A Viscoelastic Study of Scalp, Brain, and Dura, Journal of Biomechanics 3(2)211-222, March.
62. Galford, J.E., McElhaney, J.H. 1969. Some Viscoelastic Properties of Scalp, Brain, and Dura. New York: ASME Paper No. 69-BHF-7.
63. Got, C., et al. 1983. Morphological and Biomechanical Study of 146 Human Skulls Used in Experimental Impacts in Relation with the Observed Injuries. In: 27th Stapp Car Crash Conference Proceedings, pp. 241-250.
64. Gurdjian, E.S.; Hodgson, V.R.; Thomas, L.M.; Patrick, L.M. 1968. Significance of Relative Movements of Scalp, Skull, and Intracranial Contents During Impact Injury of the Head. Journal of Neurosurgery 29(1):70-72.
65. Gurdjian, E.S., et al. 1961. Intracranial Pressure and Acceleration Accompanying Head Impacts in Human Cadavers. Surgery, Gynecology, and Obstetrics 113:185-190.
66. Gurdjian, E.S.; Schawan, H.K. 1932. Management of Skull Fracture Involving the Frontal Sinus. Annals of Surgery 95:22-32.
67. Hardy, C.H.; Marcal, P.V. 1971. Elastic Analysis of a Skull. Technical Report No. 8, Office of Naval Research, Contract No. N00014-67-A-0191-0007, Div. of Engr., Brown University.
68. Hastings, G.W.; Williams, D.F. 1980. Mechanical Properties of Biomaterials, John Wiley and Son.
69. Hayashi, K., et al. 1980. Stiffness and Elastic Behavior of Human Intracranial and Extracranial Arteries. Journal of Biomechanics 13(2):175-184.

70. Hayes, W.C.; Carter, D.R. 1979. Biomechanics of Bone, Skeletal Research, Academic Press, pp. 263-300.
71. Hubbard, R.P.; McLeod, D.G. 1974. Definition and Development of a Crash Dummy Head. In: 18th Stapp Car Crash Conference Proceedings, pp. 599-628. SAE Paper No. 74-1193.
72. Hubbard, R.P. 1971. Flexure of Layered Cranial Bone. Journal of Biomechanics 4(4):251-263, July.
73. Hubbard, R.P. 1971. Flexure of Cranial Sutures. Journal of Biomechanics 4(6):491-496, Dec.
74. Hubbard, R.P. 1970. Flexure of Cranial Bone, Urbana: University of Illinois for the National Institute of Neurological Diseases and Stroke.
75. Jones, R.M. 1975. Mechanics of Composite Materials, Scripta Book Co.
76. Katz, J.L. 1980. Anisotropy of Young's Modulus of Bone. Nature 283:106-107.
77. Katz, J.L. 1971. Hard Tissue as a Composite Material - I Bounds on the Elastic Behavior. Journal of Biomechanics 4:455-473.
78. Khalil, T.B.; Smith, D.L.; Viano, D.C. 1978. Experimental Analysis of the Vibration Characteristics of the Human Skull. Publication No. GMR-2756, General Motors Research Laboratories, Warren, MI.
79. Kriewall, T.J., et al. 1981. Bending Properties and Ash Content of Fetal Cranial Bone. Journal of Biomechanics 4(2):73-79.
80. LeCount, E.R.; Appelnach, C.W. 1920. Pathologic Anatomy of Traumatic Fractures of Cranial Bones and Concomitant Brain Injuries. Journal of the American Medical Association 74:501-511.
81. Lee, S. 1981. A Model for Bone Hardness. Journal of Biomechanics 14(8):561-568.
82. Lubock, R.; Goldsmith, W. 1980. Experimental Study of Cavitation in a Model Head-Neck System. Journal of Biomechanics 13:1041-1052.
83. MacFarlane, T.W.R.; Roach, M.R.; Chan, K. 1980. The Geometry of Human Cerebral Bifurcations: Effect of Static Distending Pressure. Journal of Biomechanics 13(3):265-278.
84. McElhaney, J.H.; Fogel, J.L.; Melvin, J.W.; Haynes, R.R.; Roberts, V.L.; Alem, N.M. 1970. Mechanical Properties of Cranial Bone. Journal of Biomechanics 3(5):495-511.

85. McElhaney, J.H.; Melvin, J.W.; Roberts, V.L., Portnoy, H.D. 1973. Dynamic Characteristics of the Tissues of the Head. In: Perspectives in Biomedical Engineering, pp. 215-222. Symposium on Perspectives in Biomedical Engineering, June 1972, Glasgow. London: MacMillan Press.
86. McPherson, G.K.; Kriewall, T.J. 1980. The Elastic Modulus of Fetal Cranial Bone: A First Step Toward an Understanding of the Biomechanics of Fetal Head Molding, Journal of Biomechanics, 13:9-16, 17-26.
87. Melvin, J.W.; Fuller, P.M.; Barodawala, I.T. 1970. The Mechanical Properties of the Diploe Layer in the Human Skull. Society for Experimental Stress Analysis Spring Meeting, 19-22. May 1970, Huntsville, Alabama.
88. Melvin, J.W.; McElhaney, J.H.; Roberts, V.L. 1970. Development of a Mechanical Model of the Human Head - Determination of Tissue Properties and Synthetic Substitute Materials. In: 14th Stapp Car Crash Conference Proceedings, 17-18 November, Ann Arbor, MI., pp. 221-240. New York: SAE Paper No. 700903.
89. Merchant, H.C.; Crispino, A.J. 1974. A Dynamic Analysis of an Elastic Model of the Human Head. Journal of Biomechanics 7:219-228.
90. Metz, H., McElhaney, J.H.; Ommaya, A.K. 1970. A Comparison of the Elasticity of Live, Dead, and Fixed Brain Tissue. Journal of Biomechanics 3(4):453-458.
91. Nahum, A.M.; Smith, R.; Raasch, F.; Ward, C.C. 1979. Intracranial Pressure Relationships in the Protected and Unprotected Head. In: 23rd Stapp Car Crash Conference Proceedings, 17-19 October, San Diego, Calif., pp. 615-636. SAE Paper No. 791024.
92. Nusholtz, G.S.; Axelrod, J.B.; Melvin, J.W.; Ward, C.C. 1979. Comparison of Epidural Pressure in Live Anesthetized and Post Mortem Primates. In: 7th International Workshop on Human Subjects for Biomechanical Research Proceedings, 16 October 1979, Coronado, Calif., pp. 175-200. Washington, D.C.: Distributed by the National Highway Traffic Safety Administration.
93. Patrick, L.M.; Levine, R.S. 1975. Injury to Unembalmed Belted Cadavers in Simulated Collisions. In: 19th Stapp Car Crash Conference Proceedings, 17-19 November, San Diego, pp. 79-115. SAE Paper No. 751144.
94. Piekarski, K. 1970. Fracture of Bone. Journal of Applied Physics 41:215-223.
95. Rhea, J.T. 1980. The Disappearing Ellipse: A New Sign of a Linear Skull Fracture. Journal of Trauma 20(4):327-328, April.

96. Robbins, D.H. 1980. Impact Head Injury Data Base. Ann Arbor: University of Michigan Highway Safety Research Institute for the National Institute for Occupational Safety and Health.
97. Rowbotham, G.F. 1942. Acute Injuries of the Head. Baltimore: Williams and Wilkins Co.
98. Stalnaker, R.L.; Melvin, J.W.; Nusholtz, G.S.; Alem, N.M.; Benson, J.B. 1977. Head Impact Response. In: 21st Stapp Car Crash Conference Proceedings.
99. Stalnaker, R.L.; Mohan, D.; Melvin, J.W. 1975. Head Injury Evaluation: Criteria for Assessment of Field, Clinical and Laboratory Data. In: 19th Conference of the American Association for Automotive Medicine Proceedings, 20-22 November, San Diego, pp. 168-178. Morton Grove, IL: AAAM.
100. Stone, J.L.; Beaupre, G.S.; Hayes, W.C. 1983. Multiaxial Strength Characteristics of Trabecular Bone. Journal of Biomechanics 16(9):743-752.
101. Tarriere, C.; Sapin, C. 1969. Biokinetic Study of the Head to Thorax Linkage. In: 13th Stapp Car Crash Conference Proceedings, 2-4 December, Boston, pp. 365-380. New York: SAE Paper No. 690815.
102. Thomas, D.J. 1972. Specialized Anthropometry Requirements for Protective Equipment Evaluation. In: Current Status in Aerospace Medicine, pp. C9-1-C9-8. Aerospace Medical Panel Specialist Meeting, 7-8 September 1972, Glasgow, Scotland. Paris: AGARD Conference Proceedings, No. 110, 1973.
103. U. S. National Center for Health Statistics. 1970. Skinfolds, Body Girths, Bio-cranial Diameter, and Selected Anthropometric Indices of Adults: United States, 1960-1962. Washington, D.C.: NCHS Series II, No. 35.
104. Walker, L.B., et al. 1973. Mass, Volume, Center of Mass, and Mass Moment of Inertia of Head and Head and Neck of Human Body. In: 17th Stapp Car Crash Conference Proceedings, pp. 525-537.
105. Ward, C.C.; Nahum, A. 1979. Correlation Between Brain Injury and Intracranial Pressures in Experimental Head Impact. Presented at the International Conference on Impact Trauma, Gotenberg, Sweden, September 1979 and published in proceedings. Navy Report TM No. 51-79-15.
106. Ward, C.C.; Nikravesh, P.E.; Thompson, R.B. 1978. Biodynamic Finite Element Models Used in Brain Injury Research. Journal of Aviation, Space and Environmental Medicine 49(1).

107. Ward, C.C.; Thompson, R.B. 1972. The Development of a Detailed Finite Element Brain Model. In: 19th Stapp Car Crash Conference Proceedings, 17-19 November, San Diego, pp. 641-674. SAE Paper No. 751163.
108. Weng, G.J.; Sun, C.T. 1979. Effects of Fiber Length on Elastic Moduli of Randomly-Oriented Chopped-Fiber Composites. ASTM, STP-674, pp. 149-162.
109. Wood, J.L. 1971. Dynamic Response of Human Cranial Bone. Journal of Biomechanics 4:1-12.
110. Yamada, H. 1970. Strength of Biological Materials, Baltimore: The Williams and Wilkins Co.

SEVERITY INDICES

111. American Association of Automotive Medicine, 1980. AIS-80: The Abbreviated Injury Scale 1980 Revision, Park Ridge, IL.
112. Bittner, A.C.; Shortall, III, J.P.; Harbeson, M. 1983. Effects of Head Impact Acceleration on Human Performance: Overview and Preliminary Battery Identification, Naval Biodynamics Laboratory, New Orleans, LA, NBDL-83R004, May.
113. Brinn, J.; Staffeld, S.E. 1970. Evaluation of Impact Test Accelerations: A Damage Index for the Head and Torso (EDI). In: 14th Stapp Car Crash Conference Proceedings, 17-18 November 1970, Ann Arbor, MI, pp. 188-220, NY: SAE Paper No. 700902.
114. Bull, J.P. 1982. Injury Severity Scoring Systems, Injury 14:2-6, July.
115. Eiband, A.M. 1959. Human Tolerance to Rapidly Applied Accelerations: A Summary of the Literature. Cleveland: NASA Lewis Research Center, NASA Memorandum 5-19-59E.
116. Fan, W.R.S. 1971. Internal Head Injury Assessment. In: 15th Stapp Car Crash Conference Proceedings, 17-19 November 1971 Coronado, CA, pp. 645-665. NY: SAE Paper No. 710870.
117. Hess, R.L.; Weber, K.; Melvin, J.W. 1980. Review of Literature and Regulation Relating to Head Impact Tolerance and Injury Criteria, University of Michigan: Transportation Research Institute, UM-HSRI-80-52-1, July.
118. Gadd, C.W. 1962. Criteria for Injury Potential. In: Impact Acceleration Stress Symposium, 27-29 November 1961, Brooks AFB, Texas, pp. 141-144, Washington, D.C.: National Academy of Sciences--National Research Council Publication No. 977.

119. Gadd, C.W. 1967. Use of a Weighted Impulse Criterion for Estimating Injury Hazard. In: 10th Stapp Car Crash Conference Proceedings, 8-9 November 1966, Alamogordo, NM, pp. 164-174. NY: SAE Paper No. 660793.
120. Gadd, C.W. 1971. Tolerable Severity Index in Whole-Head, Non-Mechanical Impact. In: 15th Stapp Car Crash Conference Proceedings, pp. 809-816. New York: SAE.
121. Gennarelli, T. 1980. Analysis of Head Injury Severity by AIS-80. Proceedings of American Association for Automotive Medicine, Rochester, NY.
122. Gennarelli, T.A. 1983. Head Injury Lesion Analysis by CT Scan: Correlations to Neurological Variables and to Outcome. Final Report Contract #DOT-HS-9-02088.
123. Harris, B.S.H.; Kalsbeek, W.D.; McLaurin, R.L. 1981. The National Head and Spinal Cord Injury Survey: An Overview of the Study and Selected Findings Relative to Head Injury. In: DOT, NHTSA, Head and Neck Injury Criteria, Washington, D.C.
124. Hodgson, V.R.; Thomas, L.M. 1971. Comparison of Head Acceleration Injury Indices in Cadaver Skull Fracture. In: 15th Stapp Car Crash Conference Proceedings, pp. 190-206.
125. Hodgson, V.R., et al. 1970. Testing the Validity and Limitations of the Severity Index. In: 14th Stapp Car Crash Conference Proceedings, pp. 169-187.
126. Lissner, H.R.; Lebow, M.; Evans, F.G. 1960. Experimental Studies on the Relation Between Acceleration and Intracranial Pressure Changes in Man. Surgery, Gynecology and Obstetrics, 111:329-338.
127. Patrick, L.M.; Lissner, H.R.; Gurdjian, E.S. 1965. Survival by Design--Head Protection. In: 7th Stapp Car Crash Conference Proceedings, 11-13 November 1963, Los Angeles, pp. 483-499. Springfield, Il: Charles C. Thomas.
128. Newman, J.A. 1975. On the Use of the Head Injury Criterion (HIC) in Protective Headgear Evaluation. In: 19th Stapp Car Crash Conference Proceedings, pp. 615-640.
129. Scott, W.F. 1981. Epidemiology of Head and Neck Trauma in Victims of Motor Vehicle Accidents. In: DOT, NHTSA, Head and Neck Injury Criteria, Washington, D.C.
130. Slattenschek, A.; Tauffkirchen, W. 1970. Critical Evaluation of Assessment Methods for Head Impact Applied in Appraisal of Brain Injury Hazard, in Particular Head Impact on Windshields. In: 1970 International Automobile Safety Conference Compendium 13-15 May 1970 Detroit; 8-11 June 1970 Brussels, pp. 1084-1112. NY: SAE Paper No. 700426.

131. Stalnaker, R.L.; McElhaney, J.H. 1970. Head Injury Tolerance for Linear Impacts by Mechanical Impedance Methods. Am. Soc. Mech. Eng. Winter Annual Meeting 29 November-3 December 1970, NY. SAE Paper No. 70-WA/BHF-4.
132. Stalnaker, R.L.; McElhaney, J.H.; Roberts, V.L. 1971. MSC Tolerance Curve for Head Impacts, NY: ASME Paper No. 71-WA/BHF-10.
133. States, J.D. 1980. The Abbreviated and Comprehensive Injury Scales, Arlington Heights, Il: American Association of Medicine.
134. Teasdale, G.; Jennet, B. 1974. Assessment of Coma and Impaired Consciousness: A Practical Scale (GCS), Lancet 2:81-83.
135. Trunkey, D.D., et al. 1983. Panel: Current Status of Trauma Severity Indices, The Journal of Trauma 23(3):185-201, March.
136. Versace, J. 1971. A Review of the Severity Index. In: 15th Stapp Car Crash Conference Proceedings, 17-19 November 1971, Coronado, Ca, pp. 771-796. NY: SAE Paper No. 710881.
137. U.S. Department of Health. 1980. The International Classification of Diseases, 2nd ed., Vol. 1. Tabular List, Sept., PHS 80-1260.

REGULATION

138. Brinn, J.; Staffeld, S.E. 1970. Evaluation of Impact Test Accelerations: A Damage index for the Head and Torso. In: 14th Stapp Car Crash Conference Proceedings, 17-18 November, Ann Arbor, MI, pp. 188-220. New York: SAE Paper No. 700902.
139. Gadd, C.W. 1971. Tolerable Severity Index in Whole-Head, Nonmechanical Impact. In: 15th Stapp Car Crash Conference Proceedings, 17-19 November, Coronado, Calif., pp. 809-816. New York: Society of Automotive Engineers.
140. Gadd, C.W. 1967. Use of a Weighted Impulse Criterion for Estimating Injury Hazard. In: 10th Stapp Car Crash Conference Proceedings, 8-9 November, Alamogordo, New Mexico, pp. 164-174. New York: SAE Paper No. 660793.
141. Gadd, C.W. 1962. Criteria for Injury Potential. In: Impact Acceleration Stress Symposium, 27-29 November 1961. Brooks, AFB, Texas, pp. 141-144. Washington, D.C.: National Academy of Sciences - National Research Council Publication No. 977.
142. Gurdjian, E.S.; Roberts, V.L.; Thomas, L.M. 1966. Tolerance Curves of Acceleration and Intracranial Pressure Protective Index in Experimental Head Injury. Journal of Trauma 6(5):600-604.

143. Hess, R.L.; Weber, K.; Melvin, J.W. 1980. Review of Literature and Regulation Relating to Head Impact Tolerance and Injury Criteria, UM-HSRI-80-52-1, July.
144. Hodgson, V.R.; Thomas, L.M. 1971. Comparison of Head Acceleration Injury Indices in Cadaver Skull Fracture. In: 15th Stapp Car Crash Conference Proceedings, 17-19 November, Coronado, Calif., pp. 190-206. New York: SAE Paper No. 710854.
145. Hodgson, V.R.; Thomas, L.M.; Prasad, P. 1970. Testing the Validity and Limitations of the Severity Index. In: 14th Stapp Car Crash Conference Proceedings, 17-18 November, Ann Arbor, MI., pp. 167-187. New York: SAE Paper No. 700901.
146. Lissner, H.R.; Lebow, M.; Evans, F.G. 1960. Experimental Studies on the Relation Between Acceleration and Intracranial Pressure Changes in Man. Surgery, Gynecology, and Obstetrics 111:329-338. 1980. Introduces Wayne State Tolerance Curve (WSTC).
147. Patrick, L.M.; Lissner, H.R.; Gurdjian, E.S. 1965. Survival by Design-Head Protection. In: 7th Stapp Car Crash Conference Proceedings, 11-13 November, Los Angeles, pp. 483-499. Springfield, IL: Charles C. Thomas. Modifies WSTC.
148. Robbins, D.H. and Roberts, V.L. 1971. Michigan Injury Criteria Hypothesis and Restraint System Effectiveness Index. In: 15th Stapp Car Crash Conference Proceedings, 17-19 November, Coronado, Calif., pp. 686-709. New York: SAE Paper No. 710872.
149. Slattencheck, A.; Tauffkirchen, W.; Benedikter, G. 1971. The Quantification of Internal Head Injury by Means of the Phantom Head and the Impact Assessment Methods. In: 15th Stapp Car Crash Conference Proceedings, 17-19 November, Coronado, Calif., pp. 742-766. New York: SAE Paper No. 710879.
150. Slattencheck, A.; Tauffkirchen, W. 1970. Critical Evaluation of Assessment Methods for Head Impact Applied in Appraisal of Brain Injury Hazard, in Particular on Head Impact on Windshields. In: 1970 International Automobile Safety Conference Compendium, 13-15 May 1970, Detroit; 8-11 June 1970, Brussels, pp. 1084-1112. New York: SAE Paper No. 700426.
151. U.S. National Highway Traffic Safety Administration. 1972. Head Injury Criterion for Federal Motor Vehicle Safety Standard No. 208, Washington, D.C.: NHTSA. Supplement to '37 FR 5507.
152. Versace, S. 1971. A Review of the Severity Index. In: 15th Stapp Car Crash Conference Proceedings, 17-19 November, Coronado, Calif., pp. 771-796. New York: SAE Paper No. 710881.

CADAVER SUBJECTS

153. Got, C., et al. 1978. Results of Experimental Head Impacts on Cadavers: The Various Data Obtained and Their Relations to Some Measured Physical Properties. In: 22nd Stapp Car Crash Conference Proceedings, pp. 55-99.
154. Hodgson, V.R. et al. 1970. Fracture Behavior of the Skull Frontal Bone Against Cylindrical Surfaces. In: 14th Stapp Car Crash Conference Proceedings, pp. 241-355.
155. Hodgson, V.R.; Patrick, L.M. 1968. Dynamic Response of the Human Cadaver Head Compared to a Simple Mathematical Model. In: 12th Stapp Car Crash Conference Proceedings, pp. 280-301.
156. Lingren, S.O. 1966. Experimental Studies of Mechanical Effects in Head Injury. Acta Chirurgica Scandanavia, Suppl. 360.
157. Nahum, A., et al. 1980. Experimental Studies of Side Impact to the Human Head. In: 24th Stapp Car Crash Conference Proceedings, pp. 45-62, 161-185.
158. Nahum, A.M., et al. 1968. Impact Tolerance of the Skull and Face. In: 12th Stapp Car Crash Conference Proceedings, pp. 301-316.
159. Patrick, L.M., et al. 1967. Cadaver Knee, Chest and Head Impact Loads. In: 11th Stapp Car Crash Conference Proceedings, pp. 106-117.
160. Schneider, D.C.; Nahum, A.M. 1972. Impact Studies of Facial Bones and Skull. In: 16th Stapp Car Crash Conference Proceedings, pp. 186-203.

NON-HUMAN PRIMATE SUBJECTS

161. Abel, J.M., et al. 1978. Incidence and Severity of Cerebral Concussion in the Rhesus Monkey Following Sagittal Plane Angular Acceleration. In: 22nd Stapp Car Crash Conference Proceedings, pp. 33-53.
162. Atluri, S.; Kobayashi, A.S.; Cheng, J.S. 1975. Brain Tissue Fragility - A Finite Strain Analysis by Hybrid Finite-Element Method. Journal of Applied Mechanics:269-273. June.
163. Brinn, J.; Staffeld, S.E. 1970. Evaluation of Impact Test Accelerations. In: 14th Stapp Car Crash Conference Proceedings, pp. 188-207.
164. Brown, G.W.; Brown, M.L. 1954. Cardiovascular Response to Experimental Cerebral Concussion in the Rhesus Monkey: Discussion of Similarity of Responses to Electroconvulsive Shock and Cerebral Concussion in Dogs, Monkeys, and Man. A.M.A. Arch. Neurol. Psychiat. 71:707-713.

165. Douglass, J.M., et al. 1968. Applications of Experimental Head Injury Research. In: 12th Stapp Car Crash Conference Proceedings, pp. 317-337.
166. Flexner, L.B.; Weed, L.H. 1983. Note on Cerebrospinal Elasticity in a Chimpanzee. Am. J. Physiol. 105:571-573.
167. Hashizume, K. 1972. A Study of the Experimental Brain Injury. Brain and Nerve 14:991-1002.
168. Miller, J.D.; Becker, D.P.; Ward, J.D., et al. 1977. Significance of Intracranial Hypertension in Severe Head Injury. Journal of Neurosurgery 47:503-516.
169. Nusholtz, G.S., et al. 1979. Head Impact Response Comparisons of Human Surrogates. In: 23rd Stapp Car Crash Conference Proceedings, pp. 499-541.
170. Ommaya, A.K., et al. 1967. Scaling of Experimental Data on Cerebral Concussion in Sub-Human Primates to Concussion Threshold for Man. In: 11th Stapp Car Crash Conference Proceedings, pp. 45-52.
171. Ono, I., et al. 1980. Human Head Tolerance to Sagittal Impact Reliable Estimation Deduced from Experimental Head Injury Using Subhuman Primates and Human Cadaver Skulls. In: 24th Stapp Car Crash Conference Proceedings, pp. 101-160.
172. Portnoy, H.D., et al. 1970. Intracranial Pressure and Head Acceleration During Whiplash. In: 14th Stapp Car Crash Conference Proceedings, Paper No. 700-900, pp. 152-168.
173. Saczalski, K.J. 1976. A Critical Assessment of the Use of Non-Human Surrogates for Safety System Evaluation. In: 20th Stapp Car Crash Conference Proceedings, pp. 159-187.
174. Symon, L. 1967. A Comparative Study of Middle Cerebral Pressure in Dogs and Macaques. Journal of Physiol. 191:449-465.
175. Unterharnscheidt, F.; Higgins, L.S. 1969. Traumatic Lesions of Brain and Spinal Cord Due to Nondeforming Angular Acceleration of the Head. Texas Reports on Biol. and Med. 27:127-166.
176. Weed, L.H.; Flexner, L.B. 1932. Cerebrospinal Elasticity in the Cat and Macaque. Am. J. Physiol. 101:668-677.

ANTHROPOMORPHIC DEVICE SUBJECT (DUMMIES)

177. Hertzberg, H.T.E. 1969. The Anthropology of Anthropomorphic Dummies. In: 13th Stapp Car Crash Conference Proceedings, pp. 201-214.

178. Higgins, L.S.; Schmall, R.A. 1967. A Device for the Investigation of Head Injury Effected by Non-Deforming Head Accelerations. In: 11th Stapp Car Crash Conference Proceedings, pp. 35-46.
179. Hubbard, R.P.; McCleod, D.G. 1974. Definition and Development of a Crash Dummy Head. In: 18th Stapp Car Crash Conference Proceedings, pp. 599-628. SAE Paper No. 74-1193.
180. McElhaney, J.H., et al. 1973. A New Crash Test Device - "Repeatable Pete." In: 17th Stapp Car Crash Conference Proceedings, pp. 467-507.
181. Melvin, J.W., et al. 1970. Development of a Mechanical Model of the Human Head - Determination of Tissue Properties and Synthetic Substitute Materials. In: 14th Stapp Car Crash Conference Proceedings, pp. 221-240.
182. von Gierke, I.H.E. 1978. Technical Evaluation Report, Models and Analogues for the Evaluation of Human Biodynamic Response, Performance and Protection. AGARD Conference Proceedings, No. 253, viii-A3-4.

MODELS

183. Belytschko, T.; Privitzer, E. 1978. Refinement and Validation of a Three-Dimensional Head-Spine Model, AMRL-TR-78-7. Aerospace Medical Research Lab., Wright-Patterson Air Force Base, Ohio. August.
184. Hodgson, V.R., et al. 1972. Head Model for Impact. In: 16th Stapp Car Crash Conference Proceedings, pp. 1-13.
185. Hosey, R.R.; Liu, Y.K. 1982. A Homeomorphic Finite Element Model of the Human Head and Neck. In: Finite Elements in Biomechanics, R. H. Gallagher, pp. 379-401.
186. Kaleps, I. 1980. Models and Analogs for the Evaluation of Human Biodynamic Response, Performance and Protection. AGARD Proceedings, no. 253, PP. 1-13.
187. Khalil, T.B.; Viano, D.C. 1982. Critical Issues in Finite Element Modeling of Head Impact. In: 26th Stapp Car Crash Conference Proceedings, Ann Arbor, MI, October 20-21, pp. 87-102, SAE Paper No. 821150.
188. Melvin, J.W., et al. 1970. Development of a Mechanical Model of the Human Head - Determination of Tissue Properties and Synthetic Substitute Materials. In: 14th Stapp Car Crash Conference Proceedings, pp. 221-240.
189. Ward, C.C.; Thompson, R.B. 1975. The Development of a Detailed Finite Element Brain Model. In: 19th Stapp Car Crash Conference Proceedings, pp. 641-674.

MECHANISM OF HEAD INJURY

190. Abel, J.M.; Gennarelli, T.A.; Segawa, H. 1978. Incidence and Severity of Cerebral Concussion in the Rhesus Monkey Following Sagittal Plane Angular Acceleration. In: 22nd Stapp Car Crash Conference Proceedings, 24-26 October 1978, Ann Arbor, MI, Warrendale, PA: SAE Paper No. 780886, pp. 35-53.
191. Adams, J.H., et al. 1981. Acceleration Induced Head Injury in the Monkey. II Neuropathology Acta Neuropathol. (Berl.) Suppl. VII, pp. 26-28.
192. Aldman, B.; Thorngren, L.; Ljung, C. 1981. Patterns of Deformation in Brain Models Under Rotational Motion. In: DOT, NHTSA, Head and Neck Injury Criteria, Washington, D.C.
193. Alem, N.M. 1974. Simulation of Head Injury Due to Combined Rotation and Translation of the Brain. In: 18th Stapp Car Crash Conference Proceedings, pp. 579.
194. Becker, E.B. 1973. Preliminary Discussion of an Approach to Modeling Living Human and Neck Response to $-G_x$ Impact Acceleration. In: Human Impact Response Measurement and Simulation. Proceedings of the Symposium on Human Impact Response, 2-3 October 1972, Warren, MI: New York: Plenum Press, pp. 321-329.
195. Belytschko, T.; Privitzer, E. 1978. Refinement and Validation of a Three-Dimensional Head-Spine Model, AMRL-TR-78-7. Aerospace Medical Research Lab, Wright-Patterson Air Force Base, Ohio, August.
196. Berger, M.D.; Weiss, M.S. 1983. Effects of Impact Somatosensory Evoked Potentials. In: C.L. Ewing, et al., eds., Impact Injury of the Head and Spine, Springfield, IL: Thomas, pp. 324-328.
197. Bittner, A.C.; Shortal, J.P., III; Harbeson, M. 1983. Effects of Head Impact Acceleration on Human Performance: Overview and Preliminary Battery Identification, Naval Biodynamics Laboratory, New Orleans, LA, NBDL-83R004, May.
198. Brinn, J.; Staffield, S.E. 1970. Evaluation of Impact Test Accelerations. In: 14th Stapp Car Crash Conference Proceedings, pp. 188-207.
199. Chan, M.; Ward, C. 1981. Relative Importance of Skull Deformation. Proceedings ASME. Biomechanics Symposium, June 22-24.
230. Chan, H.S. 1974. Mathematical Model for Closed Head Impact. In: 18th Stapp Car Crash Conference Proceedings, pp. 557-578. SAE Paper No. 741191.

201. Douglas, J.M., et al. 1968. Applications of Experimental Head Injury Research. In: 12th Stapp Car Crash Conference Proceedings, pp. 317-337.
202. Engin, A.E. 1969. Axisymmetric Response of a Fluid-filled Spherical Shell to a Local Radial Impulse--A Model for Head Injury. Journal of Biomechanics 2(3):325-341.
203. Engin, A.E.; Liu, Y.K. 1970. The Axisymmetric Response of a Closed Fluid-filled Spherical Shell in Free Vibrations. Journal of Biomechanics 3(1):11-22.
204. Engin, A.E.; Roberts, V.L. 1971. A Mathematical Model for the Behavior of the Brain When the Human Head is Subjected to Impulsive Loads. Symposium on Biodynamic Models and Their Applications, 26-28 October 1970, Aerospace Medical Research Laboratory, Wright-Patterson Air Force Base, Ohio, pp. 877-905.
205. Engin, A.E.; Akkas, N. 1978. Application of a Fluid-Filled Spherical Sandwich Shell as a Biodynamic Head Injury Model for Primates. Aviation, Space and Environmental Medicine, pp. 120-124.
206. Evans, F.G.; Lissner, H.R.; Lebow, M. 1958. The Relation of Energy, Velocity and Acceleration to Skull Deformation and Fracture. Surgery, Gynecology and Obstetrics 107:593-601.
207. Ewing, C.L.; Thomas, D.J. 1973. Torque Versus Angular Displacement Response of Human Head to -G Impact Acceleration. In: 17th Stapp Car Crash Conference Proceedings, 12-13 November, Oklahoma City, pp. 309-342. New York: SAE Paper No. 730976.
208. Ewing, C.L.; Thomas, D.J. 1972. Human Head and Neck Response to Impact Acceleration, Pensacola, FLA: Naval Aerospace Medical Research Laboratory Monograph 21, Report No. USAARL 73-1.
209. Ewing, C.L., et al. 1978. Effect of Initial Position on the Human Head and Neck Response to +Y Impact Acceleration. In: 22nd Stapp Car Crash Conference Proceedings, New Orleans, pp. 101-138.
210. Ewing, C.L., et al. 1976. The Effect of Duration, Rate of Onset and Peak Acceleration on the Dynamic Response of the Human Head and Neck. In: 20th Stapp Car Crash Conference Proceedings.
211. Ewing, C.L., et al. 1977a. Dynamic Response of the Human Head and Neck to +Gy Impact Acceleration. In: 21st Stapp Car Crash Conference Proceedings, pp. 549-586.
212. Ewing, C.L., et al. 1977b. Measurement of Head, T_1 , and Pelvic Response to -Gx Impact Acceleration. In: 21st Stapp Car Crash Conference Proceedings, pp. 509-545.

213. Ewing, C.L., et al. 1975. The Effect of the Initial Position of the Head and Neck on the Dynamic Response of the Human Head and Neck to -Gx Impact Acceleration. In: 19th Stapp Car Crash Conference Proceedings, 17-19 November, San Diego.
214. Ewing, C.L., et al. 1969. Living Human Dynamic Response to -Gx Impact Acceleration II--Accelerations Measured on the Head and Neck. In: 13th Stapp Car Crash Conference Proceedings, 2-4 December, Boston, pp. 400-415. New York: SAE Paper No. 690817.
215. Ewing, C.L., et al. 1968. Dynamic Response of the Head and Neck of the Living Human to -Gx Impact Acceleration. In: 12th Stapp Car Crash Conference Proceedings, 22-23 October, Detroit, pp. 424-439. New York: SAE Paper No. 680792.
216. Fleck, J.T.; Butler, F.E. 1975. Development of an Improved Computer Model of the Human Body and Extremity Dynamics, AMRL-TR-75-14, Aerospace Medical Research Lab, Wright-Patterson Air Force Base, Ohio, July.
217. Gennarelli, T.A., et al. 1981. Acceleration Induced Head Injury in the Monkey. Acta Neuropathol. (Berl.) Suppl. VII, pp. 23-25.
218. Gennarelli, T.A., et al. 1979. Differential Tolerance of Frontal and Temporal Lobes to Contusion Induced by Angular Acceleration. In: 23rd Stapp Car Crash Conference Proceedings, 17-19 October, San Diego, pp. 563-586. SAE Paper No. 791022.
219. Gennarelli, T.A.; Ommaya, A.K.; Thibault, L.E. 1971. Comparison of Translational and Rotational Head Motions In Experimental Cerebral Concussion. In: 15th Stapp Car Crash Conference Proceedings, 17-19 November, Coronado, California, pp. 797-803.
220. Gennarelli, T.A.; Thibault, L.E.; Ommaya, A.K. 1972. Pathophysiological Responses to Rotational and Translational Accelerations of the Head. In: 16th Stapp Car Crash Conference Proceedings, 8-10 November, Detroit, pp. 296-308. New York: SAE Paper No. 720970.
221. Goldsmith, W., et al. 1978. Response of a Realistic Human Head-Neck Model to Impact. Journal of Biomechanical Engineering 100(1):25-34, February.
222. Gonza, E.R.; Harrington. 1981. Biomechanics of Musculoskeletal Injury, Williams and Wilkins.
223. Got, C., et al. 1978. Results of Experimental Head Impacts on Cadavers: The Various Data Obtained and Their Relations to Some Measured Physical Parameters. In: 22nd Stapp Car Crash Conference Proceedings, 24-26 October, Ann Arbor, MI, pp. 57-99. SAE Paper No. 780887.

224. Gross, A.G. 1978. A New Theory on the Dynamics of Brain Concussion and Brain Injury. Journal of Neurosurgery 15:548-561.
225. Gurdjian, E.S. 1975. Impact Head Injury; Mechanistic, Clinical and Preventive Correlations. Springfield, IL: Charles C. Thomas.
226. Gurdjian, E.S., et al. 1970. Studies on Mechanical Impedance of the Human Skull: Preliminary Report. Journal of Biomechanics 3(3):239-248, May.
227. Gurdjian, E., et al. 1968. Significance of Relative Movements of Scalp, Skull and Intracranial Contents During Impact Injury of the Head. Journal of Neurosurgery 29(1):70-72.
228. Gurdjian, E.S., et al. 1961. Intracranial Pressure and Acceleration Accompanying Head Impacts in Human Cadavers. Surgery, Gynecology and Obstetrics 113:185-190.
229. Gurdjian, E.S.; Webster, J.E. 1953. Recent Advances in the Knowledge of the Mechanism, Diagnosis, and Treatment of Head Injury. American Journal of the Medical Sciences 226:214-220.
230. Gurdjian, E.S.; Lissner, H.R. 1964. The Position and Motions of the Head at Impact. In: 8th Stapp Car Crash Conference Proceedings, pp. 182-193.
231. Gurdjian, E.S.; Lissner, H.R. 1946. Deformation of the Skull in Head Injury Studied by the "Stresscoat" Technique, Quantitative Determinations. Surgery, Gynecology and Obstetrics 83:219-233.
232. Gurdjian, E.S.; Lissner, H.R. 1945. Deformation of the Skull in Head Injury: A Study of the "Stresscoat" Technique. Surgery, Gynecology and Obstetrics 81:679-687.
233. Gurdjian, E.S., Lissner, H.R.; Webster, J.E. 1947. The Mechanism of Production of Linear Skull Fractures. Surgery, Gynecology and Obstetrics 85:195-210.
234. Gurdjian, E.S., et al. 1953. Quantitative Determination of Acceleration and Intracranial Pressure in Experimental Head Injury, Preliminary Report. Neurology 3(6):417-423.
235. Gurdjian, E.S.; Webster, J.E.; Lissner, H.R. 1953. Observations on Prediction of Fracture Site in Head Injury. Radiology 60:226-235.
236. Gurdjian, E.S.; Webster, J.E.; Lissner, H.R. 1955. Observations on the Mechanism of Brain Concussion, Contusion and Laceration. Surgery, Gynecology and Obstetrics 101:680-690.

237. Gurdjian, E.S.; Webster, J.E.; Lissner, H.R. 1949. Studies on Skull Fracture with Particular References to Engineering Factors. American Journal of Surgery 78:736-742.
238. Hardy, C.H.; Marcal, P.V. 1971. Elastic Analysis of a Skull, ONR Report No. N00014-0007/8, November.
239. Haut, R.C., et al. 1972. Nonlinear viscoelastic Model from Head Impact Injury Hazard. In: 16th Stapp Car Crash Conference Proceedings, p. 149.
240. Higgins, L.S.; Schmall, R.A. 1967. A Device for the Investigation of Head Injury Effected by Non-Deforming Head Accelerations. In: 11th Stapp Car Crash Conference Proceedings, pp. 35-46.
241. Hirsch, A.E., Ommaya, A.K. 1970. Protection from Brain Injury: The Relative Significance of Translational and Rotational Motions of the Head After Impact. In: 14th Stapp Car Crash Conference Proceedings, 17-18 November, Ann Arbor, MI, pp. 299-328.
242. Hodgson, V.R.; Thomas, L.M. 1979. Acceleration Induced Shear Strains on a Monkey Brain Hemisection. In: 23rd Stapp Car Crash Conference Proceedings, 17-19 October, San Diego, Calif, pp. 589-611. SAE Paper No. 791023.
243. Hodgson, V.R., et al. 1972. Head Model for Impact. In: 16th Stapp Car Crash Conference Proceedings, pp. 1-13.
244. Hodgson, V.R.; Thomas, L.M. 1972. Effect of Long-Duration Impact on Head. In: 16th Stapp Car Crash Conference Proceedings, 8-10 November, Detroit, pp. 292-295. SAE Paper No. 720956.
245. Hodgson, V.R., et al. 1970. Fracture Behavior of the Skull Frontal Bone Against Cylindrical Surfaces. In: 14th Stapp Car Crash Conference Proceedings, 17-18 November, Ann Arbor, MI, pp. 341-355. New York: SAE Paper No. 700909.
246. Hodgson, V.R. 1969. Advances in Understanding of Experimental Concussion Mechanisms. In: 13th Stapp Car Crash Conference Proceedings, 2-4 December, Boston, pp. 18-37. New York: SAE Paper No. 690796.
247. Hodgson, V.R.; Patrick, L.M. 1968. Dynamic Response of the Human Cadaver Head Compared to a Simple Mathematical Model. In: 12th Stapp Car Crash Conference Proceedings, 22-23 October, Detroit, pp. 280-301. New York: SAE Paper No. 680784.
248. Hodgson, V.R., et al. 1967. The Development of a Model for the Study of Head Injury. In: 11th Stapp Car Crash Conference Proceedings, pp. 286-292.

249. Hodgson, V.R., et al. 1967. The Determination of Response Characteristics of the Head with Emphasis on Mechanical Impedance Techniques. In: 11th Stapp Car Crash Conference Proceedings, pp. 79-85.
250. Holbourn, A.H.S. 1943. Mechanics of Head Injuries. Lancet 245:438-441.
251. Hosey, R.R.; Liu, Y.K. 1980. A Homeomorphic Finite Element Model of Impact Head and Neck Injury. Proceedings of the International Conference on Finite Elements in Biomechanics, Tuscon, Arizona, pp. 829-850.
252. Hosey, R.R.; Liu, Y.K. 1982. A Homeomorphic Finite Element Model of the Human Head and Neck. In: R. H. Gallagher, et al., eds., Finite Elements in Biomechanics, New York: John Wiley and Sons, pp. 379-401.
253. Hu, A.S. 1980. Head Impact Rotational Measurements and Frequency Response. Journal of Biomechanics 13(7):615-622.
254. Hubbard, R.P.; McLeod, D.G. 1974. Definition and Development of a Crash Dummy Head. In: 18th Stapp Car Crash Conference Proceedings, pp. 599-628. SAE Paper No. 74-1193.
255. Huston, R.L.; Sears, J. 1981. Effects of Protective Helmet Mass on Head/Neck Dynamics. JBEG 103(1): pp. 18-23, February.
256. Kabo, J.M.; Goldsmith, W.; Harris, N.M. 1983. In-Vitro Head and Neck Response to Impact. Journal of Biomechanical Engineering 105(4):316-320.
257. Kaleps, I.; Marcus, J. 1982. Predictions of Child Motion During Panic Braking and Impact. In: 26th Stapp Car Crash Conference Proceedings, pp. 207-229. SAE Paper No. 811166.
258. Kaleps, I. 1980. Models and Analogs for the Evaluation of Human Biodynamic Response, Performance and Protection. AGARD Proceedings, No. 253, pp. 1-13.
259. Kao, R.; Perrone, N. 1970. Stresses in Spherical Shells Due to Local Loading. Washington, DC: The Catholic University of America, Report No. 71-4.
260. Kenner, V.H.; Goldsmith, W. 1973. Impact on a Simple Physical Model of the Head. Journal of Biomechanics 6:1-11.
261. Khalil, T.B.; Smith, D.L.; Viano, D.C. 1978. Experimental Analysis of the Vibrational Characteristics of the Human Skull. General Motors Research Laboratories.
262. Khalil, T.B.; Hubbard, R.P. 1977. Parametric Study of Head Response by Finite Element Modeling. Journal of Biomechanics 10(2):119-132.

263. King, A.I. 1983. Human Analogues in Biomechanical Research. In: Channing L. Ewing, Daniel J. Thomas, Anthony Sances and Sanford J. Larson, Impact Injury of the Head and Neck, Springfield, IL: Charles C. Thomas, pp. 381-390.
264. King, A.I. 1975. Survey of the State of the Art of Human Biodynamic Response. In: Aircraft Crashworthiness, pp. 83-120. Charlottesville, VA: University Press of Virginia.
265. King, A.I.; Padganokar, A.J.; Krieger, K.W. 1974. Measurement of Angular Acceleration of a Rigid Body Using Linear Accelerations. In: 2nd Human Subjects for Biomechanical Research Meeting, Committee Reports and Technical Session Papers, 6 December 1974, Ann Arbor, MI, pp. 48-59. International Ad Hoc Committee on Human Subjects for Biomechanical Research.
266. Kopecky, J.A.; Ripperger, E. 1969. Closed Brain Injuries: An Engineering Analysis. Journal of Biomechanics. 2(1):250-260, March.
267. Lindenberg, R.; Freytag, E. 1969. The Mechanism of Cerebral Contusions. AMA Archives of Pathology 69:440-469.
268. Lindgren, S.O. 1966. Experimental Studies of Mechanical Effects in Head Injury. Acta Chirurgica Scand, Suppl. 360.
269. Lissner, H.R.; Lebow, M.; Evans, F.G. 1960. Experimental Studies on the Relation between Acceleration and Intracranial Pressure Changes in Man. Surgery, Gynecology, and Obstetrics 111:329-338.
270. Liu, Y.K. 1978. Biomechanics of Closed Head Impact. J. Eng. Mech., Div. Am. Soc. Civil Eng. 104(EM1):131-152.
271. McElhaney, J.H.; Stalnaker, R.L.; Roberts, V.L. 1973. Biomechanical Aspects of Head Injury. In: Human Impact Response - Measurement and Simulation, Proceedings of the Symposium on Human Impact Response, 2-3 October 1972, Warren, Mi, pp. 85-110. New York: Plenum Press.
272. Melvin, J.W.; Evans, F.G. 1971. A Strain Energy Approach to the Mechanics of Skull Fracture. In: 15th Stapp Car Crash Conference Proceedings, 17-19 November, Coronado, Calif., pp. 666-685. New York: SAE Paper No. 710871.
273. Mertz, H.J.; Patrick, L.M. 1967. Investigation of the Kinematics and Kinetics of Whiplash. In: 11th Stapp Car Crash Conference Proceedings, 10-11 October 1967, Anaheim, Calif., pp. 175-206. New York: SAE Paper No. 670919.
274. Misa, J.C.; Chakravarty, S. 1982. A Free-Vibration Analysis for the Human Cranial System. Journal of Biomechanics 15(9):635-646.

275. Mohan, D.; Bowman, B.M.; Snyder, R.G.; Foust, D.R. 1979. A Biomechanical Analysis of Head Impact Injuries to Children. Journal of Biomechanical Engineering 101(4):250-260.
276. Mucciardi, A.N.; Sanders, J.D.; Eppinger, R.H. 1977. Prediction of Brain Injury Measures of Head Motion Parameters. In: 21st Stapp Car Crash Conference Proceedings, 19-21 October, New Orleans, pp. 369-415. SAE Paper No. 770923.
277. Nahum, A.M., et al. 1981. A Study of Impacts to the Lateral Protected and Unprotected Head. In: 25th Stapp Car Crash Conference Proceedings, pp. 241-270.
278. Nahum, A., et al. 1980. Experimental Studies of Side Impact to the Human Head. In: 24th Stapp Car Crash Conference Proceedings, pp. 45-62, pp. 161-185.
279. Nahum, A.M., et al. 1979. Intracranial Pressure Relationships in the Protected and Unprotected Head. In: 23rd Stapp Car Crash Conference Proceedings, pp. 613-636.
280. Nahum, A.M., et al. 1977. Intracranial Pressure Dynamics During Head Impact. In: 21st Stapp Car Crash Conference Proceedings, 19-21 October, New Orleans, pp. 339-366. SAE Paper No. 770922.
281. Nahum, A.M.; Smith, R.W. 1976. An Experimental Model for Closed Head Impact Injury. In: 20th Stapp Car Crash Conference Proceedings, pp. 783-814. SAE Paper No. 760825.
282. Nahum, A.M., et al. 1968. Impact Tolerance of the Skull and Face. In: 12th Stapp Car Crash Conference Proceedings, pp. 301-216.
283. Nusholtz, G.S., et al. 1982. Response of the Cervical Spine to Superior-Inferior Head Impact. In: 25th Stapp Car Crash Conference Proceedings, pp. 197-237.
284. Nusholtz, G.S.; Axelrod, J.B.; Melvin, J.W.; Ward, C.C. 1979. Comparison of Epidural Pressure in Live Anesthetized and Post-Mortem Primates. In: 7th International Workshop on Human Subjects for Biomechanical Research Proceedings, 16 October 1979, Coronado, Calif., pp. 175-200. Washington, D.C.: Distributed by National Highway Traffic Safety Administration.
285. Nusholtz, G.S.; Melvin, J.W.; Alem, N.M. 1979. Head Impact Response Comparisons of Human Surrogates. In: 23rd Stapp Car Crash Conference Proceedings, 17-19 October, San Diego, Calif., pp. 499-541. SAE Paper No. 791020.

286. Ommaya, A.K.; Hirsch, A.E. 1971. Protection of the Brain from Injury During Impact: Experimental Studies in the Biomechanics of Head Injury. In: Linear Acceleration of Impact Type, pp. 7-1 and 7-19. Aerospace Medical Panel Specialist Meeting, 23-26 June 1971, Oporto, Portugal. Paris: AGARD Conference Proceedings, No. 88.
287. Ommaya, A.K.; Yarnell, P.; Hirsch, A.E.; Harris, E.H. 1967. Scaling of Experimental Data on Cerebral Concussion in Subhuman Primates to Concussion Threshold in Man. In: 11th Stapp Car Crash Conference Proceedings, pp. 47-52.
288. Ommaya, A.K.; Hirsch, A.E.; Martinez, J.L. 1966. The Role of Whiplash in Cerebral Concussion. In: 10th Stapp Car Crash Conference Proceedings, pp. 314-324. SAE Paper No. 660804.
289. Ono, K.; Kikuchi, K.; Nakamura, M. 1980. Human Head Tolerance to Sagittal Impact Reliable Estimation Deduced from Experimental Head Injury Using Subhuman Primates and Human Cadaver Skulls. In: 24th Stapp Car Crash Proceedings, pp. 104-160. SAE Paper No. 801300.
290. Patrick, L.M.; Levine, R.S. 1975. Injury to Unembalmed Belted Cadavers in Simulated Collisions. In: 19th Stapp Car Crash Conference Proceedings, 17-19 November, San Diego, pp. 79-115. PA: SAE Paper No. 751144.
291. Patrick, L.M.; Mertz, H.J.; Kroell, C.K. 1967. Cadaver Knee, Chest, and Head Impact Loads. In: 11th Stapp Car Crash Conference Proceedings, pp. 106-117. SAE Paper No. 670913.
292. Privitzer, E.; Belytschko, T. 1980. Impedance of a Three-Dimensional Head-Spine Model. Mathematical Modeling 1:189-209.
293. Reader, D.C. 1979. Head Acceleration and Psychomotor Performance. Aviation, Space and Environmental Medicine 50:267-270.
294. Roberts, S.R., et al. 1969. Head Trauma - A Parametric Dynamic Study, Journal of Biomechanics 2(4):397-416, October.
295. Roberts, V.L.; Hodgson, V.R.; Thomas, L.M. 1967. Fluid Pressure Gradients Caused by Impact to the Human Skull. In: Biomechanics Monograph, pp. 223-235. New York: American Society of Mechanical Engineers.
296. Rose, J.L., et al. 1974. Dynamic Photoelastic Model Analysis of Impact to the Human Skull. Journal of Biomechanics 7(3):193-201, May.
297. Saltzberg, B.; Burton, W.D., Jr. 1979. Analysis of Electrophysiological Signals from Animals Subject to Biodynamic Stress. ONR Report Contract N000-76-C-0911.

298. Sances, A., et al. 1984. Biodynamics of Vehicular Injuries. In: G. A. Peters and B. J. Peters, Eds., Automotive Engineering and Litigation, New York: Garland Law Publishing, pp. 449-550.
299. Sances, A., et al. 1980. The Evoked Potential: An Experimental Method for Biomechanical Analysis of Brain and Spinal Injury. In: 24th Stapp Car Crash Conference Proceedings, 15-17 October, Troy, MI, pp. 66-100. SAE Paper No. 801302.
301. Schneider, D.C.; Nahum, A.M. 1972. Impact Studies of Facial Bones and Skull. In: 16th Stapp Car Crash Conference Proceedings, pp. 186-203. SAE Paper No. 720965.
302. Shugar, T.A. 1975. Transient Structural Response of the Linear Skull-Brain System. In: 19th Stapp Car Crash Conference Proceedings, 17-19 November, San Diego, Calif., pp. 581-614. SAE Paper No. 751161.
303. Snyder, R.G. 1970. Human Impact Tolerance - State of the Art. Society of Automotive Engineers, Warrendale, Pa. SAE Paper No. 700398.
304. Stalnaker, R.L.; Alem, N.M.; Benson, J.B. 1977. Validation Studies for Head Impact Injury Model. Ann Arbor: University of Michigan Highway Safety Research Institute for the National Highway Traffic Safety Administration, Report No. DOT/HS-802566.
305. Stalnaker, R.L.; Fogle, J.L.; McElhaney, J.H. 1971. Driving Point Impedance Characteristics of the Head. Journal of Biomechanics 4(2):127-139.
306. Stalnaker, R.L.; Fogle, J.L.; McElhaney, J.H. 1970. Driving Point Impedance Characteristics of the Head. American Society of Mechanical Engineers Biochemical and Human Factors Conference, 31 May - 3 June 1970, Washington, DC. New York: ASME Paper No. 70-BHF-14.
307. Stalnaker, R.L.; McElhaney, J.H. 1970. Head Injury Tolerance for Linear Impacts by Mechanical Impedance Methods. American Society of Mechanical Engineers, Winter Annual Meetings, 29 November - 3 December 1970. ASME Paper No. 70-WA/BHF-4.
308. Stalnaker, R.L.; Melvin, J.W.; Nusholtz, G.S.; Alem, N.M.; Benson, J.B. 1977. Head Impact Response. In: 21st Stapp Car Crash Conference Proceedings, 19-21 October, New Orleans, pp. 303-335. SAE Paper No. 770921.
309. Tarriere, C.; Sapin, C. 1969. Biokinetic Study of the Head to Thorax Linkage. In: 13th Stapp Car Crash Conference Proceedings, 2-4 December, Boston, pp. 365-380. New York: SAE Paper No. 690815.

310. Thomas, D.J.; Ewing, C.L. 1971. Theoretical Mechanics for Expressing Impact Acceleration Response of Human Beings. In: Linear Acceleration of Impact Type, pp. 12-1 12-7. Aerospace Medical Panel Specialist Meeting, 23-26 June 1971, Oporto, Portugal. Paris: AGARD Conference Proceedings, No. 88.
311. Thomas, L.M., et al. 1968. Static Deformation and Volume Changes in the Human Skull. In: 12th Stapp Car Crash Conference Proceedings, pp. 260-270.
312. Unterharnscheidt, F. 1983. Neuropathology of Rhesus Monkeys Undergoing -Gx impact acceleration. In: C.L. Ewing, et al., eds., Impact Injury of the Head and Spine, Springfield, IL: Thomas, pp. 94-176.
313. Unterharnscheidt, F.J. 1971. Translational Versus Rotational Acceleration: Animal Experiments with Measured Input. In: 15th Stapp Car Crash Conference Proceedings, 17-19 November, Coronado, Calif., pp. 767-770. New York: SAE Paper No. 710880.
314. von Gierke, Ing. H.E. 1978. Technical Evaluation Report: Models and Analogues for the Evaluation of Human Biodynamic Response, Performance and Protection. AGARD Conference Proceedings, No. 253, vii 1-A3-4.
315. Viano, D.C., Gadd, C.W. 1975. Significance of Rate of Onset in Impact Injury Evaluation. In: 19th Stapp Car Crash Conference Proceedings, 17-19 November, San Diego, pp. 807-819. SAE Paper No. 751169.
316. Walker, L.B.; Harris, E.H.;; Pontius, U.R. 1973. Mass, Volume, Center of Mass, and Mass Moment of Inertia of Head and Head and Neck of Human Body. In: 17th Stapp Car Crash Conference Proceedings, 12-13 November, Oklahoma City, pp. 525-537. New York: SAE Paper No. 730985.
317. Ward, C.; Chan, M.; Nahum, A. 1980. Intracranial Pressure - A Brain Injury Criterion. In: 24th Stapp Car Crash Conference Proceedings. SAE Paper No. 801304.
318. Ward, C.C.; Nikravesch, P.E.; Thompson, R.B. 1978. Biodynamic Finite Element Models Used in Brain Injury Research. Journal of Aviation Space and Environmental Medicine 49:136-142.
319. Ward, C.C. 1977. Analytical Brain Models for Head Impact. In: 3rd International Conference on Impact Trauma Proceedings, 7-9 September 1977, Berlin, pp. 389-398. Bron, France: International Research Committee on the Biokinetics of Impacts.
320. Ward, C.C.; Thompson, R.B. 1975. The Development of a Detailed Finite Element Brain Model. In: 19th Stapp Car Crash Conference Proceedings, 17-19 November, San Diego, pp. 641-674. SAE Paper No. 751163.

321. Ward, C.C. 1974. A Dynamic Finite Element Model of the Human Brain. Ph.D. Dissertation, University of California, Los Angeles.
322. Weiss, M.S.; Berger, M.D. 1982. Neurophysiological Effects of -X Impact Accelerations. AGARD Conference Proceedings, No. 322. Neuilly-sur-Seine, France: NATO/AGARD, Paper 14, pp. 1-7.
323. Wolfe, J.W. 1974. Technique for Chronic Head Restraint and Electrophysiology Recording in the Awake Rhesus Monkey. Physiology and Behavior 13:461-464.

INERTIAL FORCE

324. Becker, E.B. 1973. Preliminary Discussion of an Approach to An Approach to Modelling Living Human and Neck Response to -Gx Impact Acceleration. In: Human Impact Response Measurement and Simulation. Proceedings of the Symposium on Human Impact Response, 2-3 October 1972, Warren, MI, New York: Plenum Press, pp. 321-329.
325. Ewing, C.L.; Thomas, D.J. 1973. Torque Versus Angular Displacement Response of Human Head to -G Impact Acceleration. In: 17th Stapp Car Crash Conference Proceedings, 12-13 November, Oklahoma City, pp. 309-342, New York: SAE Paper No. 730976.
326. Ewing, C.L., et al. 1978. Effect of Initial Position on the Human Head and Neck Response to +Y Impact Acceleration. In: 22nd Stapp Car Crash Conference Proceedings, New Orleans, pp. 101-138.
327. Ewing, C.L., et al. 1977a. Dynamic Response of the Human Head and Neck to +Gy Impact Acceleration. In: 21st Stapp Car Crash Conference Proceedings, pp. 549-586.
328. Ewing, C.L., et al. 1977b. Measurement of Head, T_1 , and Pelvic Response to -Gx Impact Acceleration. In: 21st Stapp Car Crash Conference Proceedings, pp. 509-545.
329. Ewing, C.L., et al. 1975. The Effect of the Initial Position of the Head and Neck on the Dynamic Response of the Human Head and Neck to -Gx Impact Acceleration. In: 19th Stapp Car Crash Conference Proceedings, 17-19 November, San Diego.
330. Ewing, C.L., et al. 1969. Living Dynamic Response to -Gx Impact Acceleration II - Acceleration Measured on the Head and Neck. In: 13th Stapp Car Crash Conference Proceedings, 2-4 December, Boston, pp. 400-415. New York: SAE Paper No. 690817.

331. Ewing, C.L., et al. 1968. Dynamic Response of the Head and Neck of the Living Human to -Gx Impact Acceleration. In: 12th Stapp Car Crash Conference Proceedings, 22-23 October, Detroit, pp. 424-439. New York: SAE Paper No. 680792.
332. Unterharnscheidt, F. 1983. Neuropathology of Rhesus Monkeys Undergoing -Gx Impact Acceleration. In: C.L. Ewing, et al., eds., Impact Injury of the Head and Spine, Springfield, IL: Thomas, pp. 94-176.
333. Weiss, M.S.; Berger, M.D. 1982. Neurophysiological Effects of -X Impact Accelerations. AGARD Conference Proceedings, No. 322 Neuilly-Sur-Seine, France: NATO/AGARD, Paper 114, pp. 1-7.

TRANSLATIONAL AND ROTATIONAL ACCELERATION

334. Abel, J.M.; Gennarelli, T.A.; Segawa, H. 1978. Incidence and Severity of Cerebral Concussion in the Rhesus Monkey Following Sagittal Plane Angular Acceleration. In: 22nd Stapp Car Crash Conference Proceedings, 24-26 October 1978, Ann Arbor, MI. Warrendale, PA: SAE Paper No. 780886, pp. 35-53.
335. Adams, J.H., et al. 1981. Acceleration Induced Head Injury in the Monkey. II Neuropathology Acta Neuropathol. (Berl.) Suppl. VII, pp. 26-28.
336. Aldman, B; Thorngren, L.; Ljung, C. 1981. Patterns of Deformation in Brain Models Under Rotational Motion. In: DOT, NHTSA, Head and Neck Injury Criteria, Washington, D.C.
337. Alem, N.M. 1974. Simulation of Head Injury Due to Combined Rotation and Translation of the Brain. In: 18th Stapp Car Crash Conference Proceedings, pp. 579.
338. Ewing, C.L.; Thomas, D.J. 1973. Torque Versus Angular Displacement Response of Human Head to -G Impact Acceleration. In: 17th Stapp Car Crash Conference Proceedings, 12-13 November, Oklahoma City, pp. 309-342. New York: SAE Paper No. 730976.
339. Gennarelli, T.A., et al. 1981. Acceleration Induced Head Injury in the Monkey. Acta Neuropathol. (Berl.) Suppl. VII, pp. 23-25.
340. Gennarelli, T.A., et al. 1979. Differential Tolerance of Frontal and Temporal Lobes to Contusion Induced by Angular Acceleration. In: 23rd Stapp Car Crash Conference Proceedings, 17-19 October, San Diego, pp. 563-586. SAE Paper No. 791022.
341. Gennarelli, T.A.; Ommaya, A.K.; Thibault, L.E. 1971. Comparison of Translational and Rotational Head Motions In Experimental Cerebral Concussion. In: 15th Stapp Car Crash Conference Proceedings, 17-19 November, Coronado, California, pp. 797-803.

342. Gennarelli, T.A.; Thibault, L.E.; Ommaya, A.K. 1972. Pathophysiological Responses to Rotational and Translational Accelerations of the Head. In: 16th Stapp Car Crash Conference Proceedings, 8-10 November, Detroit, pp. 296-308. New York: SAE Paper No. 720970.
343. Higgins, L.S.; Schmull, R.A. 1967. A Device for the Investigation of Head Injury Effected by Non-Deforming Head Accelerations. In: 14th Stapp Car Crash Conference Proceedings, pp. 35-46.
344. Hirsch, A.E.; Ommaya, A.K. 1970. Protection from Brain Injury: The Relative Significance of Translational and Rotational Motions of the Head After Impact. In: 14th Stapp Car Crash Conference Proceedings, 17-18 November, Ann Arbor, MI., pp. 299-328.
345. Hodgson, V.R.; Thomas, L.M. 1979. Acceleration Induced Shear Strains on a Monkey Brain Hemisection. In: 23rd Stapp Car Crash Conference Proceedings, pp. 589-611. SAE Paper No. 791023.
346. Hu, A.S. 1980. Head Impact Rotational Measurements and Frequency Response. Journal of Biomechanics 13(7):615-622.
347. Kabo, J.M.; Goldsmith, W.; Harris, N.M. 1983. In-Vitro Head and Neck Response to Impact. Journal of Biomechanical Engineering 105(4):316-320.
348. Kaleps, I.; Marcus, J. 1982. Prediction of Child Motion During Panic Braking and Impact. In: 26th Stapp Car Crash Conference Proceedings, pp. 207-229. SAE Paper No. 811166.
349. King, A.I.; Padganokar, A.J.; Krieger, K.W. 1974. Measurement of Angular Acceleration of a Rigid Body Using Linear Accelerations. In: 2nd Human Subjects for Biomechanical Research Meeting, Committee Reports, and Technical Session Papers, 6 December 1974, Ann Arbor, MI., pp. 48-59. International Ad Hoc Committee on Human Subjects for Biomechanical Research.
350. Reader, D.C. 1979. Head Acceleration and Psychomotor Performance. Aviation, Space and Environmental Medicine, 50:267-270.
351. Unterharnscheidt, F.J. 1971. Translational Versus Rotational Acceleration: Animal Experiments with Measured Input. In: 15th Stapp Car Crash Conference Proceedings, pp. 767-770. SAE Paper No. 710880.

IMPACT FORCE

352. Berger, M.D.; Weiss, M.S. 1983. Effects of Impact Somatosensory Evoked Potentials. In: C.L. Ewing, et al., eds., Impact Injury of the Head and Spine, Springfield, IL: Thomas, pp. 324-328.
353. Bittner, A.C.; Shortal, J.P., III; Harbeson, M. 1983. Effects of Head Impact Acceleration on Human Performance, Naval Biodynamics Laboratory, New Orleans, LKA, NBDL-83R004, May.
354. Brinn, J.; Staffield, S.E. 1970. Evaluation of Impact Test Accelerations. In: 14th Stapp Car Crash Conference Proceedings, pp. 188-207.
355. Chan, H.S. 1974. Mathematical Model for Closed Head Impact. In: 18th Stapp Car Crash Conference Proceedings, pp. 557-578. SAE Paper No. 741191.
356. Engin, A.E.; Roberts, V.L. 1971. A Mathematical Model for the Behavior of the Brain When the Human head is Subjected to Impulsive Loads. Symposium on Biodynamic Models and Their Applications, 26-28 October, 1970. Aerospace medical Research Laboratory, Wright-Patterson Air Force Base, Ohio, pp. 877-905.
357. Ewing, C.L., Thomas, D.J. 1972. Human Head and Neck Response to Impact Acceleration, Pensacola, FLA: Naval Aerospace Medical Research Laboratory Monograph 21, Report No. USAARL73-1.
358. Gurdjian, E.S. 1975. Impact Head Injury: Mechanistic, Clinical and Preventive Correlations. Springfield, IL: Charles C. Thomas.
359. Gurdjian, E.S., et al. 1970. Studies on Mechanical Impedance of the Human Skull: Preliminary Report. Journal of Biomechanics 3(3):239-248. May.
360. Gurdjian, E., et al. 1968. Significance of Relative Movements of Scalp, Skull and Intracranial Contents During Impact Injury of the Head. Journal of Neurosurgery, 29(1):70-72.
361. Gurdjian, E.S.; Lissner, H.R. 1964. The Position and Motions of the Head at Impact. In: 8th Stapp Car Crash Conference Proceedings, pp. 182-193.
362. Hodgson, V.R., et al. 1972. Head Model for Impact. In: 16th Stapp Car Crash Conference Proceedings, pp. 1-13.
363. Hodgson, V.R.; Thomas, L.M. 1972. Effects of Long Duration Impact on Head. In: 16th Stapp Car Crash Conference Proceedings, pp. 292-295. SAE Paper No. 720956.
364. Hodgson, V.R., et al. 1967. The Determination of Response Characteristics of the Head with Emphasis on Mechanical Impedance Techniques. In: 11th Stapp Car Crash Conference Proceedings, pp. 79-85.

365. Hosey, R.R.; Liu, Y.K. 1980. A Homeomorphic Finite Element Model of Impact Head and Neck Injury. Proceedings of the International Conference on Finite Elements in Biomechanics, Tuscon, Arizona, pp. 829-850.
366. Kenner, V.H.; Goldsmith, W. 1973. Impact on a Simple Physical Model of the Head. Journal of Biomechanics, 6:1-11.
367. Mohan, D.; Bowman, B.M.; Snyder, R.G.; Foust, D.R. 1979. A Biomechanical Analysis of Head Impact Injuries to Children. Journal of Biomechanical Engineering, 101(4):250-260.
368. Nahum, A.M., et al. 1981. A Study of Impacts to the Lateral Protected and Unprotected Head. In: 25th Stapp Car Crash Conference Proceedings, pp. 241-270.
369. Nahum, A.M., et al. 1980. Experimental Studies of Side Impact to the Human Head. In: 24th Stapp Car Crash Conference Proceedings, pp. 45-62, pp. 161-185.
370. Nahum, A.M.; Smith, R.W. 1976. An Experimental Model for Closed Head Impact Injury. In: 20th Stapp Car Crash Conference Proceedings, pp. 783-814. SAE Paper No. 760825.
371. Nahum, A.M., et al. 1968. Impact Tolerance of the Skull and Face. In: 12th Stapp Car Crash Conference Proceedings, pp. 301-316.
372. Nusholtz, G.S., et al., 1982. Response of the Cervical Spine to Superior-Inferior Head Impact. In: 25th Stapp Car Crash Conference Proceedings, pp. 197-237.
373. Nusholtz, G.S.; Melvin, J.W.; Alem, N.M. 1979. Head Impact Response Comparisons of Human Surrogates. In: 23rd Stapp Car Crash Conference Proceedings, pp. 499-541. SAE Paper No. 791020.
374. Ommaya, A.K.; Hirsch, A.E. 1971. Protection of the Brain from Injury During Impact: Experimental Studies in the Biomechanics of Head Injury. In: Linear Acceleration of Impact Type, pp. 7-1 and 7-19. Aerospace Medical Panel Specialist Meeting, 23-26 June 1971, Oporto, Portugal. Paris: AGARD Conference Proceedings, No. 88.
375. Ono, K.; Kikuchi, K.; Nakamura, M. 1980. Human Head Tolerance to Sagittal Impact Reliable Estimation Deduced from Experimental Head Injury using Subhuman Primates and Human Cadaver Skulls. In: 24th Stapp Car Crash Conference Proceedings, pp. 104-160. SAE Paper No. 801300.
376. Patrick, L.M.; Mertz, H.J.; Kroell, C.K. 1967. Cadaver Knee, Chest, and Head Impact Loads. In: 11th Stapp Car Crash Conference Proceedings, pp. 106-117. SAE Paper No. 670913.

377. Privitzer, E., Belytschko, T. 1980. Impedance of a Three-Dimensional Head-Spine Model. Mathematical Modeling 1:189-209.
378. Rose, J.L., et al. 1974. Dynamic Photoelastic Model Analysis of Impact to the Human Skull. Journal of Biomechanics 7(3):193-201, May.
379. Schneider, D.C.; Nahum, A.M. 1972. Impact Studies of Facial Bones and Skull. In: 16th Stapp Car Crash Conference Proceedings, pp. 186-203. SAE Paper No. 720965.
380. Snyder, R.G. 1970. Human Impact Tolerance - State of the Art. Society of Automotive Engineers, Warrendale, PA. SAE Paper No. 700398.
381. Stalnaker, R.L.; Alem, N.M.; Benson, J.B. 1977. Validation Studies for Head Impact Injury Model. Ann Arbor: University of Michigan, Highway Safety Research Institute for the National Highway Traffic Safety Administration, Report No. DOT-HS-802566.
382. Stalnaker, R.L.; Fogle, J.L.; McElhaney, J.H. 1971. Driving Point Impedance Characteristics of the Head. Journal of Biomechanics, 4(2):127-139.
383. Stalnaker, R.L.; Fogle, J.L.; McElhaney, J.H. 1970. Driving Point Impedance Characteristics of the Head, American Society of Mechanical Engineers Biochemical and Human Factors Conference, 31 May - 3 June 1970, Washington, D.C. ASME Paper No. 70-WA/BHF-4.
384. Stalnaker, R.L.; McElhaney, J.H. 1970. Head Injury Tolerance for Linear Impacts by Mechanical Impedance Methods. American Society of Mechanical Engineers, Winter Annual Meetings, 29 November - 3 December 1970. ASME Paper No. 70-WA/BHF-4.
385. Stalnaker, R.L.; Melvin, J.W.; Nusholtz, G.S.; Alem, N.M.; Benson, J.B. 1977. Head Impact Response. In: 21st Stapp Car Crash Conference Proceedings, pp. 303-335. SAE Paper No. 770921.
386. Thomas, D.J.; Ewing, C.L. 1971. Theoretical Mechanics for Expressing Impact Acceleration Response of Human Beings. In: Linear Acceleration of Impact Type, pp. 12-1 and 12-7. Aerospace Medical Panel Specialist Meetings, 23-26 June 1971, Oporto, Portugal. Paris: AGARD Conference Proceedings, No. 88.
387. Viano, D.C.; Gadd, C.W. 1975. Significance of Rate of Onset in Impact Injury Evaluation. In: 19th Stapp Car Crash Conference Proceedings, pp. 807-819. SAE Paper No. 751169.

DEFORMATION

388. Aldman, B.; Thorngren, L., Ljung, C. 1981. Patterns of Deformation in Brain Models Under Rotational Motion. In: DOT, NHTSA, Head and Neck Injury Criteria, Washington, DC.
389. Chan, M.; Ward, C. 1981. Relative Importance of Skull Deformation. Proceedings, ASME. Biomechanis Symposium, June 22-24.
390. Evans, F.G.; Lissner, H.R.; Lebow, M. 1958. The Relation of Energy, Velocity, and Acceleration to Skull Deformation and Fracture. Surgery, Gynecology, and Obstetrics. 107:593-601.
391. Gurdjian, E.S.; Lissner, H.R. 1946. Deformation of the Skull in Head Injury Studied by the "Stresscoat" Technique, Quantitative Determinations. Surgery, Gynecology, and Obstetrics, 83:219-233.
392. Gurdjian, E.S.; Lissner, H.R. 1945. Deformation of the Skull in Head Injury: A Study of the "Stresscoat" Technique. Surgery, Gynecology, and Obstetrics, 81:679-687.
393. Hardy, C.H.; Marcal, P.V. 1971. Elastic Analysis of a Skull. ONR Report No. N00014-0007/8, November.
394. Haut, R.C., et al. 1972. Nonlinear Viscoelastic Model from Head Impact Injury Hazard. In: 16th Stapp Car Crash Conference Proceedings, p. 149.
395. Higgs, L.S.; Schmall, R.A. 1967. A Device for the Investigation of Head Injury Effected by Non-Deforming Head Acclerations. In: 11th Stapp Car Crash Conference Proceedings, pp. 35-46.
396. Thomas, L.M., et al. 1968. Static Deformation and Volume Changes in the Human Skull. In: 12th Stapp Car Crash Conference Proceedings, pp. 260-270.

LINEAR SKULL FRACTURES

397. Gurdjian, E.S.; Lissner, H.R.; Webster, J.E. 1947. The Mechanism of Production of Linear Skull Fractures. Surgery, Gynecology, and Obstetrics, 85:195-210.
398. Gurdjian, E.S.; Webster, J.E.; Lissner, H.R. 1953. Observations on Prediction of Fracture Site in Head Injury. Radiology, 60:226-235.
399. Gurdjian, E.S.; Webser, J.E.; Lissner, H.R. 1949. Studies on Skull Fracture with Particular References to Engineering Factors. American Journal of Surgery 78:736-742.
430. Hodgson, V.R., et al. 1970. Fracture Behavior of the Skull Frontal Bone Against Cylindrical Surfaces. In: 14th Stapp Car Crash Conference Proceedings, pp. 341-355. SAE Paper No.700909.

431. Melvin, J.W.; Evans, F.G. 1971. A Strain Energy Approach to the Mechanics of Skull Fracture. In: 15th Stapp Car Crash Conference Proceedings, pp. 666-685. SAE Paper No.710871.
402. Nahum, A.M., et al. 1968. Impact Tolerance of the Skull and Face. In: 12th Stapp Car Crash Conference Proceedings, pp. 301-316.

SHAPE

403. Byars, E.F.; Haynes, D.; Durham, T.; Lilly, H., 1970. Craniometric Measurement of Human Skulls. New York: American Society of Mechanical Engineers.
404. Engin, A.E. 1969. Axisymmetric Response of a Fluid-filled Spherical Shell to a Local Radial Impulse - A Model for Head Injury. Journal of Biomechanics, 2(3):325-341.
405. Engin, A.E.; Liu, Y.K. 1970. The Axisymmetric Response of a Closed Fluid-filled Spherical Shell in Free Vibrations. Journal of Biomechanics, 3(1):11-22.
406. Engin, A.E.; Akkas, N. 1978. Application of a Fluid-filled Spherical Sandwich Shell as a Biodynamic Head Injury Model for Primates. Aviation, Space, and Environmental Medicine, pp. 120-124.
407. Kao, R.; Perrone, N. 1970. Stresses in Spherical Shells Due to Local Loading. Washington, DC: The Catholic University of American, Report No. 71-4.

TOLERANCES

408. Eiband, A.M. 1959. Human Tolerance to Rapidly Applied Accelerations: A Summary of the Literature. Cleveland: NASA Lewis Research Center. NASA Memorandum 5-19-59E.
409. Gadd, C.W. 1967. Use of a Weighted Impulse Criterion for Estimating Injury Hazard. In: 10th Stapp Car Crash Conference Proceedings, 8-9 November, Alamogordo, New Mexico, pp. 164-174. New York: SAE Paper No. 660793.
410. Gennarelli, T.A.; Abel, J.M.; Adams, H.; Graham, D. 1979. Differential Tolerance of Frontal and Temporal Lobes to Contusion Induced by Angular Acceleration. In: 23rd Stapp Car Crash Conference Proceedings, 17-19 October, San Diego, pp. 563-586. SAE Paper No. 791022.
411. Gurdjian, E.S.; Roberts, V.L.; Thomas, L.M. 1966. Tolerance Curves of Acceleration and Intracranial Pressure Protective Index in Experimental Head Injury. Journal of Trauma 6(5):600-604.

412. Hess, R.L.; Weber, K.; Melvin, J.W. 1980. Review of Literature and Regulation Relating to Head Impact Tolerance and Injury Criterion, UM-HSRI-80-52-1, July.
413. Hirsch, A.E.; Ommaya, A.K., Mahone, R.H. 1970. Tolerance of Sub-human Primate Brain to Cerebral Concussion. In: Impact Injury and Crash Protection, Springfield, IL: Charles C. Thomas, pp. 352-369.
414. Hodgson, V.R.; Thomas, L.M. 1975. Head Injury Tolerance. In: Aircraft Crashworthiness, Charlottesville, VA: University Press of Virginia, pp. 175-193.
415. Hodgson, V.R. 1973. Head Model for Impact Tolerance. In: Human Impact Response - Measurement and Simulation. Proceedings of the Symposium on Human Impact Response, 2-3 October 1972. Warren, MI:, pp. 113-128. New York: Plenum Press.
416. Hodgson, V.R. 1967. Tolerance of the Facial Bones to Impact. American Journal of Anatomy 120:113-122.
417. Melvin, J.W.; Fuller, P.M.; Darriell, R.P.; Paviscak, G.M. 1969. Human Head and Knee Tolerance to Localized Impacts. Society of Automotive Engineers Mid-Year Meeting, 19-23 May 1969, Chicago. New York: SAE Paper No. 690477.
418. Nahum, A.M.; Gatts, J.D.; Gadd, C.W.; Danforth, J. 1968. Impact Tolerance of the Skull and Face. In: 12th Stapp Car Crash Conference Proceedings, 22-23 October, Detroit, pp. 302-316. New York: SAE Paper No. 680785.
419. Ommaya, A.K.; Fisch, F.J.; Malone, R.M.; Corrao, P.; Letcher, F. 1970. Comparative Tolerances for Cerebral Concussion by Head Impact and Whiplash Injury in Primates. In: 1970 International Automobile Safety Conference Compendium, 13-15 May 1970, Detroit; 8-11 June 1970, Brussels, pp. 808-817. New York: SAE Paper No. 700401.
420. Society of Automotive Engineers. 1980. Human Tolerance to Impact Conditions as Related to Motor Vehicle Design, New York: SAE Handbook Supplement, J885 Apr80.
421. Society of Automotive Engineers. 1966. Human Tolerance to Impact Conditions as Related to Motor Vehicle Design. SAE Handbook 1968, pp. 911-913. New York: SAE J885a.
422. Stalnaker, R.L.; McElhaney, J.H. 1970. Head Injury Tolerance for Linear Impacts by Mechanical Impedance Methods. American Society of Mechanical Engineers Winter Annual Meeting, 29 November - 3 December 1970, New York. New York: ASME Paper No. 70-WA/BHF-4.

423. Stalnaker, R.L.; Roberts, V.L.; McElhaney, J.H. 1973. Side Impact Tolerance to Blunt Trauma. In: 17th Stapp Car Crash Conference Proceedings, 12-13 November, Oklahoma City, pp. 377-408. New York: SAE Paper No. 730979.
424. Stapp, J.P. 1961. Human Tolerance to Severe, Abrupt Deceleration. In: Gravitational Stress in Aerospace Medicine, Boston: Little Brown, pp. 165-188.
425. Stapp, J.P. 1955. Tolerance to Abrupt Deceleration. AGARDograph 6:122-169.
426. Swearingen, J.J. 1965. Tolerances of the Human Face to Crash Impact, Oklahoma City: Civil Aeromedical Research Institute.

INTRACRANIAL PRESSURE

427. Gurdjian, E.S., et al. 1961. Intracranial Pressure and Acceleration Accompanying Head Impacts in Human Cadavers. Surgery, Gynecology, and Obstetrics, 113:185-190.
428. Gurdjian, E.S., et al. 1953. Quantitative Determination of Acceleration and Intracranial Pressure in Experimental Head Injury Preliminary Report. Neurology, 3(6):417-423.
429. Lissner, H.R.; Lebow, M.; Evans, F.G. 1960. Experimental Studies on the Relation between Acceleration and Intracranial Pressure Changes in Man. Surgery, Gynecology, and Obstetrics. 111:329-338.
430. Nahum, A.M., et al. 1979. Intracranial Pressure Relationships in the Protected and Unprotected Head. In: 23rd Stapp Car Crash Conference Proceedings, pp. 613-636.
431. Nusholtz, G.S.; Axelrod, J.B.; Melvin, J.W.; Ward, C.C. 1979. Comparison of Epidural Pressure in Live Anesthetized and Post-Mortem Primates. In: 7th International Workshop on Human Subjects for Biomechanical Research Proceedings, pp. 175-200. Washington, DC: Distributed by National Highway Traffic Safety Administration.
432. Roberts, V.L.; Hodgson, V.R.; Thomas, L.M. 1967. Fluid Pressure Gradients Caused by Impact to the Human Skull. In: Biomechanics Monograph, pp. 223-235. New York: American Society of Mechanical Engineers.
433. Ward, C.; Chan, M.; Nahum, A. 1980. Intracranial Pressure - A Brain Injury Criterion. In: 24th Stapp Car Crash Conference Proceedings. SAE Paper No. 801304.

DIFFERENTIAL MOVEMENT

434. Gennarelli, T.A., et al. 1979. Differential Tolerance of Frontal and Temporal Lobes to Contusion Induced by Angular Acceleration. In: 23rd Stapp Car Crash Conference Proceedings, 17-19 October, San Diego, pp. 563-586. SAE Paper No. 791022.

CLOSED HEAD INJURY/HIC

435. Chan, H.S. 1974. Mathematical Model for Closed Head Impact. In: 18th Stapp Car Crash Conference Proceedings, pp. 557-578. SAE Paper No. 741191.
436. Ewing, C.L., et al. 1976. The Effect of Duration, Rate of Onset and Peak Acceleration on the Dynamic Response of the Human Head and Neck. In: 20th Stapp Car Crash Conference Proceedings.
437. Gurdjian, E.S.; Webster, J.E. 1953. Recent Advances in the Knowledge of the Mechanism, Diagnosis, and Treatment of Head Injury. American Journal of Medical Sciences 226:214-220.
438. Kopecky, J.A.; Ripperger, E. 1969. Closed Brain Injuries: An Engineering Analysis. Journal of Biomechanics, 2(1):250-260, March.
439. Liu, Y.K. 1978. Biomechanics of Closed Head Impact. Journal of Engineering Mechanics, Div. Am. Soc. Civil Eng., 104(EM1):131-152.
440. Nahum, A.M.; Smith, R.W. 1976. An Experimental Model for Closed Head Impact Injury. In: 20th Stapp Car Crash Conference Proceedings, pp. 783-814. SAE Paper No. 760825.

HUMAN SURROGATE HEAD IMPACT TRAUMA TEST PROTOCOL REFERENCES

441. Anderson, D.W.; Miller, J.D.; Kalsbeek, W.D. 1983. Findings from a Major Survey of Persons Hospitalized with Head Injuries. Public Health Reports, 98(5):475-478.
442. Insurance Institute for Highway Safety, 1982. The Year's Work, 1981-1982. Washington, DC.
443. Kraus, J.F., et al. 1984. The Incidence of Acute Brain Injury and Serious Impairment in a Defined Population. American Journal of Epidemiology. 19(2):186-201.
444. Thomas, D.J.; Robbins, D.H.; Eppinger, R.H.; King, A.I.; and Hubbard, R.P. 1974. Guidelines for the Comparison of Human and Human Analogue Biomechanical Data. A report of an ad hoc committee, Ann Arbor, Michigan, December 6.

445. Abel, J.M.; Gennarelli, T.A.; Segawa, H. 1978. Incidence and Severity of Cerebral Concussion in the Rhesus Monkey Following Sagittal Plane Angular Acceleration. In: 22nd Stapp Car Crash Conference Proceedings, 24-26 October 1978, Ann Arbor, MI., Warrendale, PA: SAE Paper No. 780886, pp. 35-53.
446. Adams, J.H.; Graham, D.I.; Gennarelli, T.A. 1981. Acceleration Induced Head Injury in the Monkey. II Neuropathology. In: K. Jellinger, F. Gullotta, M. Mossakowski, eds., Experimental Clinical Neuropathology. Acta Neuropathol. (Berl.) Suppl. vii, pp. 26-28.
447. Aldman, B.; Thorngren, L.; Ljung, C. 1981. Patterns of Deformation in Brain Models Under Rotational Motion. In: DOT, NHTSA, Head and Neck Injury Criteria, Washington, DC.
448. Alem, N.M. 1974. Simulation of Head Injury Due to Combined Rotation and Translation of the Brain. In: 18th Stapp Car Crash Conference Proceedings, pp. 579.
449. Chan, M.; Ward, C. 1981. Relative Importance of Skull Deformation. Proceedings ASME. Biomechanics Symposium, June 22-24.
450. Engin, A.E. 1969. Axisymmetric Response of a Fluid-filled Spherical Shell to a Local Radial Impulse--A Model for Head Injury. Journal of Biomechanics 2(3):395-341.
451. Engin, A.E.; Akkas, N. 1978. Application of a Fluid-filled Spherical Sandwich Shell as a Biodynamic Head Injury Model for Primates. Aviation, Space and Environmental Medicine, pp. 120-124.
452. Evans, F.G.; Lissner, H.R.; Lebow, M. 1958. The Relation of Energy, Velocity and Acceleration to Skull Deformation and Fracture. Surgery, Gynecology, and Obstetrics, 107:593-601.
453. Ewing, C.L.; Thomas, D.J. 1972. Human Head and Neck Response to Impact Acceleration. Naval Aerospace Medical Research Laboratory Detachment, New Orleans, Monograph 21, August.
454. Ewing, C.L.; Thomas, D.J. 1973. Torque Versus Angular Displacement Response of Human Head to -Gx Impact Acceleration. In: 17th Stapp Car Crash Conference Proceedings, SAE Paper No. 730976.
455. Ewing, C.L., et al. 1975. The Effect of the Initial Position of the Head and Neck on the Dynamic Response of the Human Head and Neck to -Gx Impact Acceleration. In: 19th Stapp Car Crash Conference Proceedings, SAE Paper No. 751157.

456. Gennarelli, T.A., et al. 1979. Differential Tolerance of Frontal and Temporal Lobes to Contusion Induced by Angular Acceleration. In: 23rd Stapp Car Crash Conference Proceedings, 17-19 October, San Diego, pp. 563-586. SAE Paper No. 791022.
457. Gennarelli, T.A.; Adams, J.H.; Graham, D.I. 1981. Acceleration Induced Head Injury in the Monkey. 1. The Model Its Mechanical and Physiological Correlates. In: K. Jellinger, F. Gullotta, M. Mossakowski, eds., Experimental Clinical Neuropathology. Acta Neuropathol. (Berl.) Suppl. VII, pp. 23-25.
458. Gennarelli, T.A., et al. 1982. Diffuse Axonal Injury and Traumatic Coma in the Primate. Ann. Neurol. 12:564-574.
459. Gurdjian, E.S., et al. 1961. Intracranial Pressure and Acceleration Accompanying Head Impacts in Human Cadavers. Surgery, Gynecology, and Obstetrics, 113:185-190.
460. Gurdjian, E.S., et al. 1968. Significance of Relative Movements of Scalp, Skull, and Intracranial Contents During Impact Injury of the Head. Journal of Neurosurgery 29(1):70-72.
461. Higgins, L.S.; Schmall, R.A. 1967. A Device for the Investigation of Head Injury Effected by Non-Deforming Head Accelerations. In: 11th Stapp Car Crash Conference Proceedings, pp. 35-46.
462. Hodgson, V.R.; Thomas, L.M. 1979. Acceleration Induced Shear Strains on a Monkey Brain Hemisection. In: 23rd Stapp Car Crash Conference Proceedings, 17-19 October, San Diego, CA, pp. 589-611. SAE Paper No. 791023.
463. Hosey, R.R.; Liu, Y.K. 1982. A Homeomorphic Finite Element Model of the Human Head and Neck. In: R. H. Gallagher, et al., Finite Elements in Biomechanics, NY: John Wiley and Sons, Ltd., pp. 379-401.
464. Khalil, T.B.; Hubbard, R.P. 1977. Parametric Study of Head Response by Finite Element Modeling. Journal of Biomechanics, 10(2):119-132.
465. Lissner, H.R.; Lebow, M.; Evans, F.G. 1960. Experimental Studies on the Relation Between Acceleration and Intracranial Pressure Changes in Man. Surgery, Gynecology, and Obstetrics. 111:329-338.
466. Lowenhielm, P. 1974. Strain Tolerance of the W. Cerebri Sup. (bridging veins) Calculated From Head-on Collision Tests With Cadavers. Z. Rechtsmedizin 75:131-144.

467. McElhaney, J.H.; Stalnaker, R.L.; Roberts, V.L. 1972. Biomechanical Aspects of Head Injury. In: W. F. King and H. J. Mertz, eds., Human Impact Response: Measurement and Simulation, N.Y.: Plenum Press.
468. Nahum, A.M.; Smith, R.W. 1976. An Experimental Model for Closed Head Injury. In: 20th Stapp Car Crash Conference Proceedings, SAE Paper No. 760825.
469. Nahum, A.; Smith, R.W.; Ward, C.C. 1977. Intracranial Pressure Dynamics During Head Impact. In: 21st Stapp Car Crash Conference Proceedings, pp. 337-366.
470. Nusholtz, G.S.; Melvin, J.W.; Alem, N.M. 1979. Head Impact Response Comparisons of Human Surrogates. In: 23rd Stapp Car Crash Conference Proceedings, 17-19 October, San Diego, CA., pp. 499-541. SAE Paper No. 791020.
471. Nusholtz, G.S.; Melvin, J.W.; Lux, P. 1983. The Influence of Impact Energy and Direction on Thoracic Response. In: 27th Stapp Car Crash Conference Proceedings, pp. 69-94.
472. Nusholtz, G.S., et al. 1979. Comparison of Epidural Pressure in Live Anesthetized and Post-Mortem Primates. In: 7th International Workshop on Human Subjects for Biomechanical Research Proceedings, 16 October 1979, Coronado, CA., pp. 175-200. Washington, DC: Distributed by National Highway Traffic Safety Administration.
473. Ommaya, A.K.; Hirsch, A.E.; Flamin, E.S.; Mahone, R.H. 1966. Cerebral Concussion in the Monkey: An Experimental Model. Science, 153:211-212.
474. Ono, K.; Kikuchi, K.; Nakamura, M. 1980. Human Head Tolerance to Sagittal Impact Reliable Estimation Deduced from Experimental Head Injury Using Subhuman Primates and Human Cadaver Skulls. In: 24th Stapp Car Crash Conference Proceedings, 15-17 October, Troy, MI., pp. 104-160. SAE Paper No. 801300.
475. Padgaonkar, A.J.; Krieger, K.W.; King, A.I. 1975. Measurement of Angular Accelerations of a Rigid Body Using Linear Accelerations. ASME Preprint-75-APM3, June.
476. Roberts, V.L.; Hodgson, V.R.; Thomas, L.M. 1967. Fluid Pressure Gradients Caused by Impact to the Human Skull. In: Biomechanics Monograph, pp. 223-235. New York: American Society of Mechanical Engineers.
477. Sances, A., et al. 1984. Biodynamics of Vehicular Injuries. In: G. A. Peters and B. J. Peters, Eds., Automotive Engineering and Litigation, New York: Garland Law Publishing, pp. 449-550.

478. Shugar, T. A. 1975. Transient Structural Response of the Linear Skull-Brain System. In: 19th Stapp Car Crash Conference Proceedings, pp. 581-614.
479. Stalnaker, R.L., et al. Door Crashworthiness Criteria. Final Report. 1971. Contract No. FH-11-7288, U. S. Department of Transportation, National Highway Traffic Safety Administration, Washington, DC.
480. Stalnaker, R.L., et al. 1977. Head Impact Response. In: 21st Stapp Car Crash Conference Proceedings, 19-21 October, New Orleans, pp. 303-335. SAE Paper No. 770921.
481. Thomas, L.M., et al. 1968. Static Deformation and Volume Changes in the Human Skull. In: 12th Stapp Car Crash Conference Proceedings, pp. 260-270.
482. Unterharnscheidt, F. 1983. Neuropathology of Rhesus Monkey Undergoing -gx Impact Acceleration. In: C. L. Ewing, et al., eds., Impact Injury of the Head and Spine, Springfield, IL: Thomas, pp. 94-176.
483. Ward, C.C.; Chan, M.; Nahum, A. 1980. Intracranial Pressure - A Brain Injury Criterion. In: 24th Stapp Car Crash Conference Proceedings. SAE Paper No. 801304.
484. Ward, C.C.; Nikravesh, P.E.; Thompson, R.B. 1978. Biodynamic Finite Element Models Used in Brain Injury Research. Journal of Aviation, Space and Environmental Medicine, 49(1).
485. Nusholtz, G.S., et al. 1980. Thoraco-Abdominal Response and Injury. In: 24th Stapp Car Crash Conference Proceedings, pp. 187-228.
486. Nusholtz, G.S., et al. 1983. Cervical Spine Injury Mechanisms. In: 27th Stapp Car Crash Conference Proceedings, pp. 179-188.
487. Alem, N.M.; Melvin, J.W.; Holstein, G.L. 1978. Biomechanics Applications of Direct Linear Transformation in Close-Range Photogrammetry. Proceedings of the Sixth New England Bioengineering Conference, New York: Pergamon Press.
488. Bender, M.; Melvin, J.W.; Stalnaker, R.L. 1976. A High-Speed Cineradiograph Technique for Biomechanical Impact. In: 20th Stapp Car Crash Conference Proceedings, SAE Paper No. 760824.
489. Bishop, R.L.; Goldberg, S.I. 1968. Tensor Analysis on Manifolds, New York, MacMillan.
490. Cartan, E. 1946. Lecons sur la Geometrie des Espaces de Rieman, Second Edition, Paris, Gauthier Villars.
491. O'Neill, B. 1967. Elementary Differential Geometry, New York, Academic Press.

492. Stoker, J.J. 1959. Differential Geometry, New York, Wiley Intersciences.
493. Harris, C.M.; Crede, C.E. 1976. Shock and Vibration Handbook. New York, McGraw-Hill Book Company.
494. Hartman, C.G.; Straus, Jr., W.L., eds. The Anatomy of the Rhesus Monkey (Macaca mulatta), New York: Hafner Publishing Co., 1965 edition.
495. Heimer, L. 1983. The Human Brain and Spinal Cord Functional Neuroanatomy and Dissection Guide, New York: Springer-Verlag.
496. Ommaya, A.K. 1973. Head Injury Mechanisms. Final Report. Contract No. DOT-HS-081-1-106IA, U. S. Department of Transportation, National Highway Traffic Safety Administration, Washington, DC.
497. Alem, N.M., Melvin, J.W.; Holstein, G.L. 1978. Biomechanics Applications of Direct Linear Transformation in Close-Range Photogrammetry. Proceedings of the Sixth New England Bioengineering Conference, New York: Pergamon Press.
498. Bender, M.; Melvin, J.W.; Stalnaker, R.L. 1976. A High-Speed Cineradiograph Technique for Biomechanical Impact. In: 20th Stapp Car Crash Conference Proceedings, SAE Paper No. 760824.
499. Bishop, R.L.; Goldberg, S.I. 1968. Tensor Analysis on Manifolds. New York: MacMillan.
500. Cartan, E. 1946. Lecons sur la Geometrie des Espaces de Rieman, Second Edition, Paris: Gauthier Villars.
501. Harris, C.M.; Crede, C.E. 1976. Shock and Vibration Handbook, New York: McGraw-Hill Book Company.
502. Nusholtz, G.S., et al. 1984. Head Impact Response - Skull Deformation and Angular Accelerations. In: 28th Stapp Car Crash Conference Proceedings, pp. 41-74. SAE Paper No. 841657.
503. Nusholtz, G.S., et al. 1983. Cervical Spine Injury Mechanisms. In: 27th Stapp Car Crash Conference Proceedings, pp. 179-188.
504. Nusholtz, G.S., et al. 1980. Thoraco-Abdominal Response and Injury. In: 24th Stapp Car Crash Conference Proceedings, pp. 187-228.
505. Nusholtz, G.S., et al. 1977. Comparison of Epidural Pressure in Live Anesthetized and Post-Mortem Primates. In: 7th International Workshop on Human Subjects for Biomechanical Research Proceedings, pp. 175-200. Washington, DC. Distributed by the National Highway Traffic Safety Administration.

506. Nusholtz, G.S.; Melvin, J.W.; Alem, N.M. 1979. Head Impact Response Comparisons of Human Surrogates. In: 23rd Stapp Car Crash Conference Proceedings, pp. 499-541. SAE Paper No. 791020.
507. Nusholtz, G.S.; Melvin, J.W.; Lux, P. 1983. The Influence of Impact Energy and Direction on Thoracic Response. In: 27th Stapp Car Crash Conference Proceedings.
508. O'Neill, B. 1967. Elementary Differential Geometry. New York: Academic Press.
539. Stoker, J.J. 1969. Differential Geometry. New York: Wiley Intersciences.

9.0 APPENDIX A
ANATOMY OF THE HEAD

OVERVIEW OF THE HEAD

SCALP

The scalp, averaging 5 to 7 mm in thickness, consists not only of the hair and skin but also of layered soft tissues between the skin and the skull. When a traction force is applied to the scalp, its outer three layers (the hair-and-skin layer, a subcutaneous connective tissue layer, and a muscle and facial layer) move together as one. Next there is a loose connective tissue layer plus the fibrous membrane which covers bone (the periosteum). The thickness, firmness, and mobility of the outer three layers of scalp function as protective features.

SKULL

The skull is the most complex structure of the skeleton because bone is neatly molded around and fitted to the brain, eyes, ears, nose and teeth. The thickness of the skull varies between 4-7 mm, snugly accommodating these components of the head and reinforcing the strength of the skull. The skull is composed of eight bones which form the brain case and fourteen bones which form the face plus the teeth. Excluding the face, the cranial vault (calvarium) is formed by the ethmoid, sphenoid, frontal, two temporal, two parietal, and occipital bones. The inner surface of the cranial vault is concave and relatively smooth. The base of the brain case is a thick irregular plate of bone containing depressions and ridges plus small holes for arteries, veins, nerves, and the large hole (the foramen magnum), which is the transition area between the spinal cord and the brain.

THE MEMBRANES MENINGES

Three membranes known as the meninges protect and support the brain and spinal cord (which together comprise the central nervous system).

The meninges separate the brain and spinal cord from the bones which surround them. Consisting primarily of connective tissue, the meninges also form part of the walls of blood vessels and the sheaths of nerves as they emerge from their bony covering.

The membranes meninges are known individually as the dura mater, the arachnoid, and the pia mater. The dura mater is a heavy, tough membrane that surrounds the spinal cord and brain. In the skull it is divided into two layers. The outer cranial layer of dura mater, the periosteal layer, lines the inner surface of the calvarium. The inner layer of cranial dura mater, the meningeal layer, covers the brain. In the brain case, the two layers of dura mater are closely united except where they separate to form sub-structures such as the venous sinuses which drain blood from the brain, the falx cerebri, a fold of the inner layer of dura mater which projects into the longitudinal fissure between the right and left cerebral hemispheres, and the tentorium cerebelli, a fold of the inner layer of dura mater forming a shelf on which the posterior cerebral hemispheres are supported.

The arachnoid layer is a delicate spider web-like membrane which is separated from the dura mater by a narrow space called the subdural space which contains a thin film of watery fluid known as cerebrospinal fluid. In the superior longitudinal sinus (sagittal sinus) and transverse sinuses, the arachnoid mater forms structures called arachnoid granulations which reabsorb cerebrospinal fluid into the blood. The arachnoid mater extends down the spinal canal to the level of the second sacral vertebra where it surrounds the terminal filament of the spinal cord.

The pia mater is a thin membrane of fine connective tissue filled with numerous small blood vessels. It is separated from the arachnoid by a space filled with cerebrospinal fluid known as the subarachnoid space. The pia mater covers the surface of the brain, dipping well into its furrows. The pia mater covering the spinal cord is thicker than the cranial pia mater and it becomes the terminal filament of the spinal cord.

CEREBROSPINAL FLUID

The subarachnoid space and the ventricles of the brain are filled with a clear, watery, colorless fluid (cerebrospinal fluid/CSF), which provides some nutrients for the brain and which cushions the brain from mechanical shock. For normal movement, a shrinking or expanding of the brain is quickly balanced by an increase or decrease of CSF. The specific gravity of cerebrospinal fluid is about 1.008 in the adult. About 140 ml of CSF constantly circulates so that it surrounds the brain on all sides, serving as a buffer and helping to support the brain's weight. Since the subarachnoid space of the brain is continuous with that of the spinal cord, the spinal cord is suspended in a tube of CSF.

CENTRAL NERVOUS SYSTEM

Microscopically, the central nervous system is largely a network of neurons and supportive tissue functionally arranged into areas which are gray or white in color. Named for this color distinction, gray matter is composed primarily of nerve cell bodies concentrated in locations on the surface of the brain and also deep within the brain; white matter is composed of myelinated nerve cell processes which primarily form tracts to connect parts of the central nervous system to each other. There is

a difference in density between gray matter and white matter.

Macroscopically, the CNS is the brain and the spinal cord.

THE BRAIN

The brain is structurally and functionally five parts--cerebrum, cerebellum, midbrain, pons, and medulla oblongata plus four ventricles (CSF cisterns with exits); three membranes (meninges); two glands (pituitary and pineal); twelve pairs of cranial nerves; and the cranial arteries and veins. The brain snugly fills the cranial cavity. The average length of the brain is about 165 mm and its greatest transverse diameter is about 140 mm. Due to dimorphic differences, its average mass is 1360 gm for males and a little less for females. The adult brain represents about 2 percent of the weight of the body. The specific gravity of the brain averages 1.036 and it is gelatinous in consistency. The brain constitutes 98 percent of the central nervous system. The adult brain represents about 2 percent of the weight of the body. Looking down on the brain from above, the cerebrum is two cerebral hemispheres which conceal the rest of the brain. Behind and below the cerebral hemispheres lie the two hemispheres of the cerebellum. Beneath the cerebrum and cerebellum are the smaller midbrain, pons, and medulla oblongata.

CEREBRUM

The cerebrum is $\frac{7}{8}$ ths of the brain's mass, and is hemisected into right and left cerebral hemispheres. These are incompletely separated by a deep midline cleft called the longitudinal cerebral fissure. The falx cerebri projects downwards into this fissure. Beneath the longitudinal cerebral fissure the two cerebral hemispheres are connected by a mass of white matter called the corpus callosum.

Within each cerebral hemisphere is a cistern for cerebrospinal fluid called the lateral ventricle. Each cerebral hemisphere has a surface layer of gray matter called the cerebral cortex. The cerebral cortex is arranged into a number of folds, which are separated by fissures. These fissures further separate the cerebral hemispheres into lobes so that each hemisphere is divided into four lobes, each lobe being named by its association to the nearest cranial bone. Thus, the four lobes are the frontal, parietal, temporal and occipital lobes.

The interior of each cerebral hemisphere is composed of white matter or nerve fibers. These are arranged in tracts and serve to connect one part of a cerebral hemisphere with another, or to connect the cerebral hemispheres to each other, or to connect the cerebral hemispheres to the other parts of the central nervous system. In addition, within these interior areas of white matter are a number of areas of gray matter.

MIDBRAIN

The midbrain connects the cerebral hemispheres above to the pons below. Anteriorly the midbrain is composed of two stalks which are mainly fibers passing to and from the cerebral hemispheres above. Within the midbrain is a narrow canal which connects the third ventricle above to the fourth ventricle below.

PONS

The pons lies below the midbrain, in front of the cerebellum and above the medulla oblongata. It is composed of white matter nerve fibers connecting the cerebellar hemispheres. Lying deeply within its white matter are areas of gray matter which are nuclei for some of the cranial nerves.

MEDULLA OBLONGATA

The medulla oblongata appears continuous with the pons above and the spinal cord below. In the lower part of the medulla oblongata motor fibers cross from one side to the other so that fibers from the right cerebral cortex pass to the left side of the body. Some sensory fibers passing upwards towards the cerebral cortex also cross from one side to the other in the medulla oblongata. The medulla oblongata also contains areas of gray matter within its white matter. These are nuclei for cranial nerves and relay stations for sensory fibers passing upwards from the spinal cord.

CEREBELLUM

The cerebellum lies behind the pons and the medulla oblongata. Its two hemispheres are joined at the midline by a narrow strip-like structure called the vermis. The outer cortex of the cerebellar hemispheres is gray matter; the inner cortex is white matter. The outer surface of the cerebellum forms into narrow folds separated by deep fissures. Nerve fibers enter the cerebellum in three pairs of stalks which connect the cerebellar hemispheres to the midbrain, pons, and the medulla oblongata.

SPINAL CORD

The spinal cord comprises 2 percent of the central nervous system and averages 45 cm in length. Thirty-one pairs of nerves arise from the spinal cord. The spinal cord is protected by the spinal column, the membranes meninges, and pressurized CSF. The spinal dura mater forms a one-layer loose protective covering for the spinal cord and corresponds to the inner layer of cranial dura mater. The space between the bones

of the spinal column and the dura mater, the extradural space, is filled with fat and a venous network.

10.0 APPENDIX B
TEST PROTOCOL

DEPARTMENT OF TRANSPORTATION

MULTIPLE IMPACT TESTS

_____ Through _____

as performed by

the Biomechanics Department of

the Highway Safety Research Institute

Ann Arbor, Michigan

1982-1983 E Series

This protocol for the use of cadavers in this test series was approved by the Committee to Review Grants for Clinical Research of the University of Michigan Medical Center and follows guidelines established by the U.S. Public Health Service and those recommended by the National Academy of Sciences, National Research Council.

TABLE OF CONTENTS

Head Impact	2
Head Impact	4
Front Tap	6
Left Side Tap	8
Left Side Tap - Arms Up	10
Left Side Tap - Arms Down	12
Left Side Impact	14
Pelvic Impact	16
PRE-SURGERY	24
ANTHROPOMETRY	25
Anatomical Anomalies	26
MOUNTS	27
Rib and Sternum Mounts	27
Pressurization	28
Head 9-AX Mount	31
Head Transducers	32
Pelvis Mount	34
Spinal Mounts	36
Cerebrospinal Pressurization	37
POST-SURGERY	38
X-Ray	38
Preparation	38
ELECTRONICS	39
PRETEST TRIAL RUN	39
HEAD IMPACT 1	40
Final Checklist	43

HEAD IMPACT 2	44
Timer Box Setup	45
Final Checklist	46
THORAX TAPS	47
Thorax Front Tap	47
Timer Box Setup	49
Final Checklist	50
45° Thorax Tap	51
Timer Box Setup	53
Final Checklist	54
Optional Arms-Up Thorax Tap	55
Timer Box Setup	57
Final Checklist	58
Arms-Down Thorax Tap	59
Timer Box Setup	61
Final Checklist	62
THORAX IMPACT	63
Timer Box Setup	64
Final Checklist	65
PELVIS IMPACT	66
Timer Box Setup	68
Final Checklist	69
POST TEST PROCEDURE	70
AUTOPSY	72
APPENDICES	75
Anatomy Room Setup	76
Sled Lab Setup	80

Cart Setup	81
Autopsy Setup	83
Timer Box Setup	85
Pendulum Wierdness	86

TEST DESCRIPTION

Cadaver No. _____ Sex: _____ Height: _____ Weight: _____

Test No. _____ (Head, Shoulder, Pelvis)

Test

description: Head impact, subject in a normal seated
position, neck angle approx. 10° forward, impact to

forehead, angle of head determined by tangent forehead
plane.

Type of Impactor: PENDULUM

Type of Bumper: WHITE VIBRATHANE

Type of Striker: 25 Kg PISTON, 15cm DIA.

Impactor Angle: 50° (5.0m/s)

Padding: _____

Pre-Impact Travel: 14cm

Post-Impact Travel: 16cm

35mm stills:

 Black and White

 Color

CAMERAS

POSITION

Photosonics 1: 1000

 P-A, S-I

Photosonics 2:

HyCam: 3000

 P-A, S-I

INSTRUMENTATION

ACCELEROMETERS

TARGETS

TRANSDUCERS

Head (9 AX)	<u>X</u>	Head	<u>X</u>	Trachea	<u> </u>
Up. Sternum (3-AX)	<u> </u>	Acromion	<u>X</u>	Ascending Aorta	<u> </u>
Lwr. Sternum (1)	<u> </u>	Sternum (2)	<u> </u>	Internal Carotid	<u>X</u>
Spine (2 triax)	<u>X</u>	Spine	<u> </u>		
Pelvis (9 AX)	<u> </u>	Pelvis	<u> </u>	Subdural 1:	<u>X</u>
Lwr. Rib R8 (2)	<u> </u>			2:	<u>X</u>
Up. Rib R4 (2 triax)	<u> </u>			3:	<u>X</u>
				4:	<u>?</u>

Test Description - 3

TEST DESCRIPTION

Cañaver No. _____ Sex: _____ Height: _____ Weight: _____

Test No. _____ (Head, Shoulder, Pelvis)

Test description: _____
Head impact, same as previous.

Type of Impactor: PENDULUM

Type of Bumper: WHITE VIBRATHANE

Type of Striker: 25 Kg PISTON, 15cm DIA.

Impactor Angle: 50° (5.0m/s)

Padding: _____

Pre-Impact Travel: 14cm

Post-Impact Travel: 16cm

35mm stills:

 Black and White

 Color

CAMERAS	POSITION
Photosonics 1: <u>1000</u>	<u>P-A, S-I</u>
Photosonics 2: _____	_____
HyCam: <u>3000</u>	<u>P-A, S-I</u>

INSTRUMENTATION

ACCELEROMETERS

TARGETS

TRANSDUCERS

Head (9 AX)	<u>X</u>	Head	<u>X</u>	Trachea	___
Up. Sternum (3-AX)	___	Acromion	<u>X</u>	Ascending Aorta	___
Lwr. Sternum (1)	___	Sternum (2)	___	Internal Carotid	<u>X</u>
Spine (2 triax)	<u>X</u>	Spine	___		
Pelvis (9 AX)	___	Pelvis	___	Subdural 1:	<u>X</u>
Lwr. Rib R8 (2)	___			2:	<u>X</u>
Up. Rib R4 (2 triax)	___			3:	<u>X</u>
				4:	<u>?</u>

COMMENTS:

TEST DESCRIPTION

Cadaver No. _____ Sex: _____ Height: _____ Weight: _____

Test No. _____ (Head, Shoulder, Pelvis)

Test description: Front tap, mid-sternum, angle of thorax
determined by sternum tangent plane, top of impact 54 cm
from seat pan.

Type of Impactor: PENDULUM

Type of Bumper: WHITE VIBRATHANE

Type of Striker: 25 Kg PISTON, 21cm. sq.

Impactor Angle: 17° (2m/s)

Padding: .5cm ensolite

Pre-Impact Travel: 8cm

Post-Impact Travel: 22cm

35mm stills:

 Black and White

 Color

CAMERAS	POSITION
Photosonics 1: <u>1000</u>	<u>P-A, S-I</u>
Photosonics 2: _____	_____
HyCam: <u>3000</u>	<u>P-A, S-I</u>

INSTRUMENTATION

ACCELEROMETERS

TARGETS

TRANSDUCERS

Head (9-AX)	<u>X</u>	Head	<u>X</u>	Trachea	<u>X</u>
Up. Sternum (3-AX)	<u>X</u>	Acromion	<u>X</u>	Ascending Aorta	<u>X</u>
Lwr. Sternum (1)	<u>X</u>	Sternum (2)	<u>X</u>	Internal Carotid	___
Spine (2 triax)	<u>X</u>	Spine	___		
Pelvis (9-AX)	___	Pelvis	___	Subdural 1:	___
Lwr. Rib R8 (2)	<u>X</u>			2:	___
Up. Rib R4 (2 triax)	<u>X</u>			3:	___
				4:	___

COMMENTS:

TEST DESCRIPTION

Cadaver No. _____ Sex: _____ Height: _____ Weight: _____

Test No. _____ (Head, Shoulder, Pelvis)

Test description: Left side tap, 45° P-A into R-L,
normal seated posture, move arm if

necessary, top of impact 54 cm above seat pan.

Type of Impactor: PENDULUM

Type of Bumper: WHITE VIBRATHANE

Type of Striker: 25 Kg PISTON, 21cm. sq.

Impactor Angle: 17° (2m/s)

Padding: .5cm ensolite

Pre-Impact Travel: 8cm

Post-Impact Travel: 22cm

35mm stills:

 Black and White

 Color

CAMERAS

POSITION

Photosonics 1: 1000

45° P-A into R-L, S-I

Photosonics 2: _____

HyCam: 3000

45° P-A into R-L, S-I

INSTRUMENTATION

ACCELEROMETERS

TARGETS

TRANSDUCERS

Head (9-AX)	<u>X</u>	Head	<u>X</u>	Trachea	<u>X</u>
Up. Sternum (3-AX)	<u>X</u>	Acromion	<u>X</u>	Ascending Aorta	<u>X</u>
Lwr. Sternum (1)	<u>X</u>	Sternum (2)	<u>X</u>	Internal Carotid	___
Spine (2 triax)	<u>X</u>	Spine	___		
Pelvis (9-AX)	___	Pelvis	___	Subdural 1:	___
Lwr. Rib R8 (2)	<u>X</u>			2:	___
Up. Rib R4 (2 triax)	<u>X</u>			3:	___
				4:	___

COMMENTS:

TEST DESCRIPTION

Cadaver No. _____ Sex: _____ Height: _____ Weight: _____

Test No. _____ (Head, Shoulder, Pelvis)

Test description: Left side tap arms up,
position arms to minimize interference from scapula

as well as centering piston in the R-L/I-S plane,

normal seated posture. Top of impact 54 cm

above seat pan. (This test may be dropped.)

Type of Impactor: PENDULUM

Type of Bumper: WHITE VIBRATHANE

Type of Striker: 25 Kg PISTON, 21cm sq.

Impactor Angle: 17° (2m/s)

Padding: .5cm ensolite

Pre-Impact Travel: 8cm

Post-Impact Travel: 22cm

35mm stills:

 Black and White

 Color

CAMERAS	POSITION
Photosonics 1: <u>1000</u>	<u>R-L, S-I</u>
Photosonics 2: _____	_____
HyCam: <u>3000</u>	<u>R-L, S-I</u>

INSTRUMENTATION

ACCELEROMETERS

TARGETS

TRANSDUCERS

Head (9-AX)	<u>X</u>	Head	<u>X</u>	Trachea	<u>X</u>
Up. Sternum (3-AX)	<u>X</u>	Acromion	<u>X</u>	Ascending Aorta	<u>X</u>
Lwr. Sternum (1)	<u>X</u>	Sternum (2)	<u>X</u>	Internal Carotid	—
Spine (2 triax)	<u>X</u>	Spine	—		
Pelvis (9-AX)	—	Pelvis	—	Subdural 1:	—
Lwr. Rib R8 (2)	<u>X</u>			2:	—
Up. Rib R4 (2 triax)	<u>X</u>			3:	—
				4:	—

COMMENTS:

TEST DESCRIPTION

Cadaver No. _____ Sex: _____ Height: _____ Weight: _____

Test No. _____ (Head, Shoulder, Pelvis)

Test description: Left side tap arms down, normal
seated posture, in the R-L/I-S

plane, top of impact 54 cm above seat pan.

Type of Impactor: PENDULUM

Type of Bumper: WHITE VIBRATHANE

Type of Striker: 25 Kg PISTON, 21cm sq.

Impactor Angle: 17° (2m/s)

Padding: .5cm ensolite

Pre-Impact Travel: 8cm

Post-Impact Travel: 22cm

35mm stills:

 Black and White

 Color

CAMERAS	POSITION
Photosonics 1: <u>1000</u>	<u>R-L, S-I</u>
Photosonics 2: _____	_____
HyCam: <u>3000</u>	<u>R-L, S-I</u>

INSTRUMENTATION

ACCELEROMETERS

TARGETS

TRANSDUCERS

Head (9-AX)	<u>X</u>	Head	<u>X</u>	Trachea	<u>X</u>
Up. Sternum (3-AX)	<u>X</u>	Acromion	<u>X</u>	Ascending Aorta	<u>X</u>
Lwr. Sternum (1)	<u>X</u>	Sternum (2)	<u>X</u>	Internal Carotid	___
Spine (2 triax)	<u>X</u>	Spine	___		
Pelvis (9-AX)	___	Pelvis	___	Subdural 1:	___
Lwr. Rib R8 (2)	<u>X</u>			2:	___
Up. Rib R4 (2 triax)	<u>X</u>			3:	___
				4:	___

COMMENTS:

TEST DESCRIPTION

Cadaver No. _____ Sex: _____ Height: _____ Weight: _____

Test No. _____ (Head, Shoulder, Pelvis)

Test description: Left side impact, same as left side
arms down tap.

Type of Impactor: PENDULUM

Type of Bumper: WHITE VIBRATHANE

Type of Striker: 25 Kg PISTON, 21cm sq.

Impactor Angle: 100° (8.8m/s)

Padding: 15cm APR pads

Pre-Impact Travel: 9cm

Post-Impact Travel: 21cm

35mm stills:

 Black and White

 Color

CAMERAS	POSITION
Photosonics 1: <u>1000</u>	<u>R-L, S-I</u>
Photosonics 2: _____	_____
HyCam: <u>3000</u>	<u>R-L, S-I</u>

INSTRUMENTATION

ACCELEROMETERS

TARGETS

TRANSDUCERS

Head (9-AX)	<u>X</u>	Head	<u>X</u>	Trachea	<u>X</u>
Up. Sternum (3-AX)	<u>X</u>	Acromion	<u>X</u>	Ascending Aorta	<u>X</u>
Lwr. Sternum (1)	<u>X</u>	Sternum (2)	<u>X</u>	Internal Carotid	___
Spine (2 triax)	<u>X</u>	Spine	___		
Pelvis (9-AX)	___	Pelvis	___	Subdural 1:	___
Lwr. Rib R8 (2)	<u>X</u>			2:	___
Up. Rib R4 (2 triax)	<u>X</u>			3:	___
				4:	___

COMMENTS:

TEST DESCRIPTION

Cadaver No. _____ Sex: _____ Height: _____ Weight: _____

Test No. _____ (Head, Shoulder, Pelvis)

Test Description: Pelvic impact, right side, 8cm anterior to trochanterion, centered on femur.

Type of Impactor: PENDULUM

Type of Bumper: WHITE VIBRATHANE

Type of Striker: 25 Kg PISTON, 15cm DIA.

Impactor Angle: 100° (8.8m/s)

Padding: .5cm ensolite

Pre-Impact Travel: 12cm

Post-Impact Travel: 18cm

35mm stills:

 Black and White

 Color

CAMERAS	POSITION
Photosonics 1: <u>1000</u>	<u>R-L, S-I</u>
Photosonics 2: _____	_____
HyCam: <u>3000</u>	<u>R-L, S-I</u>

INSTRUMENTATION

ACCELEROMETERS

TARGETS

TRANSDUCERS

Head (9-AX)	___	Head	___	Trachea	___
Up. Sternum (3-AX)	___	Acromion	___	Ascending Aorta	___
Lwr. Sternum (1)	___	Sternum (2)	___	Internal Carotid	___
Spine (2 triax)	<u>X</u>	Spine	<u>X</u>		
Pelvis (9-AX)	<u>X</u>	Pelvis	<u>X</u>	Subdural 1:	___
Lwr. Rib R8 (2)	___			2:	___
Up. Rib R4 (2 triax)	___			3:	___
				4:	___

COMMENTS:

TEST DESCRIPTION

Cadaver No. _____ Sex: _____ Height: _____ Weight: _____

Test No. _____ (Head, Shoulder, Pelvis)

Test description: _____

Type of Impactor: _____

Type of Bumper: _____

Type of Striker: _____

Impactor Angle: _____

Padding: _____

Pre-Impact Travel: _____

Post-Impact Travel: _____

35mm stills:

___ Black and White

___ Color

CAMERAS

POSITION

Photosonics 1: _____

Photosonics 2: _____

HyCam: _____

INSTRUMENTATION

ACCELEROMETERS

TARGETS

TRANSDUCERS

Head (9-AX) _____	Head _____	Trachea _____
Up. Sternum (3-AX) _____	Acromion _____	Ascending Aorta _____
Lwr. Sternum (1) _____	Sternum (2) _____	Internal Carotid _____
Spine (2 triax) _____	Spine _____	
Pelvis (9-AX) _____	Pelvis _____	Subdural 1: _____
Lwr. Rib R8 (2) _____		2: _____
Up. Rib R4 (2 triax) _____		3: _____
		4: _____

COMMENTS:

TEST DESCRIPTION

Cadaver No. _____ Sex: _____ Height: _____ Weight: _____

Test No. _____ (Head, Shoulder, Pelvis)

Test description: _____

Type of Impactor: _____

Type of Bumper: _____

Type of Striker: _____

Impactor Angle: _____

Padding: _____

Pre-Impact Travel: _____

Post-Impact Travel: _____

35mm stills:

___ Black and White

___ Color

CAMERAS

POSITION

Photosonics 1: _____

Photosonics 2: _____

HyCam: _____

INSTRUMENTATION

ACCELEROMETERS

TARGETS

TRANSDUCERS

Head (9-AX) _____	Head _____	Trachea _____
Up. Sternum (3-AX) _____	Acromion _____	Ascending Aorta _____
Lwr. Sternum (1) _____	Sternum (2) _____	Internal Carotid _____
Spine (2 triax) _____	Spine _____	
Pelvis (9-AX) _____	Pelvis _____	Subdural 1: _____
Lwr. Rib R8 (2) _____		2: _____
Up. Rib R4 (2 triax) _____		3: _____
		4: _____

COMMENTS:

TEST DESCRIPTION

Cadaver No. _____ Sex: _____ Height: _____ Weight: _____

Test No. _____ (Head, Shoulder, Pelvis)

Test description: _____

Type of Impactor: _____

Type of Bumper: _____

Type of Striker: _____

Impactor Angle: _____

Padding: _____

Pre-Impact Travel: _____

Post-Impact Travel: _____

35mm stills:

___ Black and White

___ Color

CAMERAS

POSITION

Photosonics 1: _____

Photosonics 2: _____

HyCam: _____

INSTRUMENTATION

ACCELEROMETERS

TARGETS

TRANSDUCERS

Head (9-AX) _____	Head _____	Trachea _____
Up. Sternum (3-AX) _____	Acromion _____	Ascending Aorta _____
Lwr. Sternum (1) _____	Sternum (2) _____	Internal Carotid _____
Spine (2 triax) _____	Spine _____	
Pelvis (9-AX) _____	Pelvis _____	Subdural 1: _____
Lwr. Rib R8 (2) _____		2: _____
Up. Rib R4 (2 triax) _____		3: _____
		4: _____

COMMENTS:

PRE-SURGERY

TASK	TIME	COMMENTS
Pick up cadaver from U of M Anatomy Dept. and transport to HSRI Biomedical lab.		
Weigh cadaver and log cadaver information.		
Store cadaver if necessary.		
Sanitary preparation.		
Pretest X-rays: <u>(KV/MA/T)</u> head A-P <u>(100/10/1)</u> // // thorax A-P <u>(90/10/1)</u> // // thorax A-P(2) <u>(90/10/1)</u> // // pelvis <u>(105/10/1)</u> // // femur <u>(80/10/1)</u> // //		
Anthropometry.		

ANTHROPOMETRY

Height: _____

Weight: _____

Sex: _____

Age: _____

Stature: left: _____ right: _____

Suprasternale height: _____

Substernale height: _____

Substernale depth: _____

Substernale breadth: _____

Substernale circumference: _____

Vertex to 12th rib: _____

Head to C7: _____

Mastoid to vertex: left: _____ right: _____

Tragon to vertex: left: _____ right: _____

Menton to vertex: _____

Bitragon diameter: _____

Acromion height: left: _____ right: _____

Acromion to tip of finger: _____

Biacromion: _____

Axillary breadth: _____

Axillary depth: _____

Axillary circumference: _____

Head breadth (R-L): _____

Head depth (A-P): _____

Head circumference: _____

Neck circumference: _____

Bitrochanteric breadth: _____

Symphysion depth: _____

Vertex to Symphysion: _____

Bispinous (ASIS) diameter: _____

Biiliocristale breadth: _____

ASIS to Symphysion: _____

Anatomical Anomalies / Clinical Observations

1. Head: a. Brain b. Skull

2. Neck:

3. Thorax: a. Ribs b. Heart c. Lungs d. Diaphragm

4. Pelvis:

5. Femur

6. Abdomen

RIB AND STERNUM MOUNTS

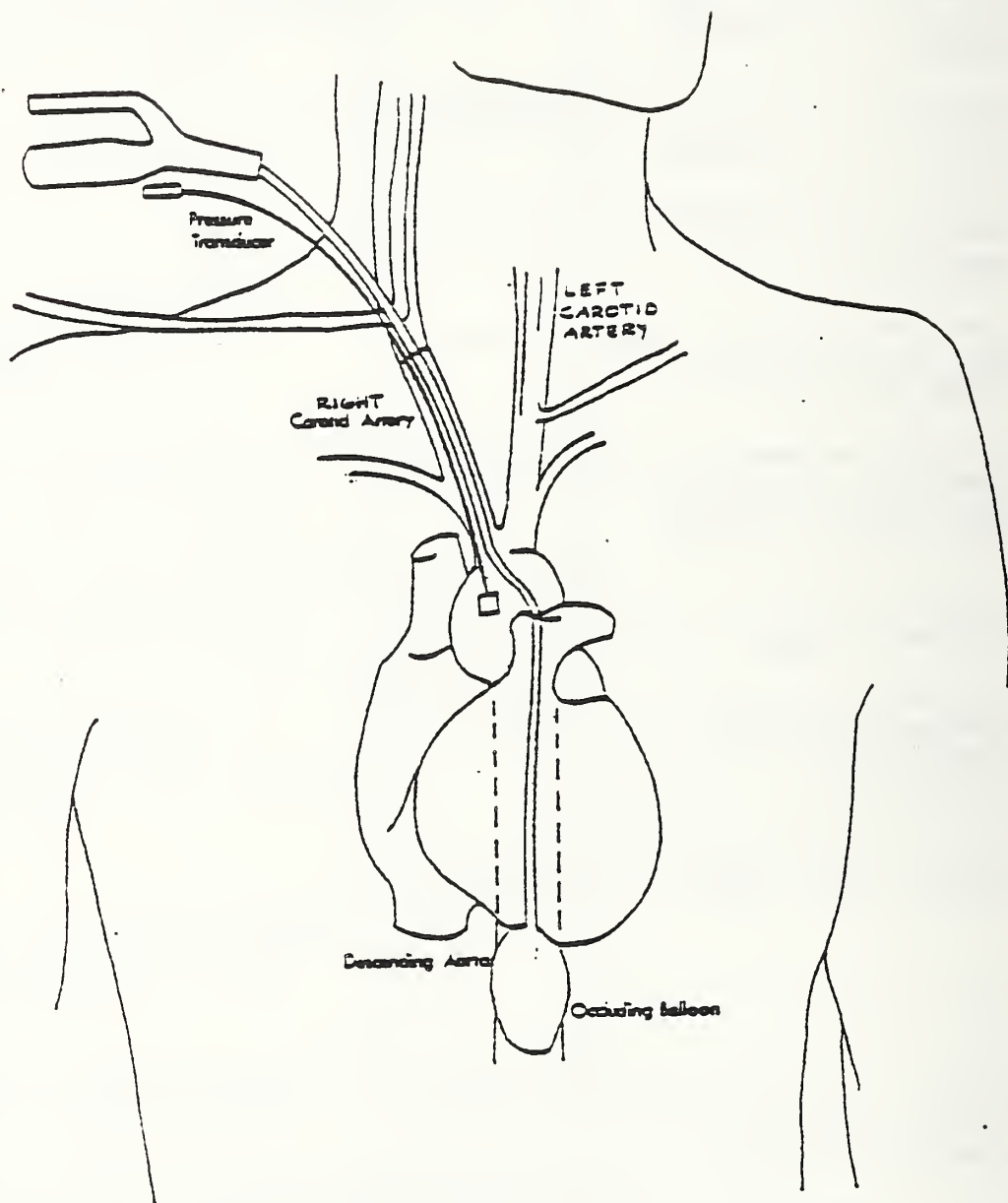
TASK	TIME	COMMENTS
Locate right and left R4 by palpation.		
Make incisions over ribs near flat region. Surface must be normal to the R-L vector.		
Loop two pieces of wire (1/2" apart) around each rib.		
Locate R8 by counting down from R4 and up from R12.		
Make incision over rib near flat region. Surface must be normal to the R-L vector.		
Make incisions over suprasternale and substernale.		
Secure mounts to rib by anchoring with pins and wire.		
Screw lag bolt into each acromion.		

PRESSURIZATION

TASK	TIME	COMMENTS
Locate right carotid and cut lengthwise.		
Locate right vertebral artery and ligate.		
Loop six pieces of string around carotid artery.		
Insert fabricated Foley catheter (#18 or #20) into descending aorta.		
Insert Kulite shield into ascending aorta.		
Insert Kulite shield into carotid artery.		
Insert arterial pressurization catheters into carotid artery.		
Using syringe, squirt acrylic into artery. Tie and sew.		
Locate left carotid, cut, loop strings.		
Locate left vertebral artery and ligate.		

PRESSURIZATION (CONT'D)

TASK	TIME	COMMENTS
Insert arterial pressurization catheters (#10, #12, or #14) into carotid artery.		
Acrylic, tie and sew.		
Locate trachea and cut lengthwise.		
Loop two Tie Wraps around trachea.		
Insert polyethylene tube snugly, tie and sew.		
Calibrate lungs.		
Pulmonary pressure relief valve calibration.		
Vascular flow check.		
Sternal geometry if necessary.		

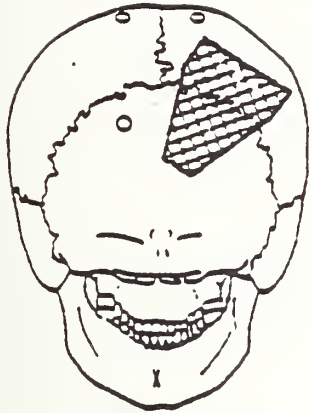


HEAD 9-AX MOUNT

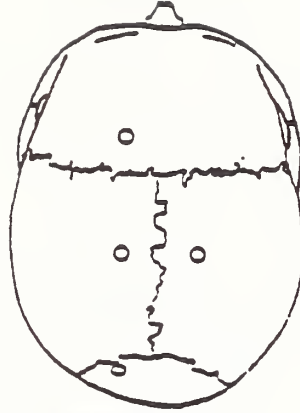
TASK	TIME	COMMENTS
With cadaver facing down, remove a 2x2" area of scalp spanning the right parietal and occipital bones.		
Drill three holes in a triangular pattern, approximately the size of the 9-ax plate.		
Insert three screws.		
Attach four feet to the 9-ax plate such that three of the feet can be positioned near the screws on the exposed forehead.		
Place acrylic around screws.		
Place plate on top of acrylic base, making sure the acrylic goes through the center holes in the plate.		
Insert a strain relief bolt in the acrylic base of the head platform. Make sure bolt does not contact plate.		

HEAD TRANSDUCERS

TASK	TIME	COMMENTS
Holes for transducers go on frontal, parietal, and occipital bones. Make sure no Xducers will contact the impacting surface. Also, the holes should not be drilled into suture.		
To drill holes, remove a 1/4" dia. circle of scalp.		
Drill through skull with a #7 drill. Be sure not to drill through the dura.		
Perforate the dura without cutting brain.		
Tap hole with a No.7 tap.		
Pinhead screws are attached 2cm from each transducer. Acrylic is applied to each area, carefully molding around the transducers.		
Note positions of head transducers on the figure.		



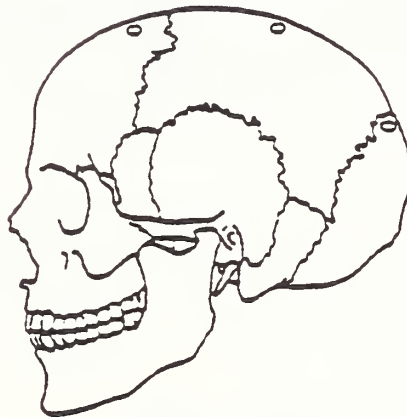
Posterior View



Superior View



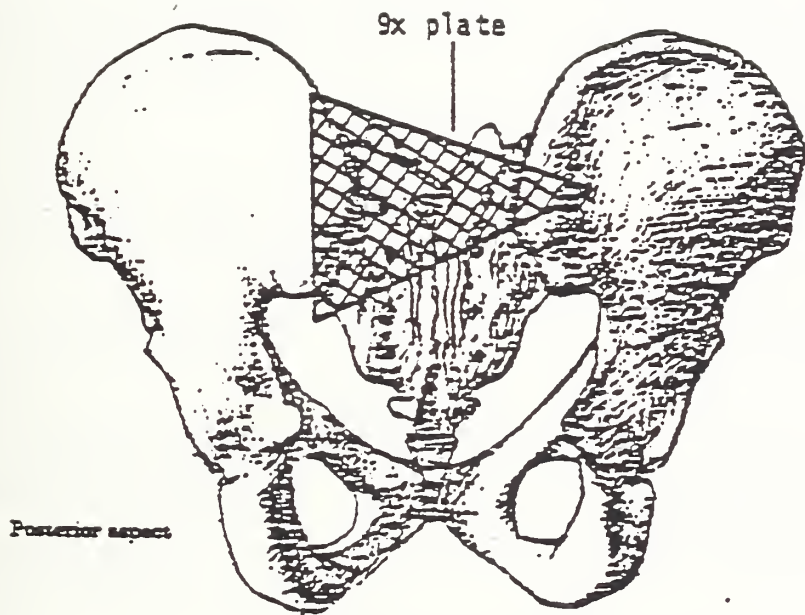
Right Lateral View



Left Lateral View

PELVIS MOUNT

TASK	TIME	COMMENTS
Locate the posterior-superior iliac spines.		
Screw two lag bolts into each spine such that the large 9-ax plate spans the bolts.		
Attach four feet to the plate such that the feet are near the lag bolts.		
Place acrylic around screws and feet.		
Imbed feet and posterior surface into acrylic.		
Test plate to see that it is secure.		



SPINAL MOUNTS

TASK	TIME	COMMENTS
Spinal mounts go on T1 and T12.		
Make incisions over T1 and T12. Clear muscle and tissue away from process, but do not cut between processes.		
Drill a small hole 1/4" deep in each process.		
Screw mounts on with wood screws (be sure screws are in process).		
Place stabilizing and mooring probic devices on each side of the laminae. Secure with Tie Wraps.		
Mold acrylic around (and under) mounts and mooring devices and allow to dry.		
Make sure accelerometers are anatomically oriented.		
Spinal geometry if necessary.		

CEREBROSPINAL PRESSURIZATION

TASK	TIME	COMMENTS
Locate L2 by palpation and counting from T12.		
Core a small hole in the lamina.		
Insert Foley catheter (#14 or #16) such that balloon is in mid-thorax.		
Insert small screws in lamina and process.		
Seal off hole with acrylic.		
Check for structural integrity of vertebra.		
Cerebral-spinal flow check.		
Check pressurization.		

PREPARATION

TASK	TIME	COMMENTS
Dress cadaver.		
Place head and body harnesses on cadaver.		
Store cadaver if necessary.		
Transport cadaver to sled lab, being careful not to damage mounts.		
Place head, sternum, and rib transducers on cadaver. Stuff and sew.		
Set up pressurization equipment (pulmonary, cerebro-spinal, vascular head and vascular thorax).		

ELECTRONICS CHECK AND PRETEST TRIAL RUN

Electronics Check

- ___ check accelerometers (excitation and zero)
- ___ check wiring and cables
- ___ mount accelerometers in triax clusters
- ___ check amplifiers
- ___ calibrate tape with impedance-matching amp recorder
- ___ complete wiring
- ___ check pendulum accelerometer
- ___ check velocity, strobe, gate, timer, rope cutters
- ___ run trial test
- ___ load cell mounted on pendulum day before test
- ___ load Photosonics and HyCam cameras with Kodak 16mm 7242-#FB-430 color film

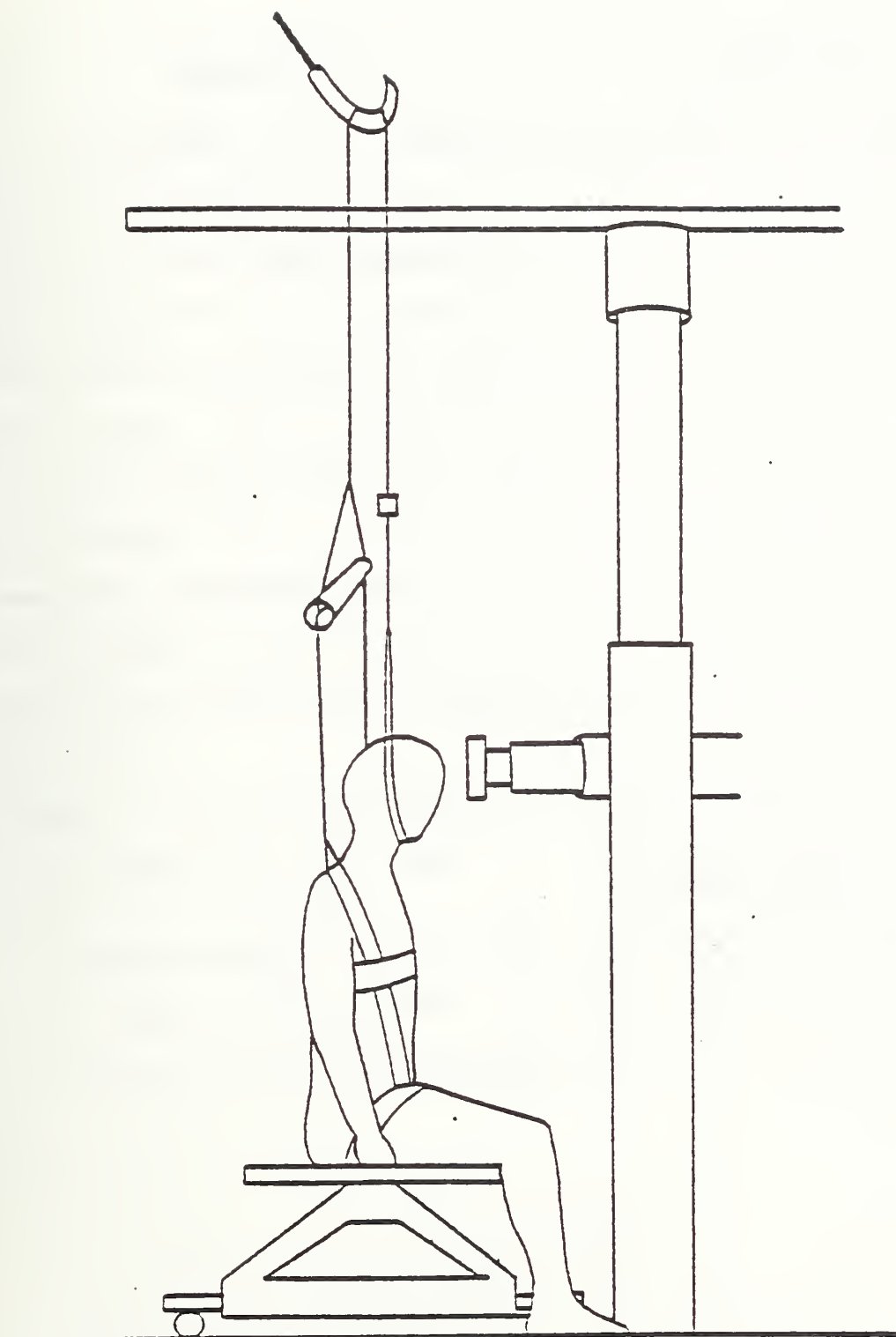
Pretest Trial Run

1. ___ Suspend rubber tube five inches from pendulum with fiber tape.
2. ___ Tape all accelerometers to seat with paper tape.
3. ___ Attach the contact switches to the load cell and shock absorber with paper tape.
4. ___ Run trial test.
5. ___ Record all signals, gate, and strobe.
6. ___ Put a one-volt signal on a junk tape and check to see if one volt is played back. Use signal generator or impedance-matching amp with the scope to calibrate output.

HEAD IMPACT 1

Test No. _____

TASK	TIME	COMMENTS
Head impact 1.		
Attach ball targets and phototargets.		
Change padding on impactor head surface.		
Set up head catch and spinal backup.		
Final positioning (see figure).		
Measure and record head and neck angles		
Setup photos.		
Final checklist.		
Start pressurization of vascular and cerebrospinal systems.		
Finish pressurizations.		
Run test.		



HEAD IMPACT 1
Timer Box Setup

EQUIPMENT	TIMER VALUES		
	Impact	Delay	Run
Gate (from strobe 1)	0011	1	0170
Lights (start)	0001	2	2600
HyCam (start)	1200	3	1600
Pendulum rope cutter(start)	1390	4	0050
Photosonics (start)	1000	5	1600
		6	
Head, pelvis, rope cutter (from velocity probe)	0001	7	0050
Piston Acceleration Corridor	0009	8	0050

FINAL CHECKLIST

- ___ check transducers
- ___ tape positioned
- ___ slots for velocity probe lined up
- ___ both strobes charged
- ___ timer box values correct
- ___ all timer box switches to 'off'
- ___ rope cutter threaded and ready
- ___ nylon (rope cutter) string unfrayed
- ___ rope cutter cable free
- ___ cameras set
- ___ Newtonian reference
- ___ calibration target
- ___ targets in view of cameras
- ___ padding
- ___ correct timers charged
- ___ gate trigger established
- ___ timing lights on
- ___ doors locked
- ___ final positioning
- ___ correct pressure system used
- ___ pendulum raised
- ___ power on
- ___ all pressure connections secured
- ___ zero piston accelerometer
- ___ head and neck angles

HEAD IMPACT 2

Test No. _____

TASK	TIME	COMMENTS
Reposition as for tap.		
Check spinal brace and head catch.		
Final positioning		
Measure and record head and neck angles		
Setup photos.		
Start pressurization of vascular and cerebrospinal systems.		
Final checklist.		
Finish pressurization.		
Run test.		

HEAD IMPACT 2

Timer Box Setup

EQUIPMENT	TIMER VALUES		
	Impact	Delay	Run
Gate (from strobe 1)	0008	1	0170
Lights (start)	0001	2	2600
HyCam (start)	1200	3	1600
Pendulum rope cutter(start)	1290	4	0050
Photosonics (start)	1000	5	1600
		6	
Head, pelvis, rope cutter (from velocity probe)	0001	7	0050
Piston Acceleration Corridor	0009	8	0050

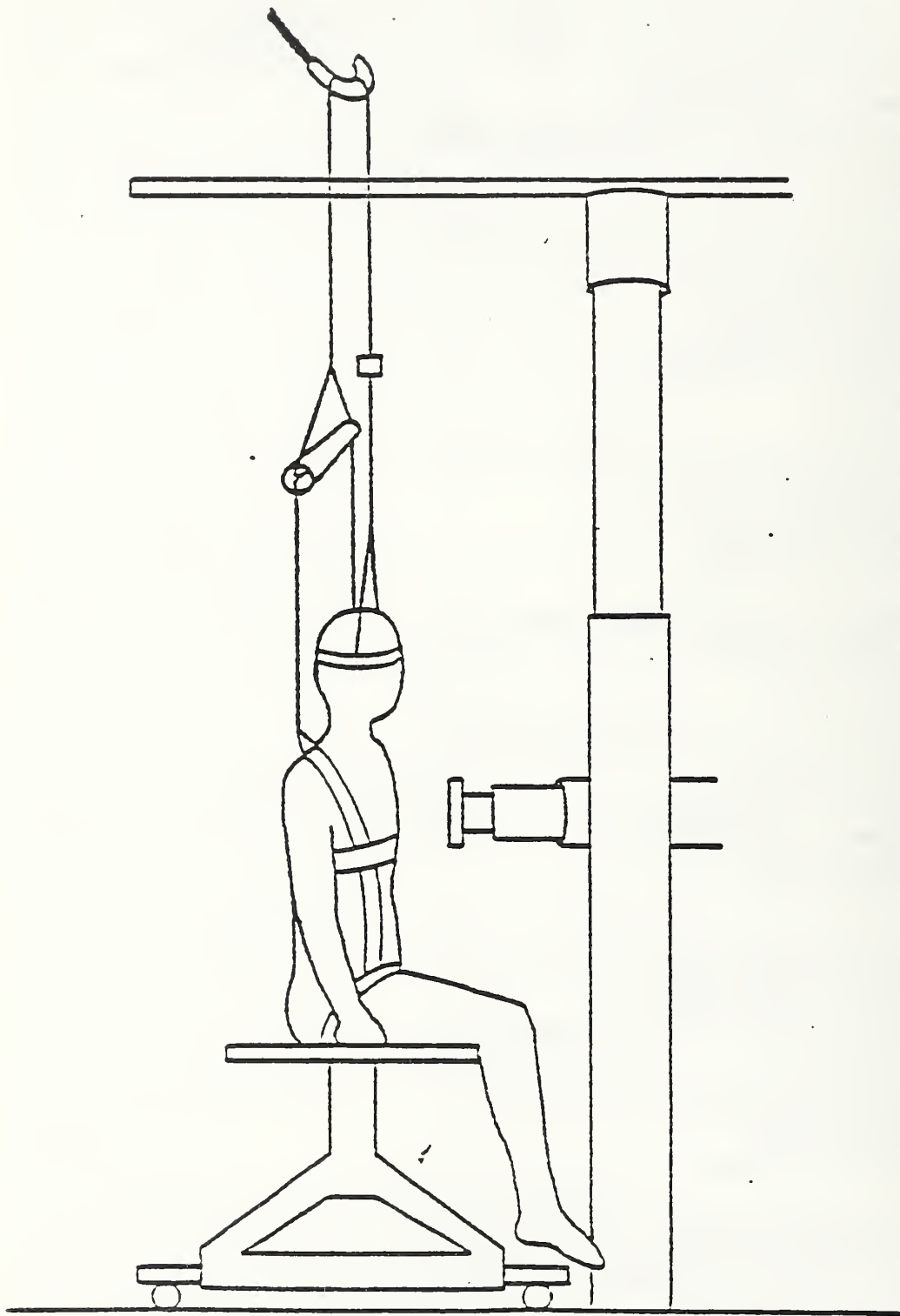
FINAL CHECKLIST

- ___ check transducers
- ___ tape positioned
- ___ slots for velocity probe lined up
- ___ both strobes charged
- ___ timer box values correct
- ___ all timer box switches to 'off'
- ___ rope cutter threaded and ready
- ___ nylon (rope cutter) string unfrayed
- ___ rope cutter cable free
- ___ cameras set
- ___ Newtonian reference
- ___ calibration target
- ___ targets in view of cameras
- ___ padding
- ___ correct timers charged
- ___ gate trigger established
- ___ timing lights on
- ___ doors locked
- ___ final positioning
- ___ correct pressure system used
- ___ pendulum raised
- ___ power on
- ___ all pressure connections secured
- ___ zero piston accelerometer
- ___ head and neck angles

THORAX FRONT TAP

Test No. _____

TASK	TIME	COMMENTS
Place seat in position and square on pendulum.		
String up rope cutters.		
Position subject as per figure with body and head harnesses. Protect any mounts that may be hit with gauze and padding.		
Subject should be in normal sitting position with back inclined approx. 10° forwards.		
Attach ball targets and phototargets.		
Place one of the pressure transducers that was in the head in the trachea, and place the Kulite in the descending aorta.		
Final positioning and setup photos (see fig)		
Final checklist.		
Start pressurization of vascular and respiratory systems.		
Finish pressurization.		
Run test.		



THORAX FRONT TAP

Timer Box Setup

EQUIPMENT	TIMER VALUES		
	Impact	Delay	Run
Gate (from strobe 1)	0021	1	0170
Lights (start)	0001	2	2500
HyCam (start)	1200	3	1600
Pendulum rope cutter(start)	1400	4	0050
Photosonics (start)	1000	5	1600
		6	
Head, pelvis, rope cutter (from velocity probe)	0001	7	0050
Piston Acceleration Corridor	0012	8	0150

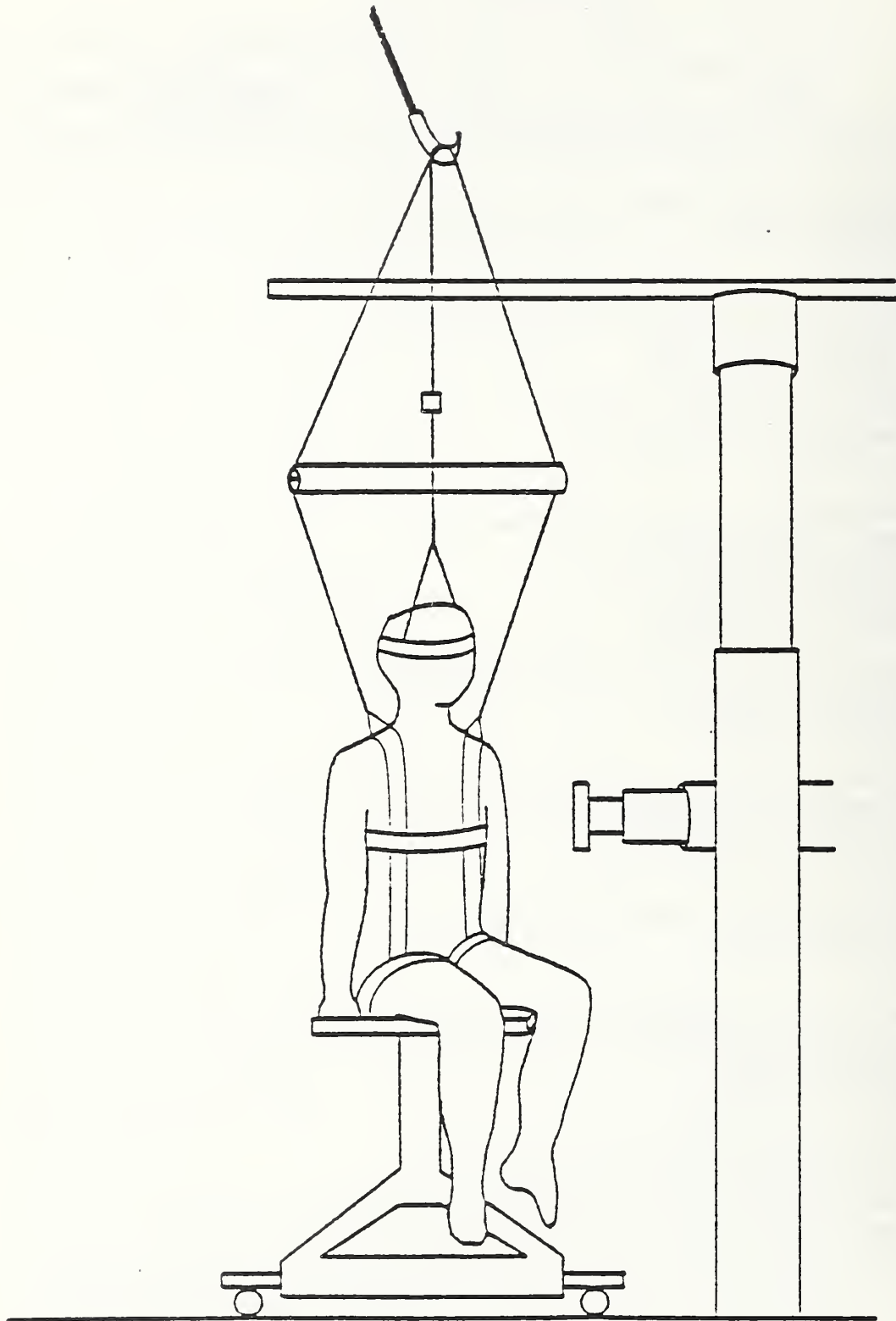
FINAL CHECKLIST

- ___ check transducers
- ___ tape positioned
- ___ slots for velocity probe lined up
- ___ both strobes charged
- ___ timer box values correct
- ___ all timer box switches to 'off'
- ___ rope cutter threaded and ready
- ___ nylon (rope cutter) string unfrayed
- ___ rope cutter cable free
- ___ cameras set
- ___ Newtonian reference
- ___ calibration target
- ___ targets in view of cameras
- ___ padding
- ___ correct timers charged
- ___ gate trigger established
- ___ timing lights on
- ___ doors locked
- ___ final positioning
- ___ correct pressure system used
- ___ pendulum raised
- ___ power on
- ___ all pressure connections secured
- ___ zero piston accelerometer
- ___ head and neck angles

45° THORAX TAP

Test No. _____

TASK	TIME	COMMENTS
Place seat in position.		
String up rope cutters.		
Position subject as per figure with body and head harnesses. Protect any mounts that may be hit with gauze and padding.		
Subject should be in normal sitting position with back inclined approx. 10° forwards.		
Attach ball targets and phototargets.		
Final positioning and setup photos (see fig)		
Final checklist.		
Start pressurization of vascular and respiratory systems.		
Finish pressurization.		
Run test.		



45° THORAX TAP

Timer Box Setup

EQUIPMENT	TIMER VALUES		
	Impact	Delay	Run
Gate (from strobe 1)	0021	1	0170
Lights (start)	0001	2	2600
HyCam (start)	1200	3	1600
Pendulum rope cutter (start)	1400	4	0050
Photosonics (start)	1000	5	1600
		6	
Head, pelvis, rope cutter (from velocity probe)	0001	7	0050
Piston Acceleration Corridor	0012	8	0150

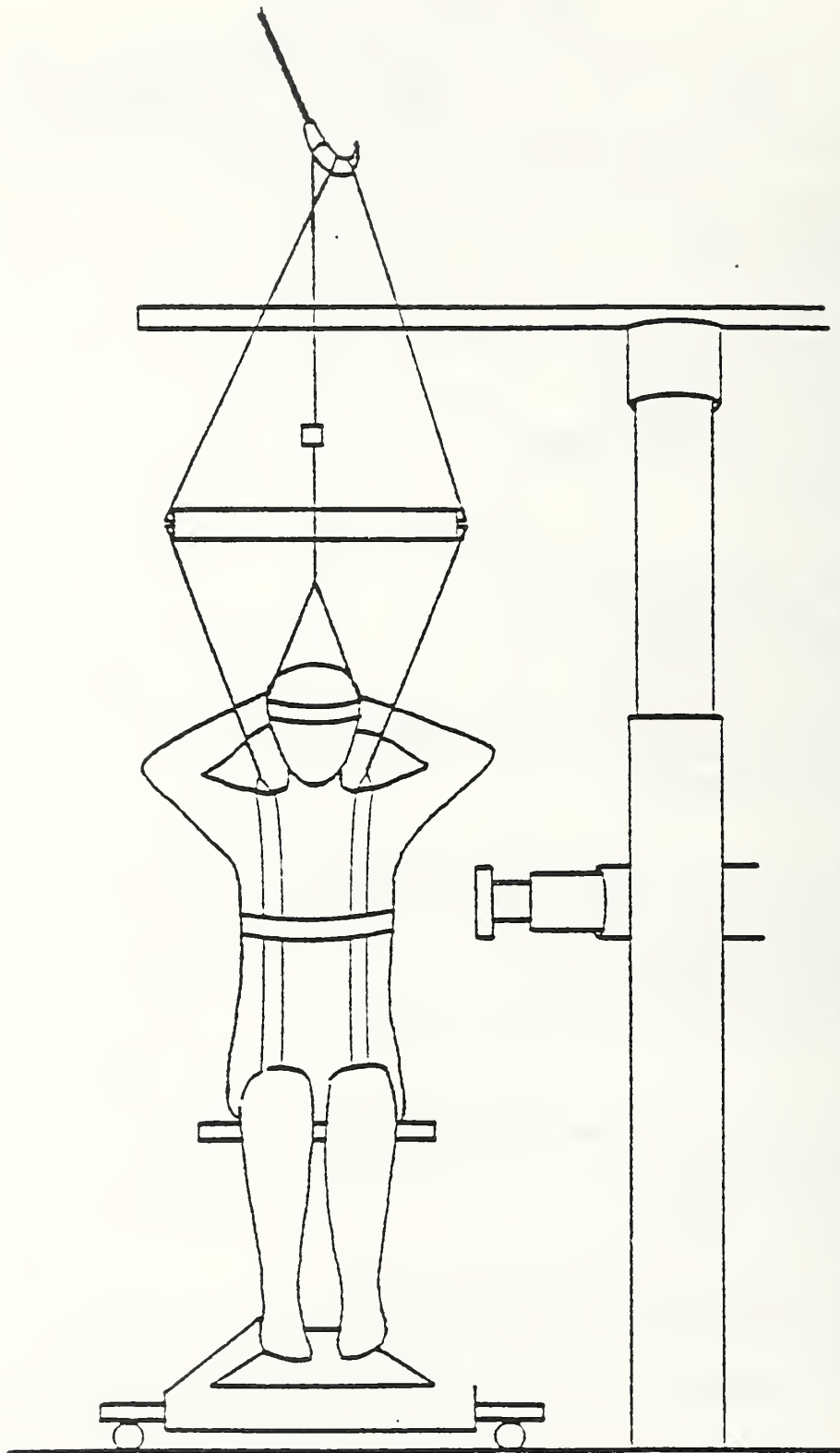
FINAL CHECKLIST

- ___ check transducers
- ___ tape positioned
- ___ slots for velocity probe lined up
- ___ both strobes charged
- ___ timer box values correct
- ___ all timer box switches to 'off'
- ___ rope cutter threaded and ready
- ___ nylon (rope cutter) string unfrayed
- ___ rope cutter cable free
- ___ cameras set
- ___ Newtonian reference
- ___ calibration target
- ___ targets in view of cameras
- ___ padding
- ___ correct timers charged
- ___ gate trigger established
- ___ timing lights on
- ___ doors locked
- ___ final positioning
- ___ correct pressure system used
- ___ pendulum raised
- ___ power on
- ___ all pressure connections secured
- ___ zero piston accelerometer
- ___ head and neck angles

OPTIONAL ARMS-UP THORAX TAP

Test No. _____

TASK	TIME	COMMENTS
Place seat in position.		
String up rope cutters.		
Position subject as per figure with body and head harnesses. Protect any mounts that may be hit with gauze and padding.		
Subject should be in normal sitting position with back inclined approx. 10° forwards.		
Attach ball targets and phototargets.		
Final positioning and setup photos see drawings and figures by ***PAULA LUX***		
Final checklist.		
Start pressurization of vascular and respiratory systems.		
Finish pressurization.		
Run test.		



B60

OPTIONAL ARMS-UP THORAX TAP

Timer Box Setup

EQUIPMENT	TIMER VALUES		
	Impact	Delay	Run
Gate (from strobe 1)	0021	1	0170
Lights (start)	0001	2	2600
HyCam (start)	1200	3	1600
Pendulum rope cutter(start)	1400	4	0050
Photosonics (start)	1000	5	1600
		6	
Head, pelvis, rope cutter (from velocity probe)	0001	7	0050
Piston Acceleration Corridor	0012	8	0150

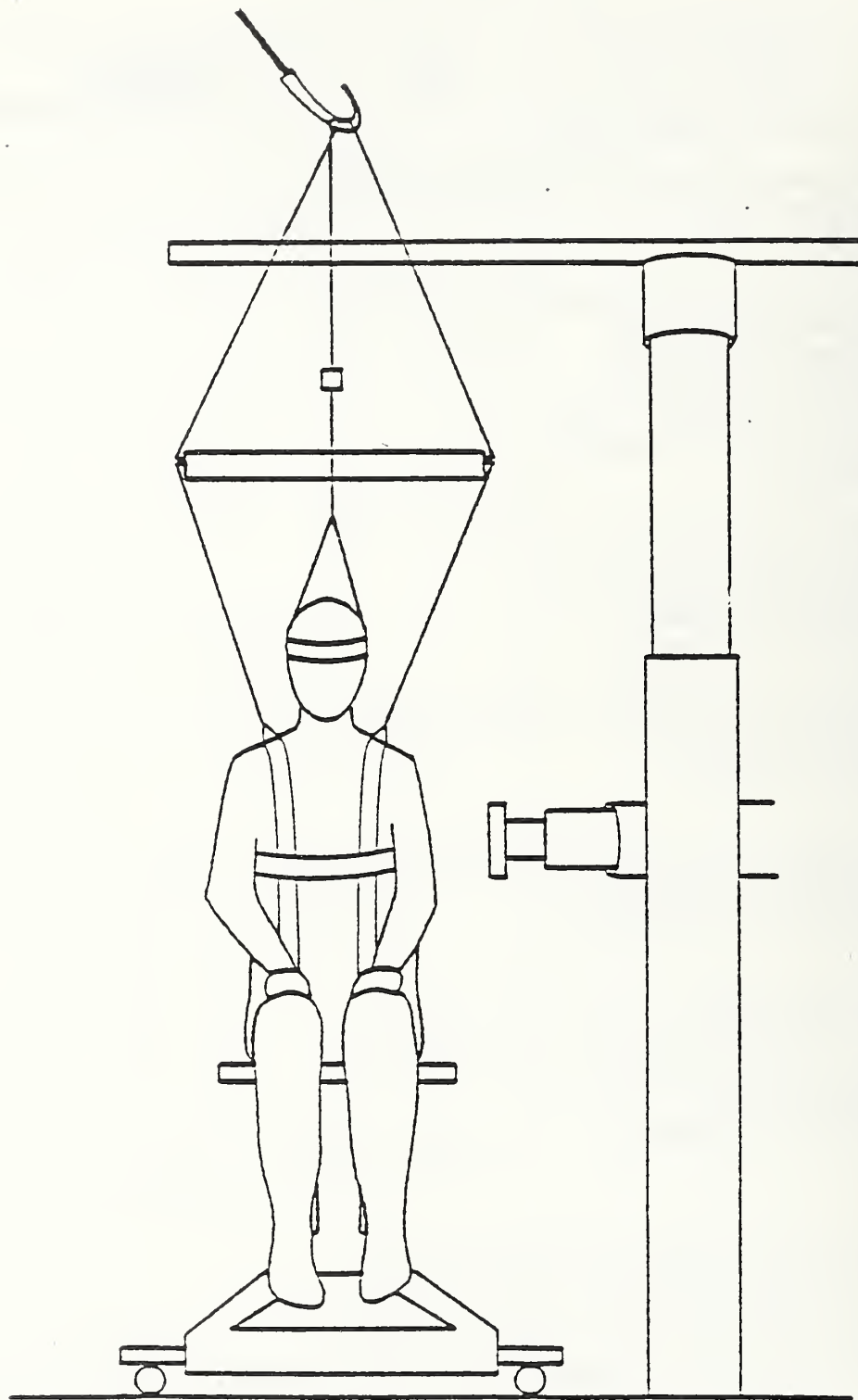
FINAL CHECKLIST

- ___ check transducers
- ___ tape positioned
- ___ slots for velocity probe lined up
- ___ both strobes charged
- ___ timer box values correct
- ___ all timer box switches to 'off'
- ___ rope cutter threaded and ready
- ___ nylon (rope cutter) string unfrayed
- ___ rope cutter cable free
- ___ cameras set
- ___ Newtonian reference
- ___ calibration target
- ___ targets in view of cameras
- ___ padding
- ___ correct timers charged
- ___ gate trigger established
- ___ timing lights on
- ___ doors locked
- ___ final positioning
- ___ correct pressure system used
- ___ pendulum raised
- ___ power on
- ___ all pressure connections secured
- ___ zero piston accelerometer
- ___ head and neck angles

ARMS-DOWN THORAX TAP

Test No. _____

TASK	TIME	COMMENTS
Place seat in position.		
String up rope cutters.		
Position subject as per figure with body and head harnesses. Protect any mounts that may be hit with gauze and padding.		
Subject should be in normal sitting position with back inclined approx. 10° forwards.		
Attach ball targets and phototargets.		
Final positioning and setup photos (see fig)		
Final checklist.		
Start pressurization of vascular and respiratory systems.		
Finish pressurization.		
Run test.		



ARMS-DOWN THORAX TAP

Timer Box Setup

EQUIPMENT	TIMER VALUES		
	Impact	Delay	Run
Gate (from strobe 1)	0021	1	0170
Lights (start)	0001	2	2600
HyCam (start)	1200	3	1600
Pendulum rope cutter(start)	1400	4	0050
Photosonics (start)	1000	5	1600
		6	
Head, pelvis, rope cutter (from velocity probe)	0001	7	0050
Piston Acceleration Corridor	0012	8	0150

FINAL CHECKLIST

- ___ check transducers
- ___ tape positioned
- ___ slots for velocity probe lined up
- ___ both strobes charged
- ___ timer box values correct
- ___ all timer box switches to 'off'
- ___ rope cutter threaded and ready
- ___ nylon (rope cutter) string unfrayed
- ___ rope cutter cable free
- ___ cameras set
- ___ Newtonian reference
- ___ calibration target
- ___ targets in view of cameras
- ___ padding
- ___ correct timers charged
- ___ gate trigger established
- ___ timing lights on
- ___ doors locked
- ___ final positioning
- ___ correct pressure system used
- ___ pendulum raised
- ___ power on
- ___ all pressure connections secured
- ___ zero piston accelerometer
- ___ head and neck angles

THORAX IMPACT

Test No. _____

TASK	TIME	COMMENTS
Reposition for shoulder (arms down) impact.		
Set up catch net.		
Slacken body harness.		
Start pressurization of vascular and respiratory systems.		
Final checklist.		
Finish pressurization.		
Run test		

ARMS-DOWN THORAX IMPACT

Timer Box Setup

EQUIPMENT	TIMER VALUES		
	Impact	Delay	Run
Gate (from strobe 1)	0006	1	0170
Lights (start)	0001	2	2600
HyCam (start)	1200	3	1600
Pendulum rope cutter(start)	1220	4	0050
Photosonics (start)	1000	5	1600
		6	
Head, pelvis, rope cutter (from velocity probe)	0002	7	0050
Piston Acceleration Corridor	0006	8	0050

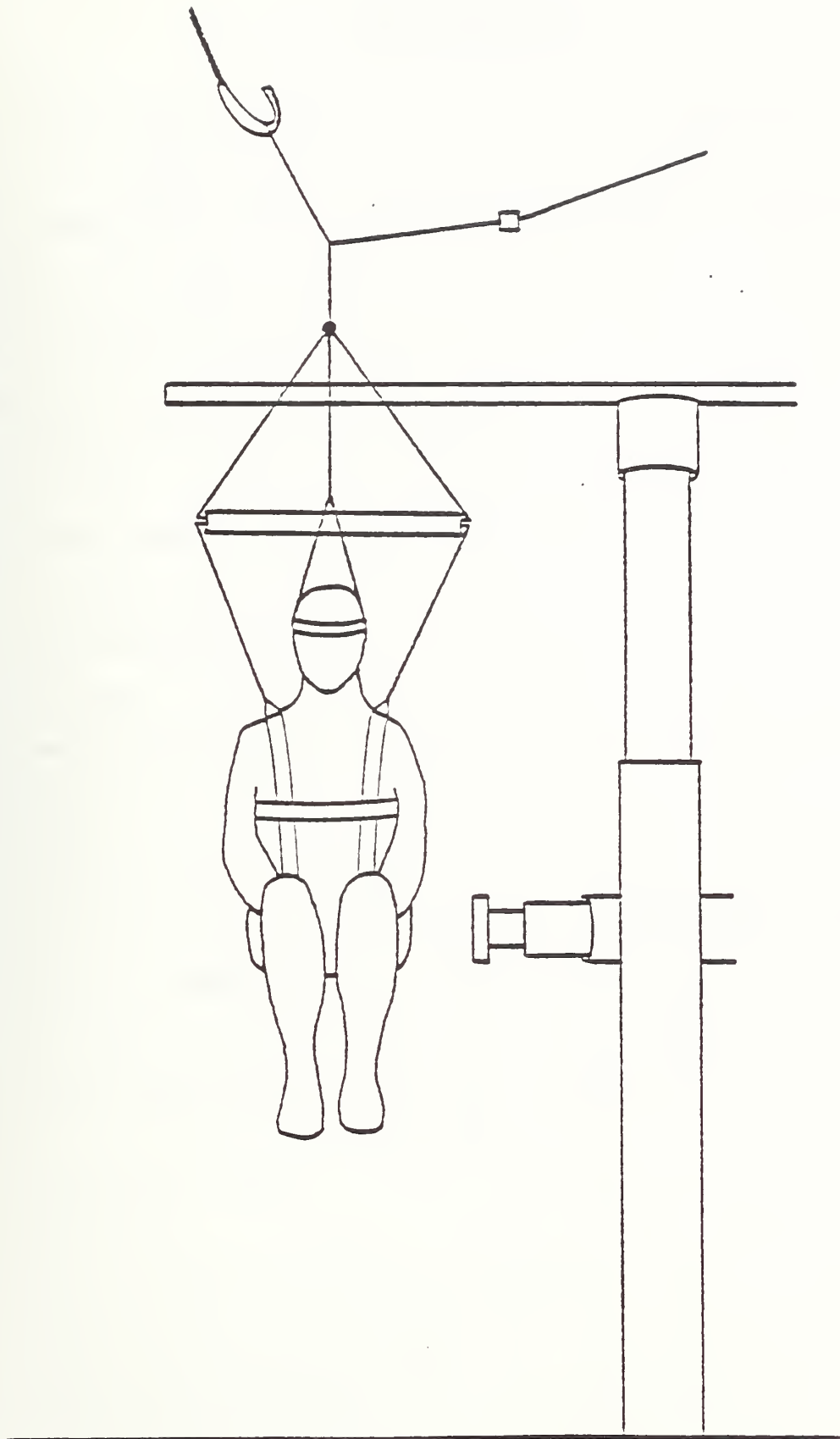
FINAL CHECKLIST

- ___ check transducers
- ___ tape positioned
- ___ slots for velocity probe lined up
- ___ both strobes charged
- ___ timer box values correct
- ___ all timer box switches to 'off'
- ___ rope cutter threaded and ready
- ___ nylon (rope cutter) string unfrayed
- ___ rope cutter cable free
- ___ cameras set
- ___ Newtonian reference
- ___ calibration target
- ___ targets in view of cameras
- ___ padding
- ___ correct timers charged
- ___ gate trigger established
- ___ timing lights on
- ___ doors locked
- ___ final positioning
- ___ correct pressure system used
- ___ pendulum raised
- ___ power on
- ___ all pressure connections secured
- ___ zero piston accelerometer
- ___ head and neck angles

PELVIS IMPACT

Test No. _____

TASK	TIME	COMMENTS
Install pelvic and spinal accelerometers. Stuff and sew. Pad pelvic plate.		
Attach ball targets and phototargets.		
Change padding on impact head surface.		
Final positioning, setup photos (see fig)		
Final checklist.		
Run test.		



PELVIS IMPACT

Timer Box Setup

EQUIPMENT	TIMER VALUES		
	Impact	Delay	Run
Gate (from strobe 1)	0006	1	0170
Lights (start)	0001	2	2600
HyCam (start)	1200	3	1600
Pendulum rope cutter(start)	1220	4	0050
Photosonics (start)	1000	5	1600
		6	
Head, pelvis, rope cutter (from velocity probe)	0002	7	0050
Piston Acceleration Corridor	0006	8	0050

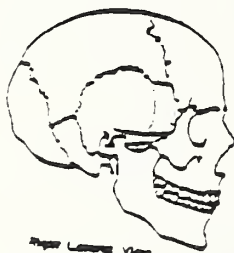
FINAL CHECKLIST

- check transducers
- tape positioned
- slots for velocity probe lined up
- both strobes charged
- timer box values correct
- all timer box switches to 'off'
- rope cutter threaded and ready
- nylon (rope cutter) string unfrayed
- rope cutter cable free
- cameras set
- Newtonian reference
- calibration target
- targets in view of cameras
- padding
- correct timers charged
- gate trigger established
- timing lights on
- doors locked
- final positioning
- correct pressure system used
- pendulum raised
- power on
- all pressure connections secured
- zero piston accelerometer
- head and neck angles

POST TEST PROCEDURE

TASK	TIME	COMMENTS
Remove all targets and triax clusters.		
Store cadaver if necessary.		
Transport cadaver to anatomy lab.		
Remove all instrumentation, except for SAX head plate.		
Remove head and transport it to X-Ray Room for post test radiographs.		

Z-X
(Profile)



Z-Y
(Frontal)



X-RAYS (X-RAY ROOM)

Reference Point	Z-X Distance from Table	Z-Y Distance from Table
R. Eye		
L. Eye		
R. Ear		
L. Ear		
Q1		
Q2		
Q3		
CG		

	KVP	MA	SEC	LABEL	
Z-X	_____ /	_____ /	_____ /	_____	(100/10/1)
Z-Y	_____ /	_____ /	_____ /	_____	(100/10/1)

AUTOPSY

TASK	TIME	COMMENTS
After completion of radiographs, transport head to Anatomy Room for commencement of Autopsy.		
Autopsy		
SAVE RIBS RIGHT SIDE 4, 5, 6		

Observed Injuries

1. Head: a. Brain b. Skull

2. Neck:

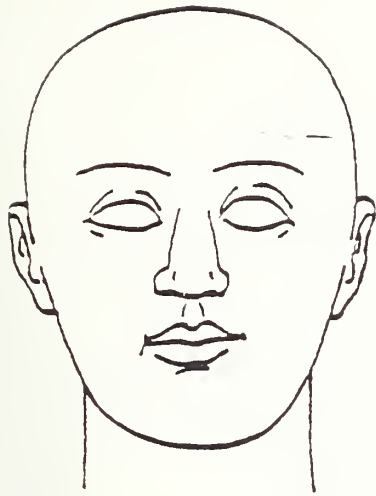
3. Thorax: a. Ribs b. Heart c. Lungs d. Diaphragm

4. Pelvis:

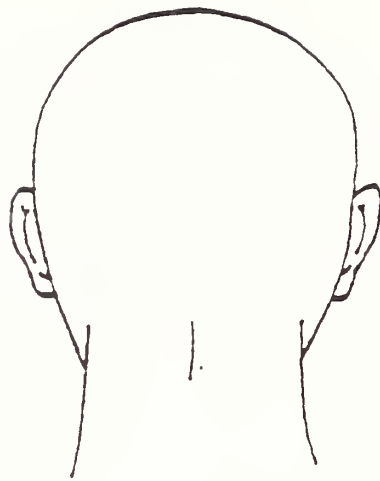
5. Femur

6. Abdomen

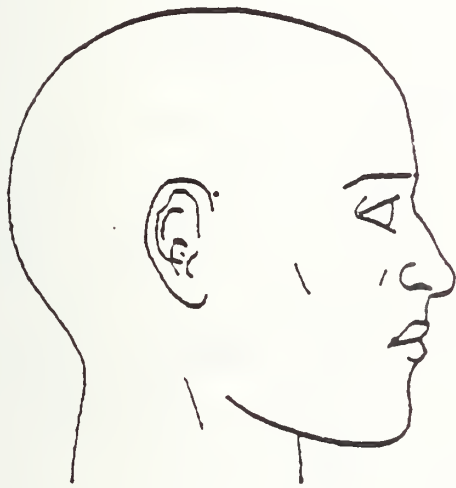
COMMENTS :



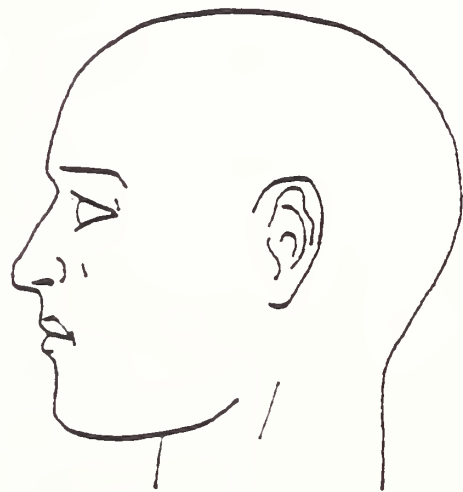
Anterior View



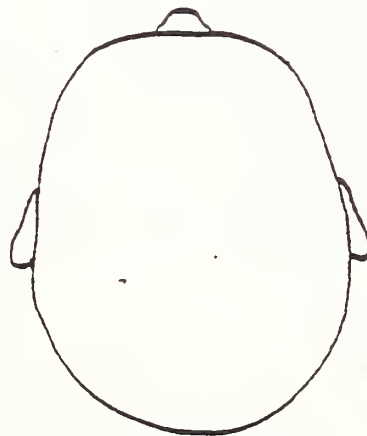
Posterior View



Right Lateral View

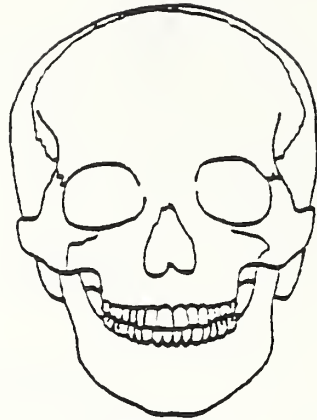


Left Lateral View

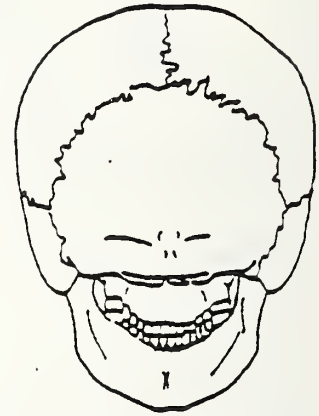


Superior View

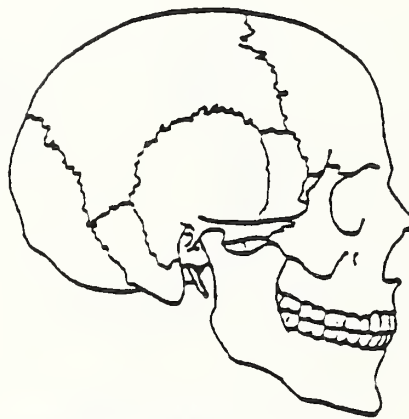
TEST NO. _____



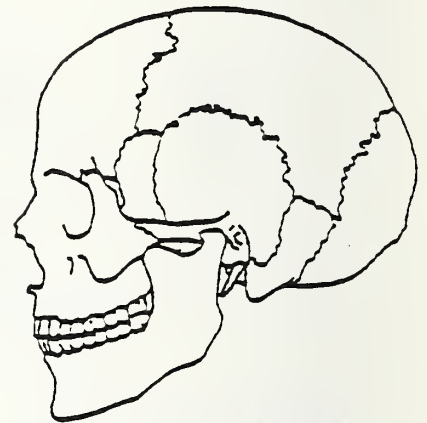
Anterior View



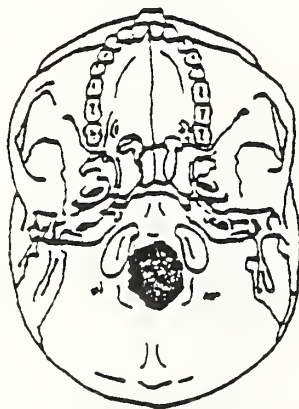
Posterior View



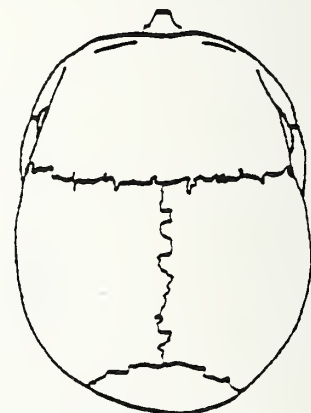
Right Lateral View



Left Lateral View



Inferior View



Superior View

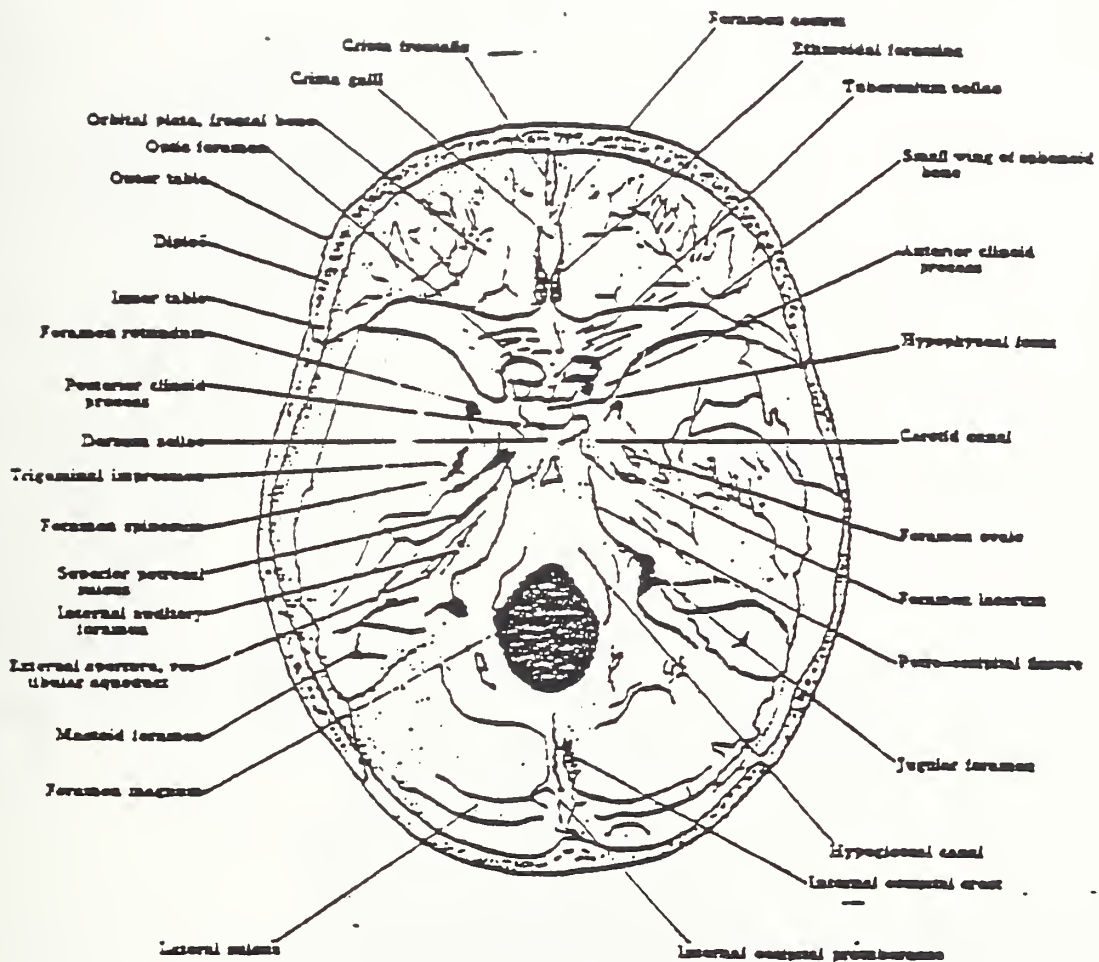
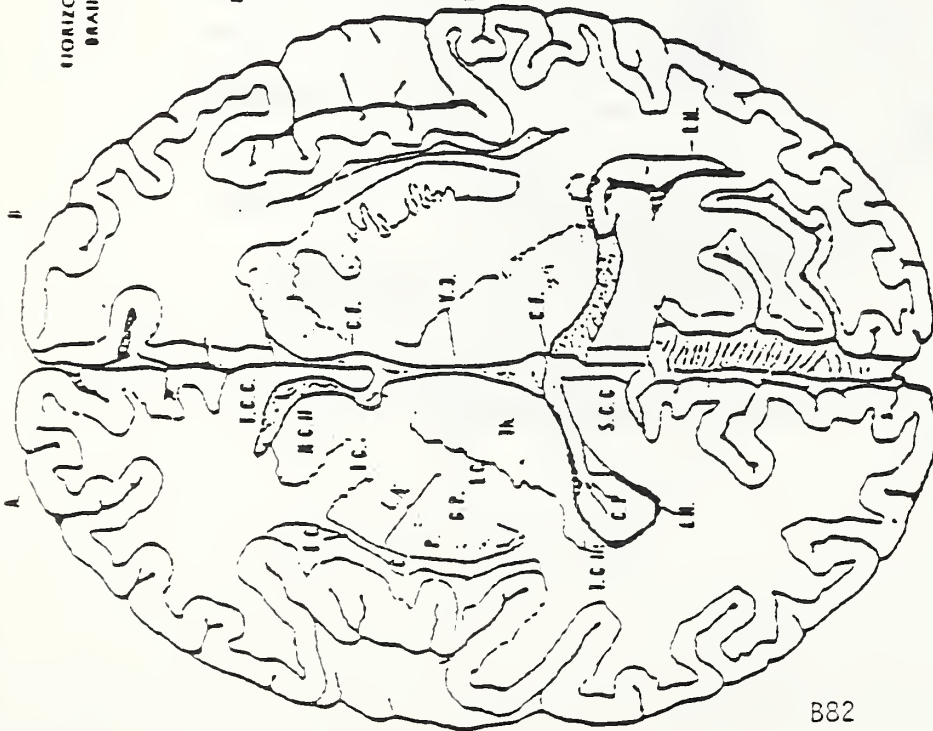
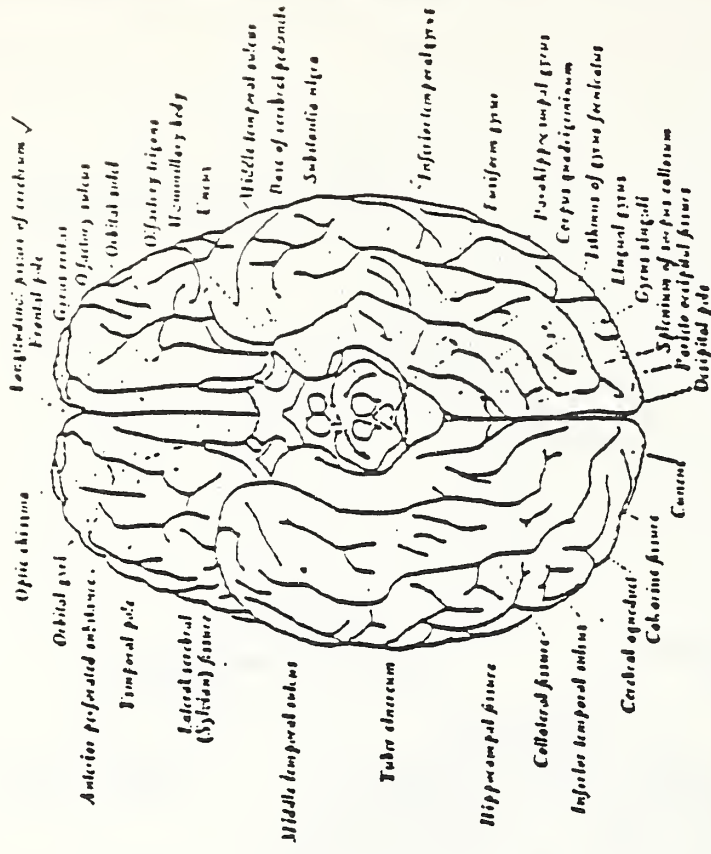


FIG. 109.—THE SKULL, INTERNAL ASPECT OF THE BASE.

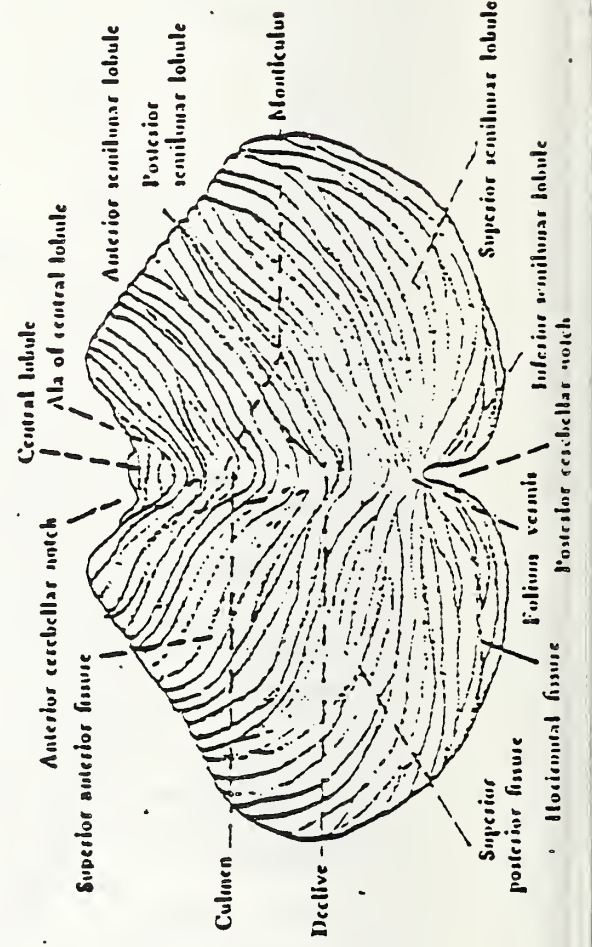
HORIZONTAL SECTIONS OF BRAIN AT TWO LEVELS

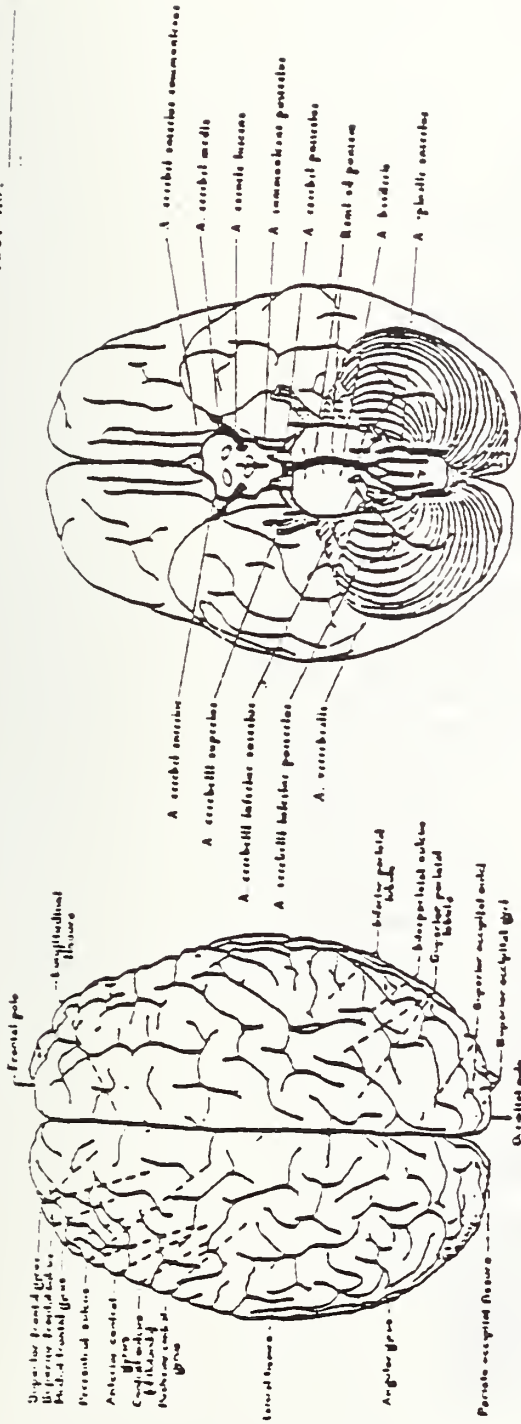


- C. — Cavities
- C.C. — Corpus Callosum
- C.P. — Cerebral Peduncle
- I.C. — Internal Cerebral Cavity
- O.P. — Optic Chiasm
- H.C. — Head of Caudate Nucleus
- I.C. — Internal Cerebral Cavity
- H. — Horn of Lateral Ventricle
- L.V. — Lateral Ventricle
- P. — Putamen
- S.C.C. — Splenium of Corpus Callosum
- I.C.C. — Body of Corpus Callosum
- I.C.H. — Tail of Caudate Nucleus
- H. — Hemisphere
- V.B. — 2nd Ventricle

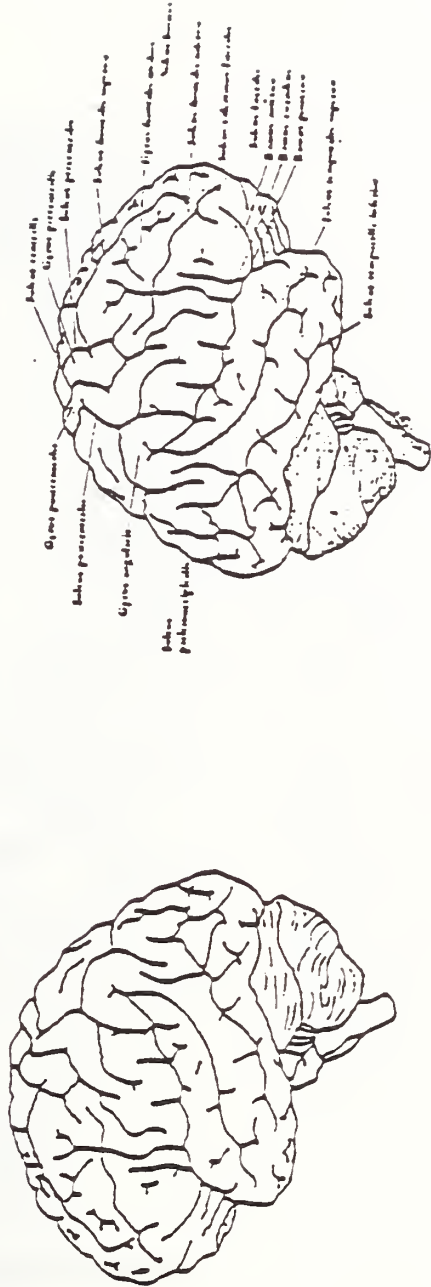


Basal aspect of the human cerebral hemisphere. (Schultz, McMurich)

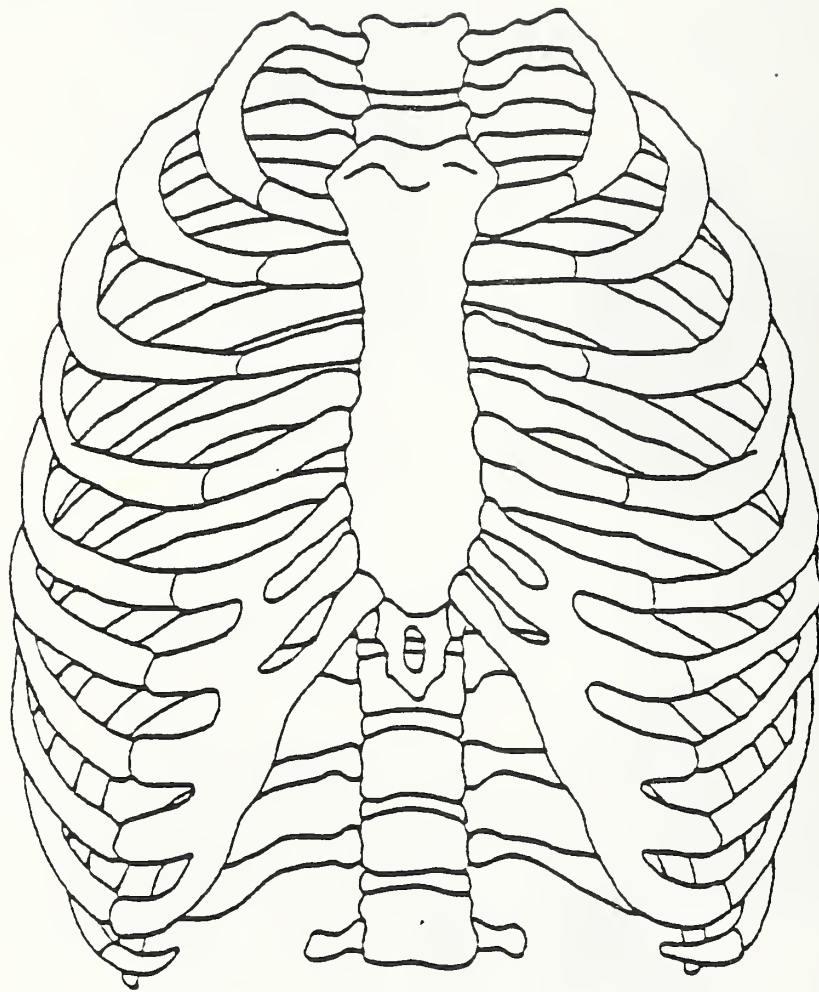




— Cerebrum et cerebellum in homine —

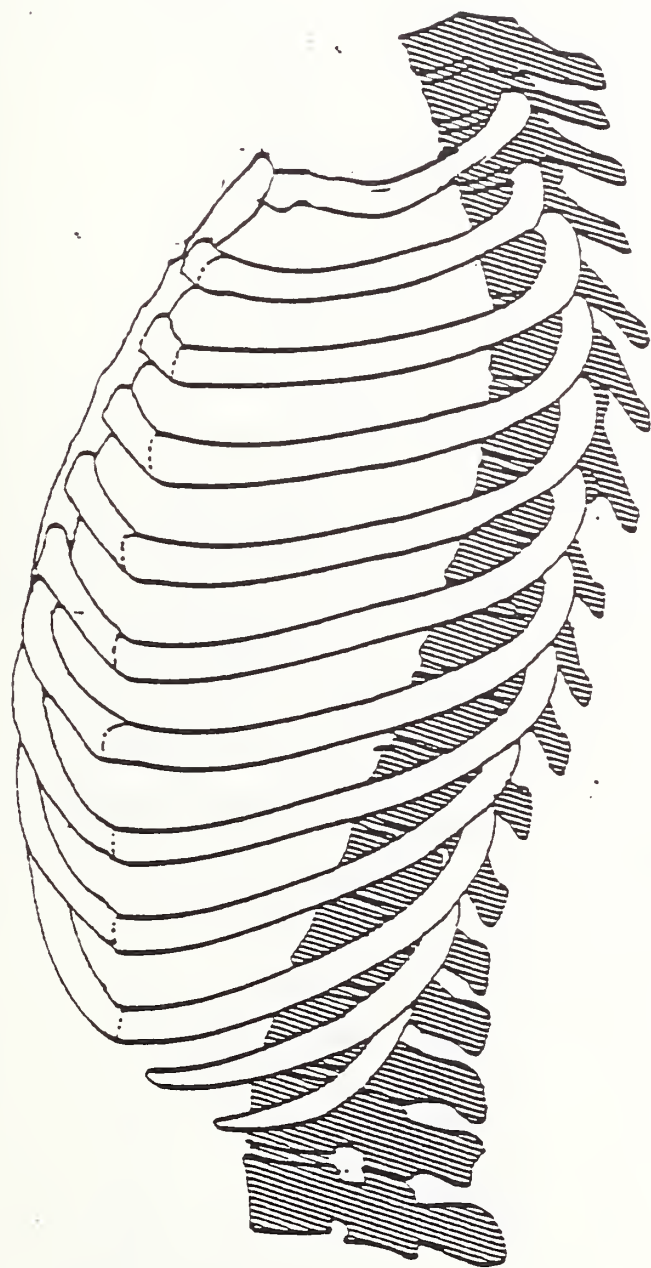


TEST NO. _____

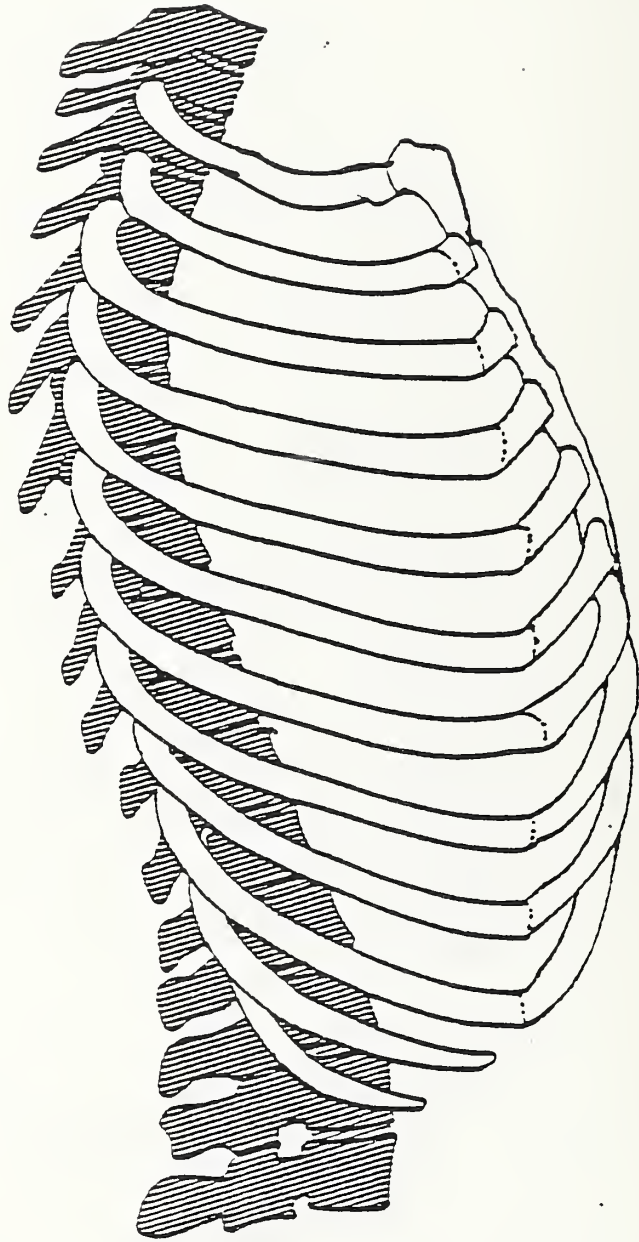


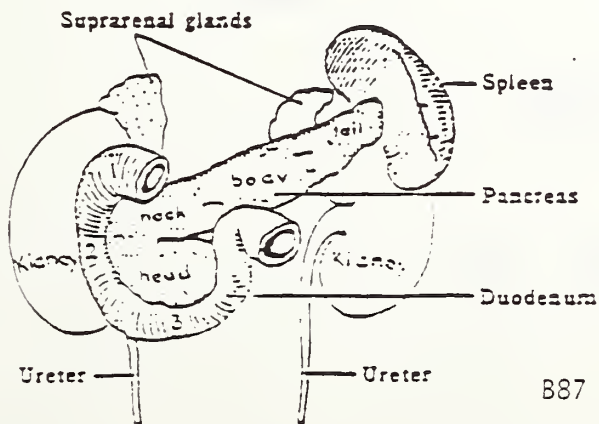
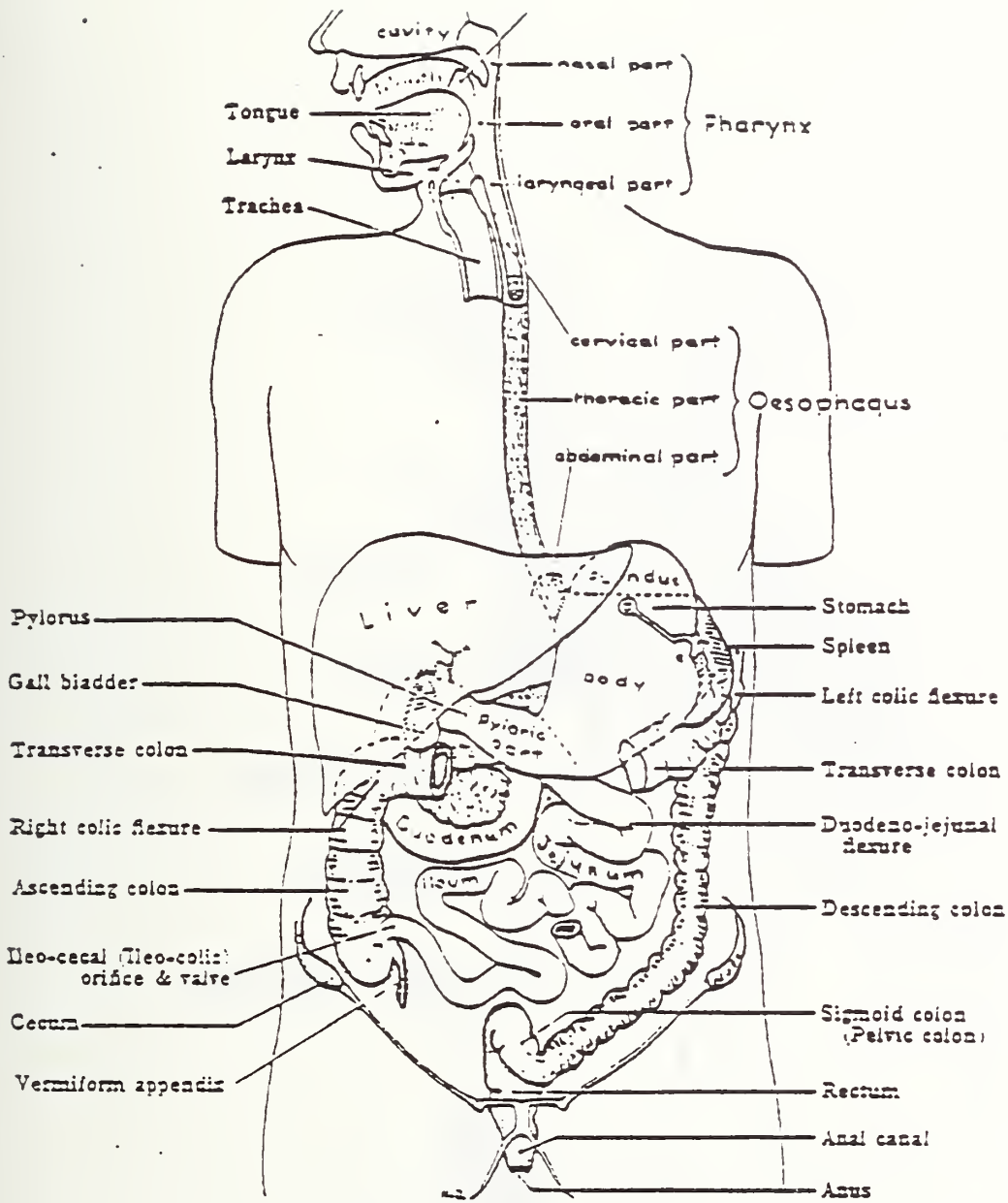
ANTERIOR THORAX

Test No. _____

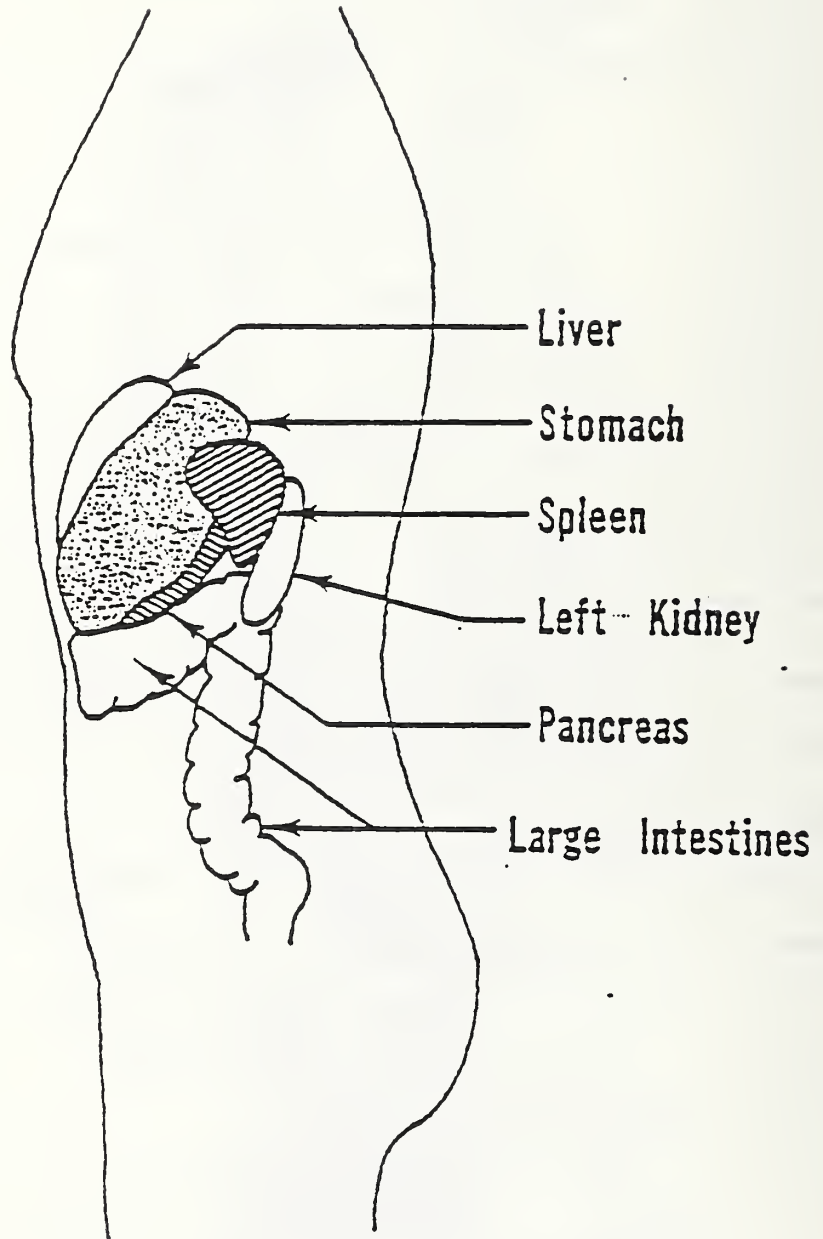


Test No. _____



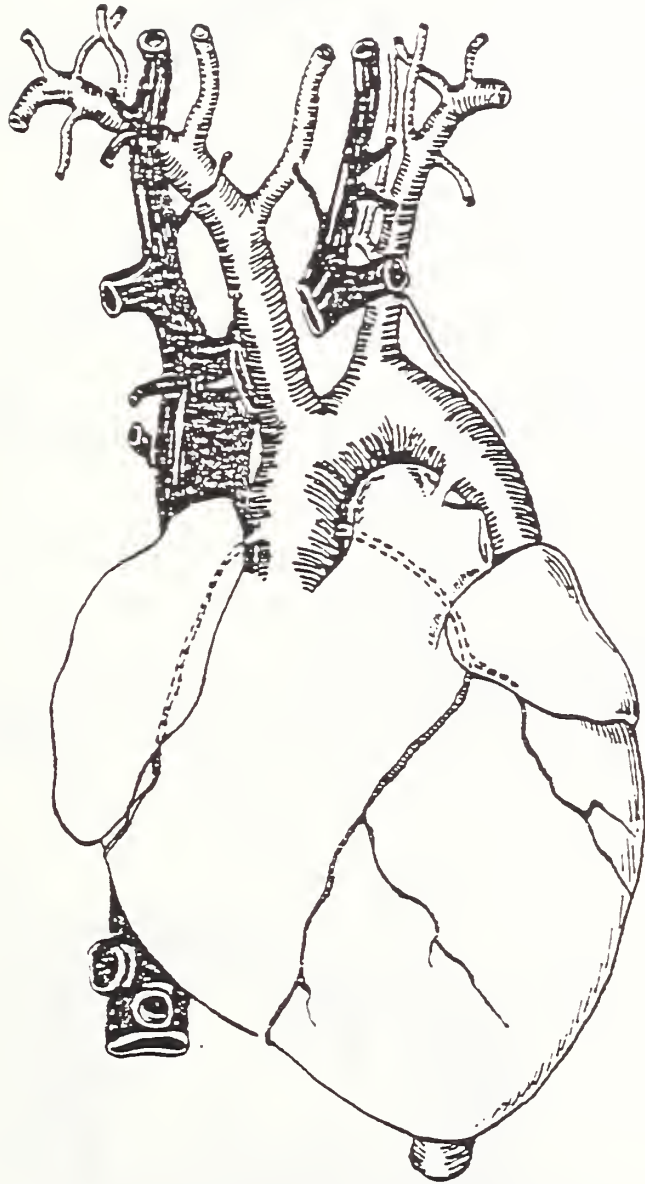


Test No. _____

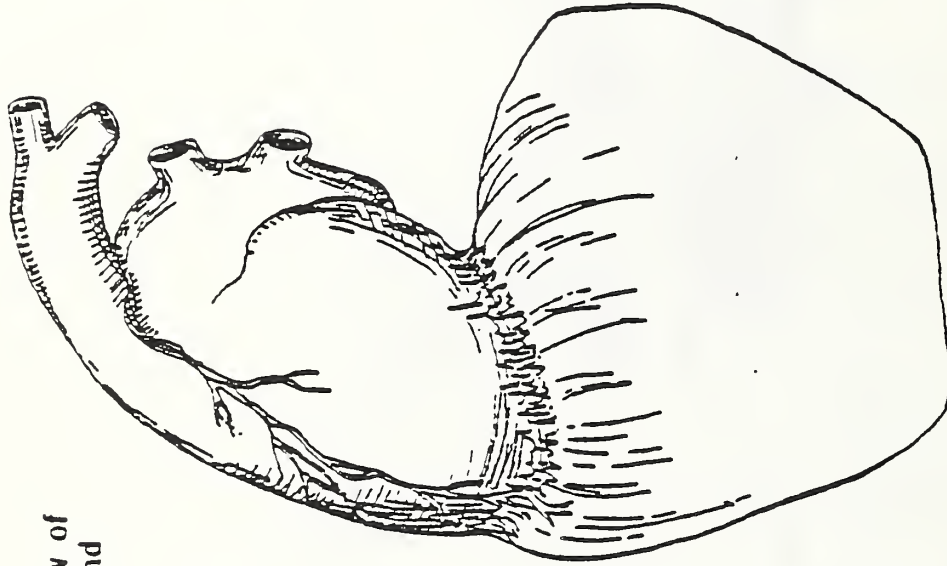


LEFT SIDE

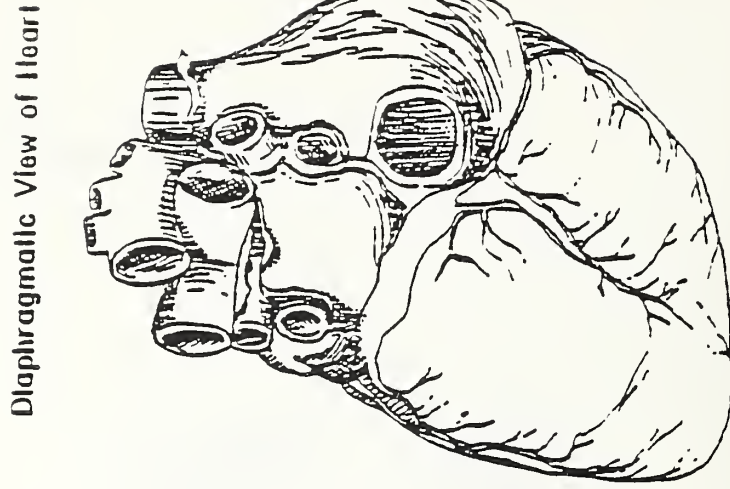
TEST NO. _____



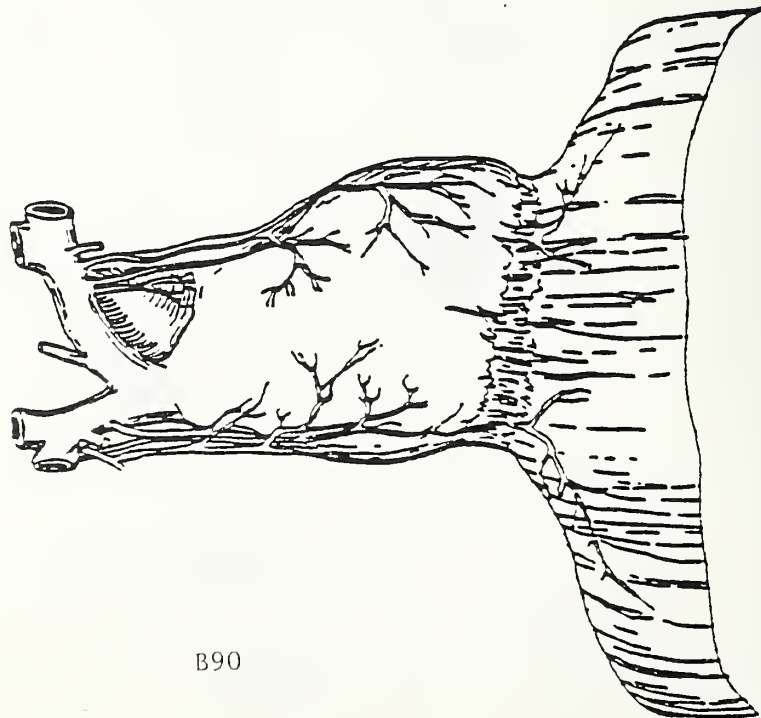
TEST NO.



Left Side View of
Pericardium and
Diaphragm



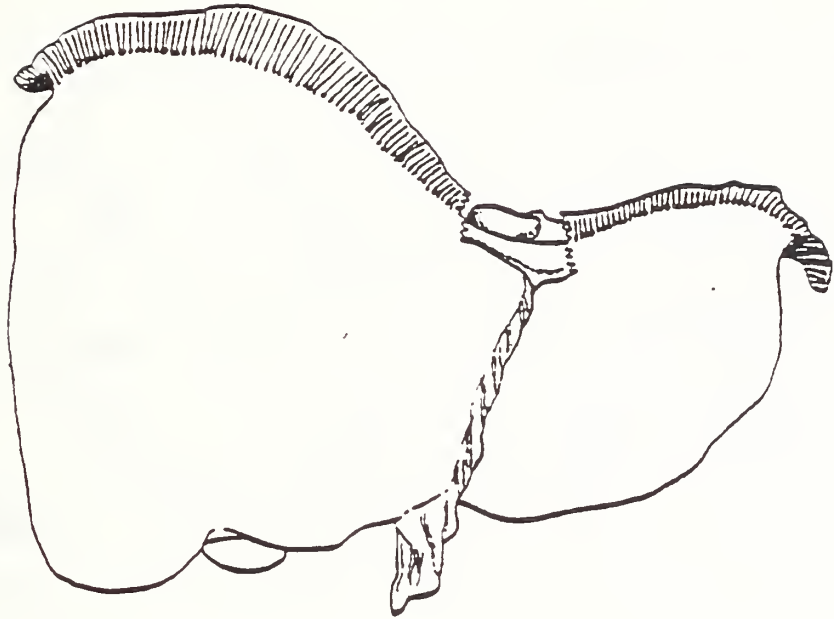
Diaphragmatic View of Heart



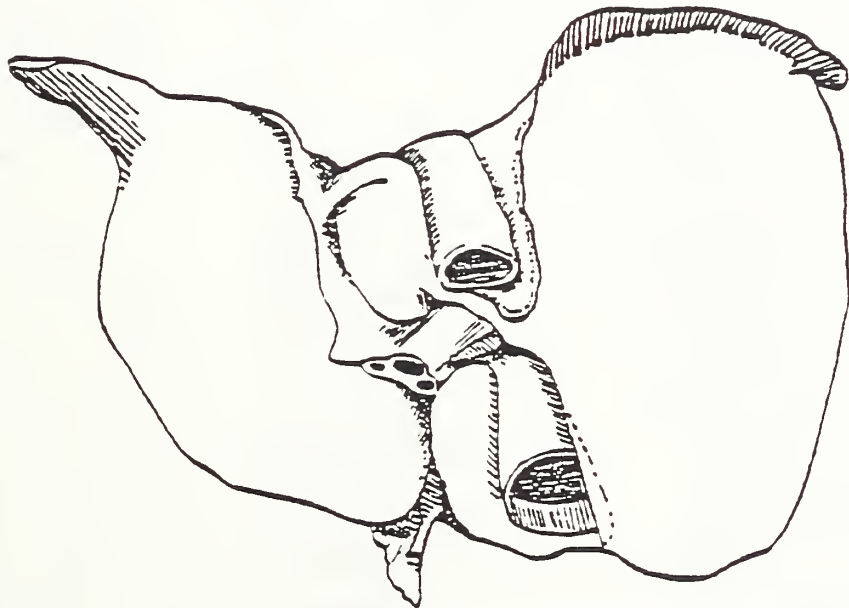
Anterior View of Pericardium and Diaphragm

LIVER IMPACT AUTOPSY SUMMARY

NC. _____



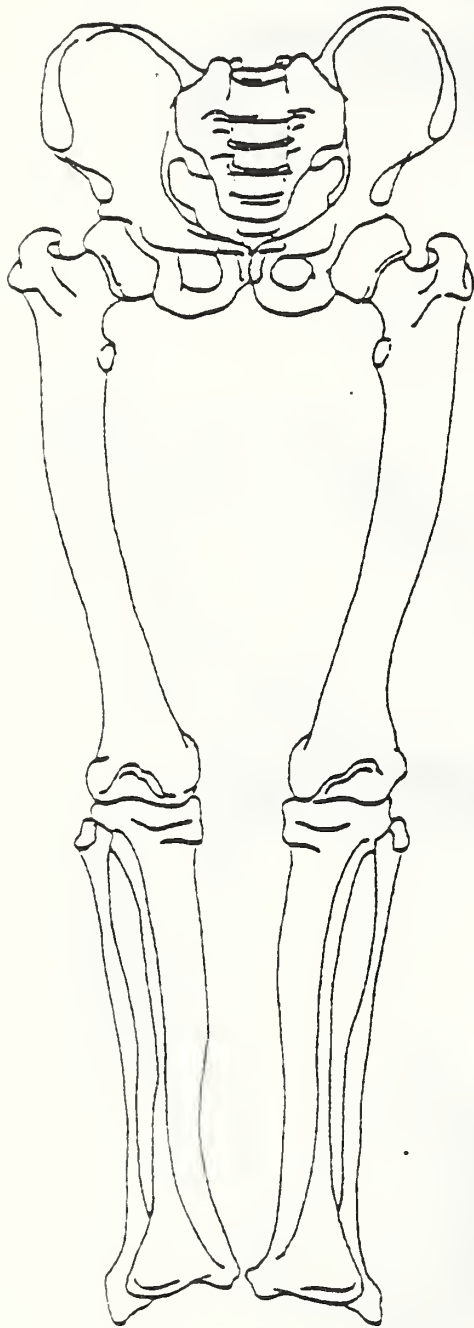
SUPERIOR SURFACE OF THE LIVER



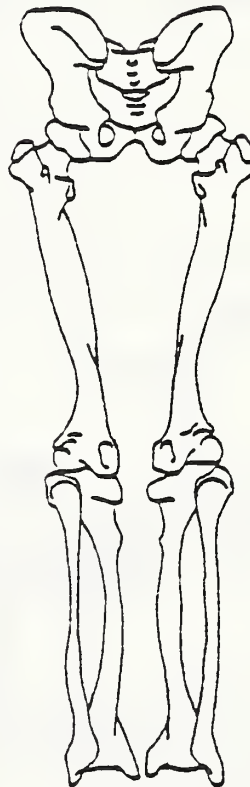
VISCERAL SURFACE OF THE LIVER

TEST NO. _____

DATE _____



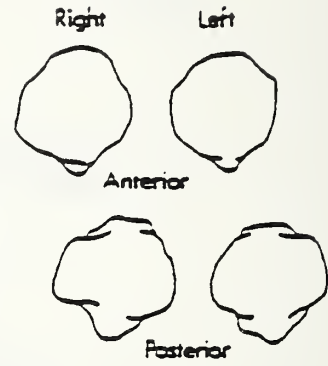
Anterior



Posterior

LOWER EXTREMITIES

PATELLA



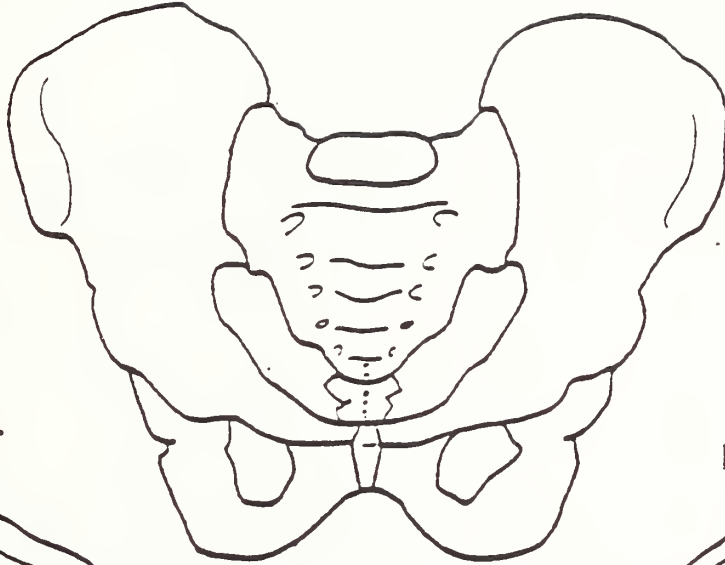
Right

Left

Anterior

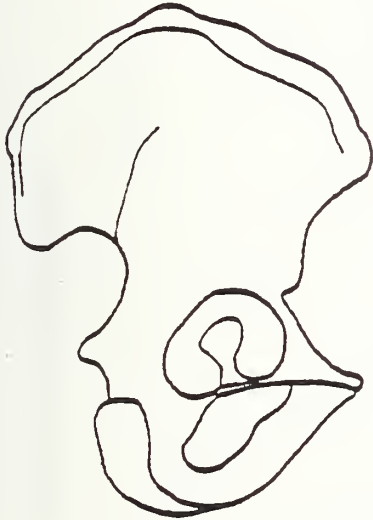
Posterior

TEST NO. _____

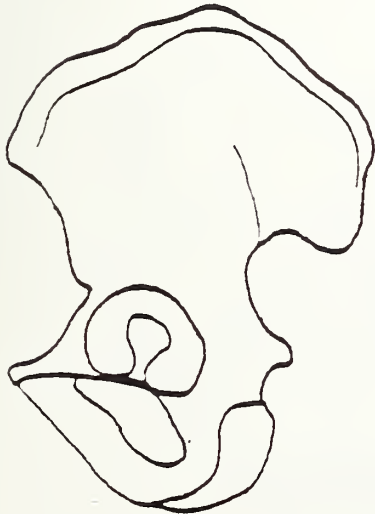
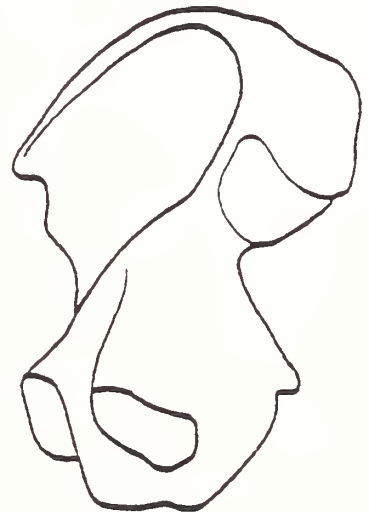


OUTER ASPECT

INNER ASPECT



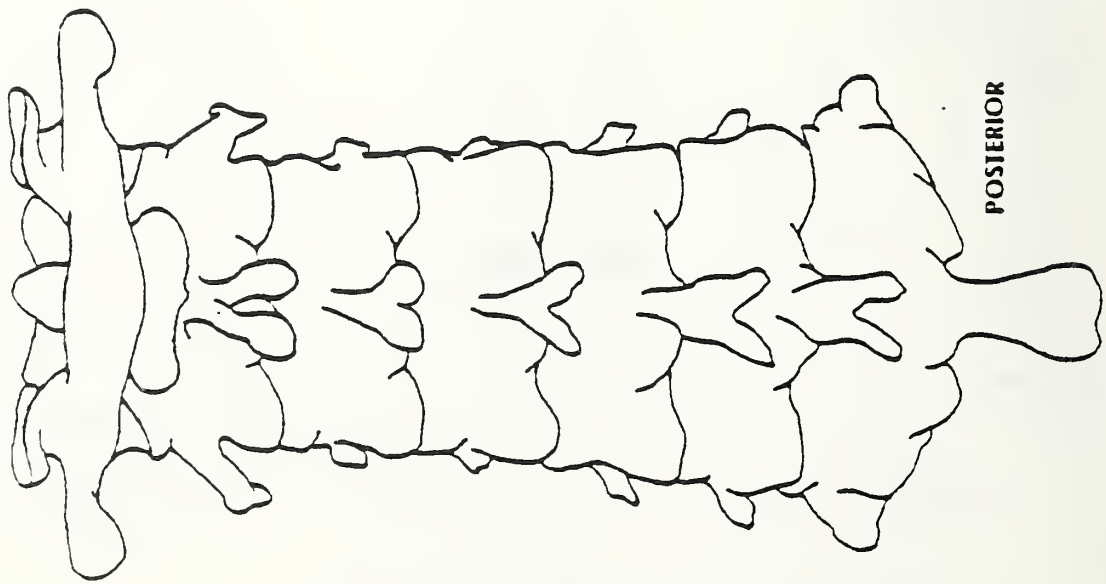
RIGHT ILIUM



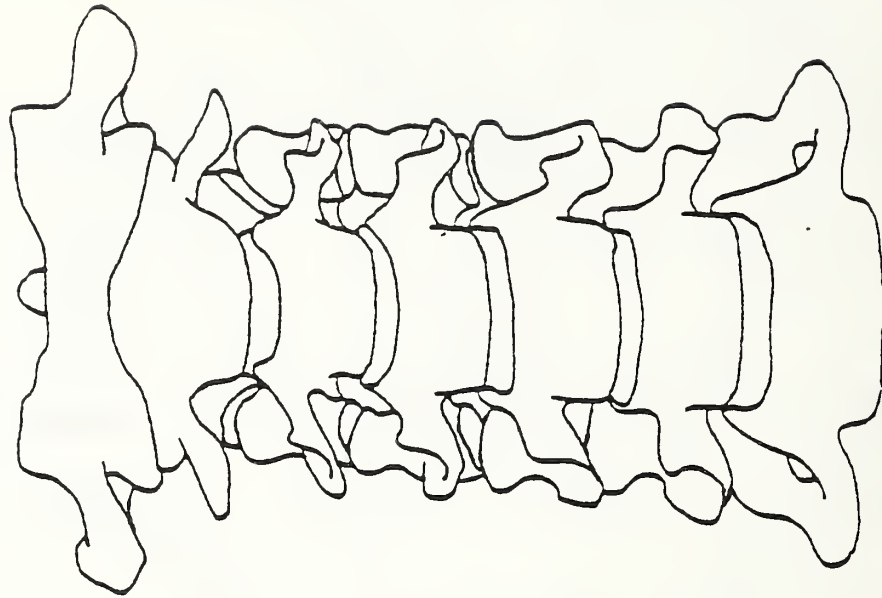
LEFT ILIUM



TEST NO. _____



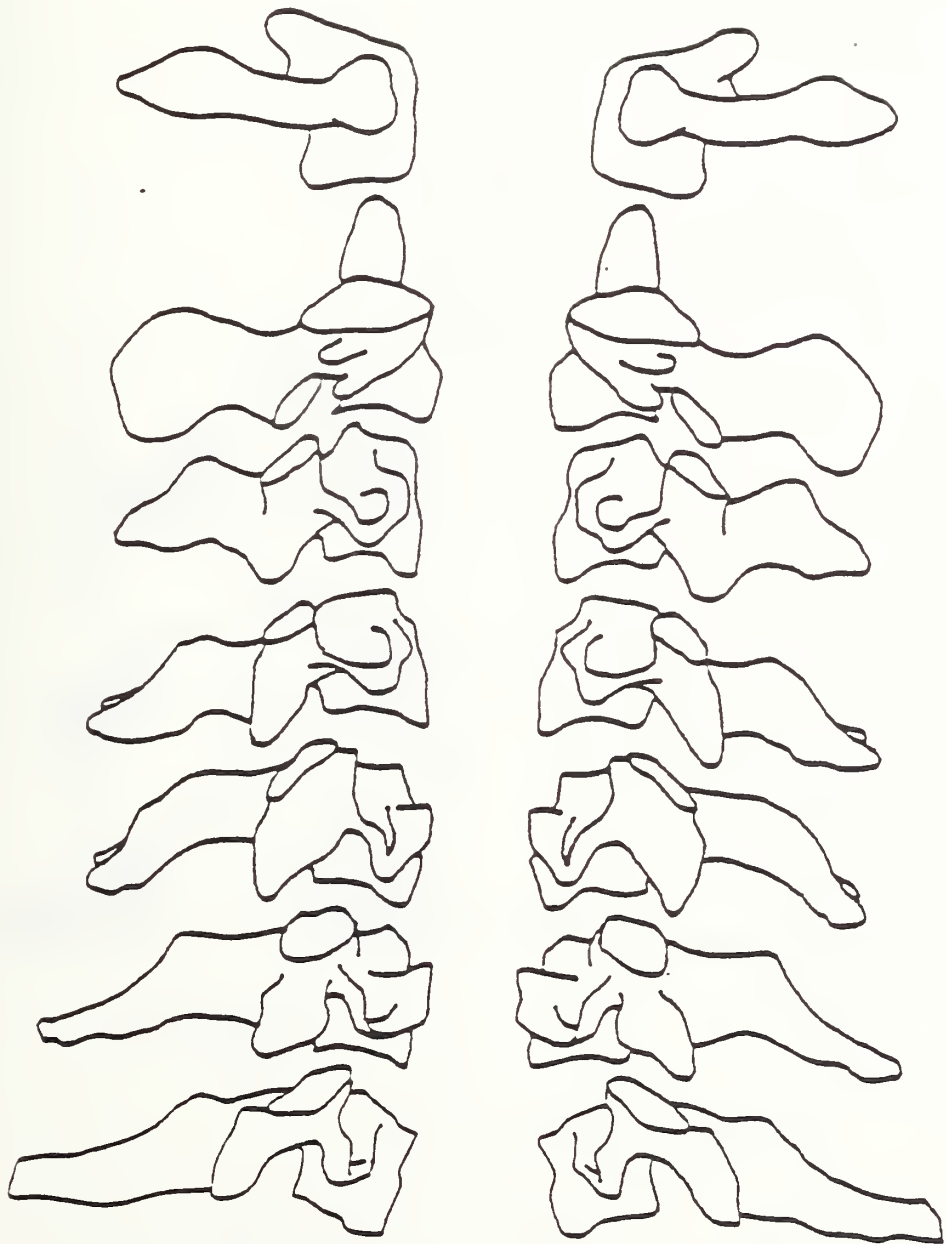
POSTERIOR



ANTERIOR

CERVICAL VERTEBRAE

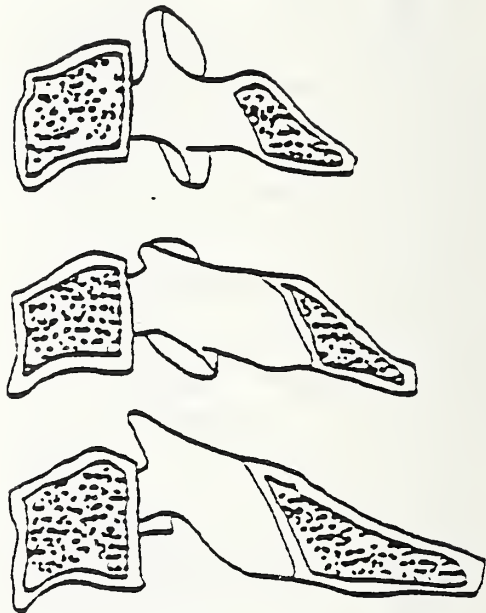
TEST NO. _____



Right Profile

Left Profile

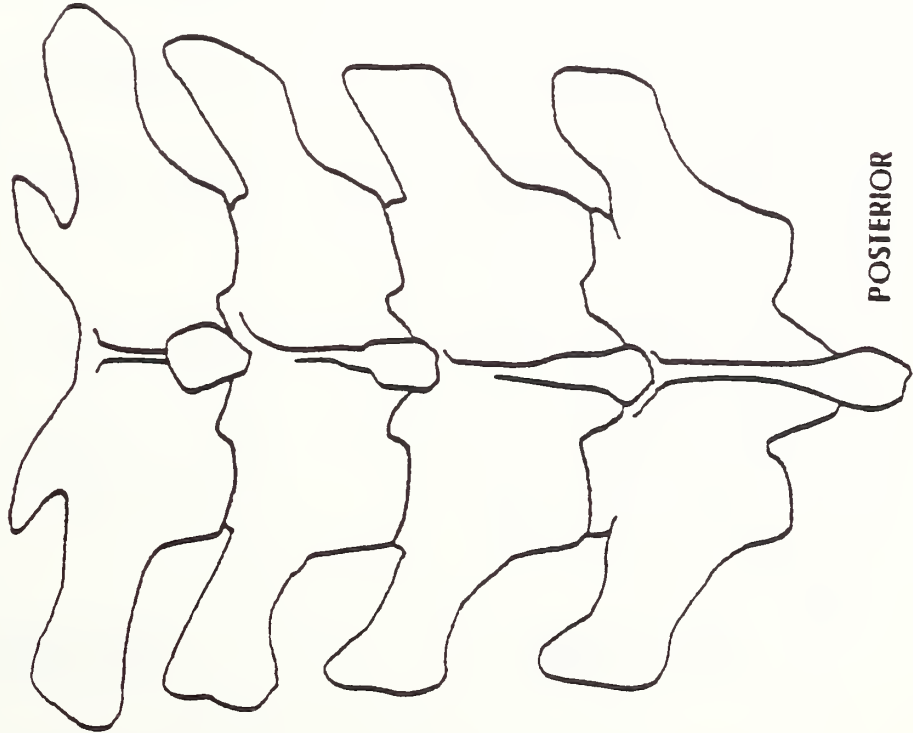
TEST NO. _____



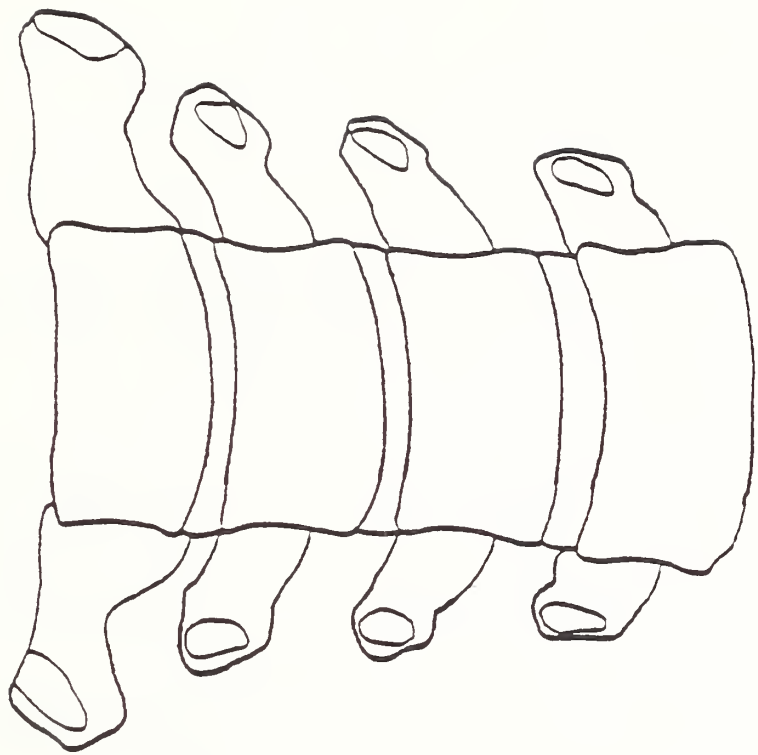
Cross Section

TEST NO. _____

THORACIC VERTEBRAE (T1 - T4)



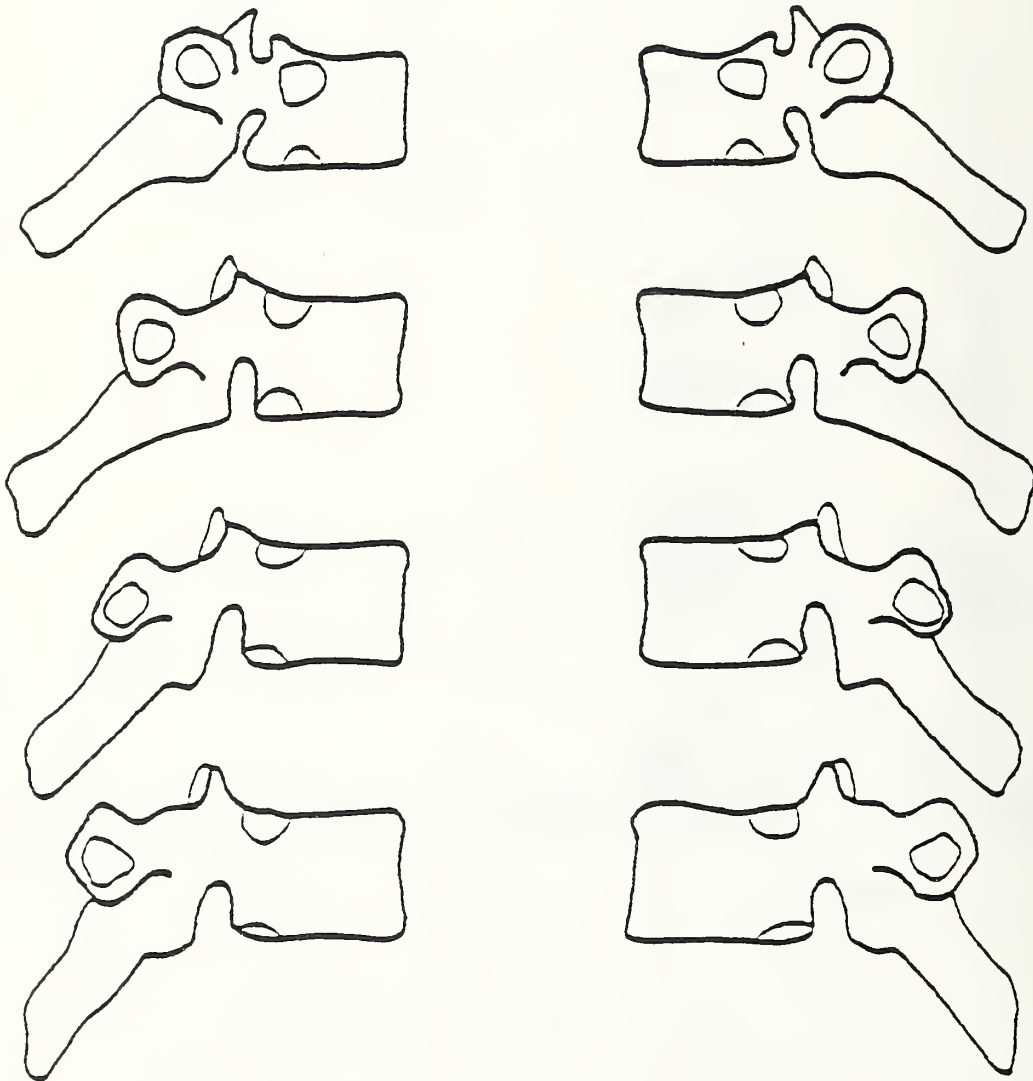
POSTERIOR



ANTERIOR

TEST NO. _____

THORACIC VERTEBRAE (T1-T4)



RIGHT PROFILE

LEFT PROFILE

APPENDICES

Anatomy Room Setup
Sled Lab Setup
Cart Setup
Autopsy Setup
Timer Box Setup
Pendulum Wierdness

MEASUREMENT

- ___ Anthropometer
- ___ Metric measuring tape

PAPER AND PLASTICS

- ___ Visqueen on autopsy table
- ___ Blue pads on table
- ___ Gauze

TAPES AND STRINGS

- ___ Silver tape
- ___ Masking tape
- ___ Adhesive tape
- ___ Fiber tape
- ___ Flat waxed string

SCALPELS

- ___ 2 large (#8) handles
- ___ 2 medium (#4) handles
- ___ 2 small (#3) handles
- ___ 2 #60 blades
- ___ 5 #22 blades
- ___ 5 #15 blades
- ___ 2 #12 blades

FORCEPS

- ___ 2 hooked
- ___ 2 large plain
- ___ 2 small plain

HEMOSTATS

- ___ needle
- ___ small straight
- ___ small curved
- ___ large straight
- ___ large curved

SCISSORS

- ___ 2 small
- ___ 2 medium
- ___ 2 large

SPREADERS

- ___ 2 large
- ___ 2 medium

NEEDLES

- ___ 2 double curved
- ___ 8 Trocar with stainless steel lockwire
- ___ 2 5cc syringes

CLOTHING

- ___ Tampons
- ___ Thermoknit longjohns and top
- ___ Cotton socks
- ___ Blue vinyl pants and top
- ___ Head and body harnesses

PRESSURIZATION

- ___ Modified Foley (#18 or #20) balloon catheters
- ___ Kulite shield
- ___ Tracheal tube
- ___ Right and left carotid pressurization catheters (Foley #10-14)
- ___ Cerebral spinal catheter (Foley #14-16)
- ___ Respiratory pressure tank
- ___ Manometer
- ___ Fluid pressure tank
- ___ 7% saline solution with India ink

BOLTS AND SCREWS

- ___ 6 self-tapping lag bolts
- ___ 3 lengths of wood screws
- ___ 1-72 screws
- ___ 10-32 tap
- ___ Strain relief bolt
- ___ Wood and metal self-tapping screw boxes

MOUNTS

- ___ Spine(2)
- ___ Rib (2, triax)
- ___ Rib (2, uniax, R-L)
- ___ Nine-accelerometer plates (large, small, and 8 feet)
- ___ Sternum
- ___ Substernale
- ___ Suprasternale (triax)
- ___ Dental acrylic
- ___ Bone wax

TOOLS

- ___ Electric hair clippers
- ___ Electric drill
- ___ Drill bits (No. 7, approx. 1/16", etc.)
- ___ large and small screwdrivers
- ___ nut driver (for lag bolts)
- ___ wire twisters
- ___ bone shears
- ___ Executive Slinky object space calibrated and nearly functional

MATERIALS

- ___ balsa wood
- ___ rags
- ___ foam (at least 2 sheets of 3x4 ft 6")
- ___ Ensolite
- ___ Styrofoam
- ___ Dow Ethafoam
- ___ Overhead support bar

ROPE CUTTERS

- ___ head, 1/8"
- ___ pendulum (with spring, 3/16")
- ___ nylon strings (10 24" 3/16"; 10 18" 1/8")
- ___ shock absorber and styrofoam bumper

WEIGHTS

- ___ steel blocks on pendulum

MISCELLANEOUS

- ___ calculator
- ___ bone wax
- ___ Pressurization equipment (pulmonary, thoracic arterial, head arterial, cerebral spinal)
- ___ Timer box
- ___ Strobes
- ___ Head impact back brace and foam padding

TAPES

- adhesive
- fiber
- silver
- masking
- black
- double stick

PAPER AND PLASTIC

- blue pads
- gauze
- gloves
- plastic garbage bags

SCALPELS

- 1 medium (#4) handle
- 1 small (#3) handle
- 2 #22 blades
- 2 #15 blades
- 1 #12 blade

SURGICAL TOOLS

- 2 forceps
- 2 hemostats
- large scissors
- 2 double curved needles

STRING

- flat waxed string
- black thread

TOOLS

- ___ small (1-72) screwdriver
- ___ large screwdriver
- ___ nut driver
- ___ ball driver (6-32, 0-80)
- ___ 1-72 screws
- ___ 2-56 screws
- ___ 0-80 screws
- ___ wiretwisters

MISCELLANEOUS

- ___ ball targets
- ___ paper targets
- ___ bone wax
- ___ vaseline
- ___ Q-tips
- ___ tubing connectors
- ___ tie wraps
- ___ lockwire
- ___ 50cc syringe
- ___ pulmonary pressurization relief valves

AUTOPSY SETUP

PAPER AND PLASTICS

- ___ Visqueen on autopsy table
- ___ blue pads
- ___ gauze

TAPE

- ___ silver tape
- ___ masking tape
- ___ fiber tape

SCALPELS

- ___ 2 large (#8) handles
- ___ 2 medium (#4) handles
- ___ 2 small (#3) handles
- ___ 2 #60 blades
- ___ 5 #22 blades
- ___ 5 #15 blades
- ___ 2 #12 blades

FORCEPS

- ___ 2 hooked
- ___ 2 large plain
- ___ 2 small plain

HEMOSTATS

- ___ needle
- ___ small straight
- ___ small curved
- ___ large straight
- ___ large curved

SCISSORS

- ___ 2 small
- ___ 2 medium
- ___ 2 large

SPREADERS

- ___ 3 medium
- ___ 3 large

MISCELLANEOUS

- ___ Stryker saw and blade
- ___ bone shears
- ___ wedge
- ___ rib cutters

TIMER BOX SETUP

EQUIPMENT	TIMER VALUES		
	Impact	Delay	Run
Gate (from strobe 1)	0012-y	1	0150
Lights (start)	0001	2	2600
HyCam (start)	1200	3	1600
Pendulum rope cutter (start)	2200-x*	4	0050
Photosonics (start)	1000	5	1600
		6	
Head, pelvis, rope cutter (from velocity probe)	0001	7	0050
Piston Acceleration Corridor	1 + 2	8	0050-0150

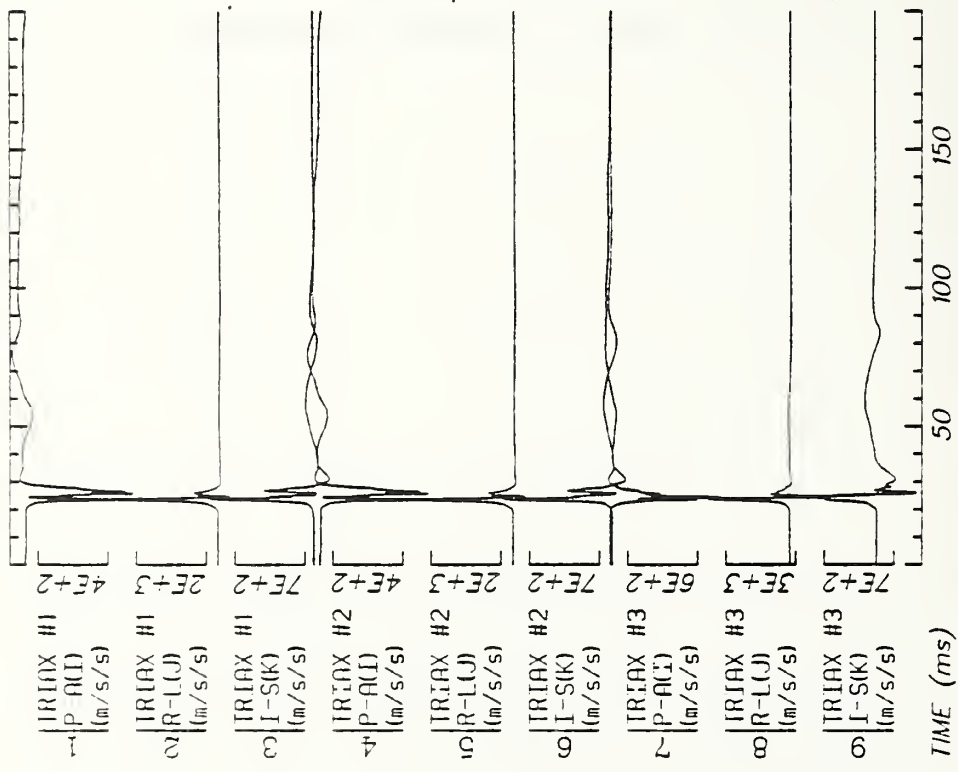
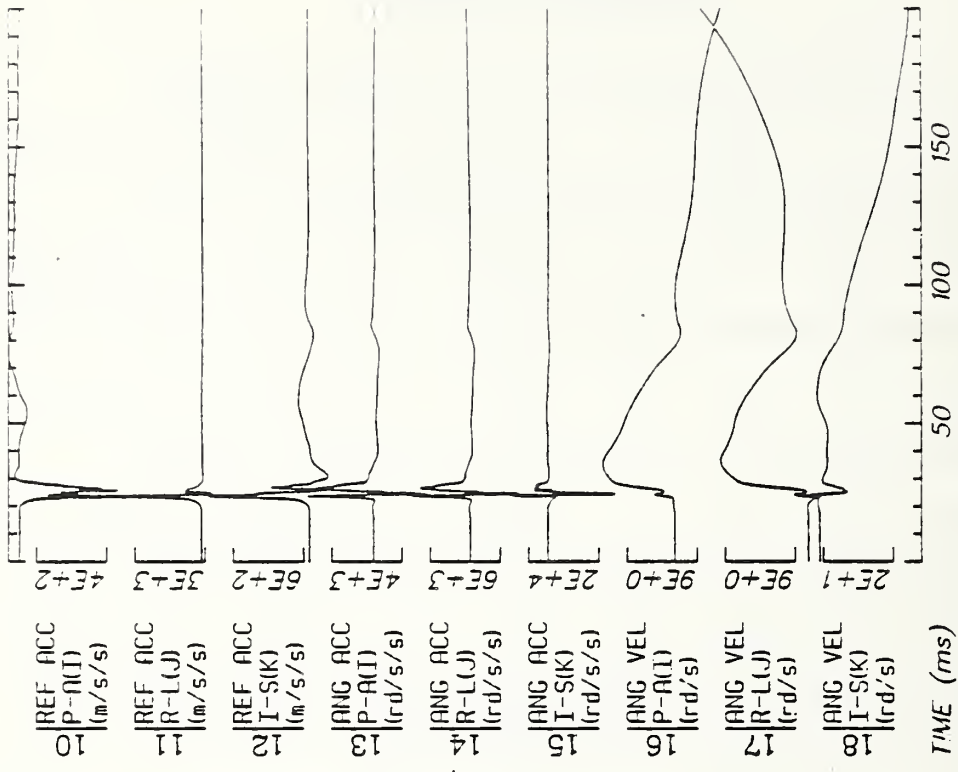
* x obtained from elliptic integral of the first kind. For
100° .87 sec, 20° .70 sec. $y = \text{angle}/20$ $z = 210/\text{angle}$

PENDULUM WEIRDNESS

Average	60.84	61.00	61.26	61.56
Standard Deviation	±.28	±.37	±.05	±.23
Period	3.042	3.050	3.063	3.078
(MGL/I)±2	2.065	2.060	2.051	2.041
t/2pi	.484	.485	.487	.489

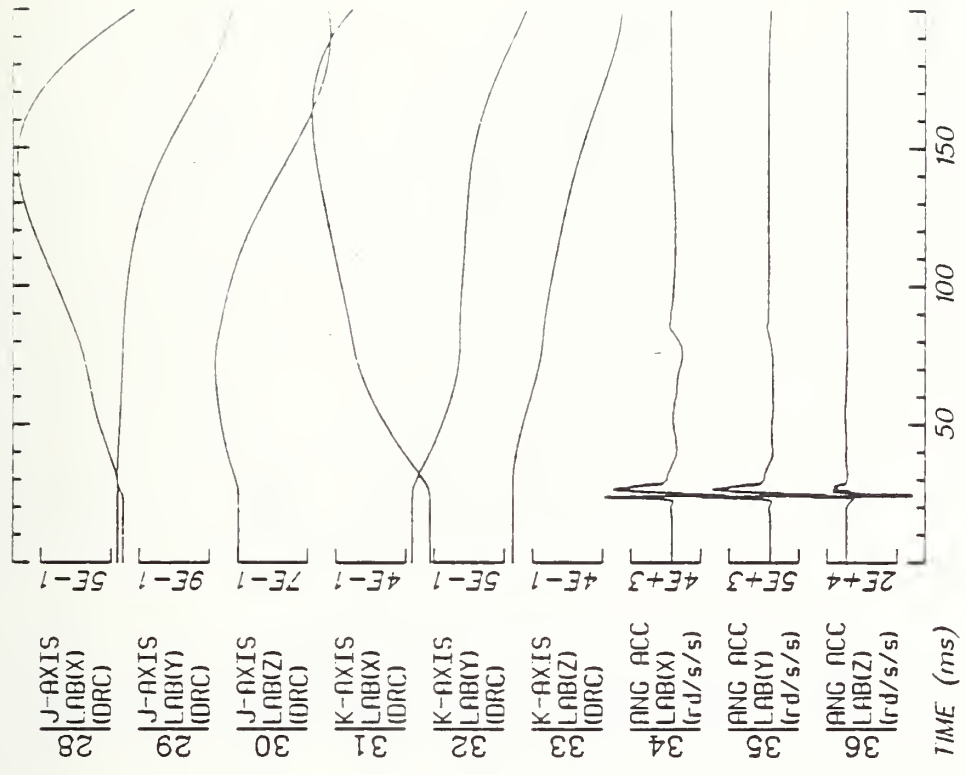
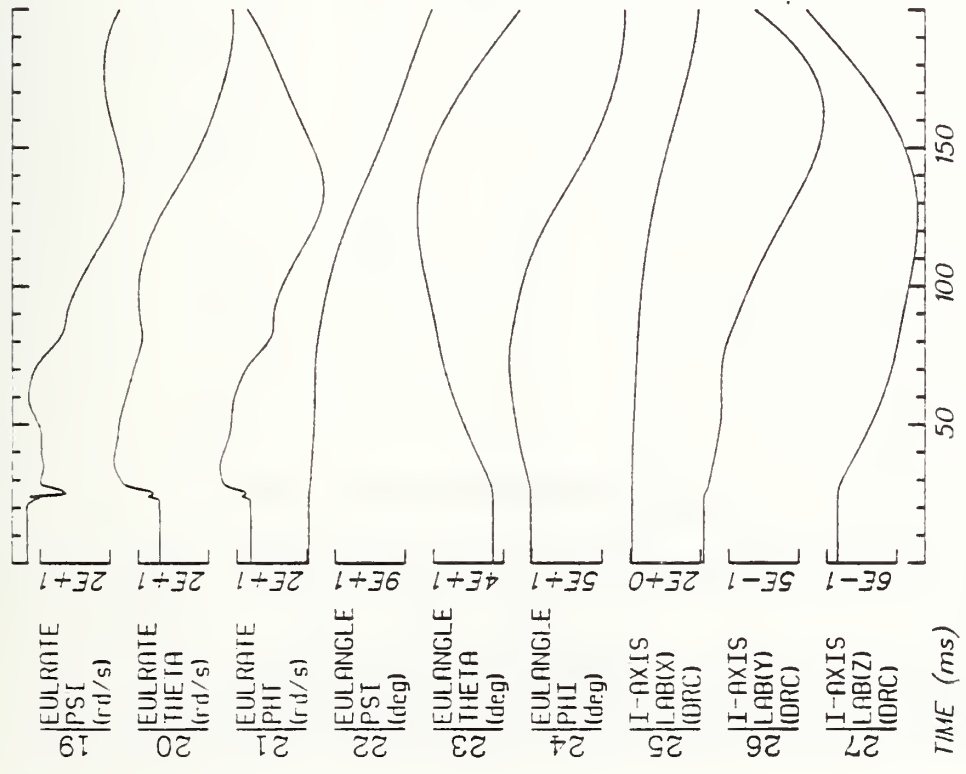
11.0 APPENDIX C

HEAD IMPACT SERIES - SELECTED TIME-HISTORIES



Run ID: 82E001 Disk: --HEAD File: 1 Date: MAR 11, 1985 Sheet: 1

Filter: 1600*4C



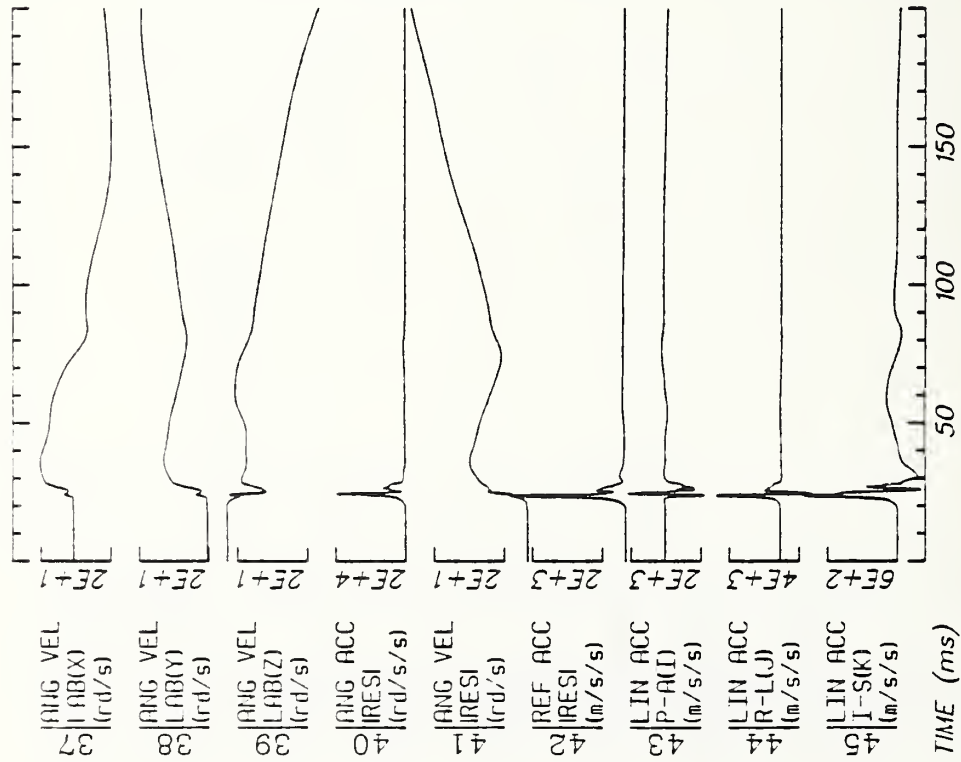
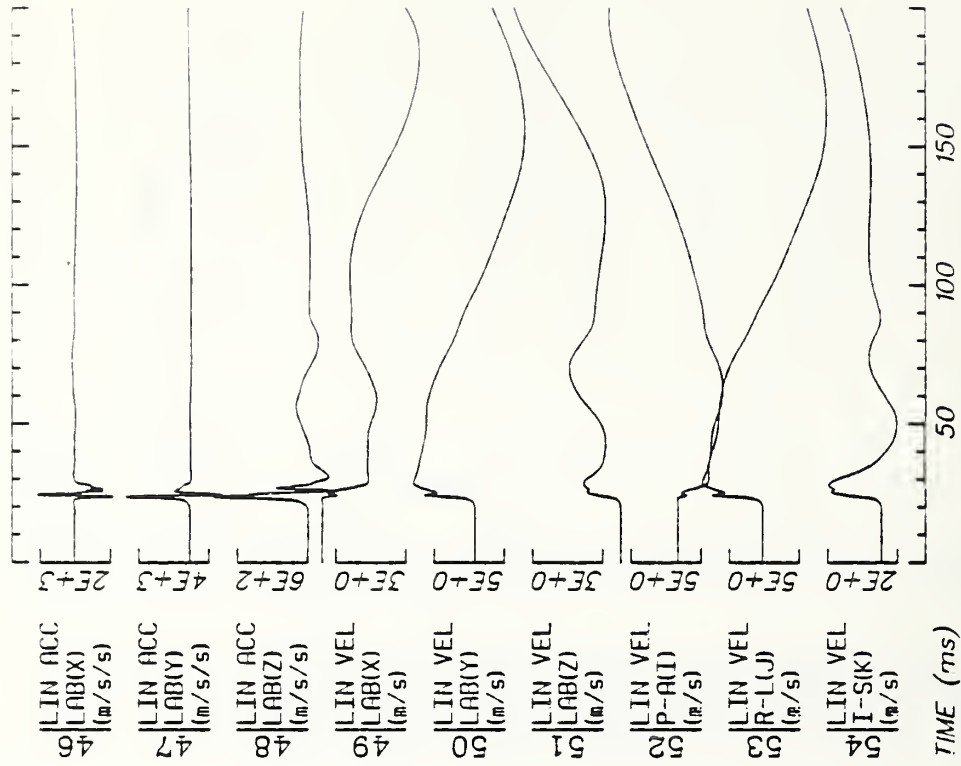
Run ID: B2E001
 Filter: 1600*4C

Disk: -HEAD

File: 1

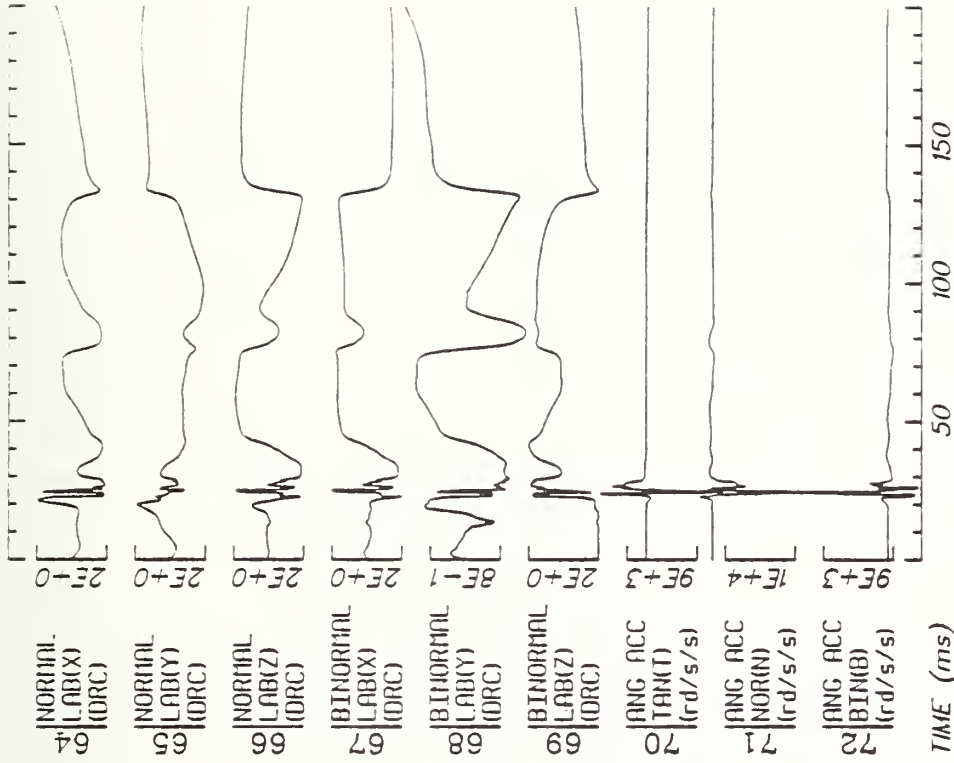
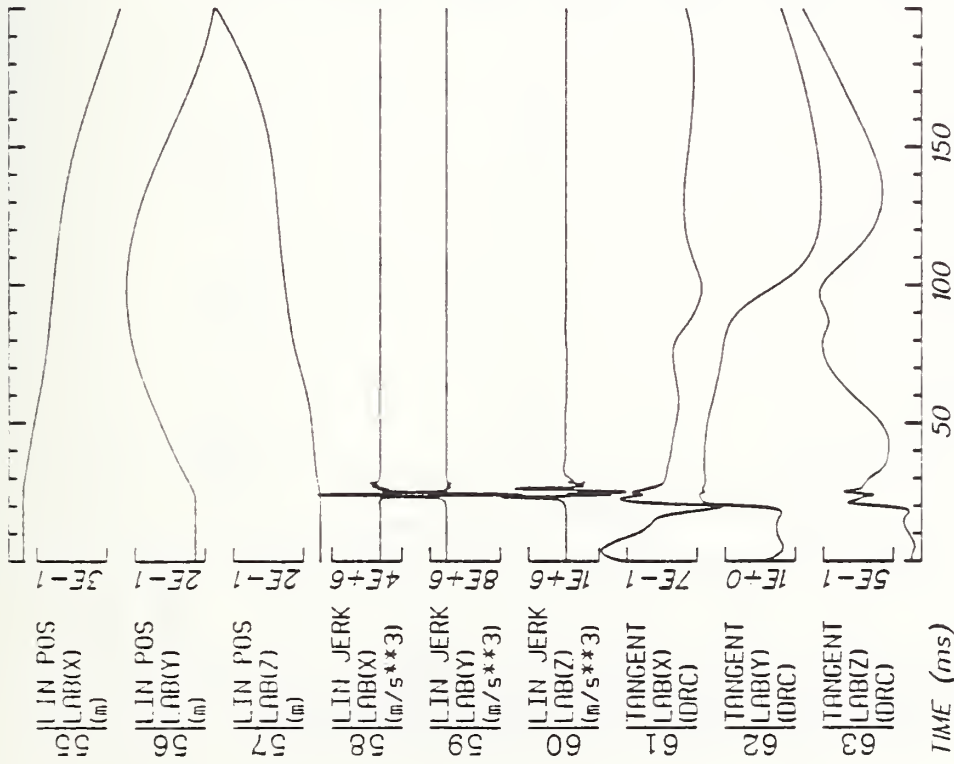
Date: MAR 11, 1985

Sheet: 2



Run ID: 82E001 Disk: -HEAD File: 1 Date: MAR 11, 1985 Sheet: 3

Filter: 1600*4C



Run ID: 82E001

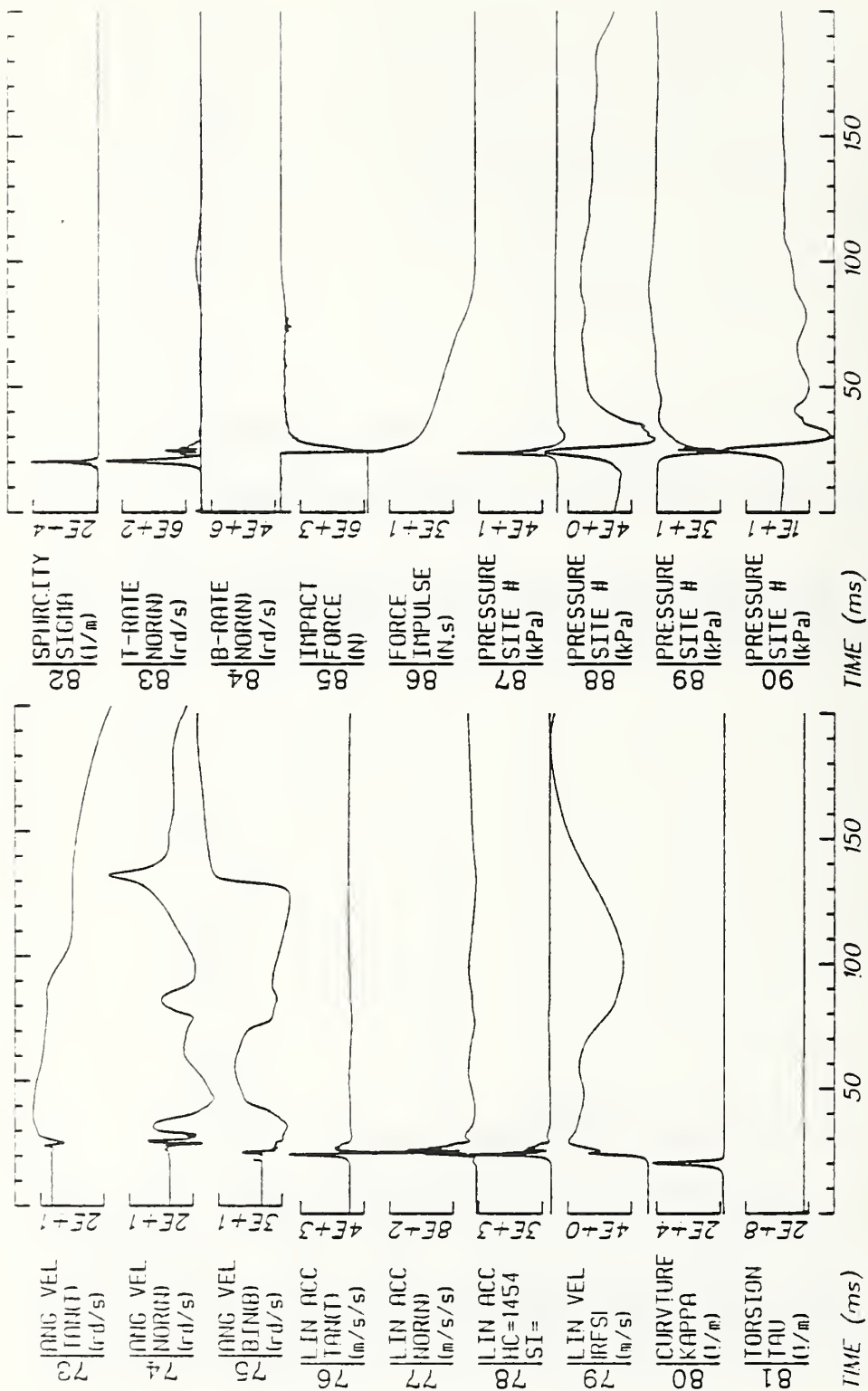
Disk: -HEAD

File: 1

Date: MAR 11, 1985

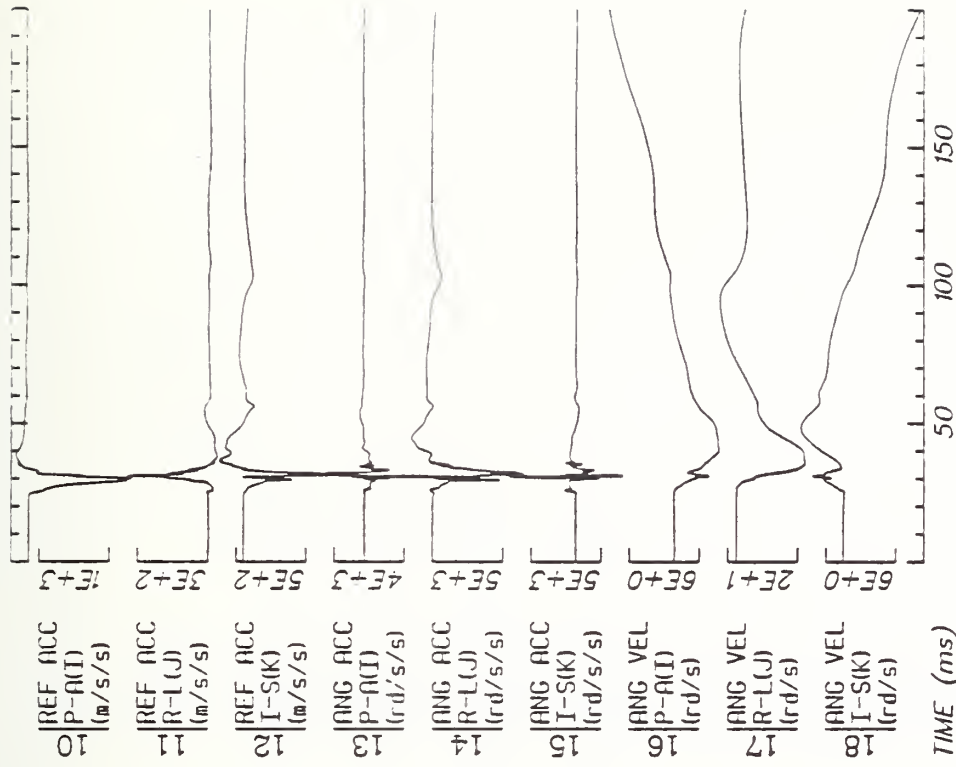
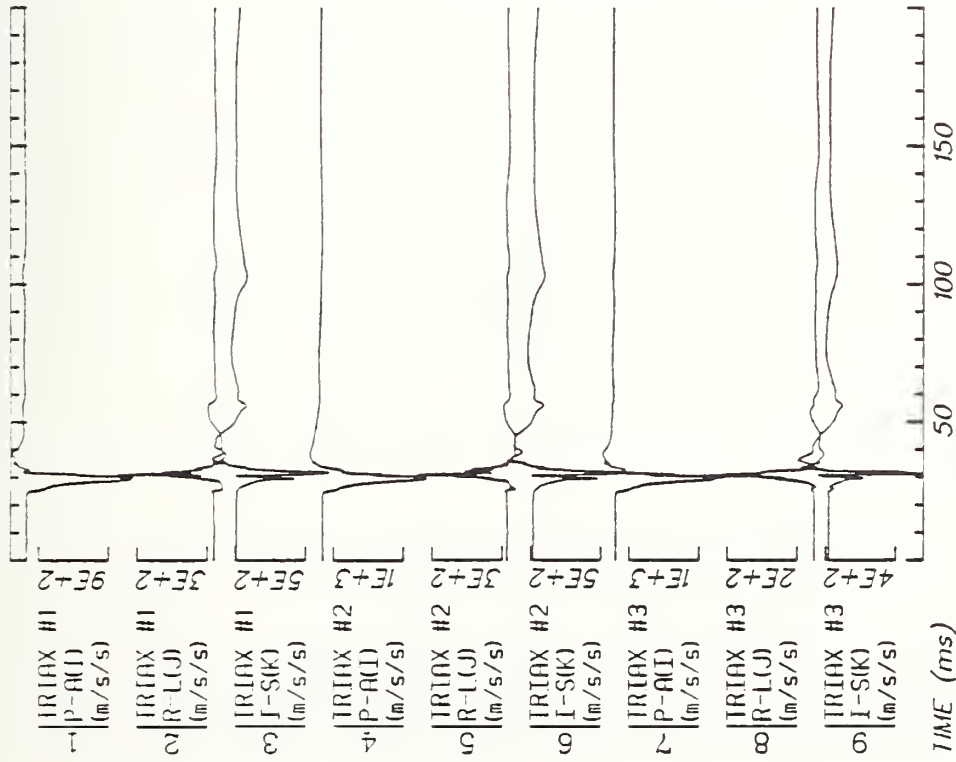
Sheet: 4

Filter: 1600*4C



Run ID: 82F001 Disk: -HEAD File: 1 Date: MAR 11, 1985 Sheet: 5

Filter: 1600*4C



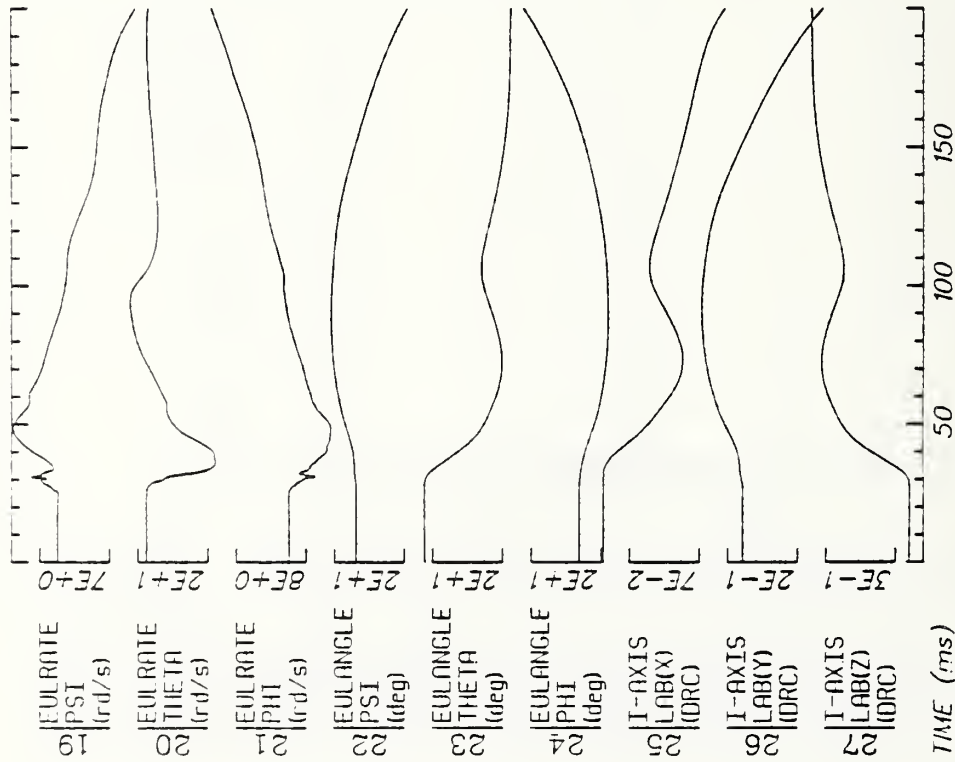
Run ID: 82E021

Disk: -HEAD

File: 2

Date: MAR 11, 1985 Sheet: 1

Filter: 1600*4C



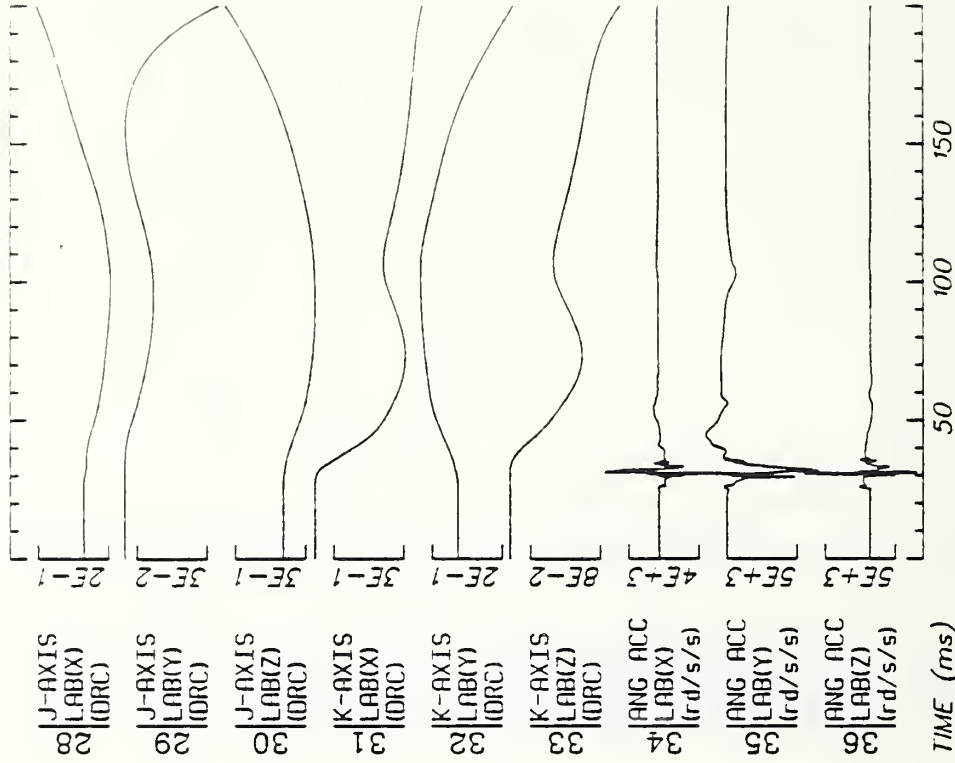
Run ID: 82F021

Disk: -HEAD

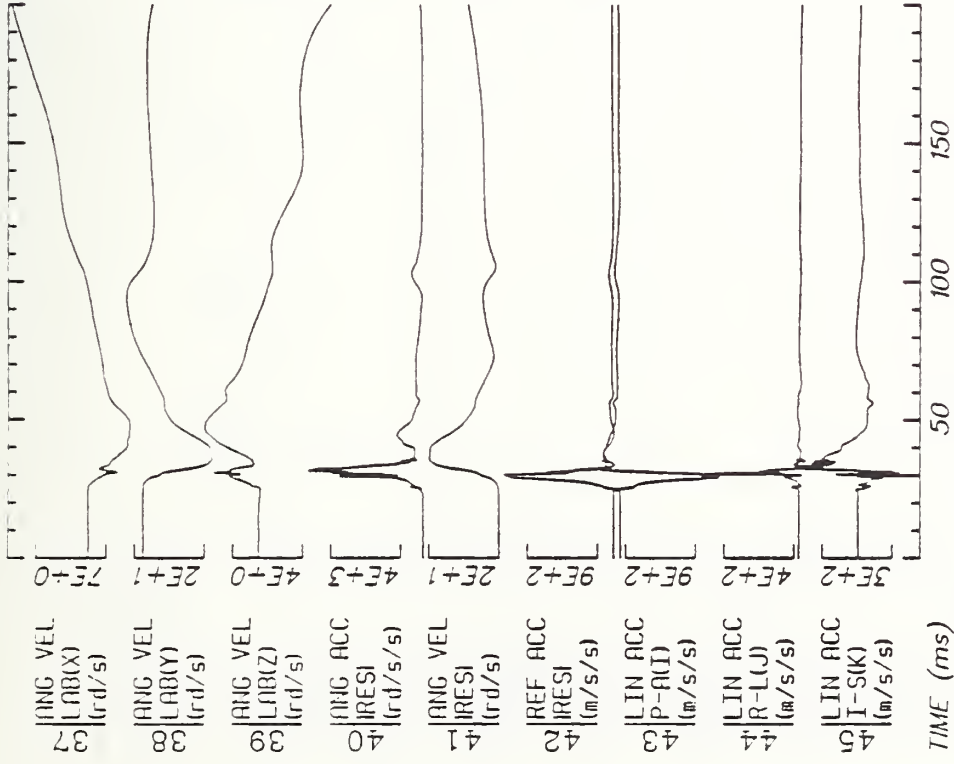
File: 2

Date: MAR 11, 1985

Sheet: 2



Filter: 1600*4C



TIME (ms)

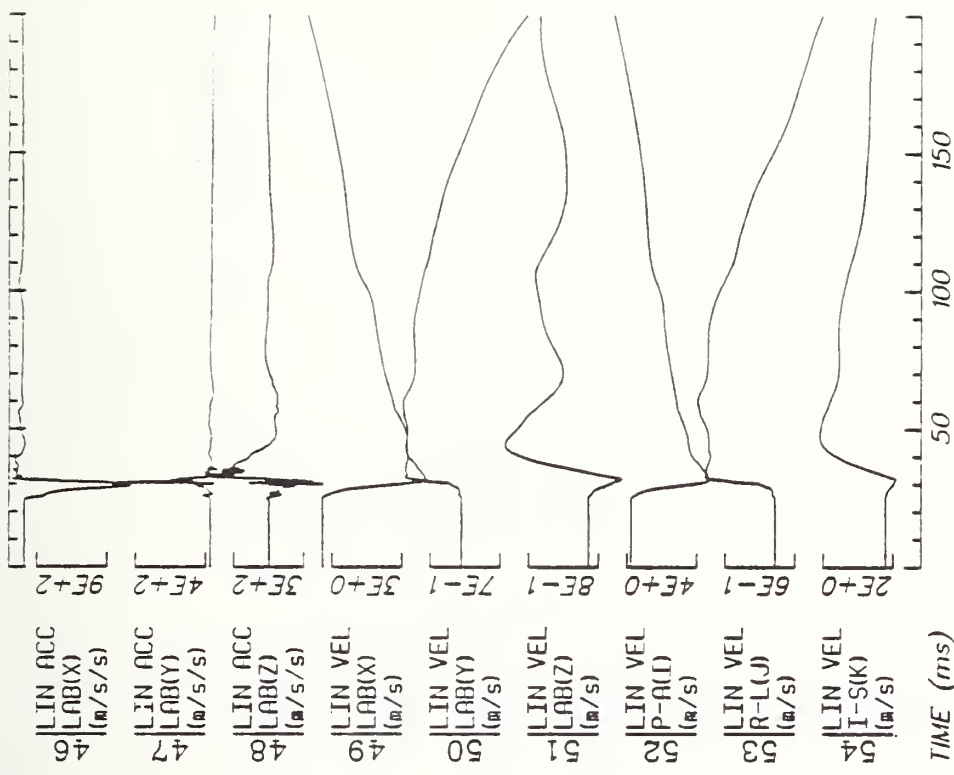
Run ID: 82E021

Disk: -HEAD

File: 2

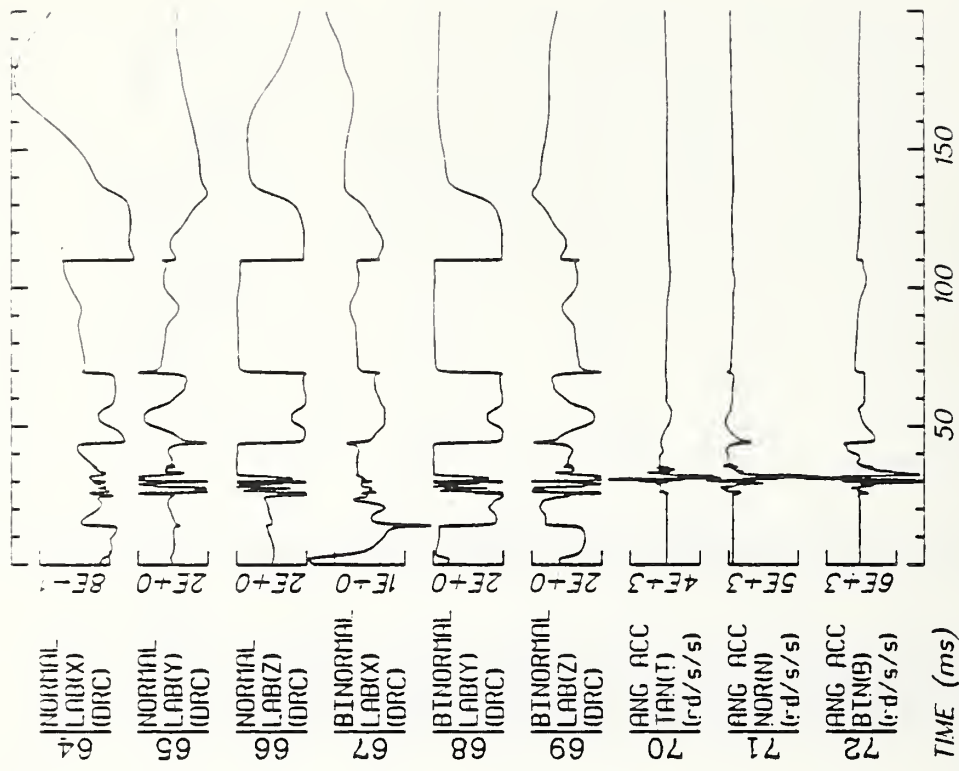
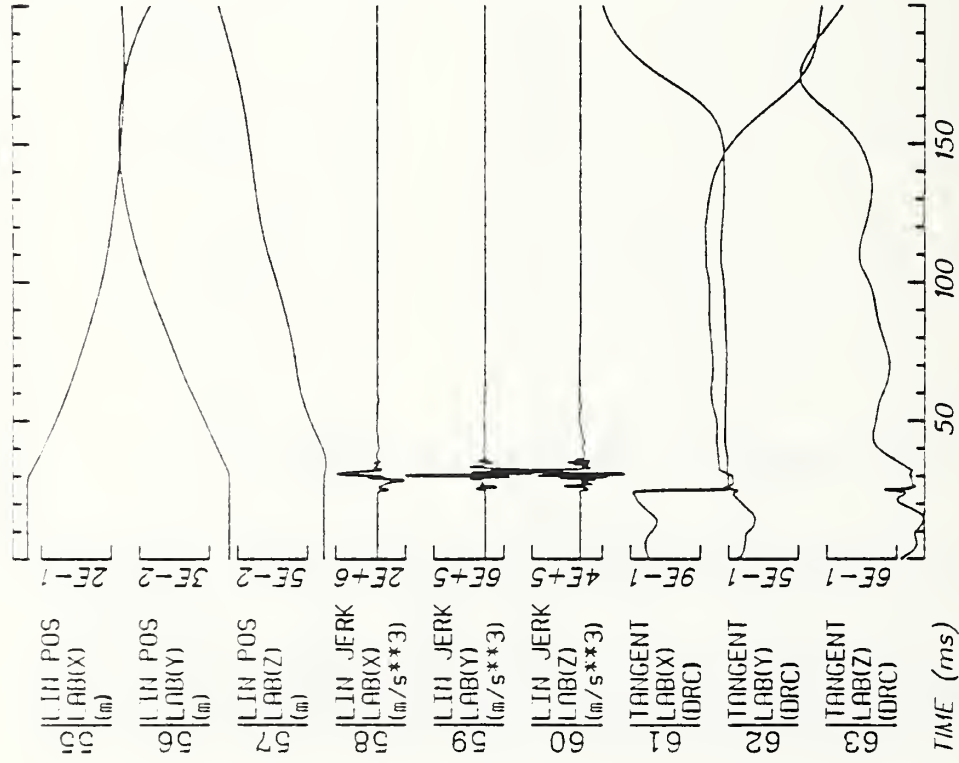
Date: MAR 11, 1985

Sheet 3



TIME (ms)

Filter: 1600*4C



Run ID: 82E021

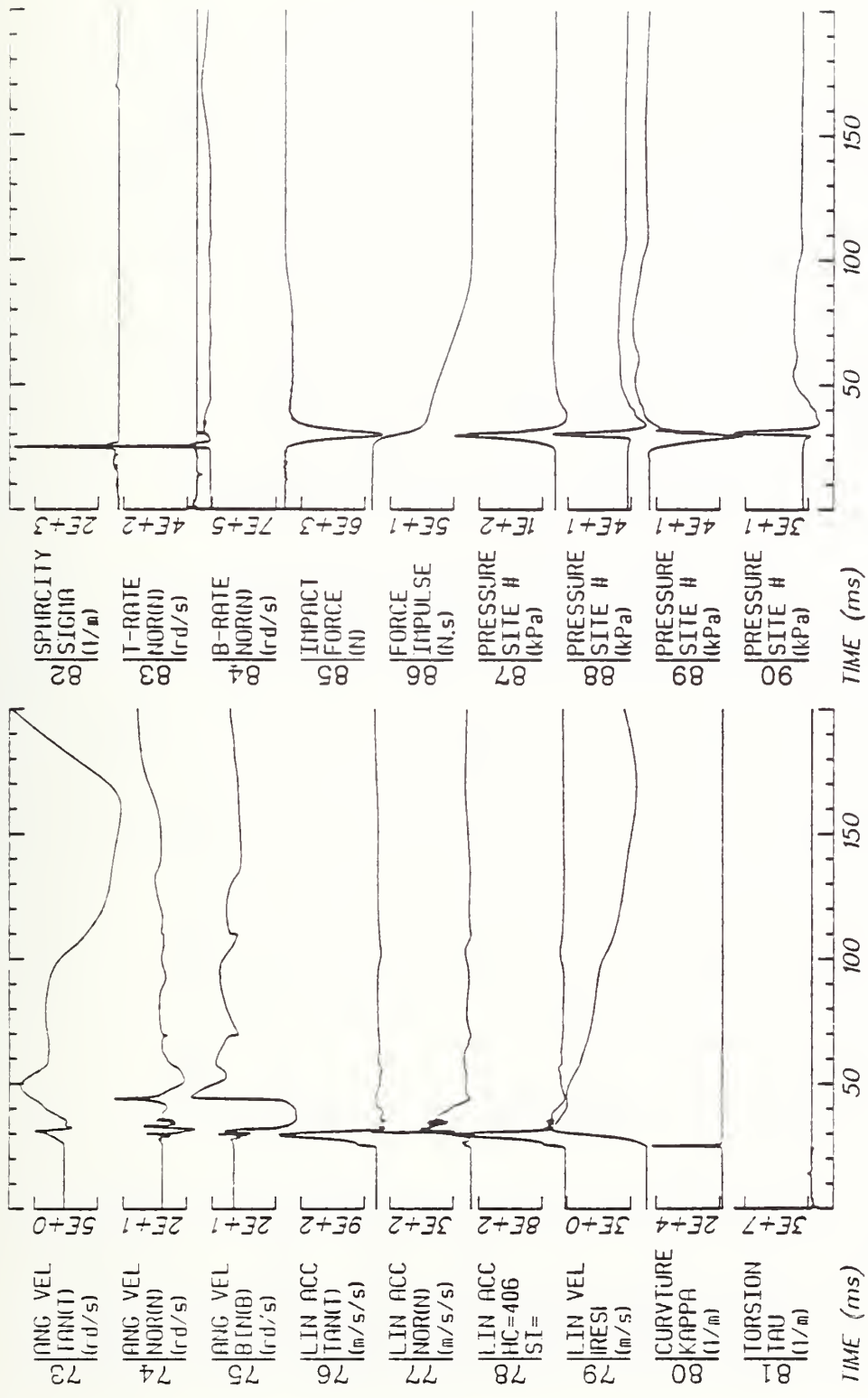
Disk: -HEAD

File: 2

Date: MAR 11, 1985

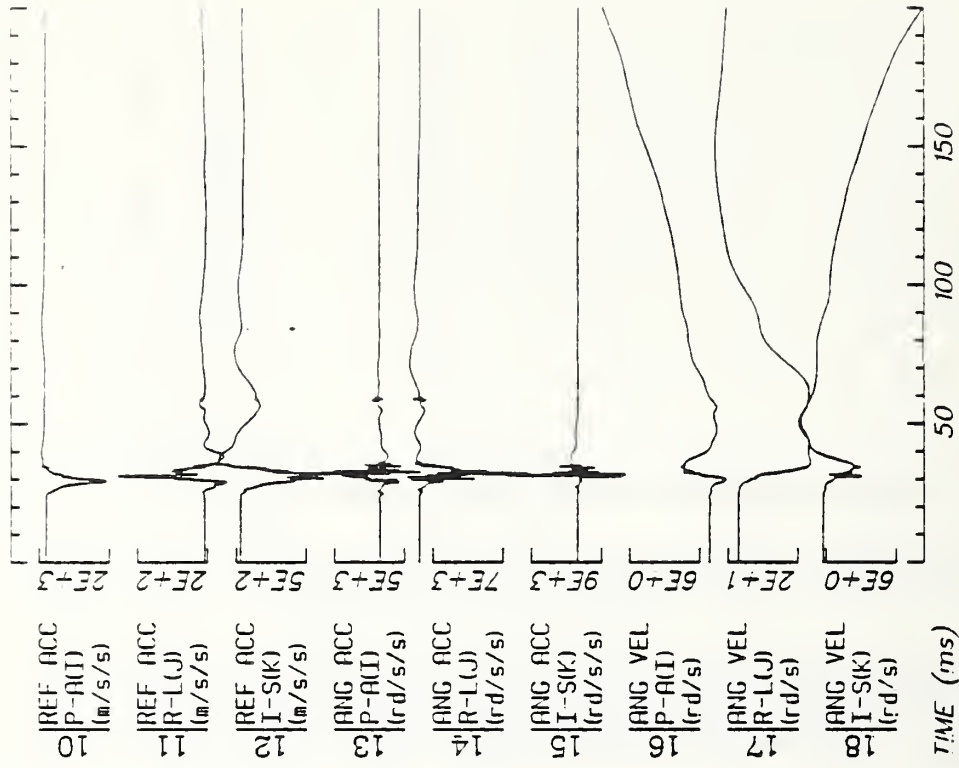
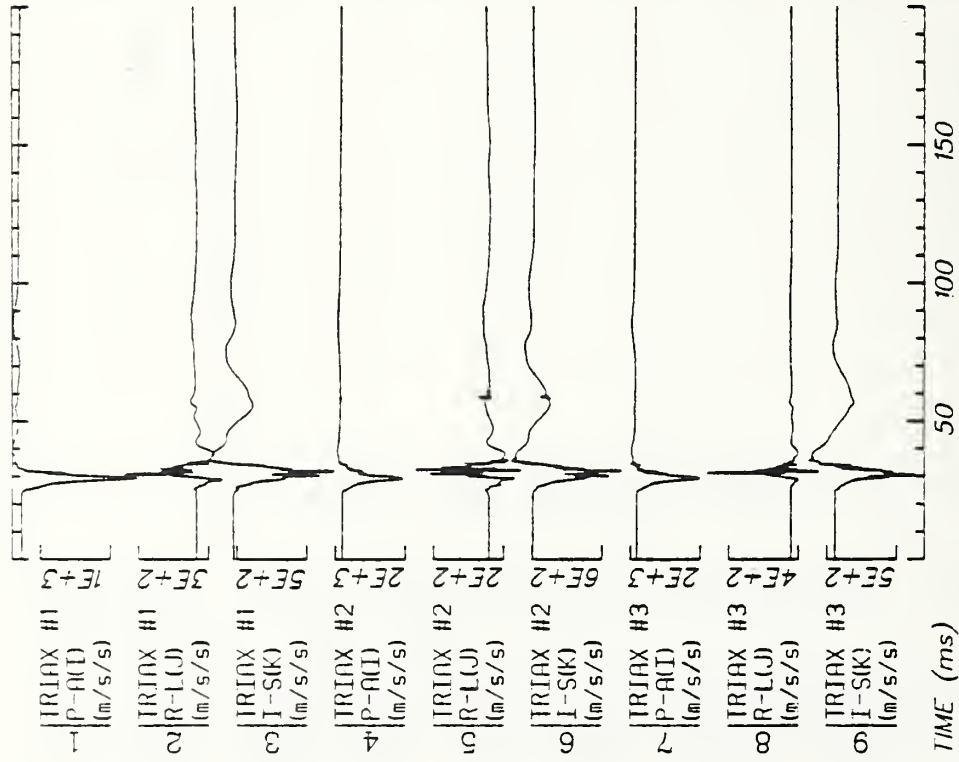
Sheet: 4

Filter: 1600*4C



Run ID: 82E021 Disk: -HEAD File: 2 Date: MAR 11, 1985 Sheet: 5

Filter: 1600*4C



Run ID: 82E022

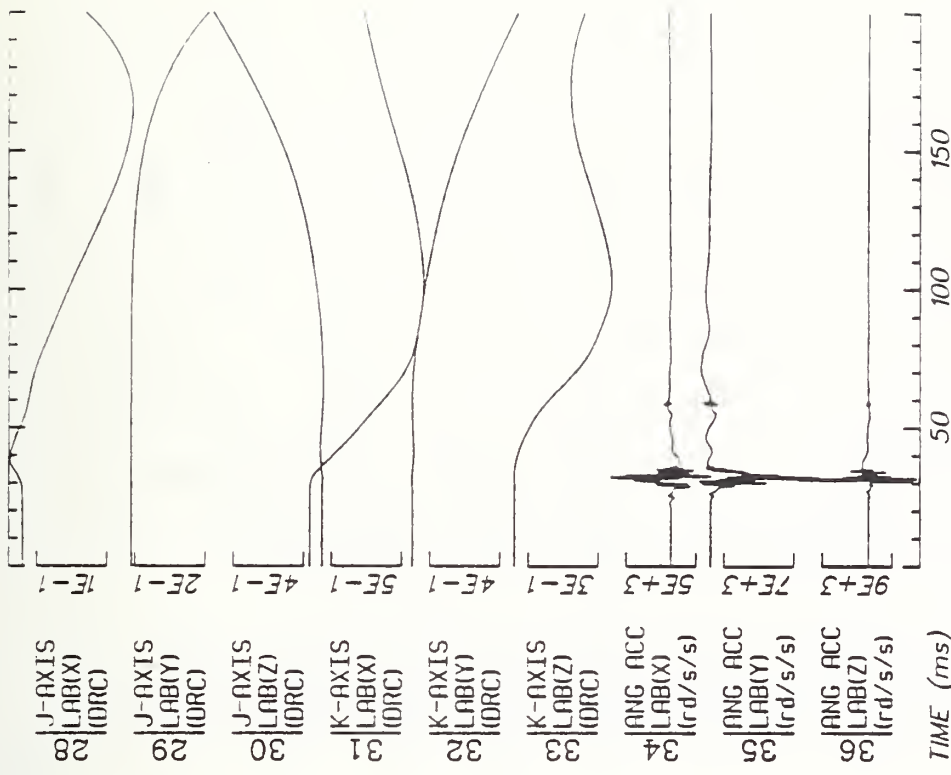
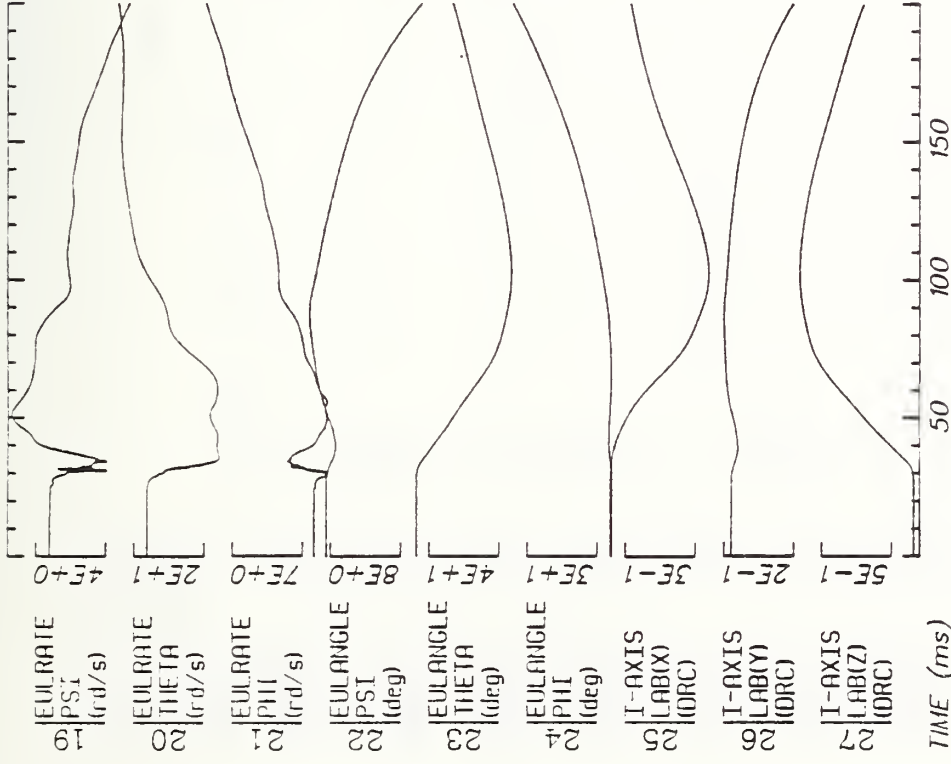
Disk: -HEAD

File: 3

Date: MAR 11, 1985

Sheet: 1

Filter: 1600*4C



Run ID: 82E022

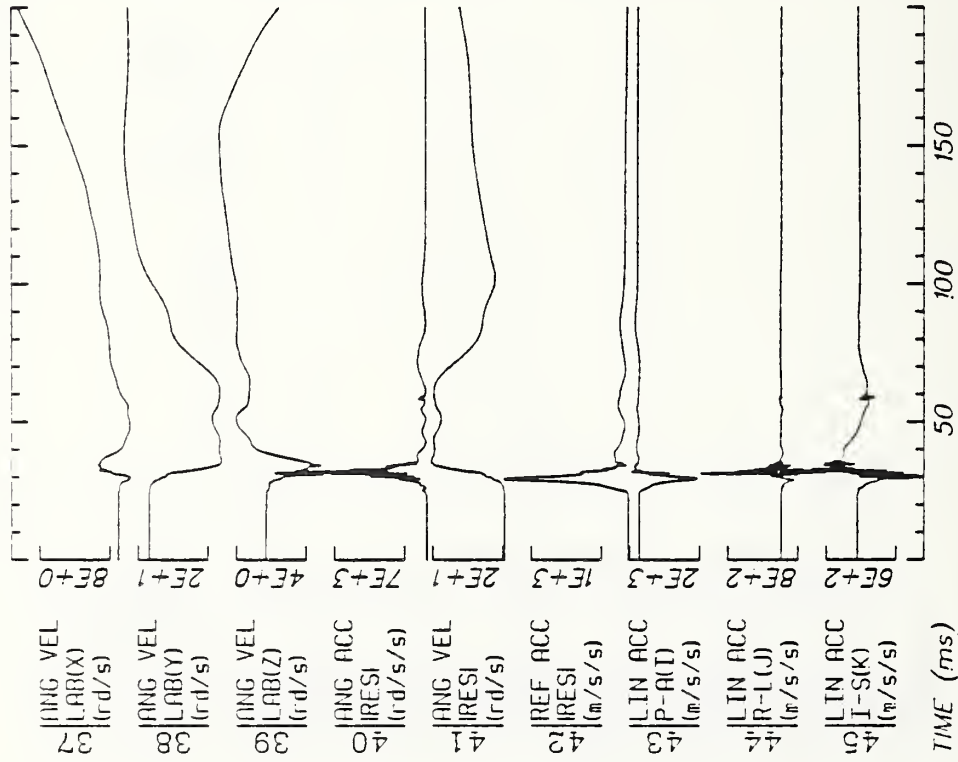
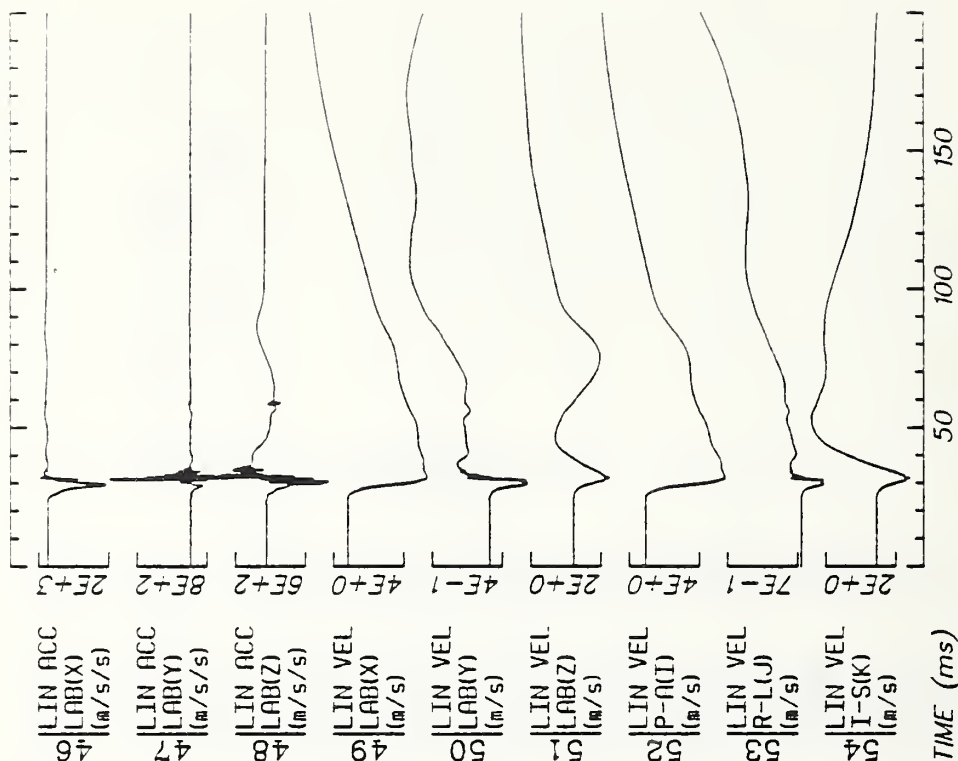
Disk: -HEAD

File: 3

Date: MAR 11, 1985

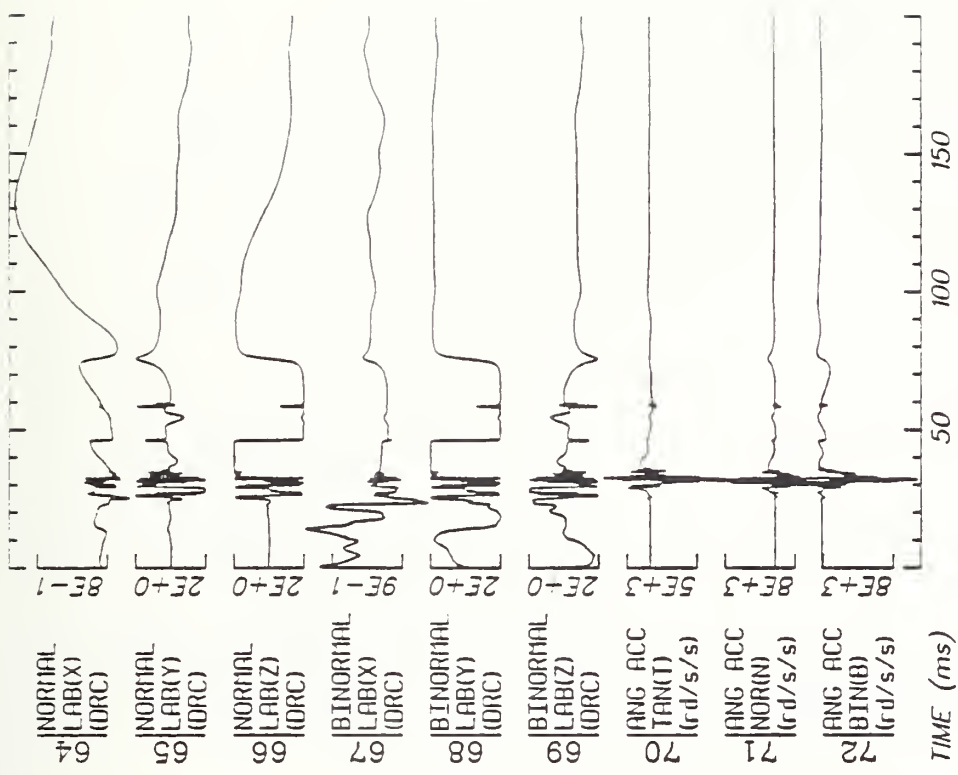
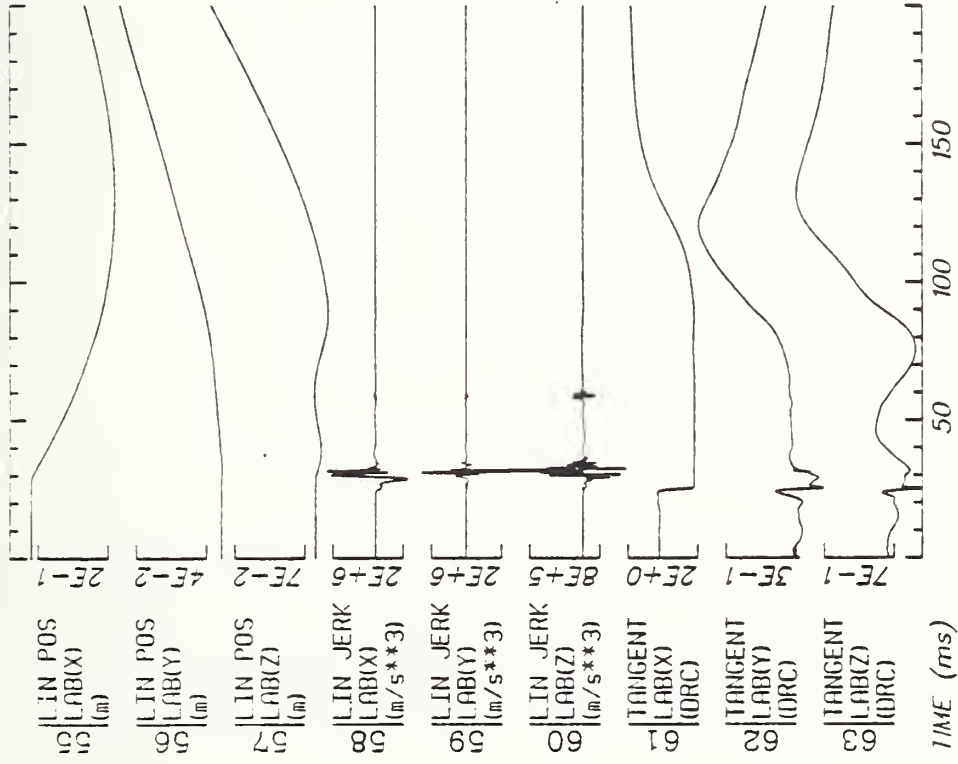
Sheet: 2

Filter: 1600*4C



Run ID: 821022 Disk: -HEAD File: 3 Date: MAR 11, 1985 Sheet: 3

Filter: 1600*4C



Run ID: 82F022

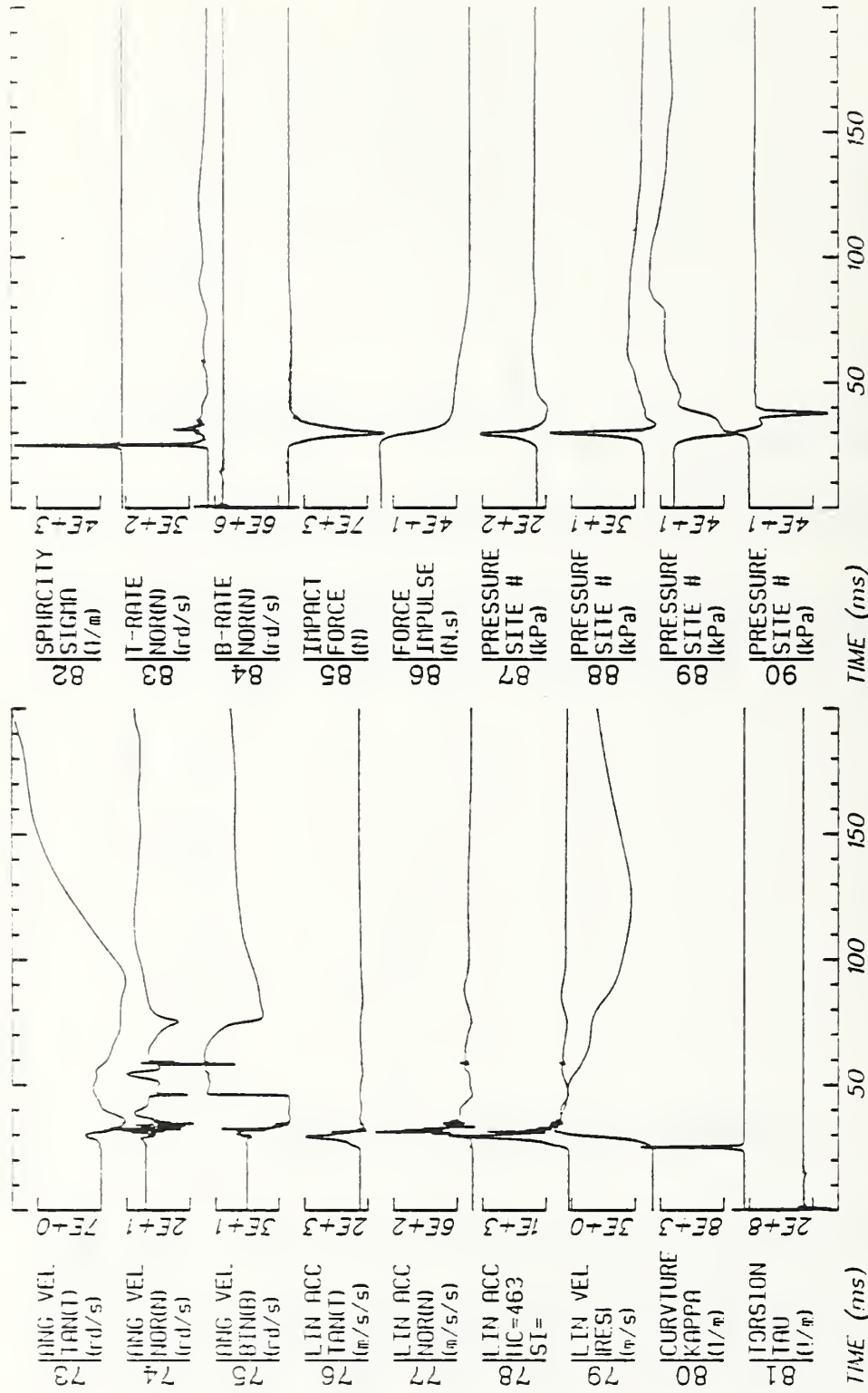
Disk: -HEAD

File: 3

Date: MAR 11, 1985

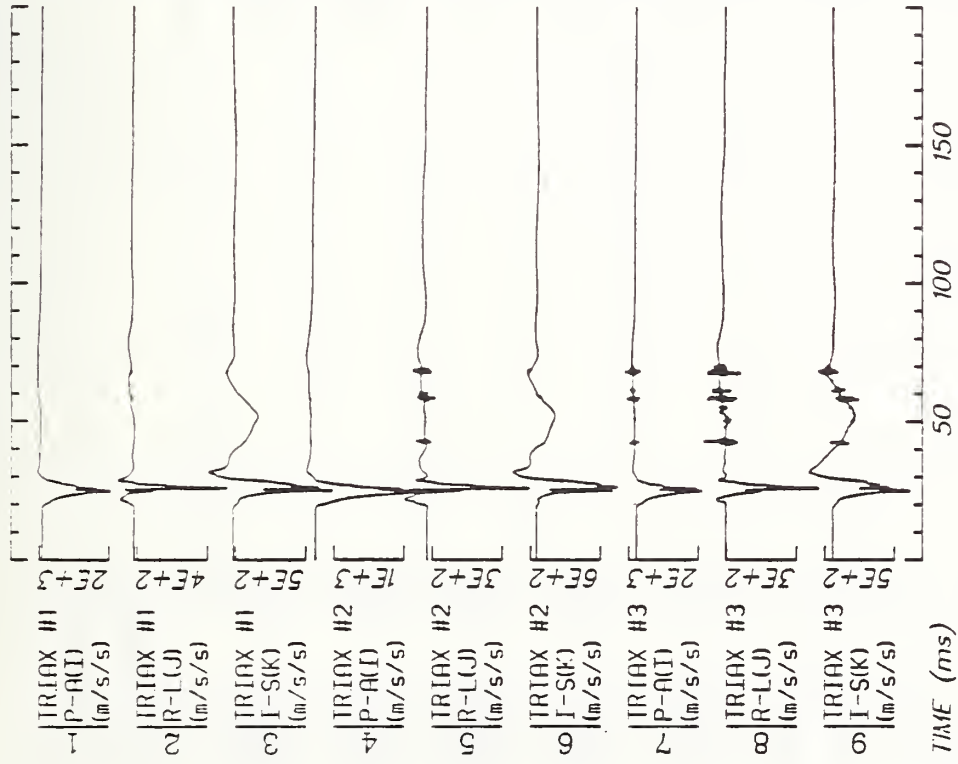
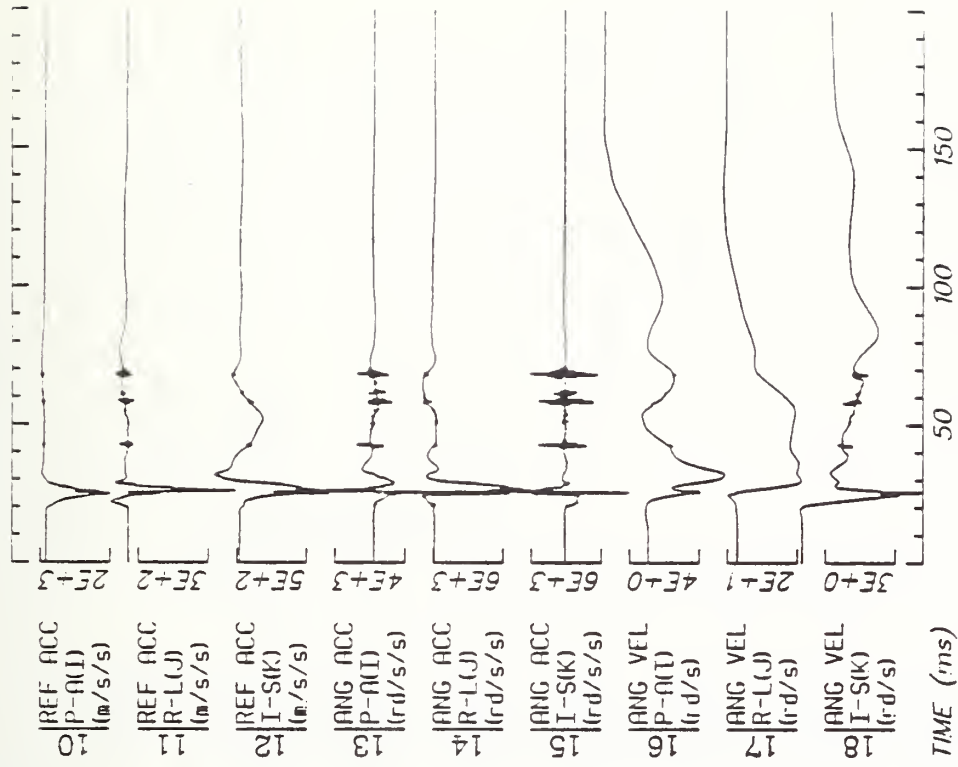
Sheet: 4

Filter: 1600*4C



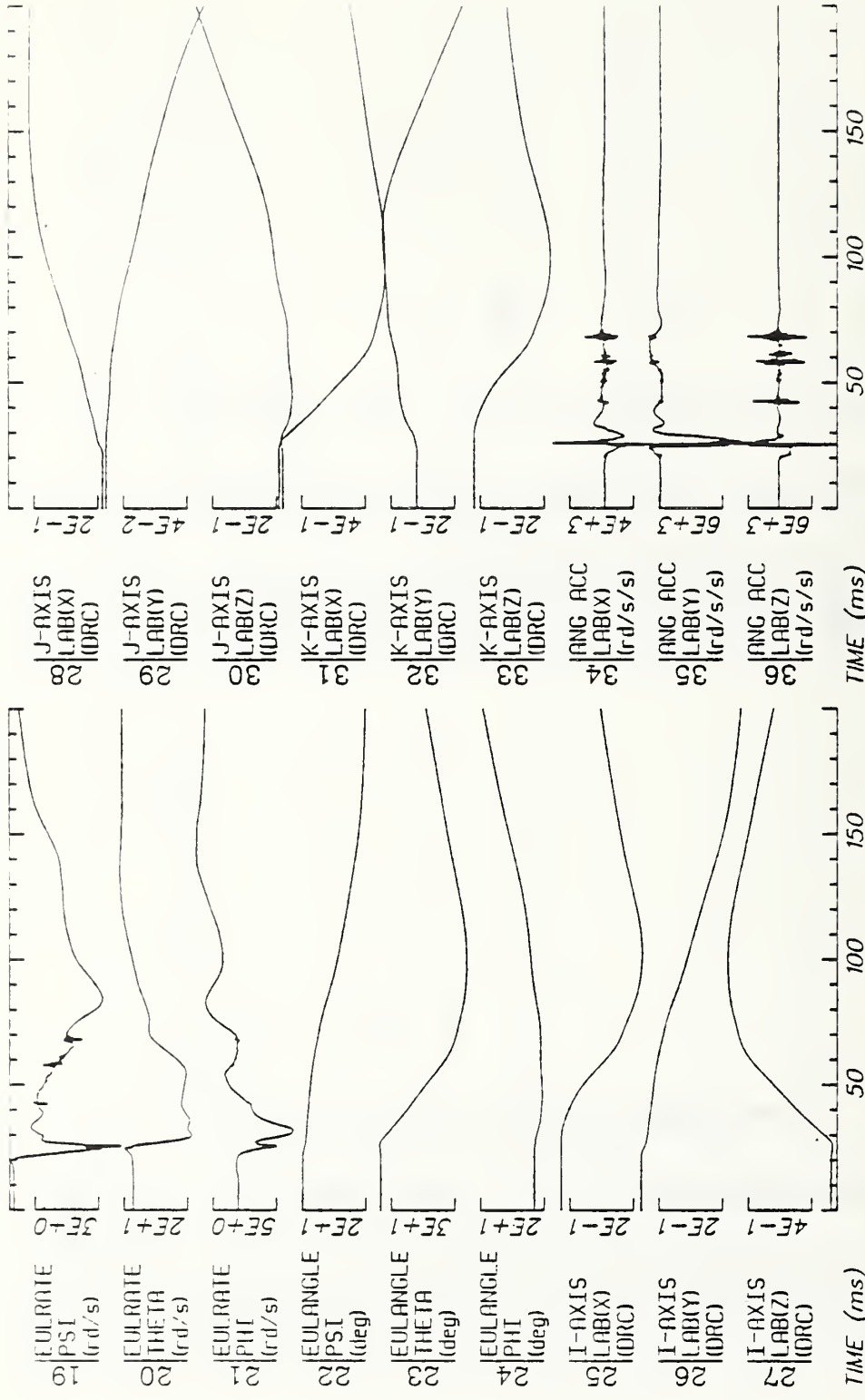
Run ID: 82E022 Disk: -HEAD File: 3 Date: MAR 11, 1985 Sheet: 5

Filter: 1600*4C



Run ID: 82E041 Disk: -HEAD File: 1 Date: MAR 11, 1985 Sheet: 1

Filter: 1600*4C



Run ID: 82E041

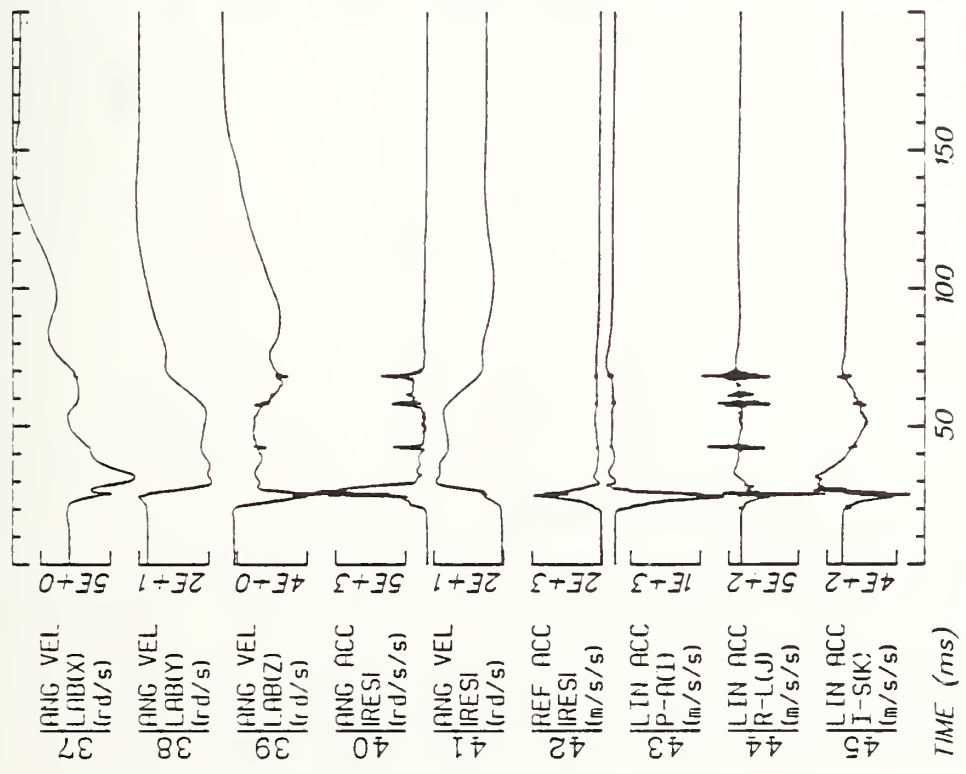
Disk: --HEAD

File: 1

Date: MAR 11, 1985

Sheet: 2

Filter: 1600*4C



Run ID: 82E041

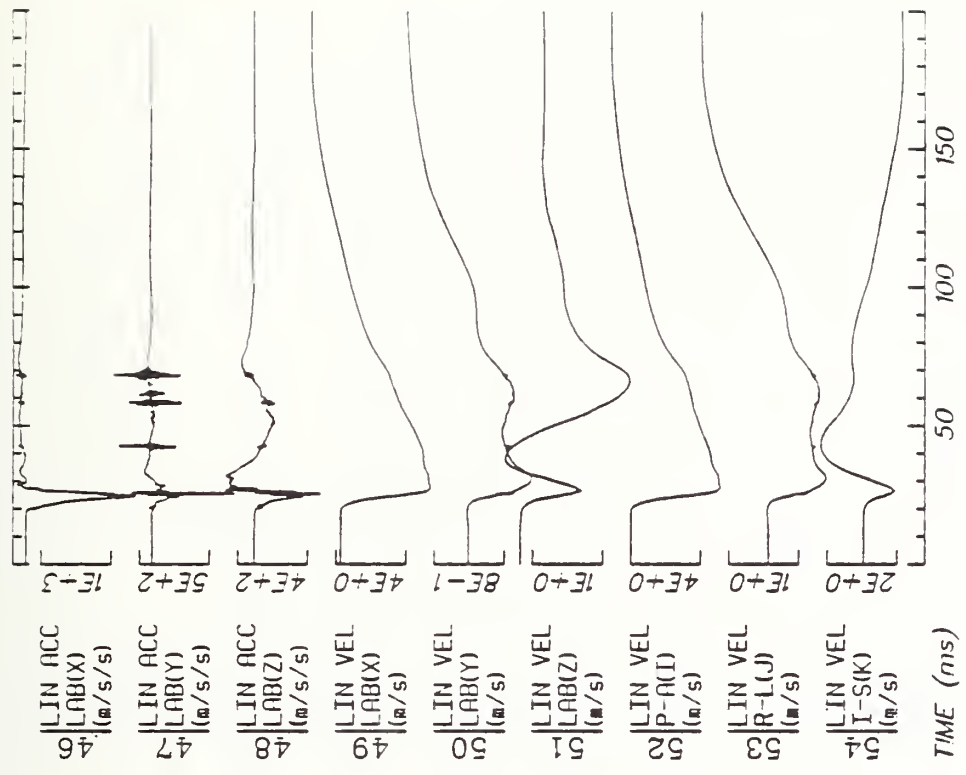
Disk: -HEAD

File: 1

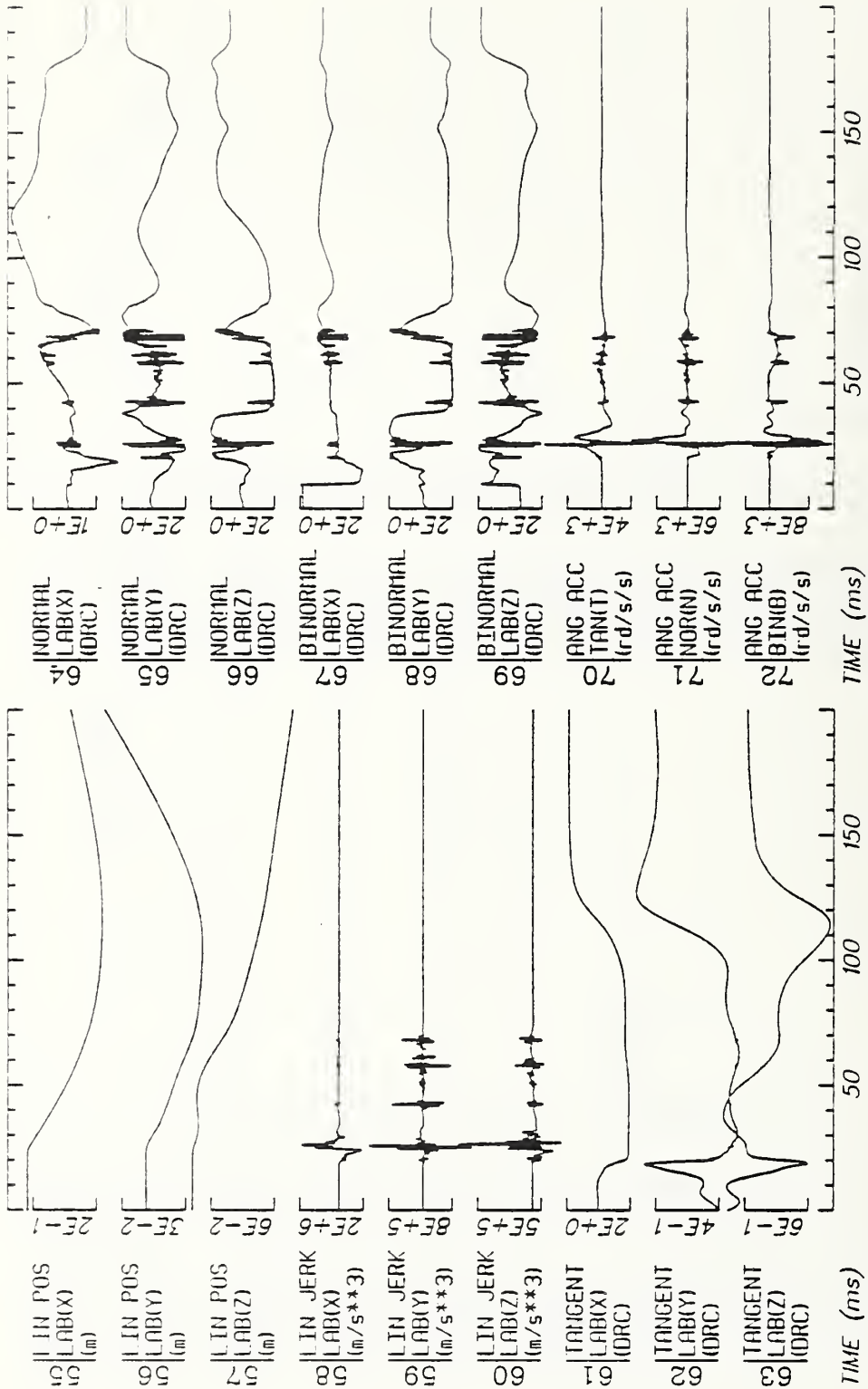
Date: MAR 11, 1985

Sheet: 3

Filter: 1600*4C

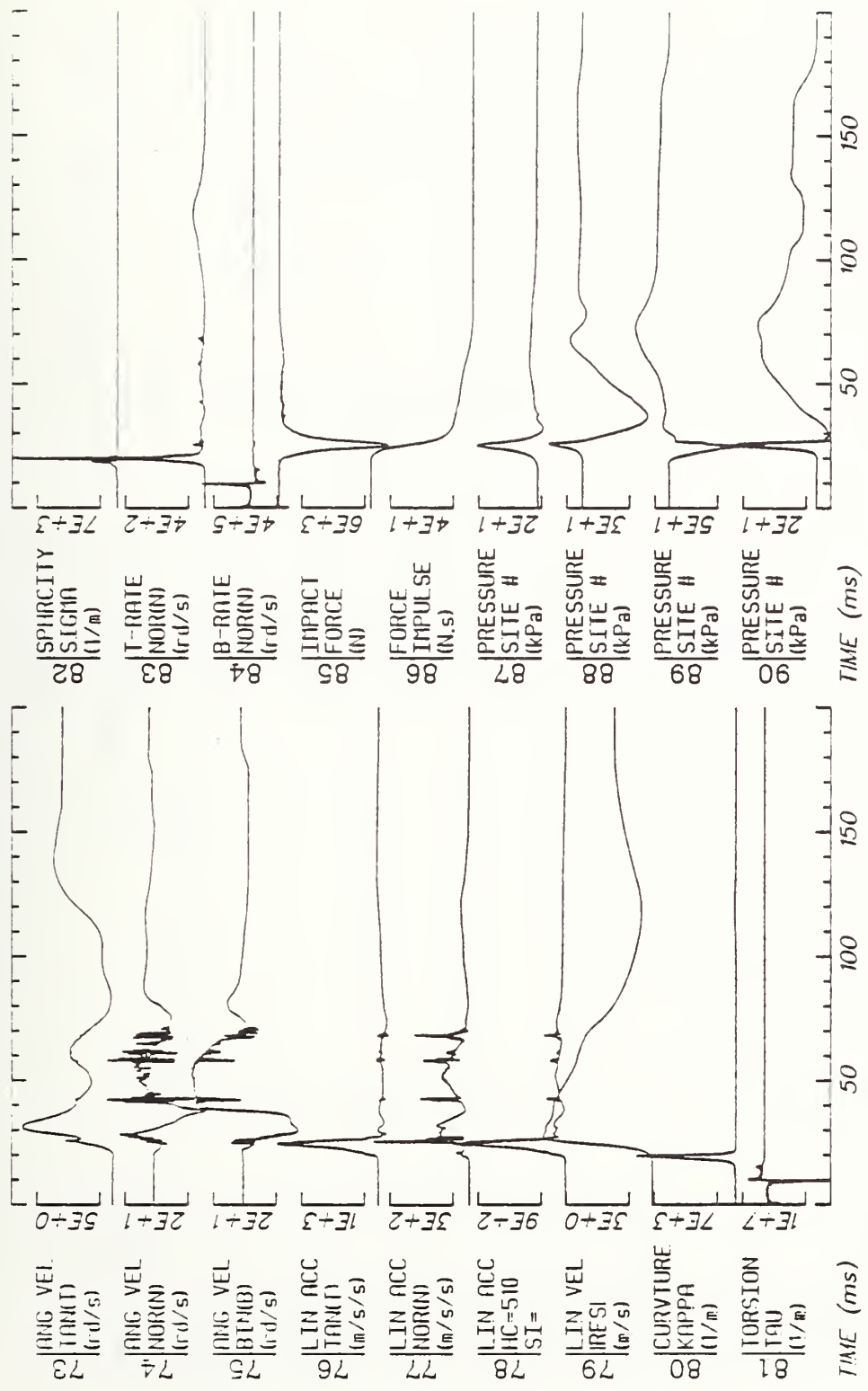


C19



Run ID: 82E041 Disk: -HEAD File: 1 Date: MAR 11, 1985 Sheet: 4

Filter: 1600*4C



Run ID: 82E041 Disk: -HEAD File: 1 Date: MAR 11, 1985 Sheet: 5

Filter: 1600*4C



TIME (ms)

Run ID: 82E041

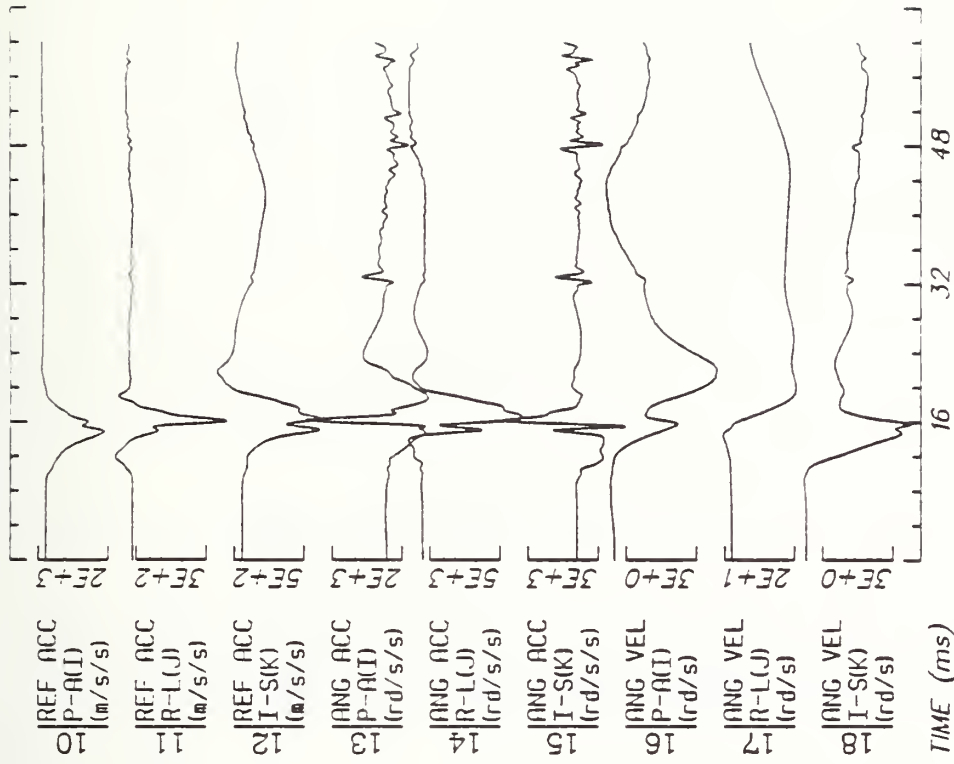
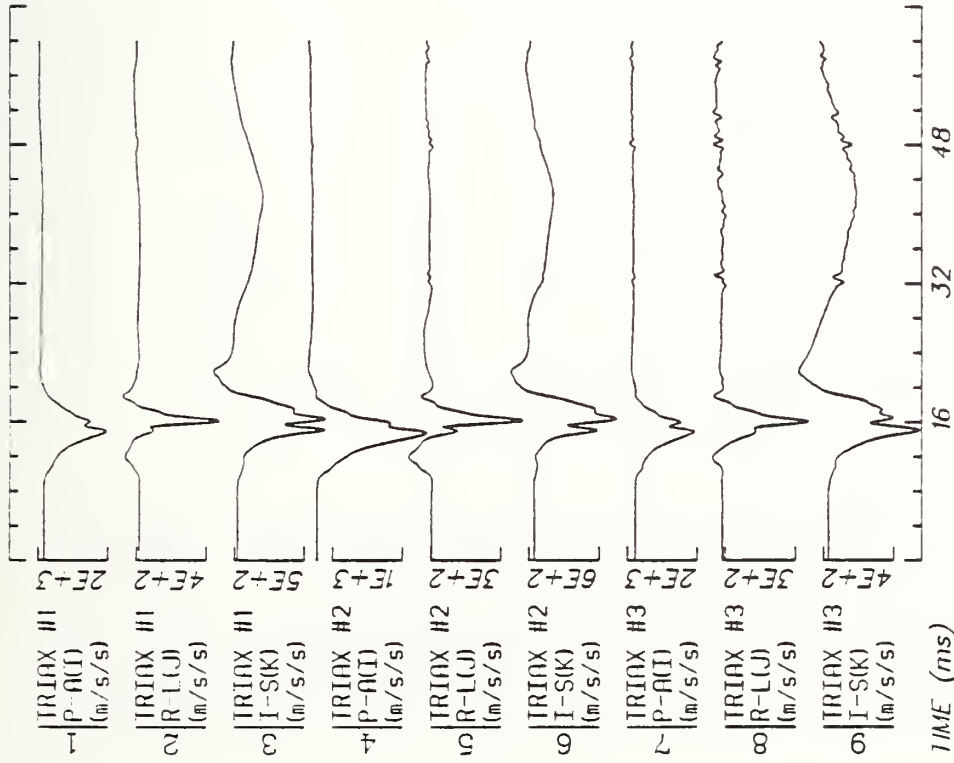
Disk: --HEAD

File: 1

Date: MAR 11, 1985

Sheet: 6

Filter: 1600*4C

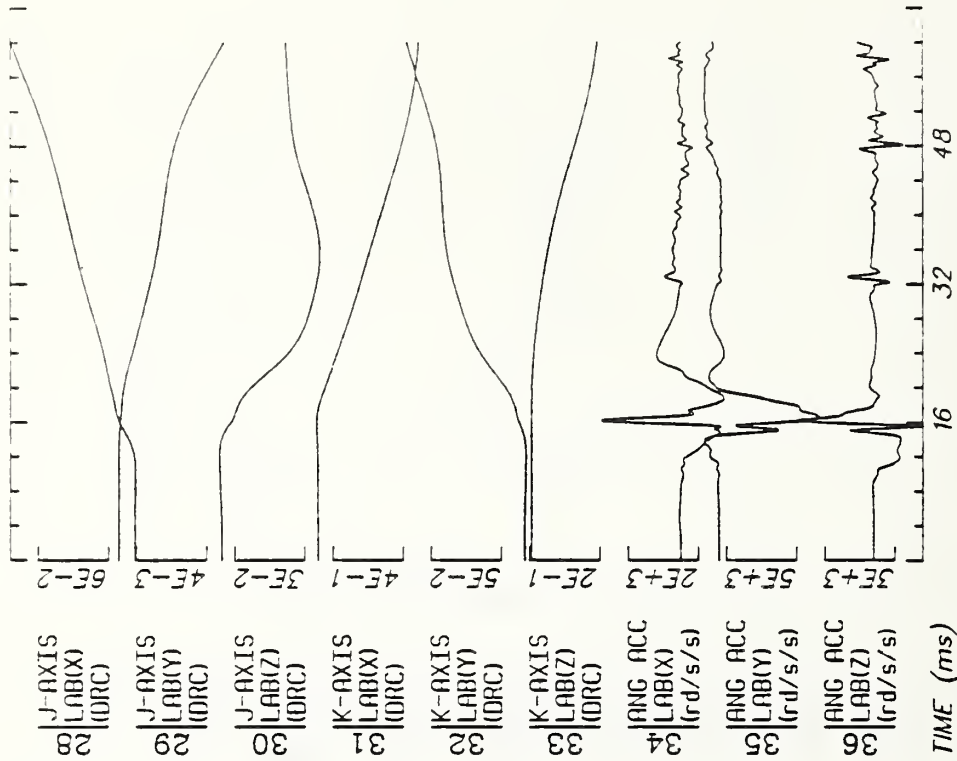
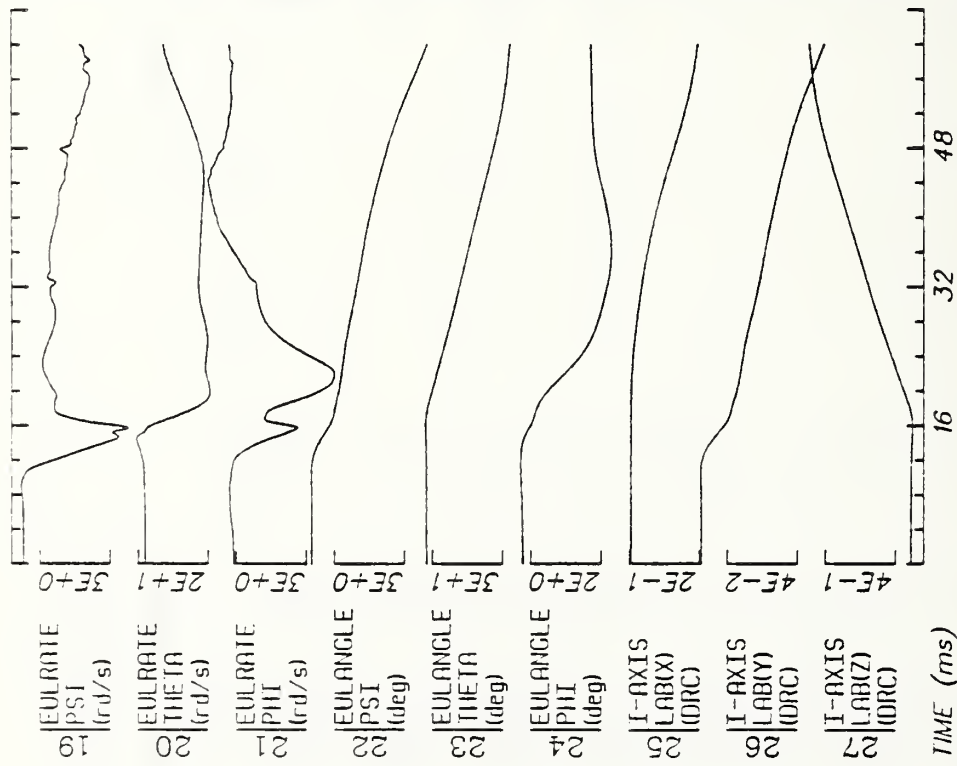


Run ID: 82E041

Disk: E041.3D. File: 1

Date: MAR 7, 1985 Sheet: 1

Filter: 800*4C

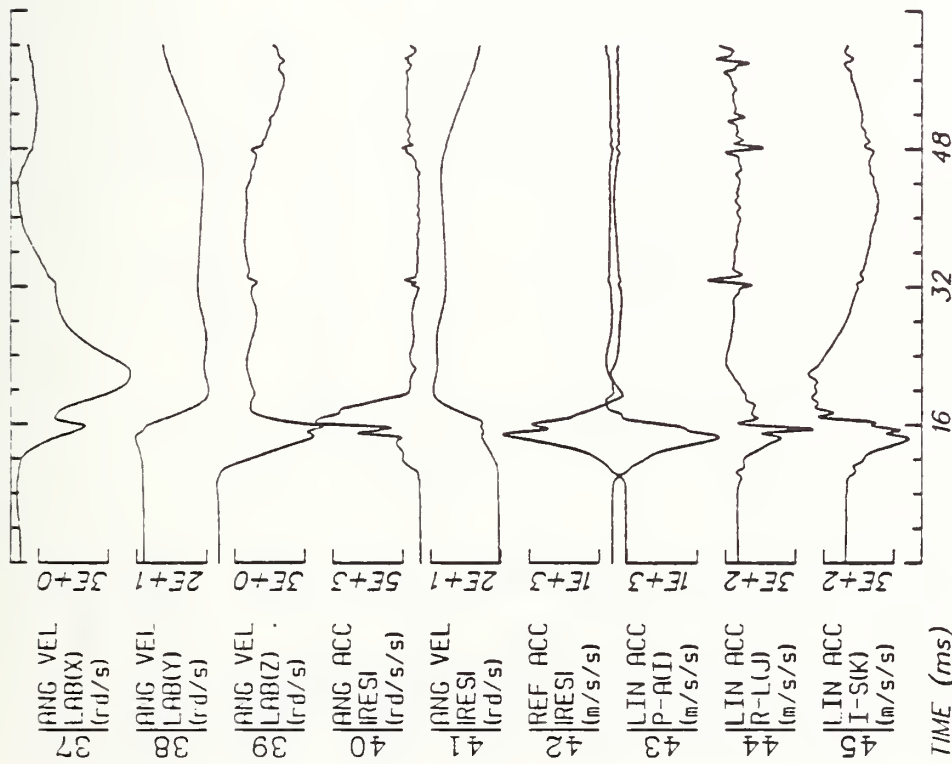
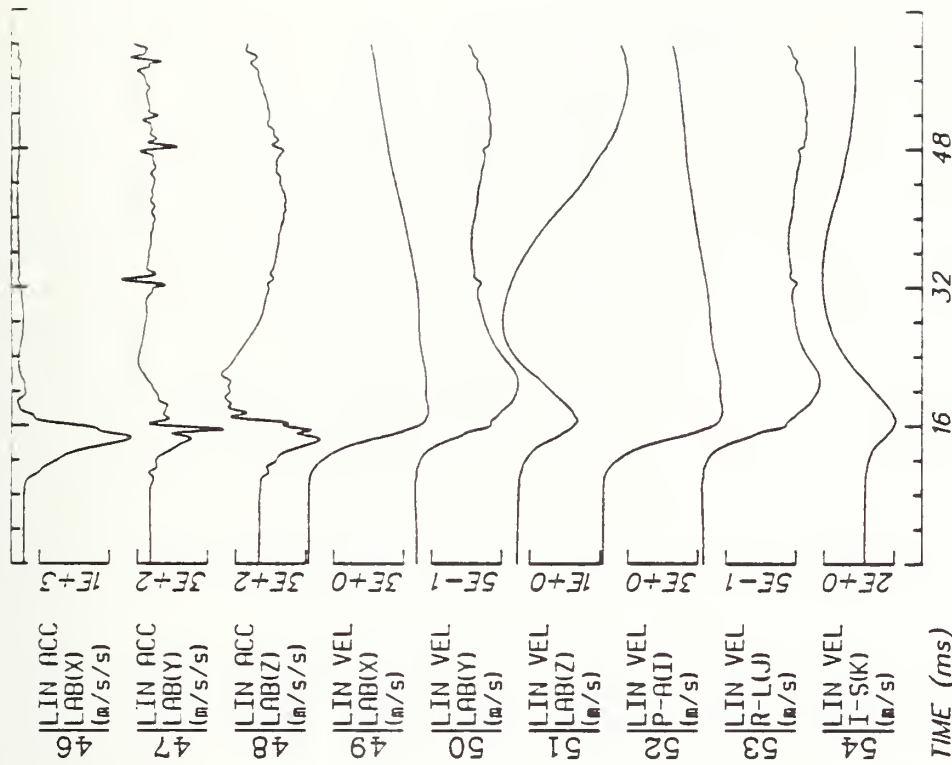


Run ID: 82E041

Disk: E041.3D. File: 1

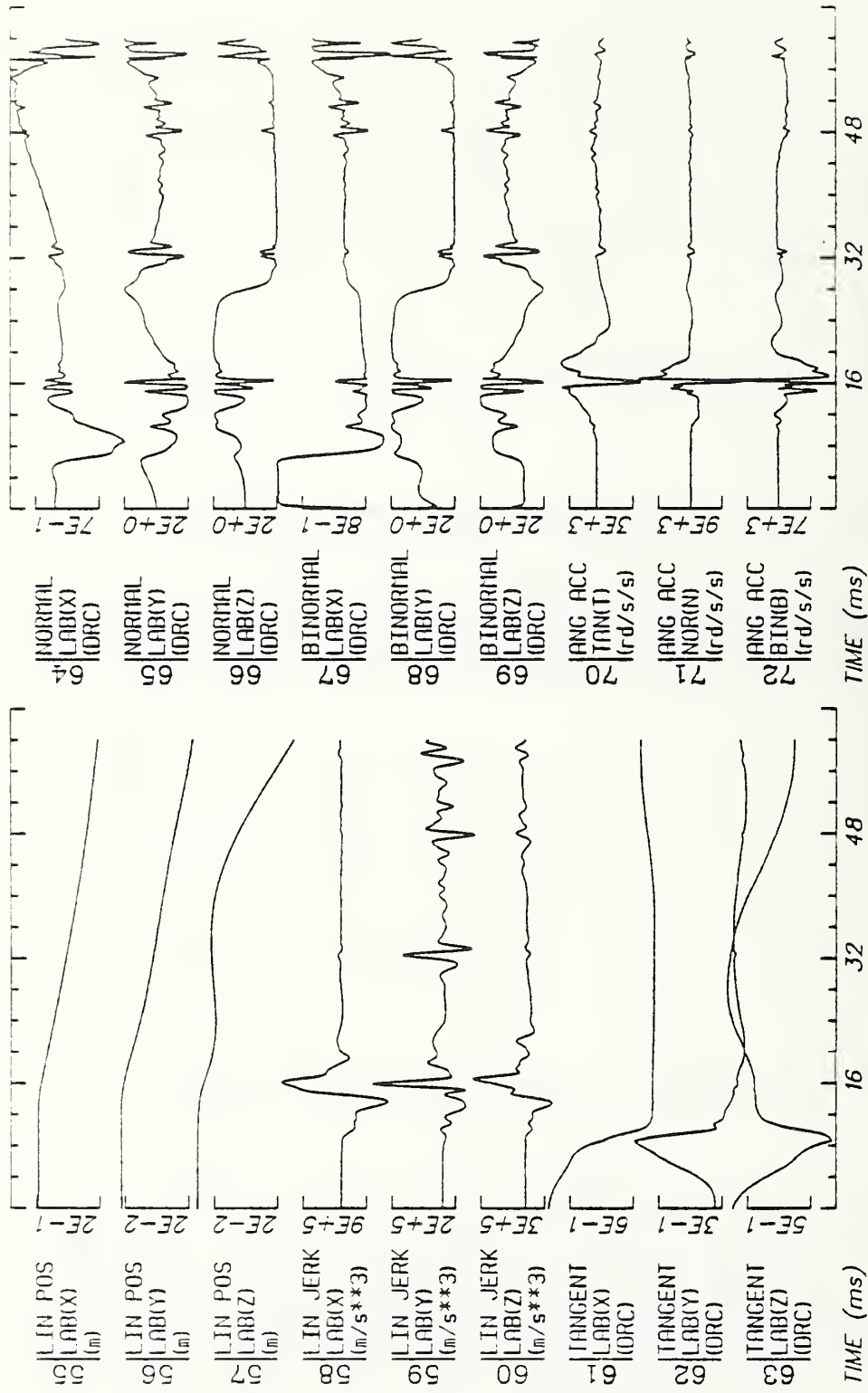
Date: MAR 7, 1985 Sheet: 2

Filter: 800*4C



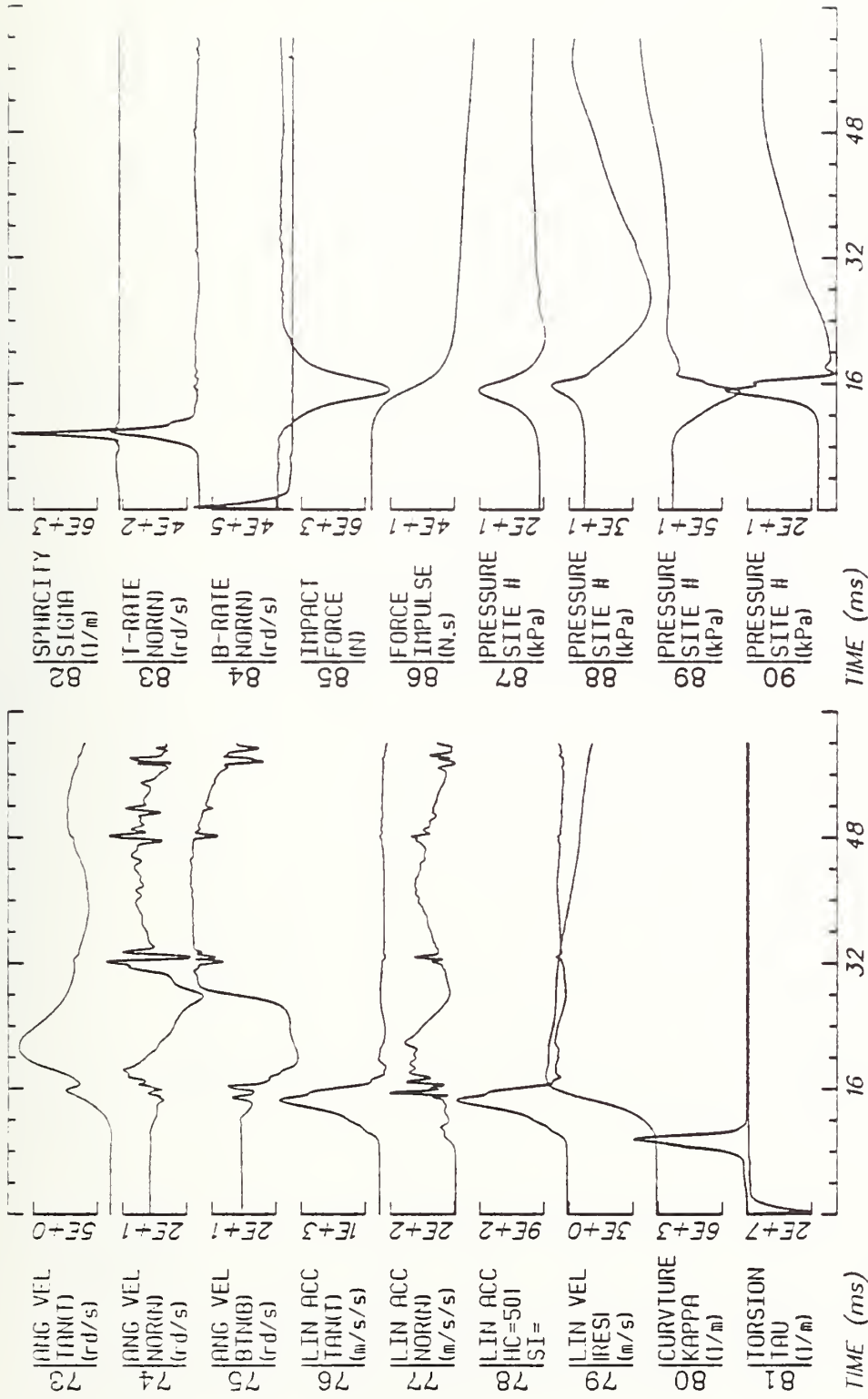
Run ID: 82E041 Disk: E041.3D. File: 1 Date: MAR 7, 1985 Sheet: 3

Filter: 800*4C



Run ID: 82E041 Disk: E041.3D. File: 1 Date: MAR 7, 1985 Sheet: 4

Filter: 800*4C



Run ID: 82E041 Disk: E041.3D. File: 1 Date: MAR 7, 1985 Sheet: 5

Filter: 800*4C



TIME (ms)

Run ID: 82E041

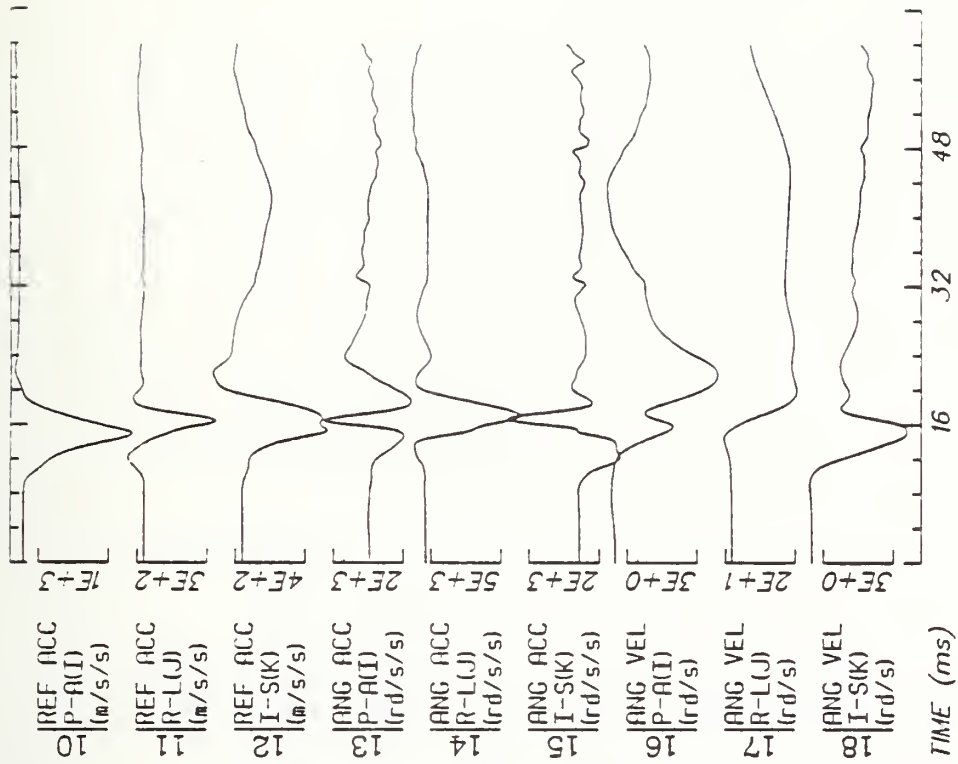
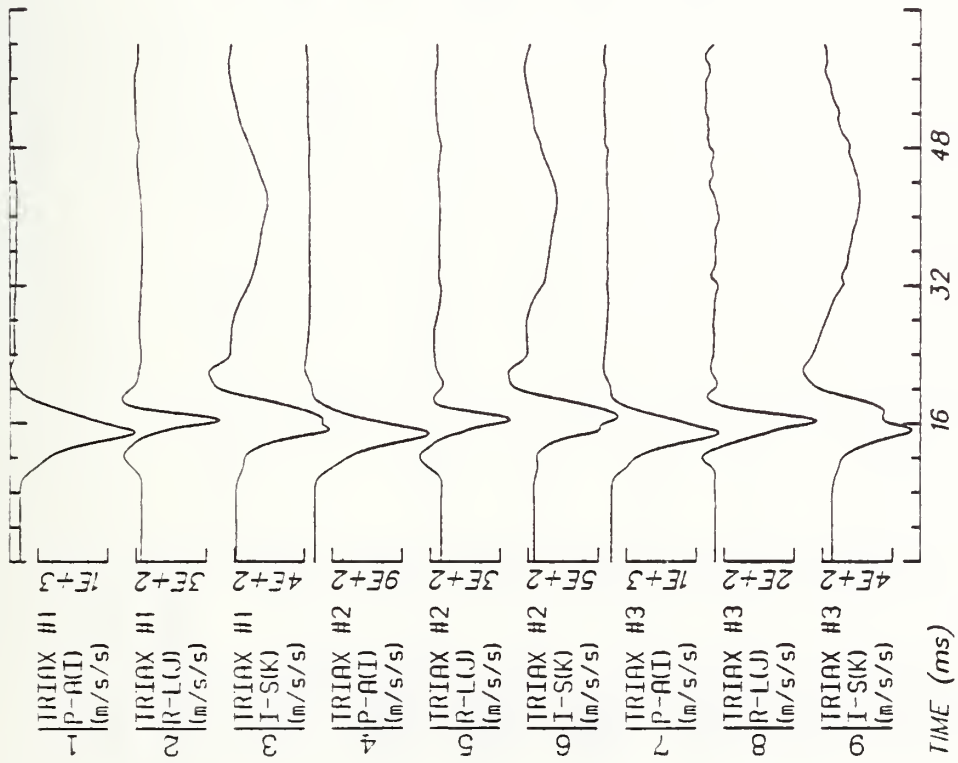
Disk: E041.3D.

File: 1

Date: MAR 7, 1985

Sheet: 6

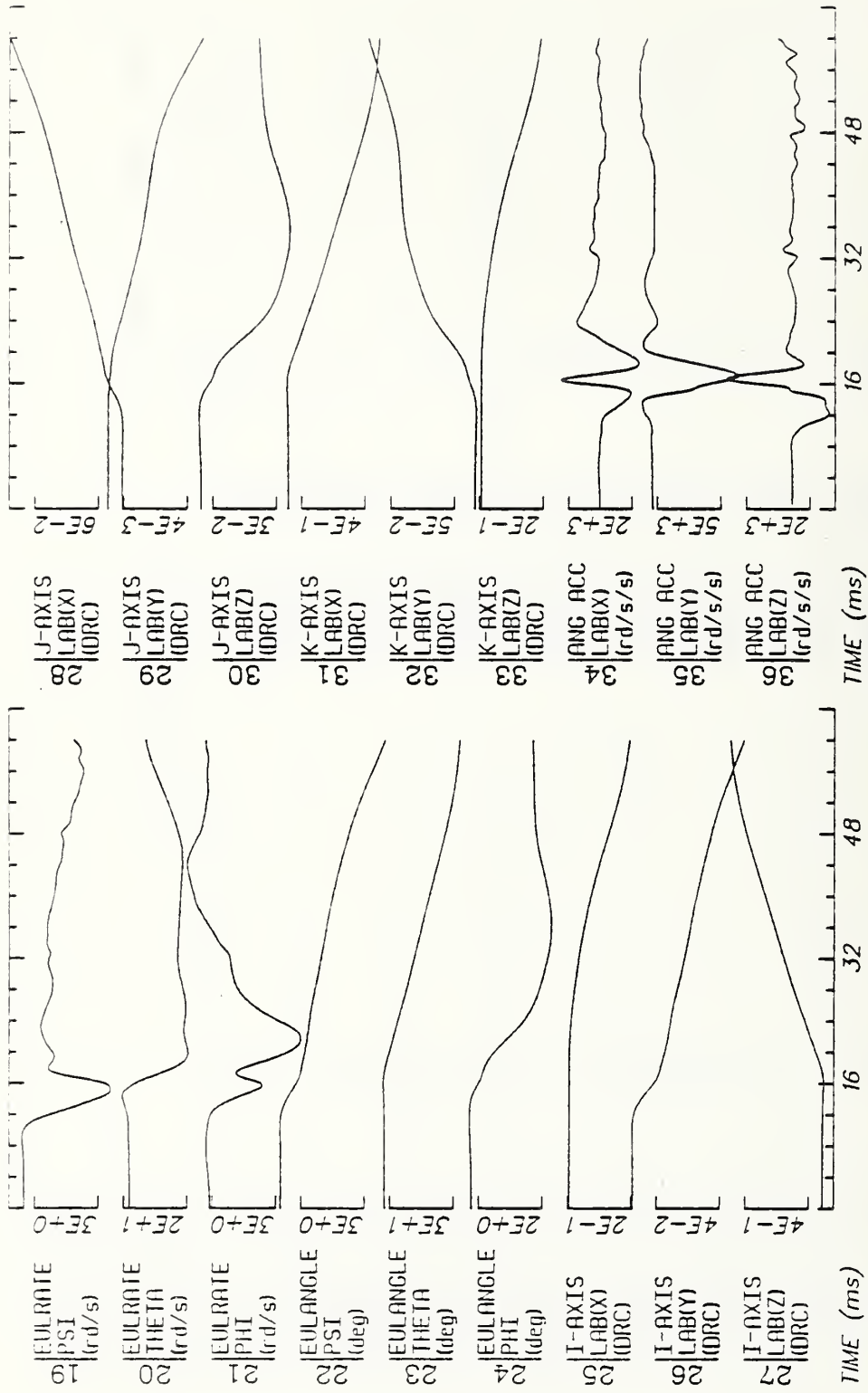
Filter: 800*4C



Run ID: 82E041
 Filter: 400*4C

Disk: E041.3D. File: 1

Date: MAR 7, 1985 Sheet: 1

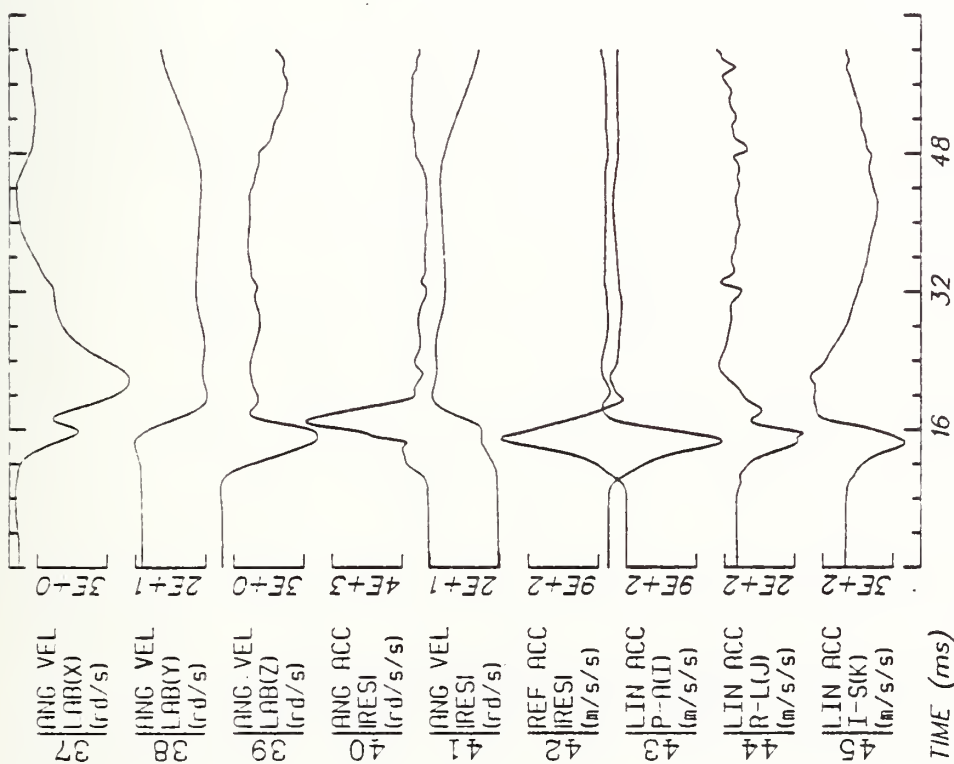
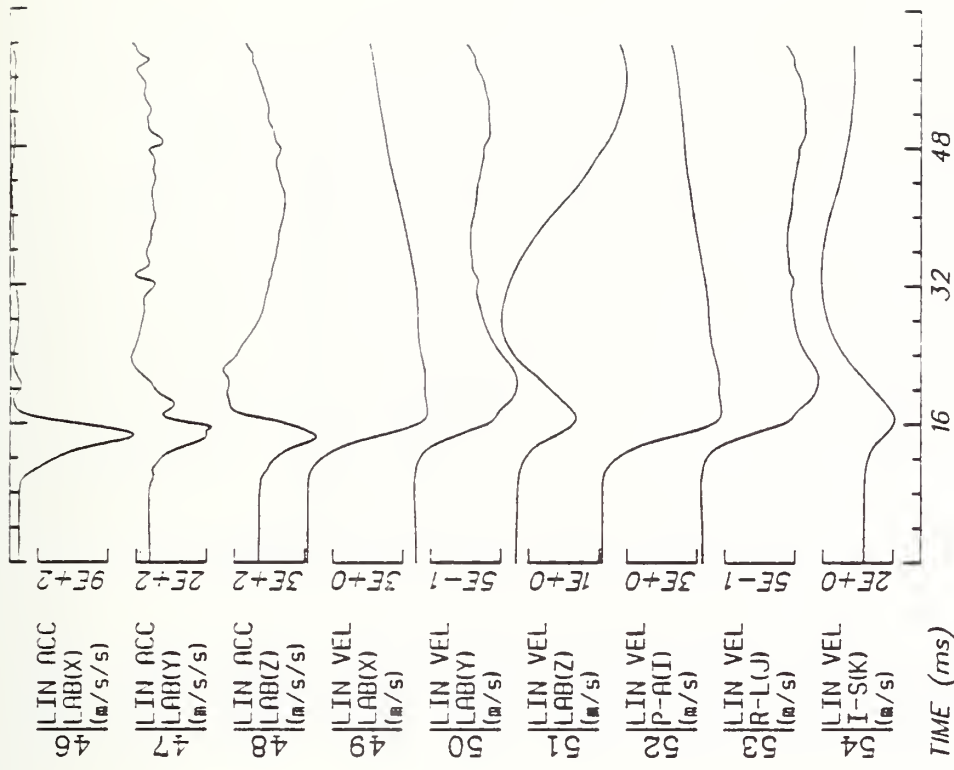


Run ID: 82E041

Disk: E041.3D. File: 1

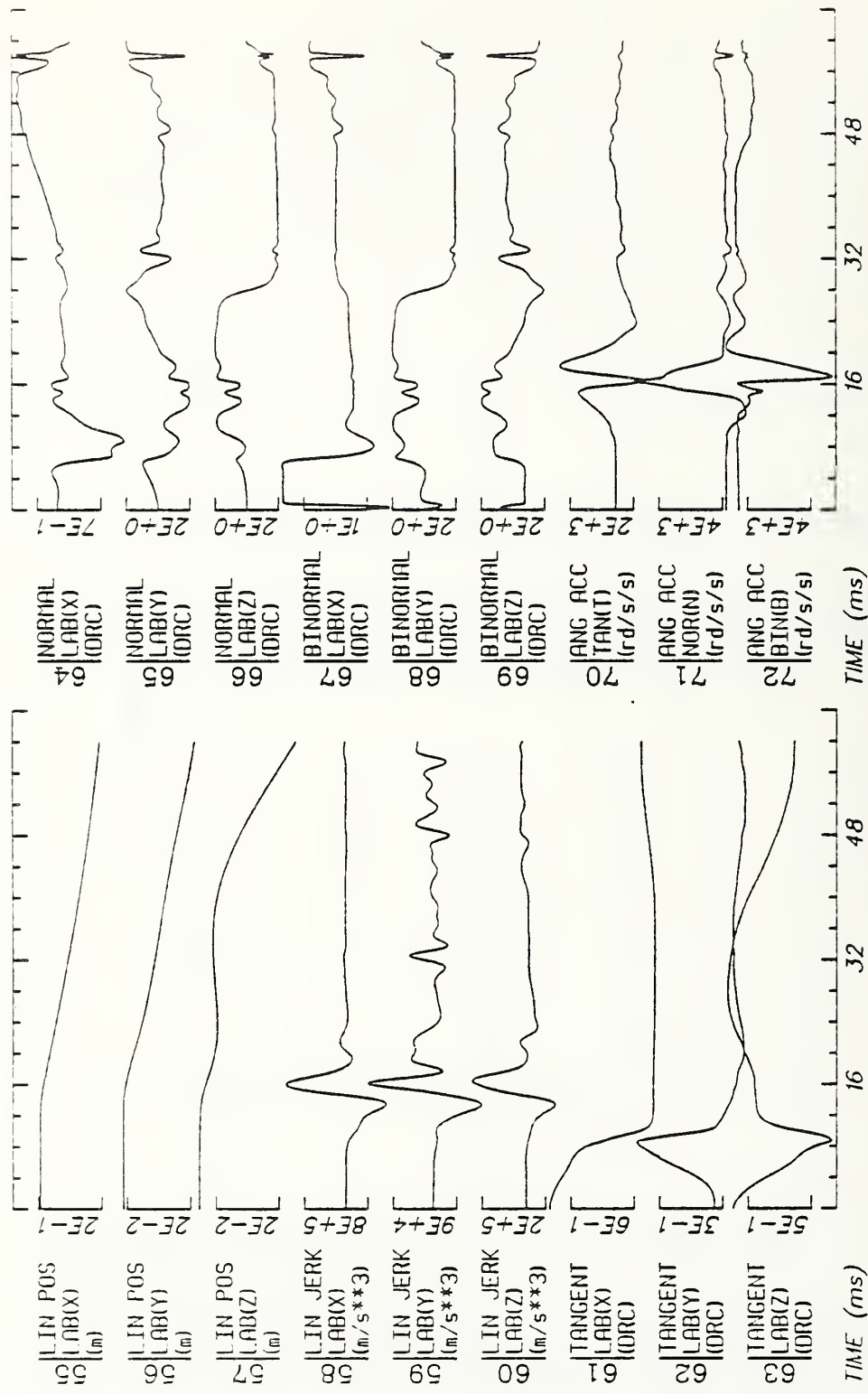
Date: MAR 7, 1985 Sheet: 2

Filter: 400*4C



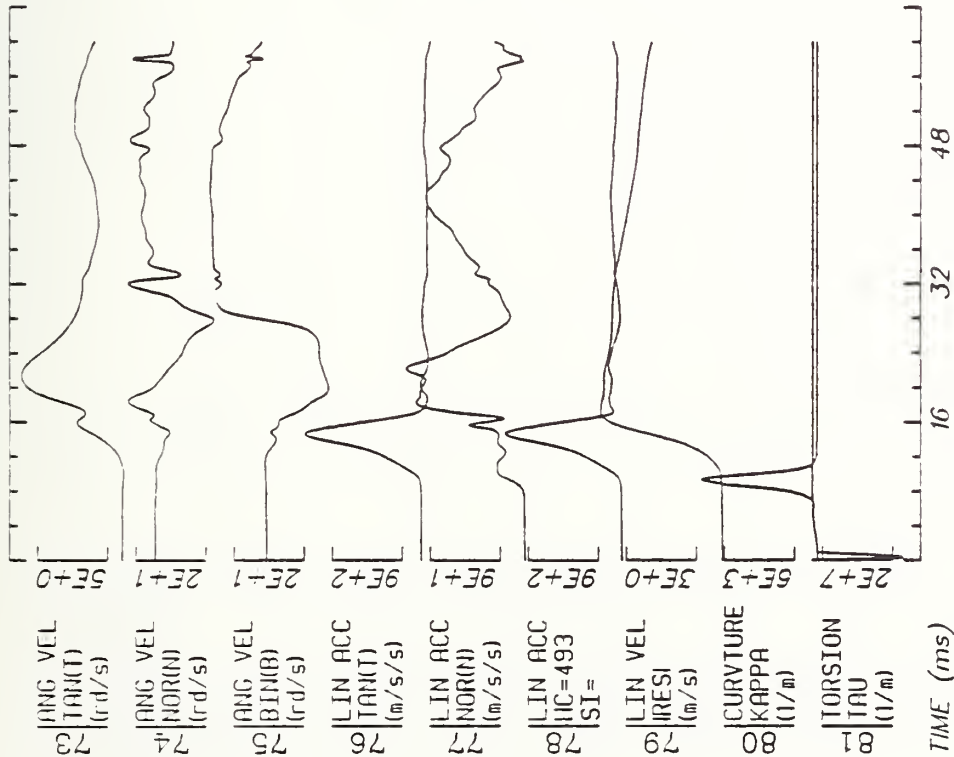
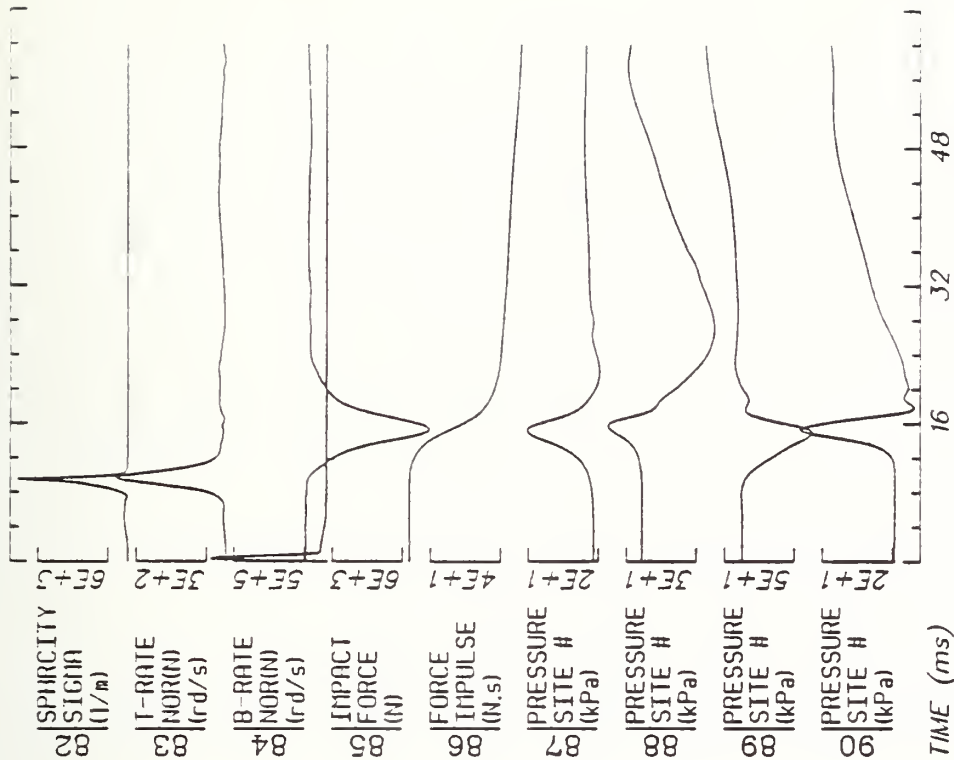
Run ID: 82E041 Disk: E041.3D. File: 1 Date: MAR 7, 1985 Sheet: 3

Filter: 400*4C



Run ID: 82E041 Disk: E041.3D. File: 1 Date: MAR 7, 1985 Sheet: 4

Filter: 400*4C



Run ID: 82E041

Disk: E041.3D. File: 1

Date: MAR 7, 1985

Sheet: 5

Filter: 400*4C



TIME (ms)

16 32 48

Run ID: 82E041

Disk: E041.3D.

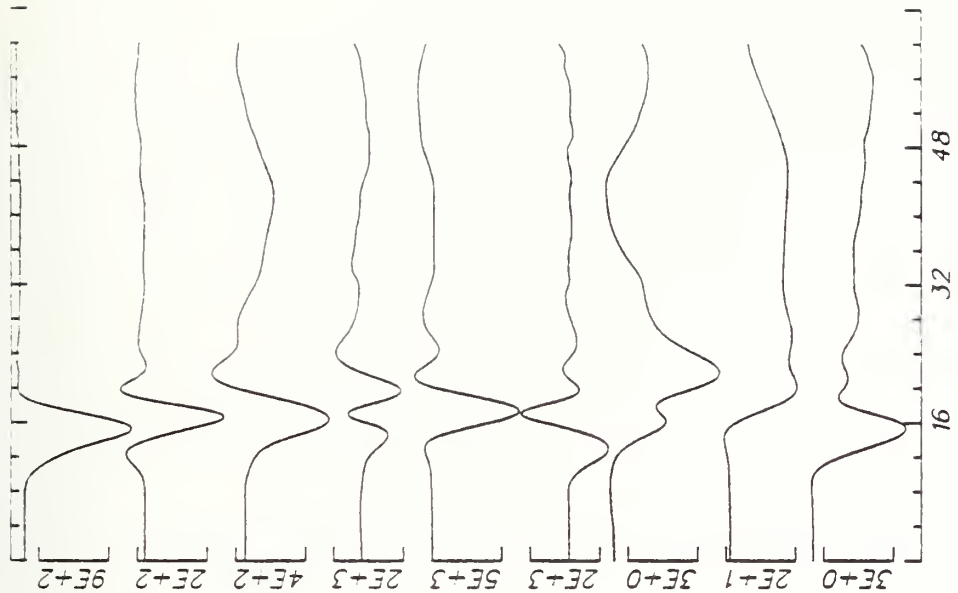
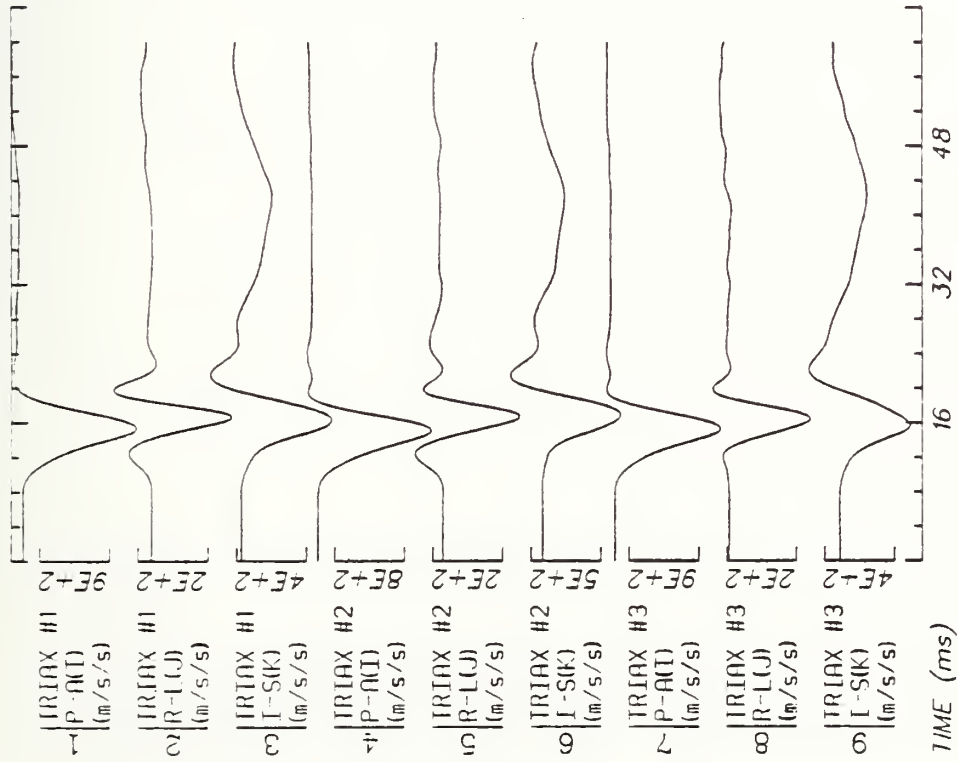
File: 1

Date: MAR 7, 1985

Sheet: 6

Filter: 400*4C

C34



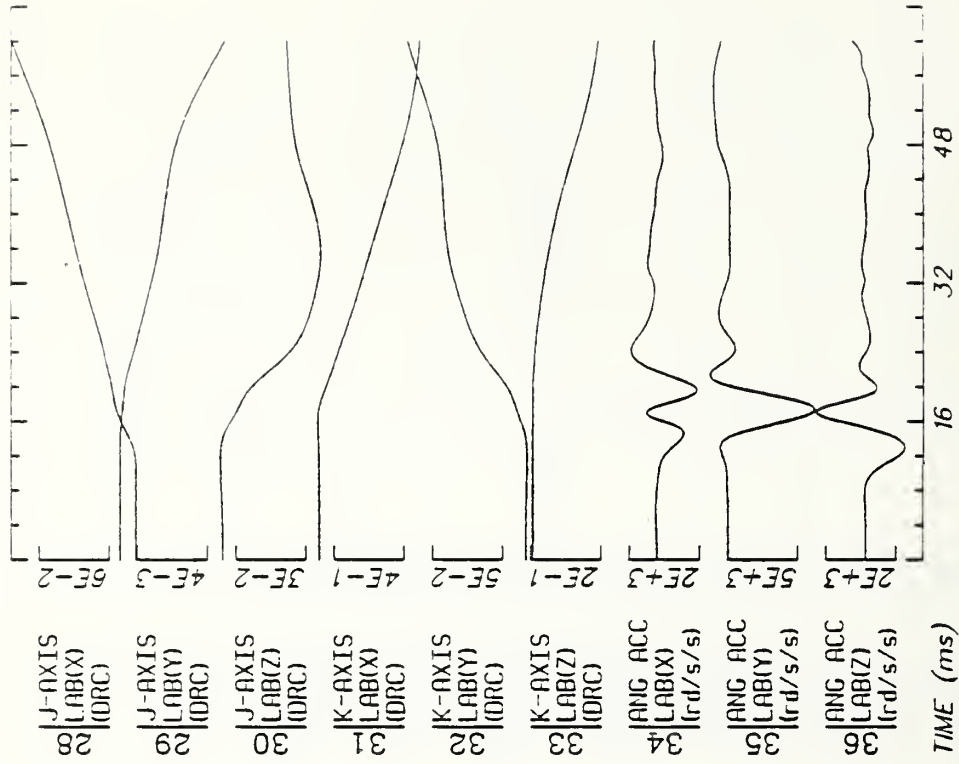
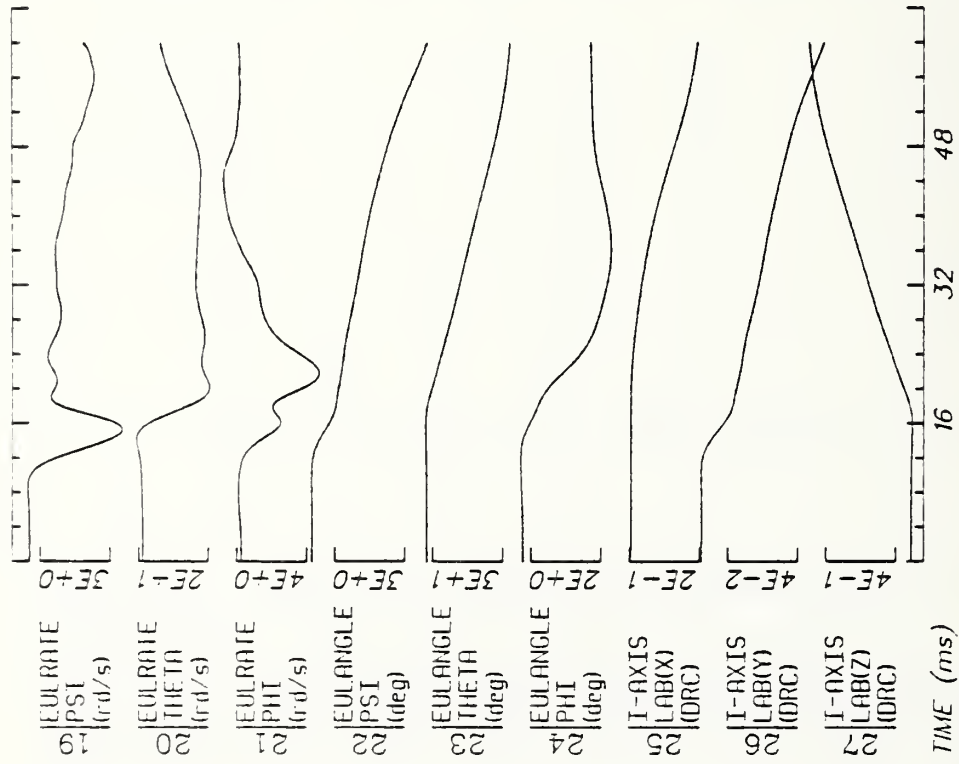
Run ID: 82E041

Disk: E041.3D. File: 1

Date: MAR 7, 1985 Sheet: 1

Filter: 200*4C

C35

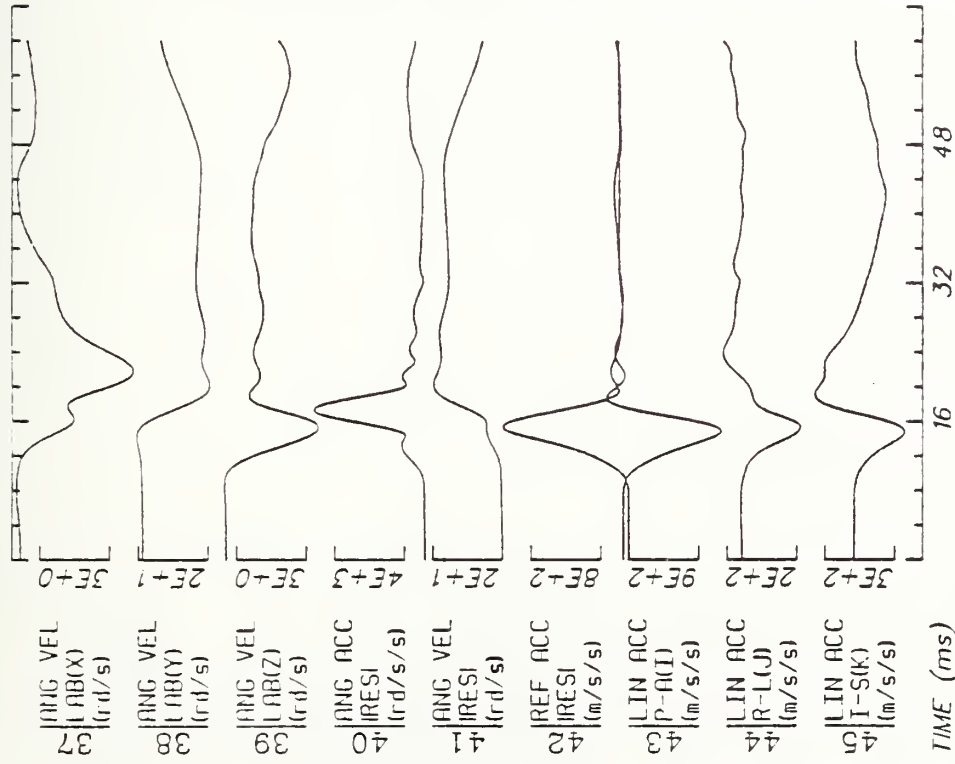


Run ID: 82E041

Disk: E041.3D. File: 1

Date: MAR 7, 1985 Sheet: 2

Filter: 200*4C



TIME (ms)

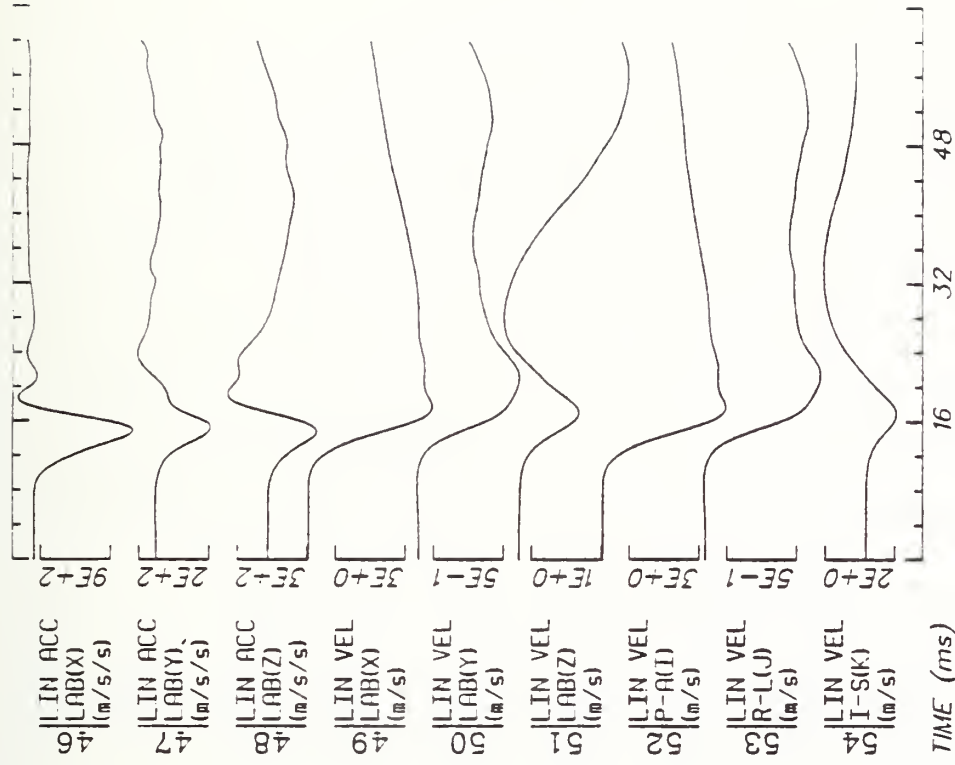
Run ID: 82E041

Disk: E041.3D.

File: 1

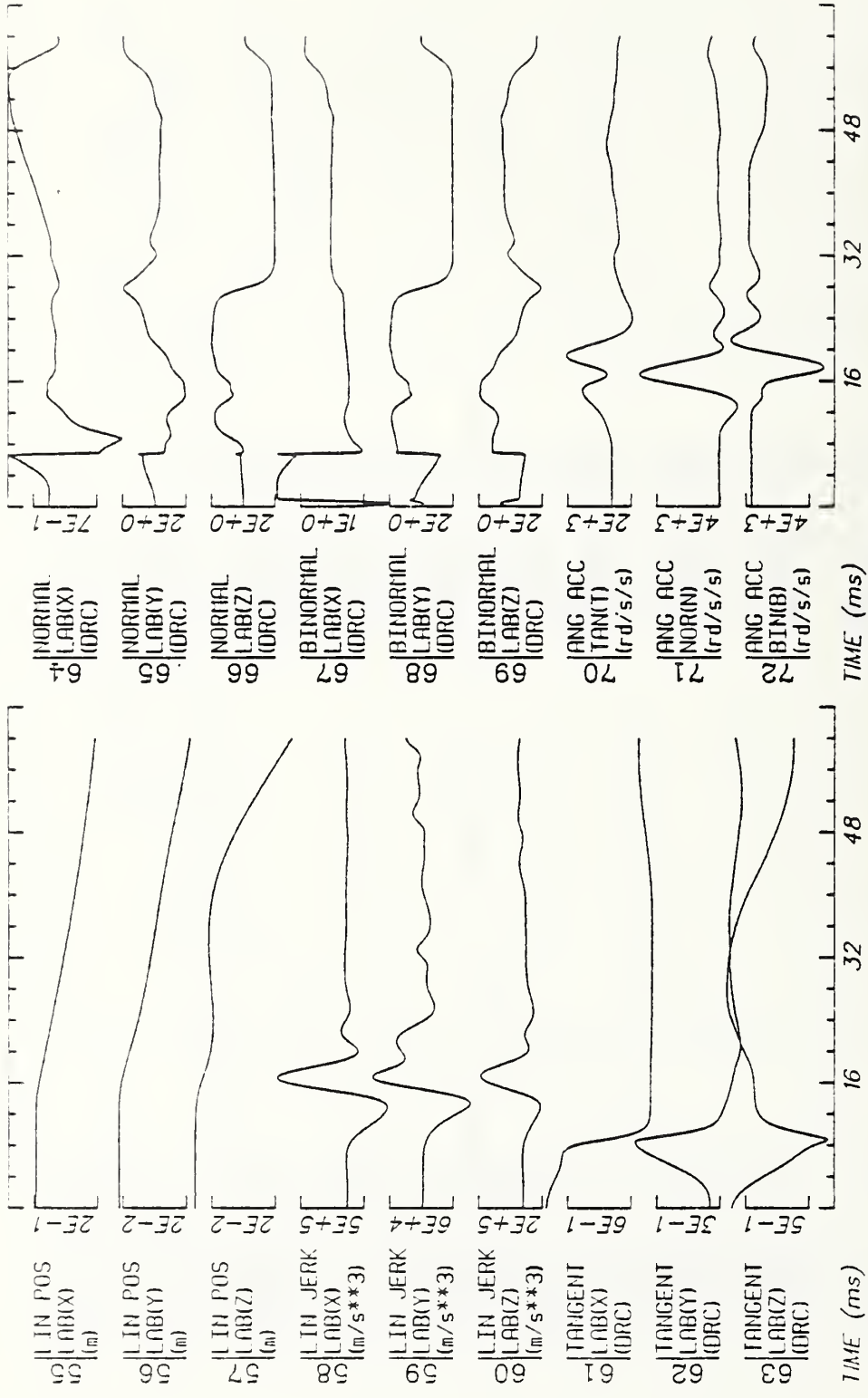
Date: MAR 7, 1985

Sheet: 3



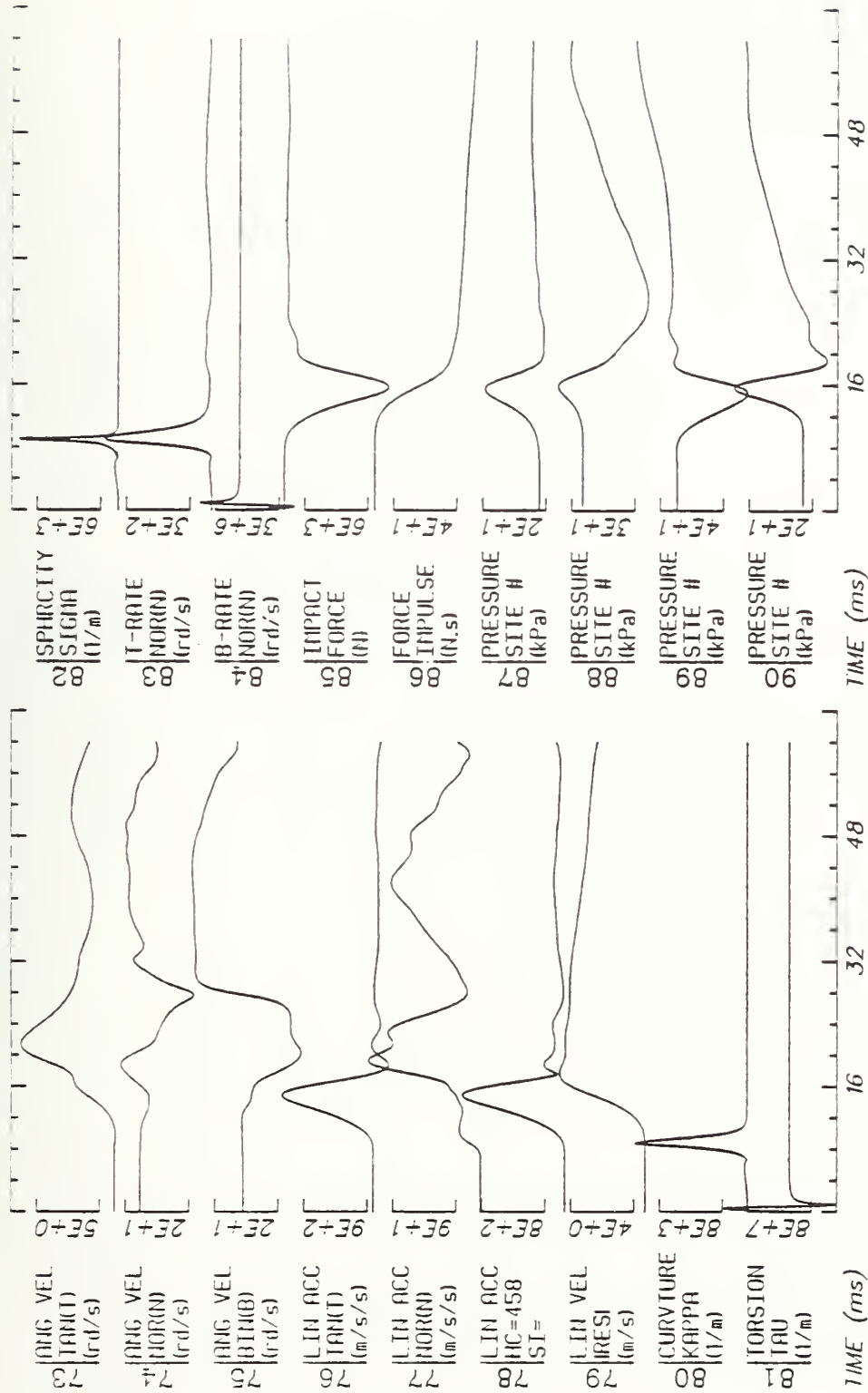
TIME (ms)

Filter: 200*4C



Run ID: 82E041 Disk: E041.3D. File: 1 Date: MAR 7, 1985 Sheet: 4

Filter: 200*4C



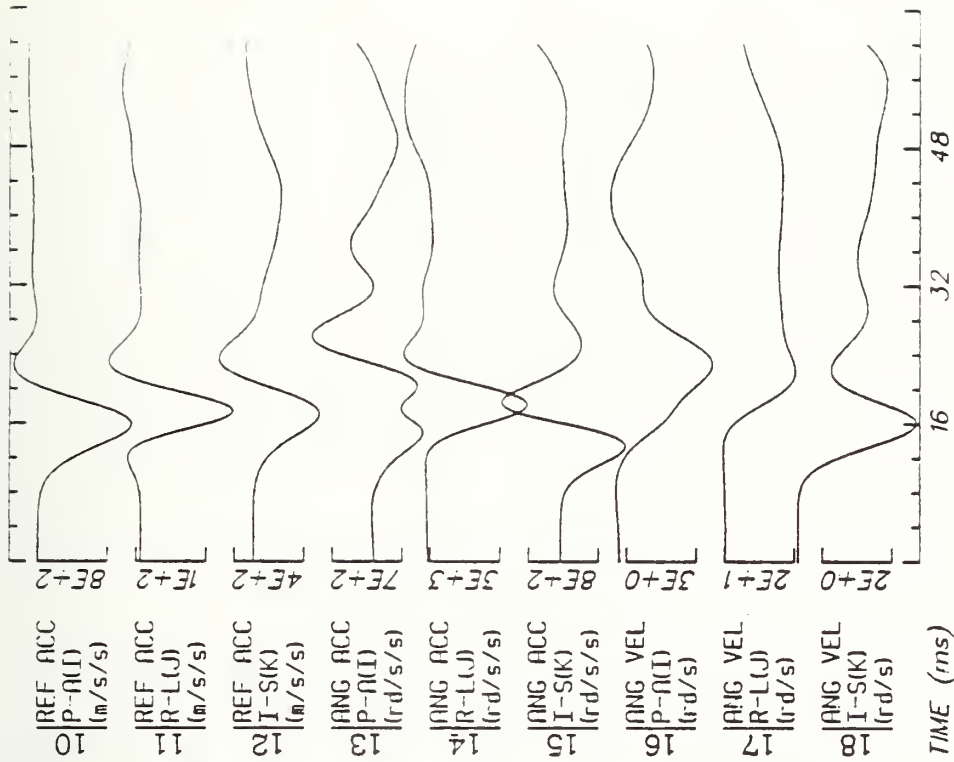
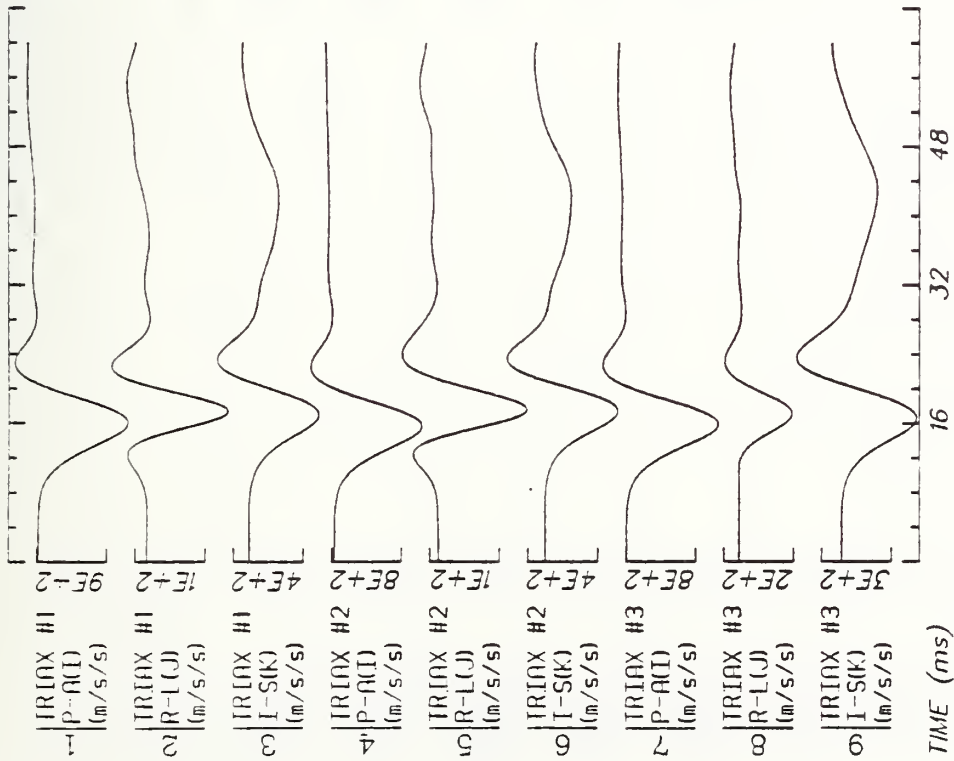
Run ID: 82E041 Disk: E041.3D. File: 1 Date: MAR 7, 1985 Sheet: 5

Filter: 200*4C



Run ID: 82E041
 Disk: E041.3D.
 Filter: 200*4C

File: 1
 Date: MAR 7, 1985
 Sheet: 6



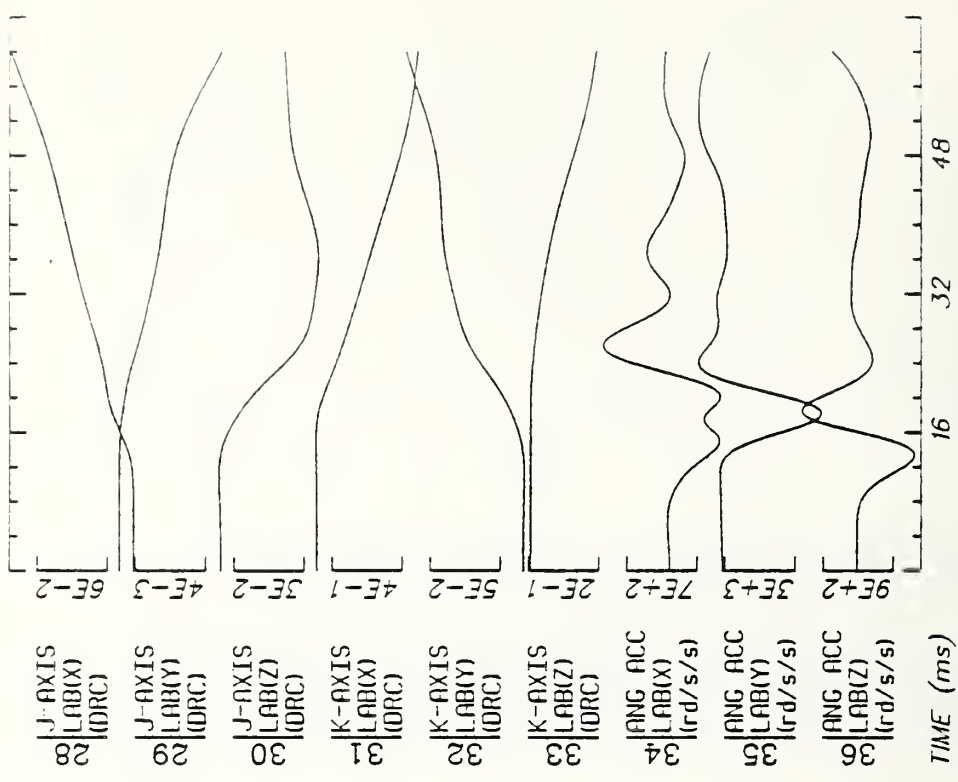
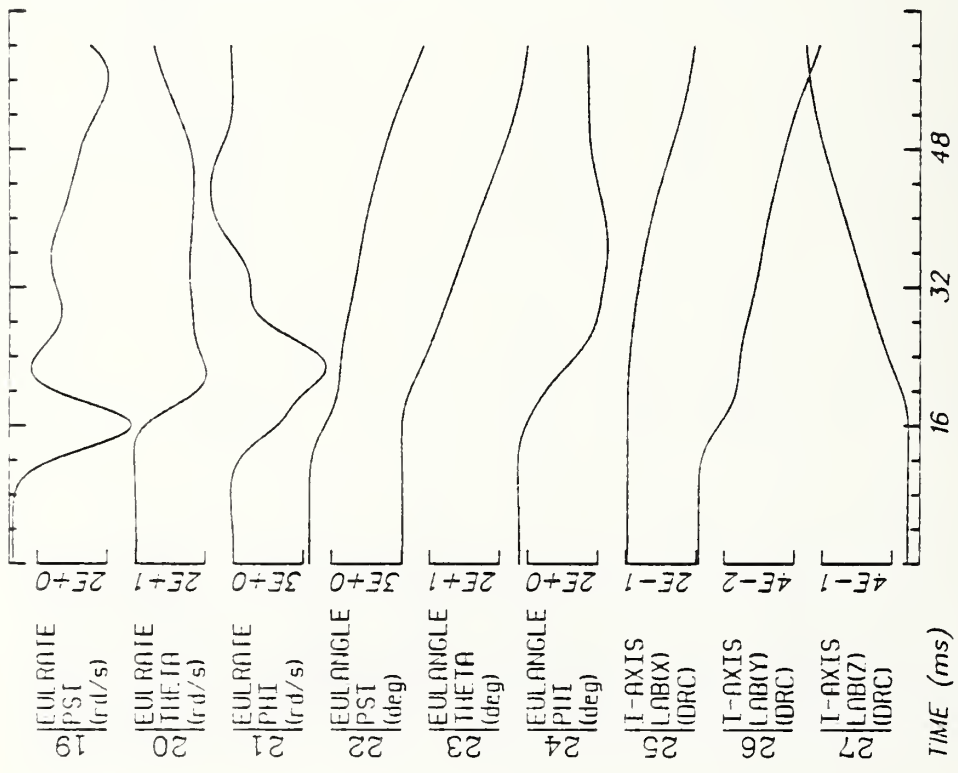
Run ID: 82E041

Disk: E041.3D. File: 1

Date: MAR 7, 1985 Sheet: 1

Filter: 100*4C

C41



Run ID: 82E041

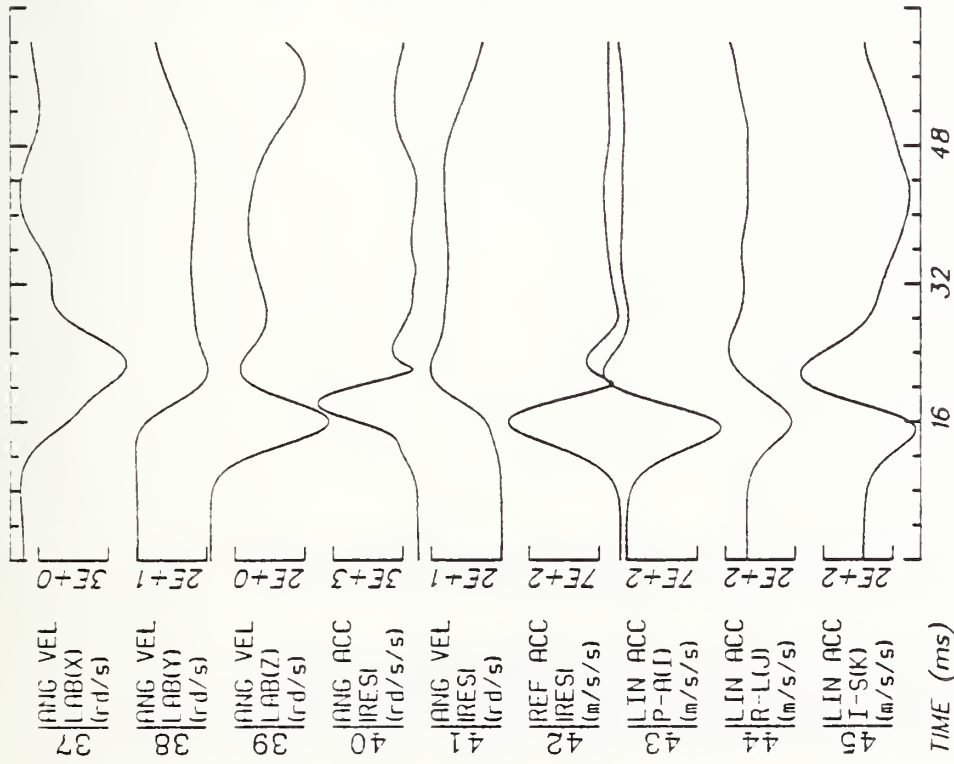
Disk: E0413D. File: 1

Date: MAR 7, 1985 Sheet: 2

Filter: 100*4C

7.1

C42



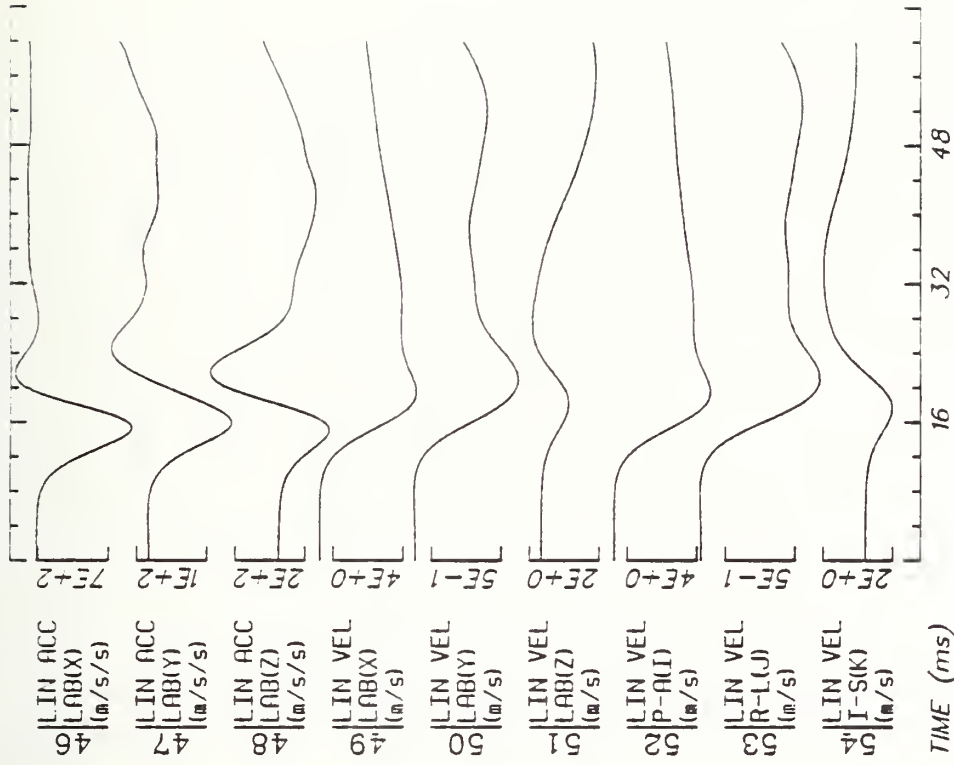
TIME (ms)

Run ID: 82E041

Disk: E041.3D. File: 1

Date: MAR 7, 1985 Sheet: 3

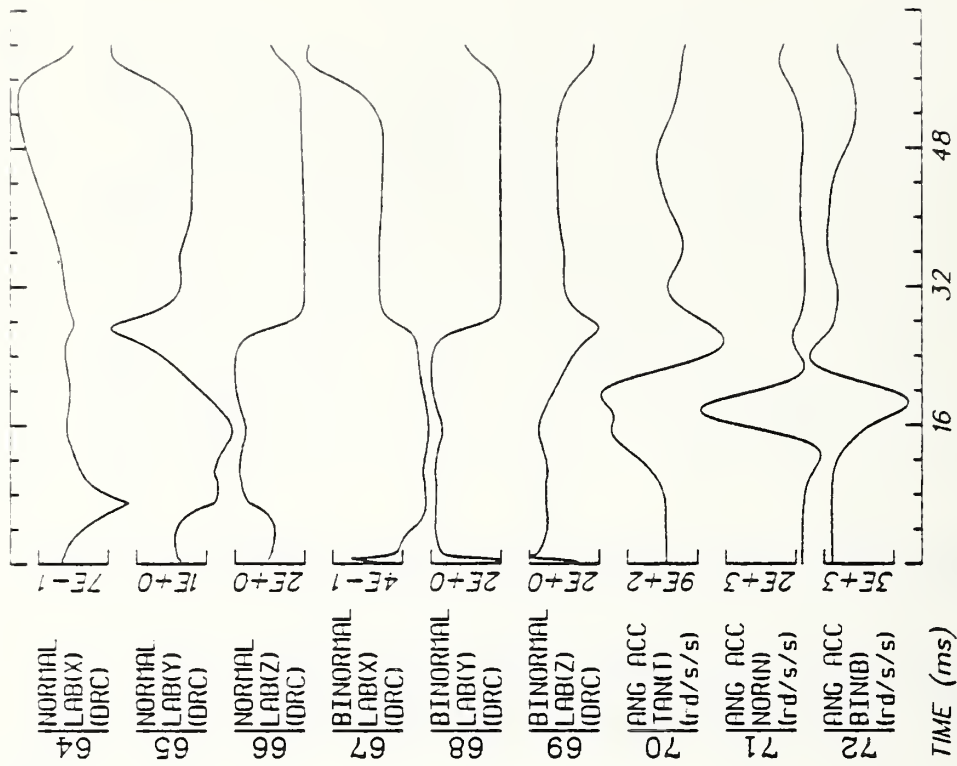
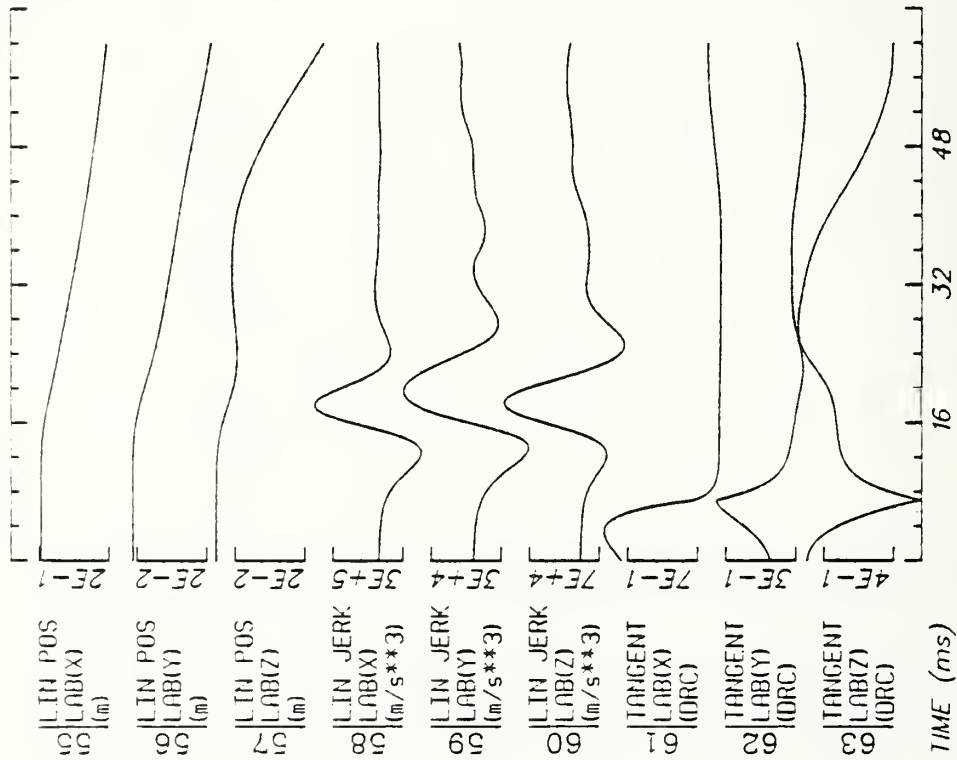
Filter: 100*4C



TIME (ms)

041

C43

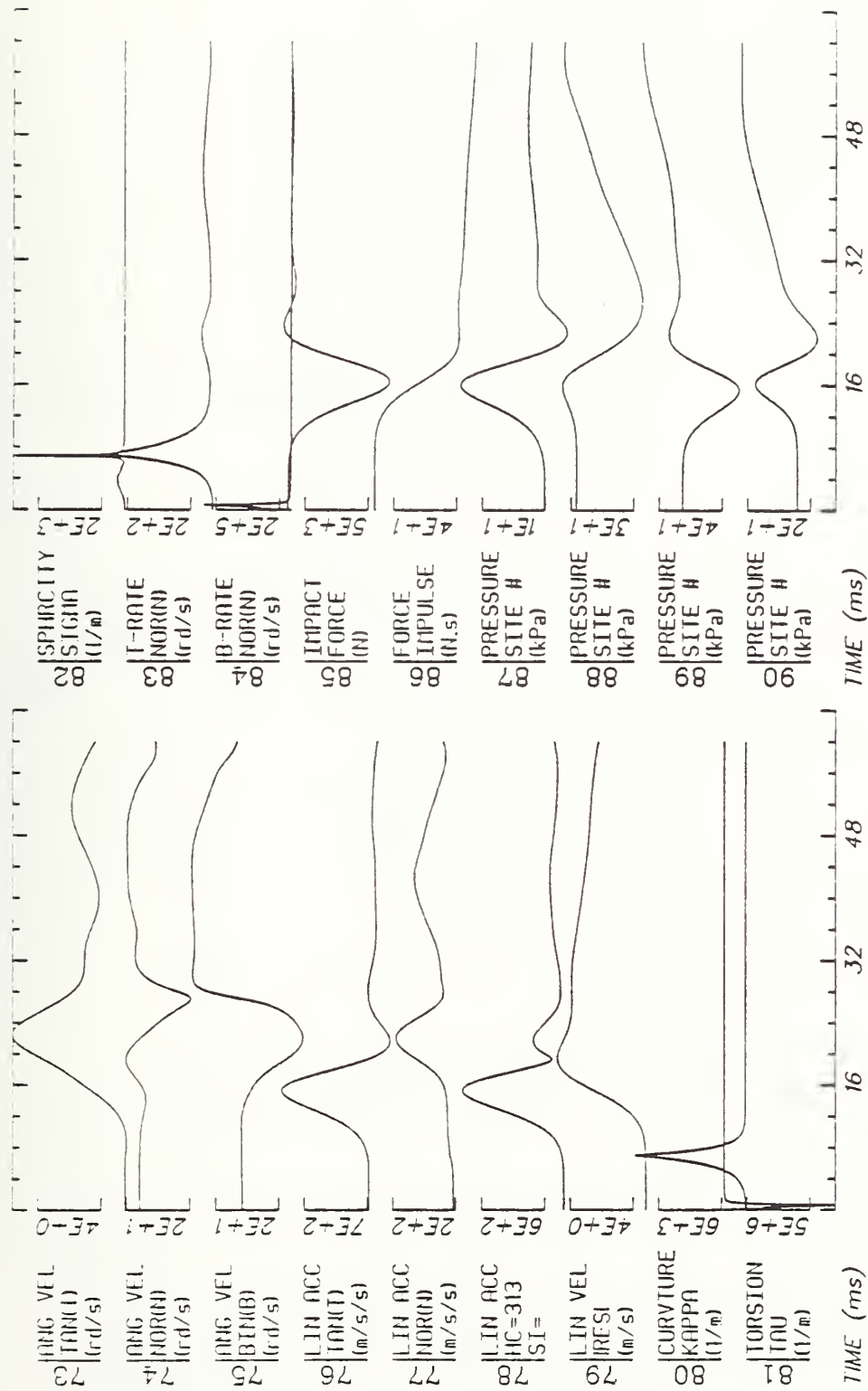


Run ID: 82E041

Disk: E041.3D. File: 1

Date: MAR 7, 1985 Sheet: 4

Filter: 100*4C



Run ID: 82E041

Disk: E041.3D.

File: 1

Date: MAR 7, 1985

Sheet: 5

Filter: 100*4C



Run ID: 82E041

Disk: E041.3D.

File: 1

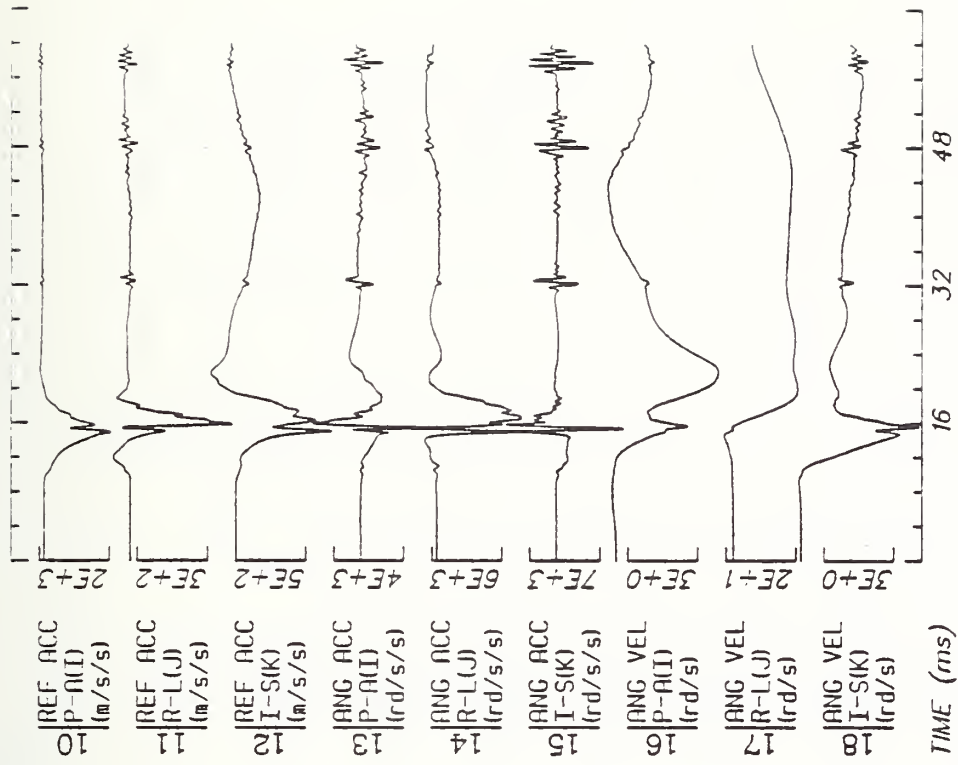
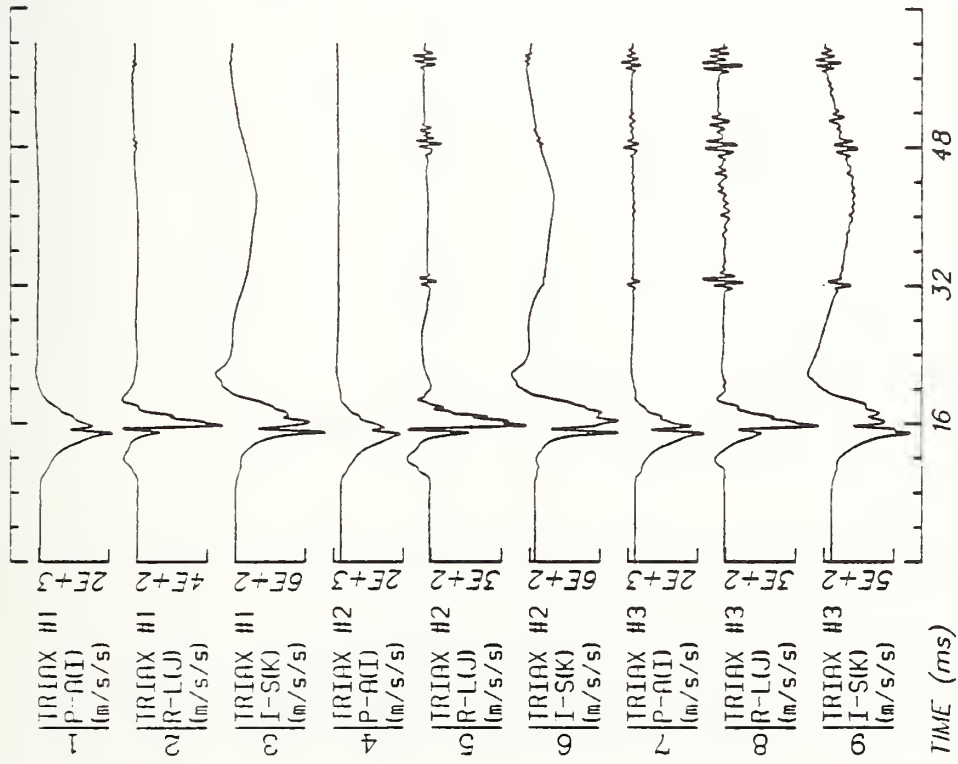
Date: MAR 7, 1985

Sheet: 6

Filler: 100*4C

境

C46



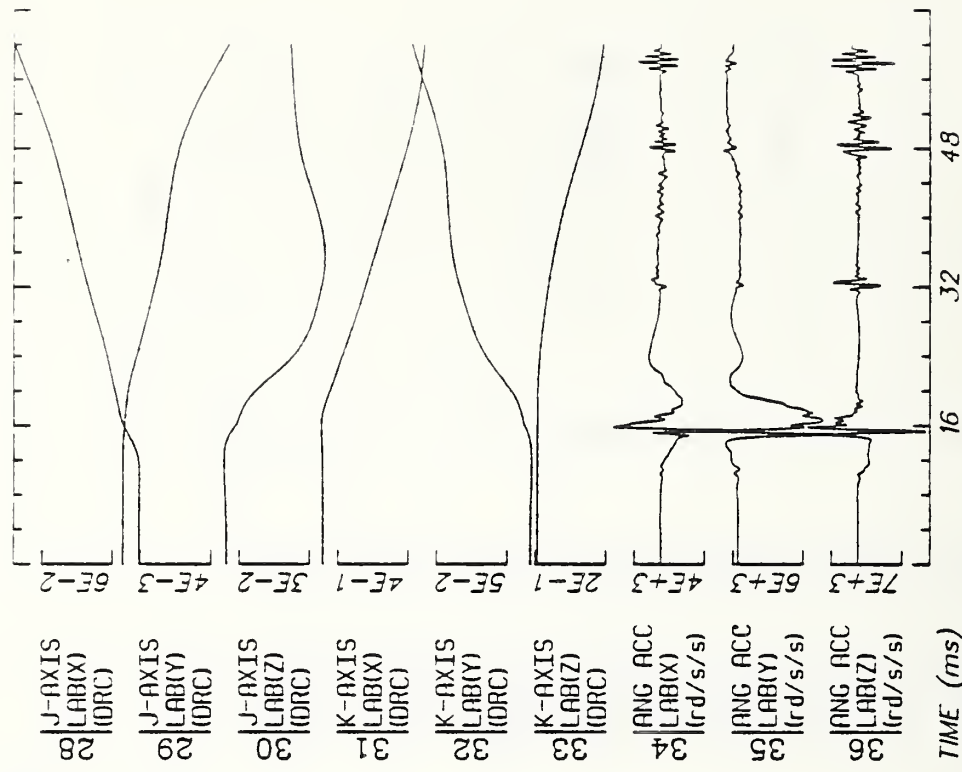
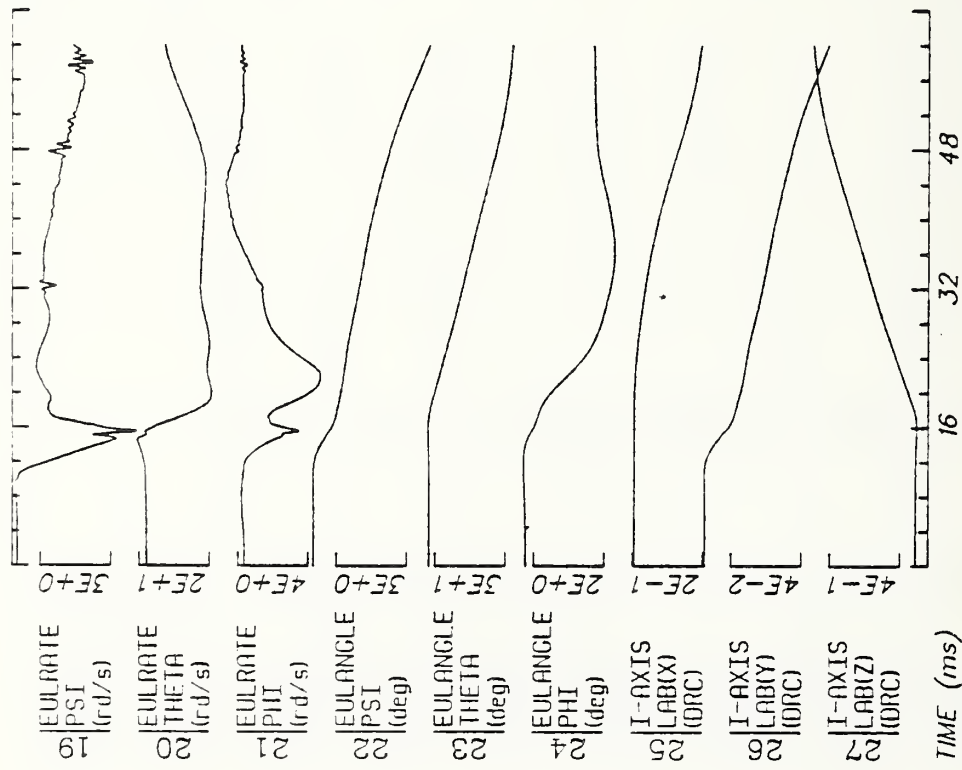
Run ID: 82E041

Disk: E041.3D. File: 1

Date: MAR 7, 1985 Sheet: 1

No Filtering

C47



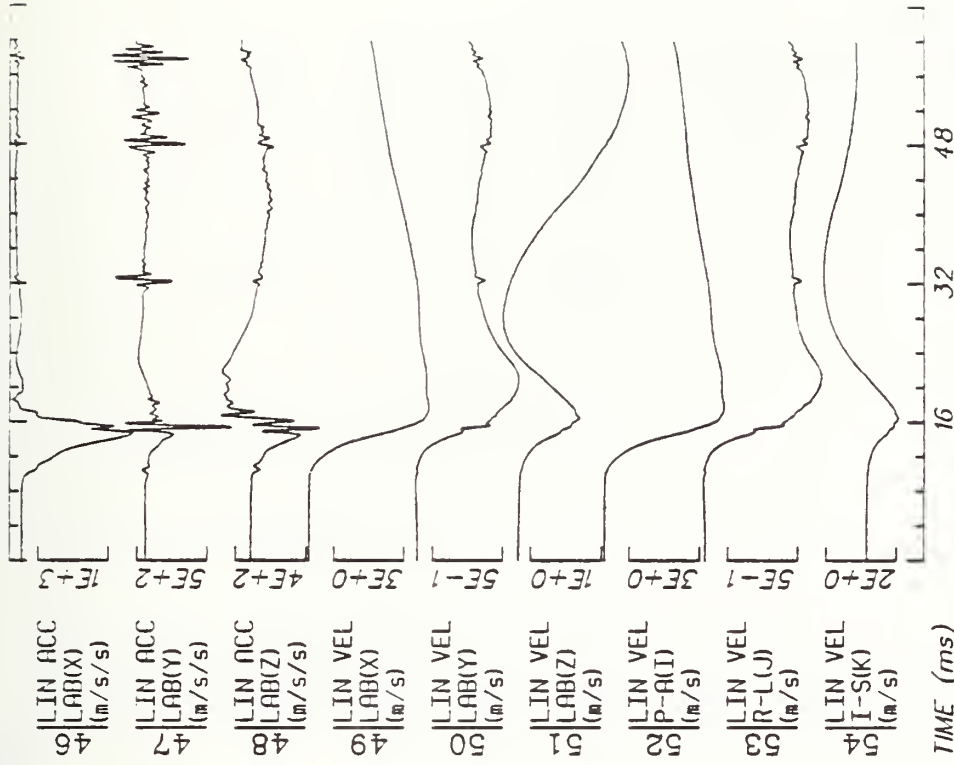
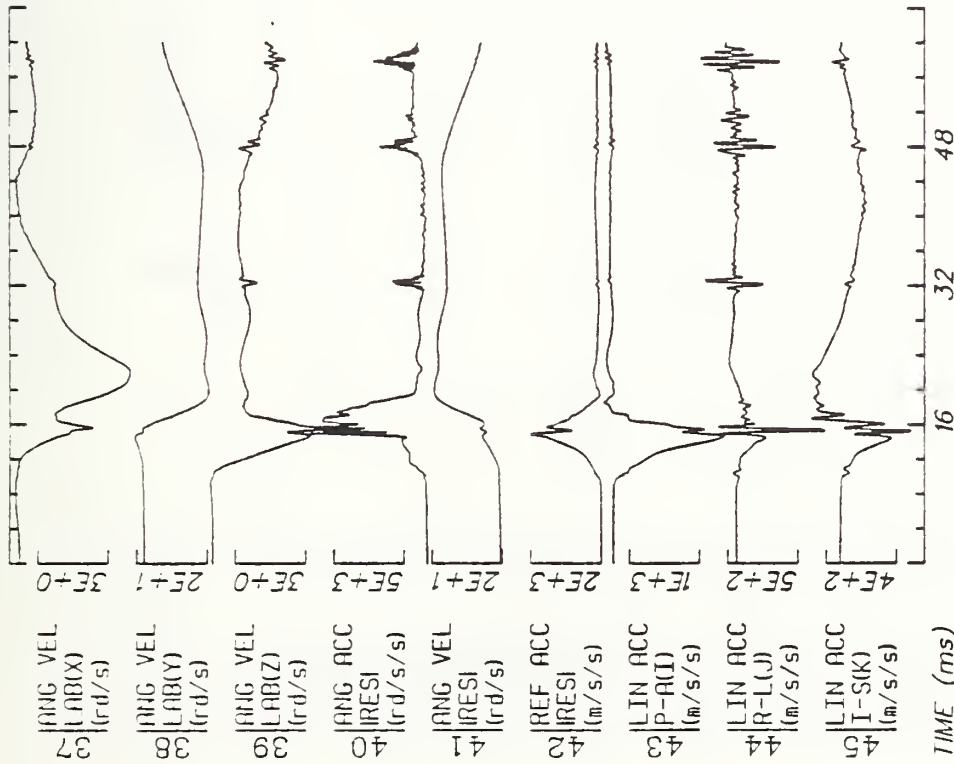
Run ID: 02E041

Disk: E041.3D. File: 1

Date: MAR 7, 1985 Sheet: 2

No Filtering

67 C48



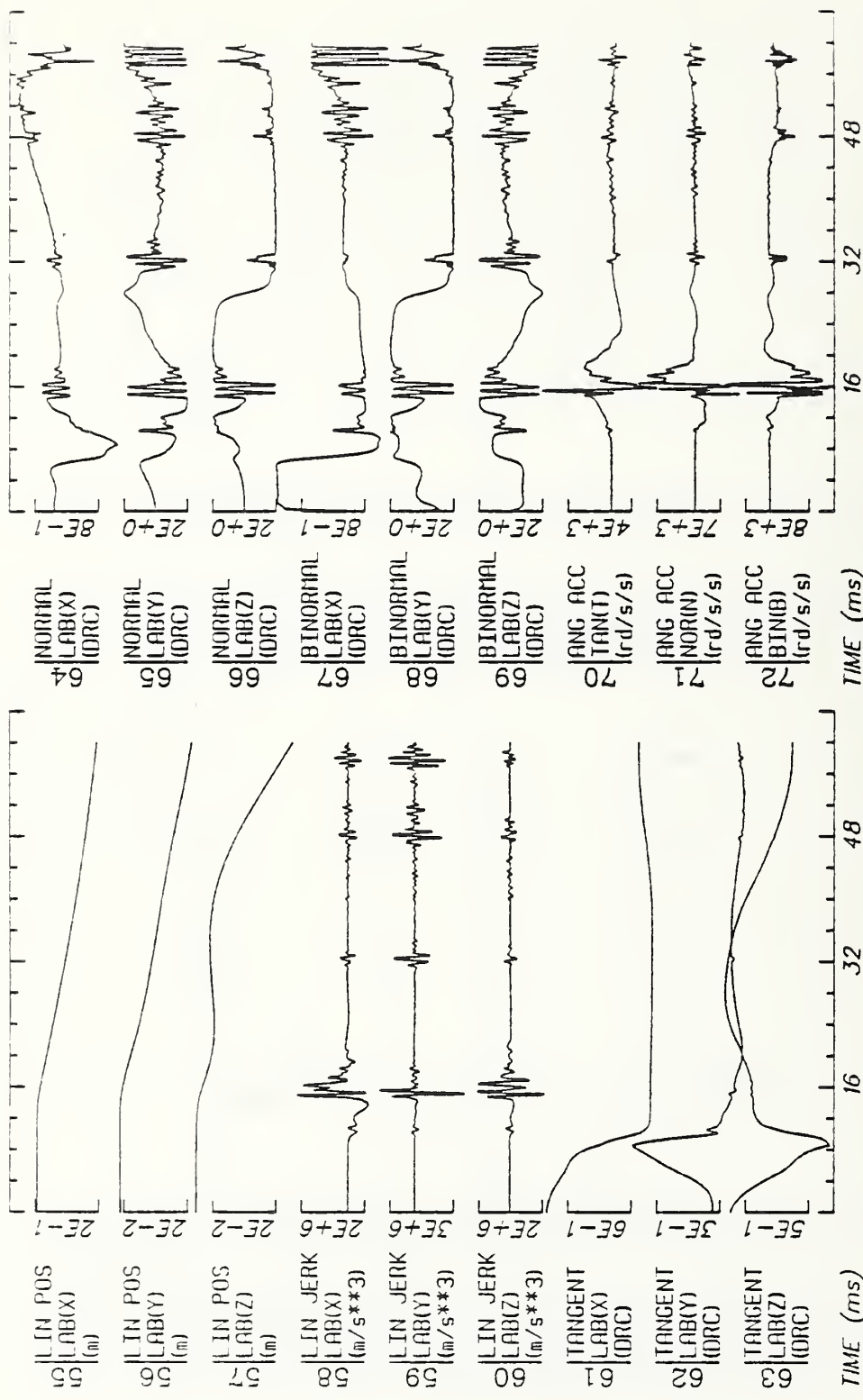
Run ID: 82E041

Disk: E041.3D. File: 1

Date: MAR 7, 1985 Sheet: 3

No Filtering

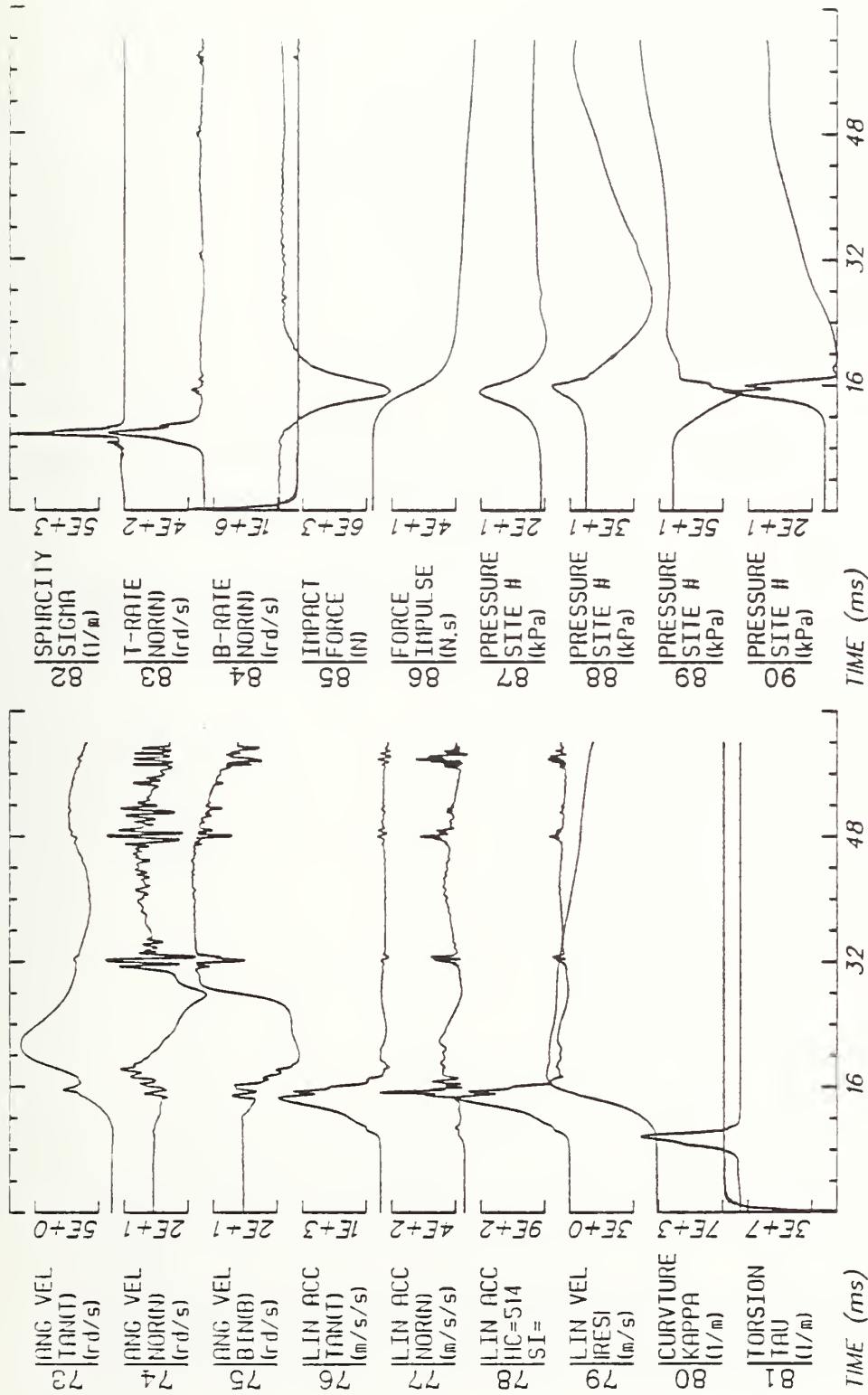
C49



Run ID: 82E041 Disk: E041.3D. File: 1 Date: MAR 7, 1985 Sheet: 4

No Filtering

C50

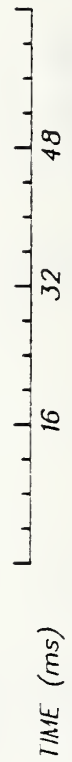


Run ID: 82E041

Disk: E041.3D. File: 1

Date: MAR 7, 1985 Sheet: 5

No Filtering



Run ID: 82E041

Disk: E041.3D.

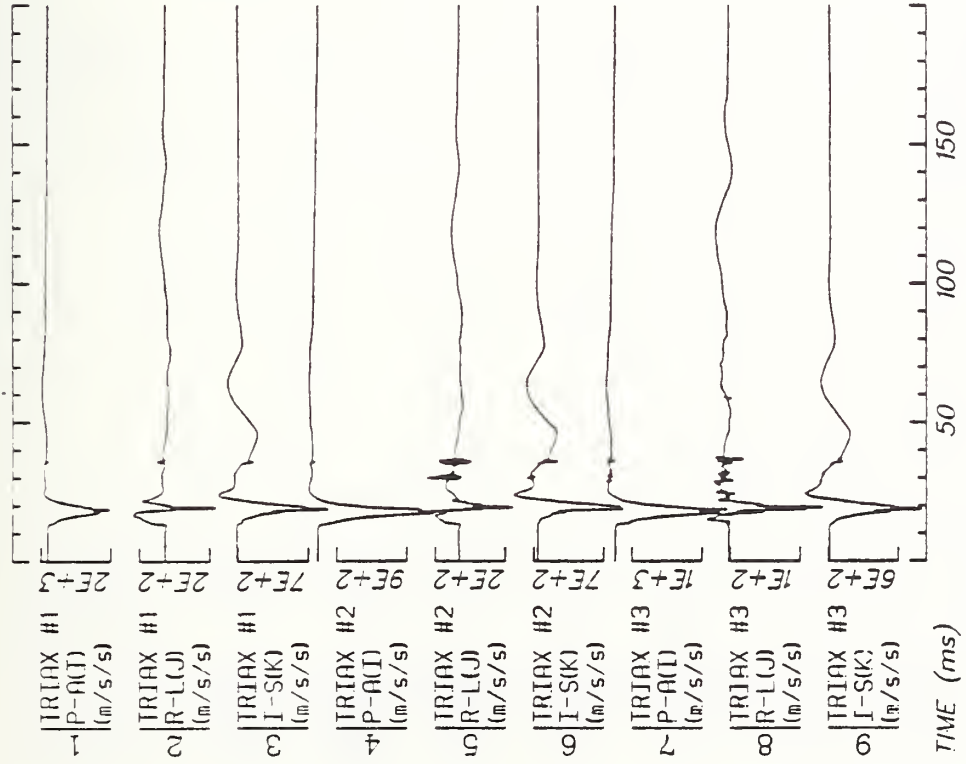
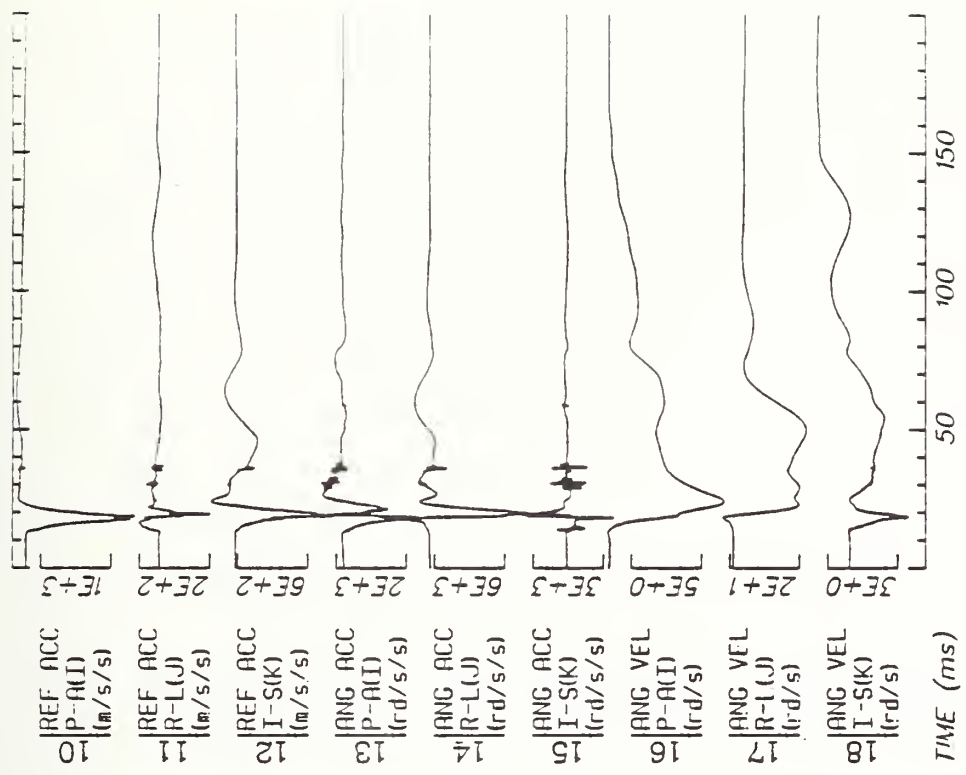
File: 1

Date: MAR 7, 1985

Sheet: 6

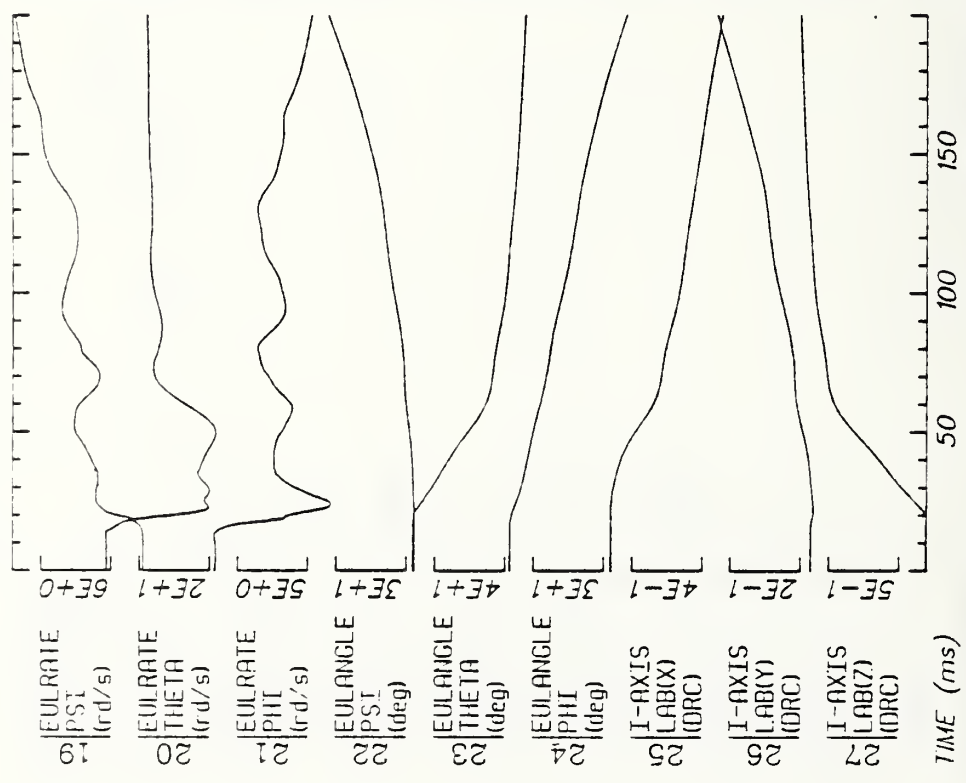
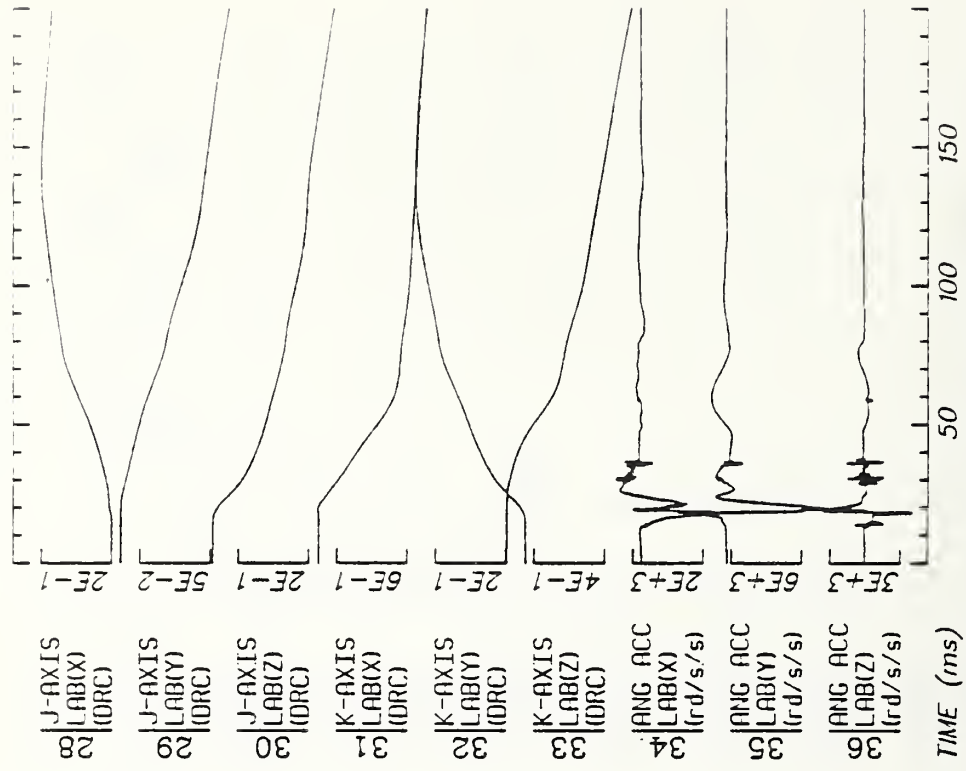
No Filtering

C52



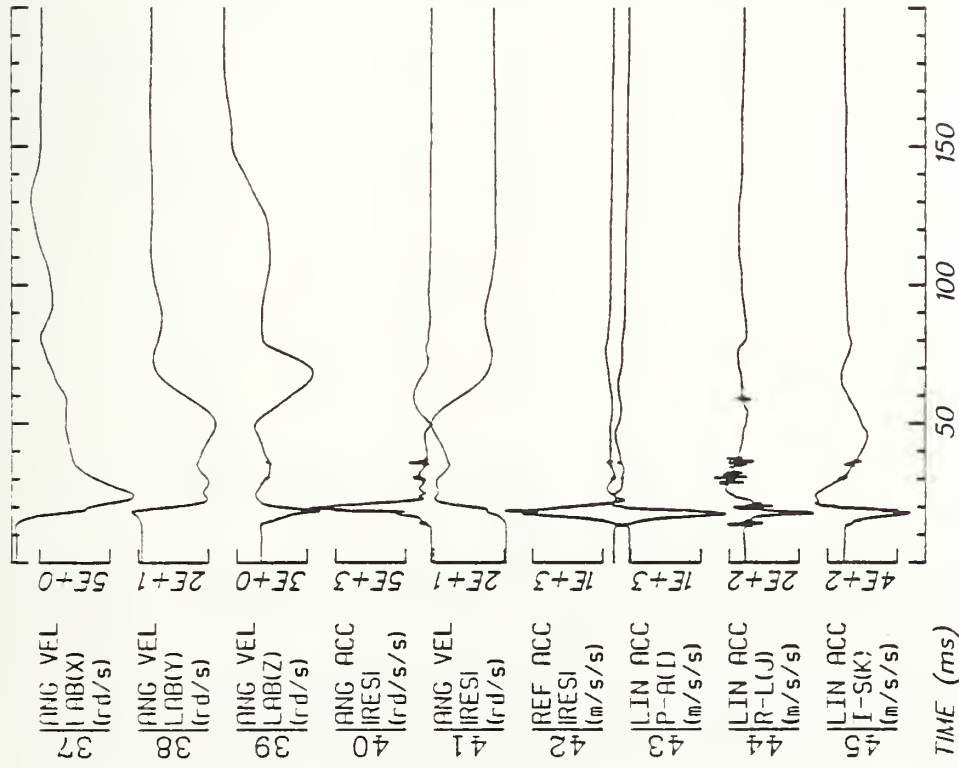
Run ID: 82E042 Disk: -HEAD File: 2 Date: MAR 11, 1985 Sheet: 1

Filter: 1600*4C



Run ID: 82E042 Disk: -HEAD File: 2 Date: MAR 11, 1985 Sheet: 2

Filter: 1600*4C



TIME (ms)

Run ID: 82E042

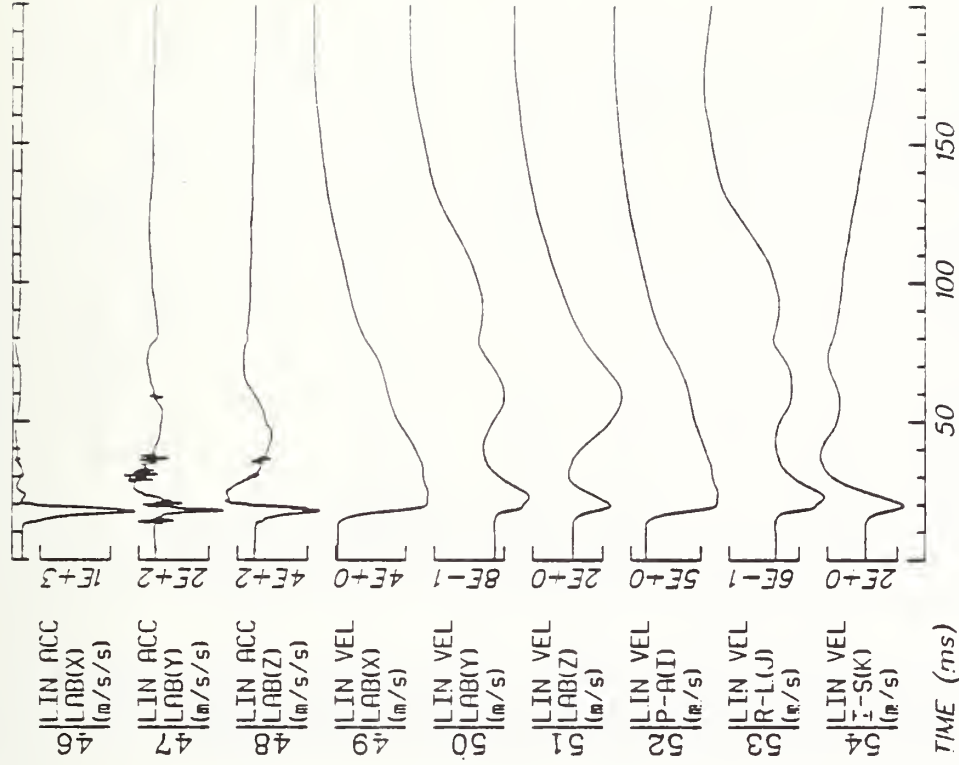
Disk: -HEAD

File: 2

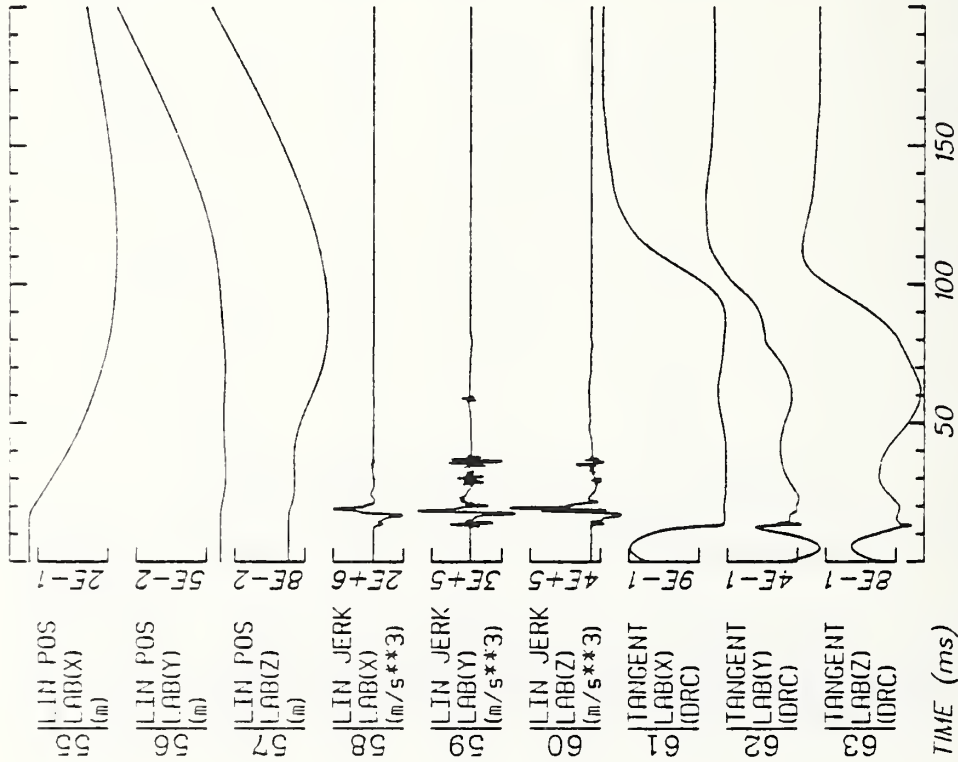
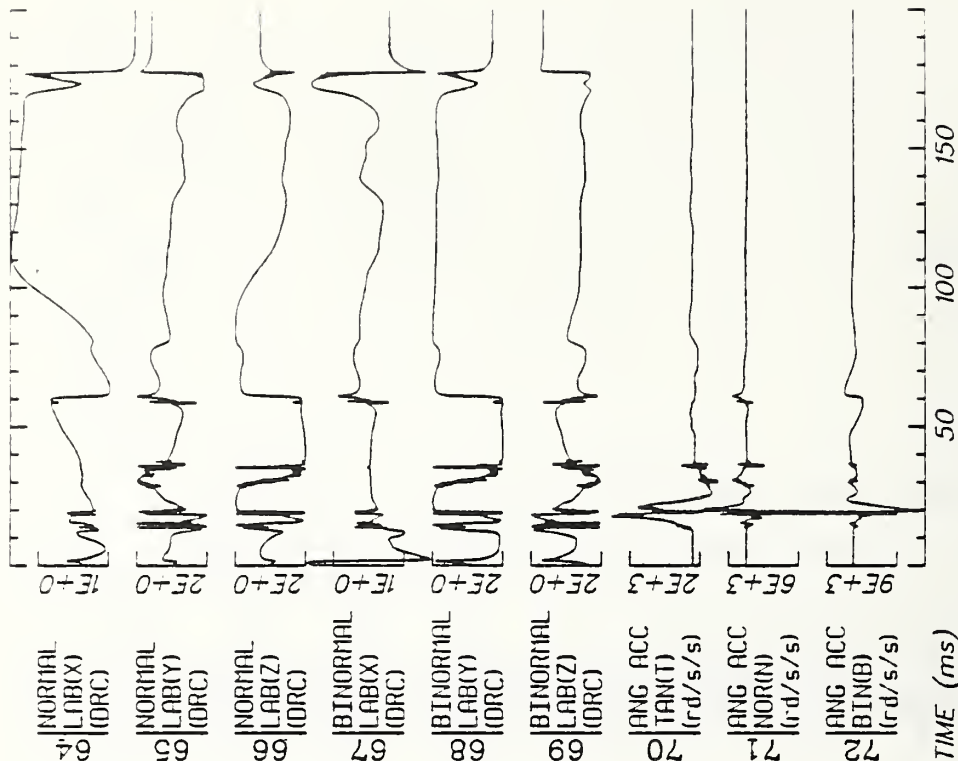
Date: MAR 11, 1985

Sheet: 3

Filter: 1600*4C

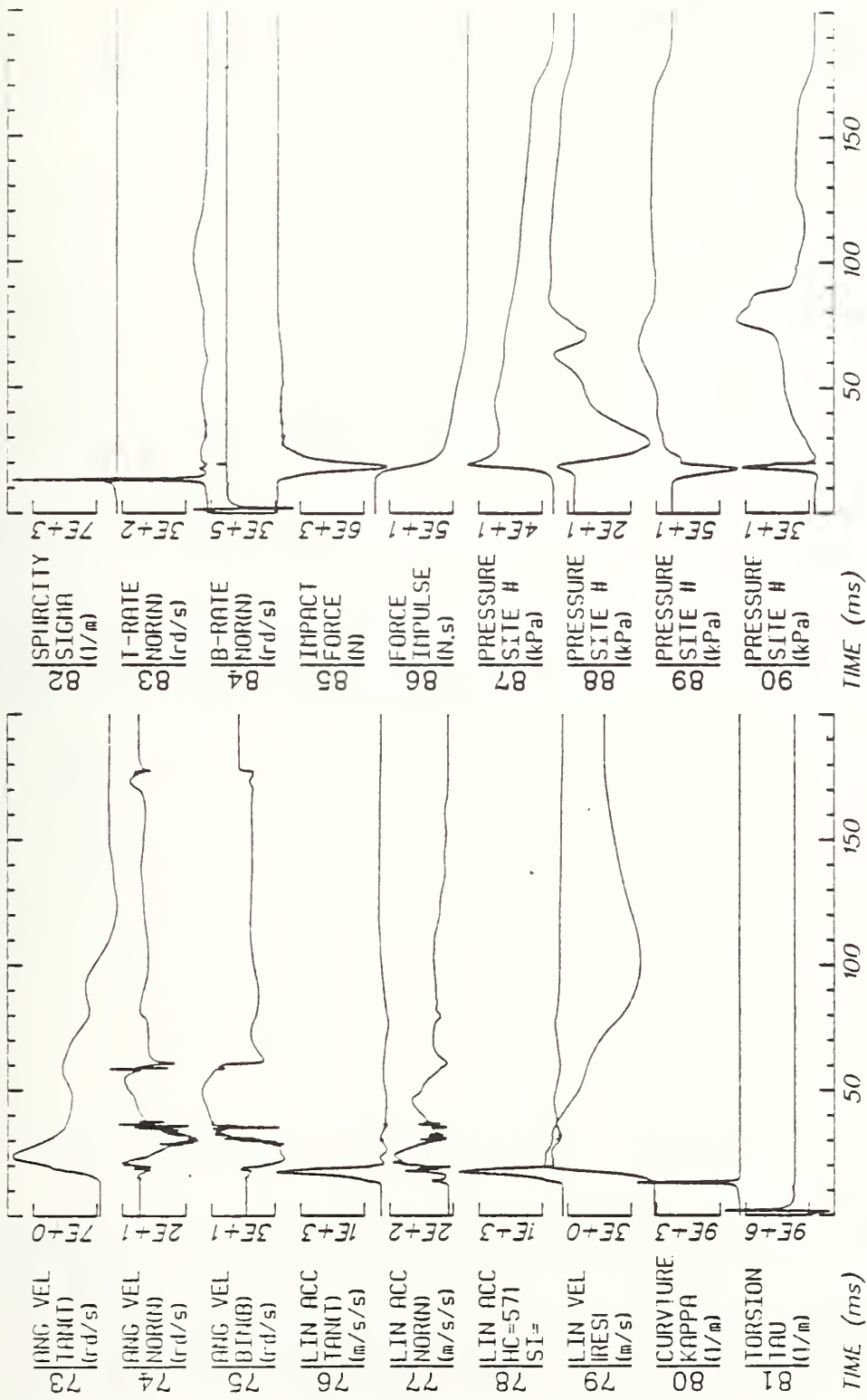


TIME (ms)



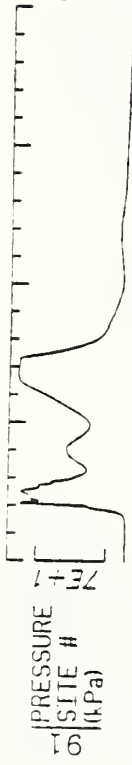
Run ID: 82E042 Disk: -HEAD File: 2 Date: MAR 11, 1985 Sheet: 4

Filter: 1600*4C



Run ID: 82E042 Disk: -HEAD File: 2 Date: MAR 11, 1985 Sheet: 5

Filter: 1600*4C



TIME (ms)

Run ID: 82E042

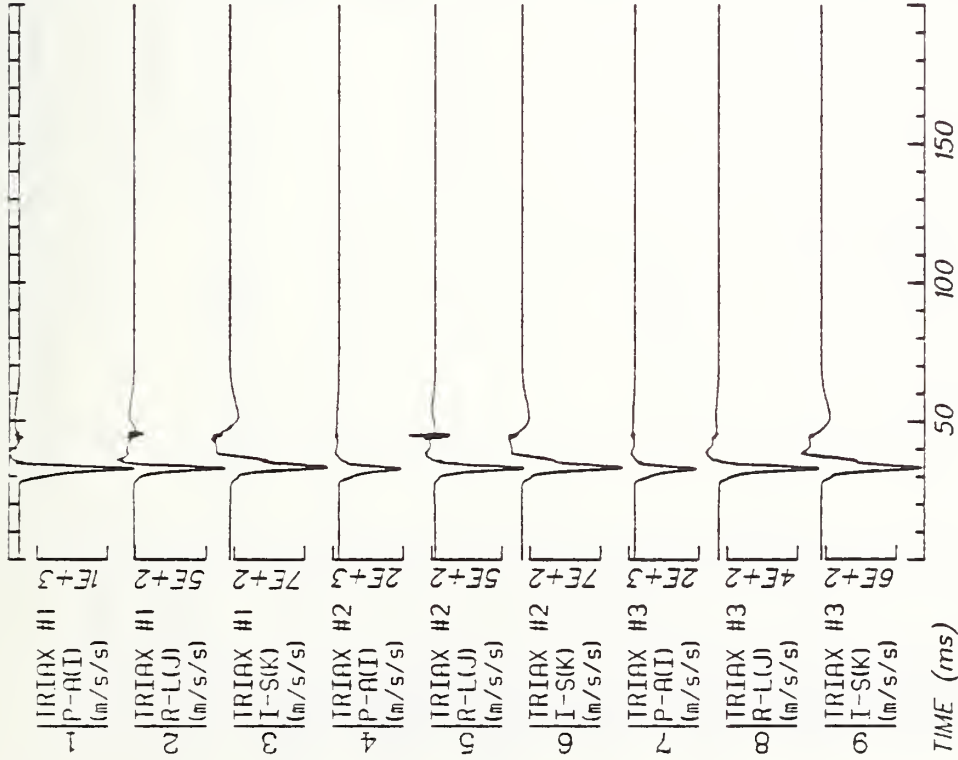
Disk: -HEAD

Filter: 1600*4C

File: 2

Date: MAR 11, 1985

Sheet: 6

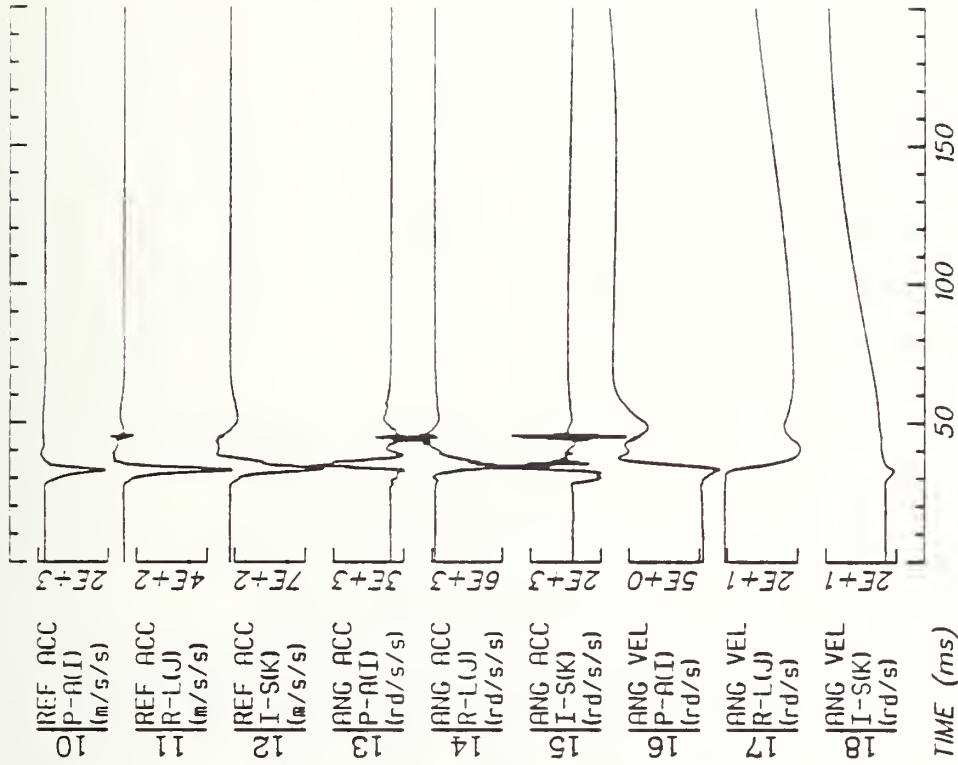


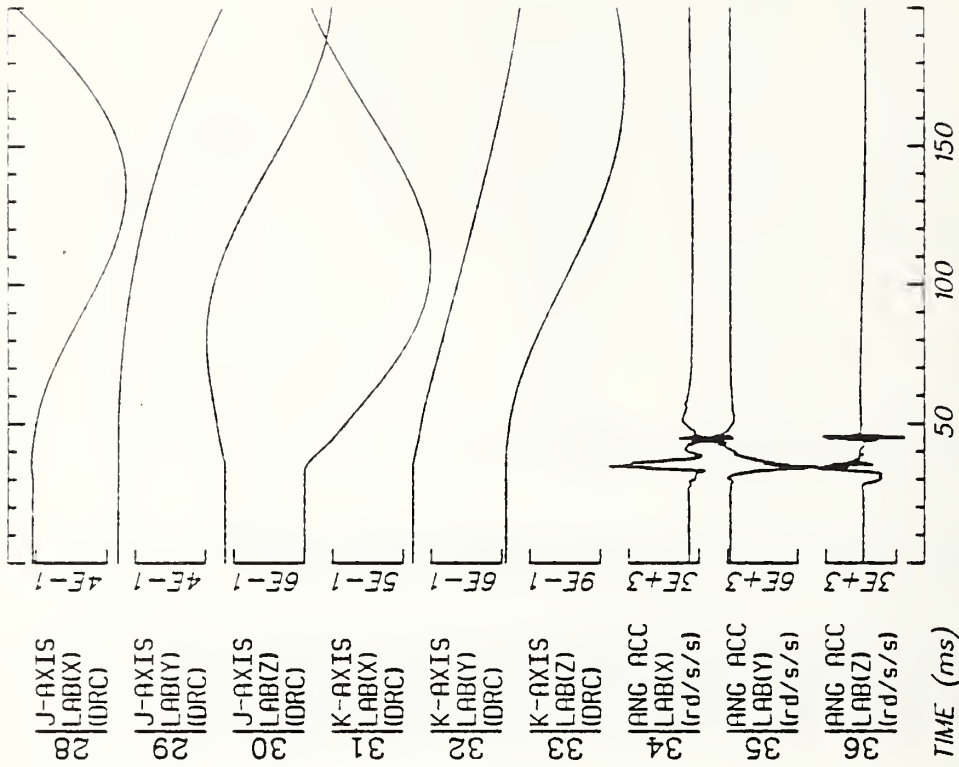
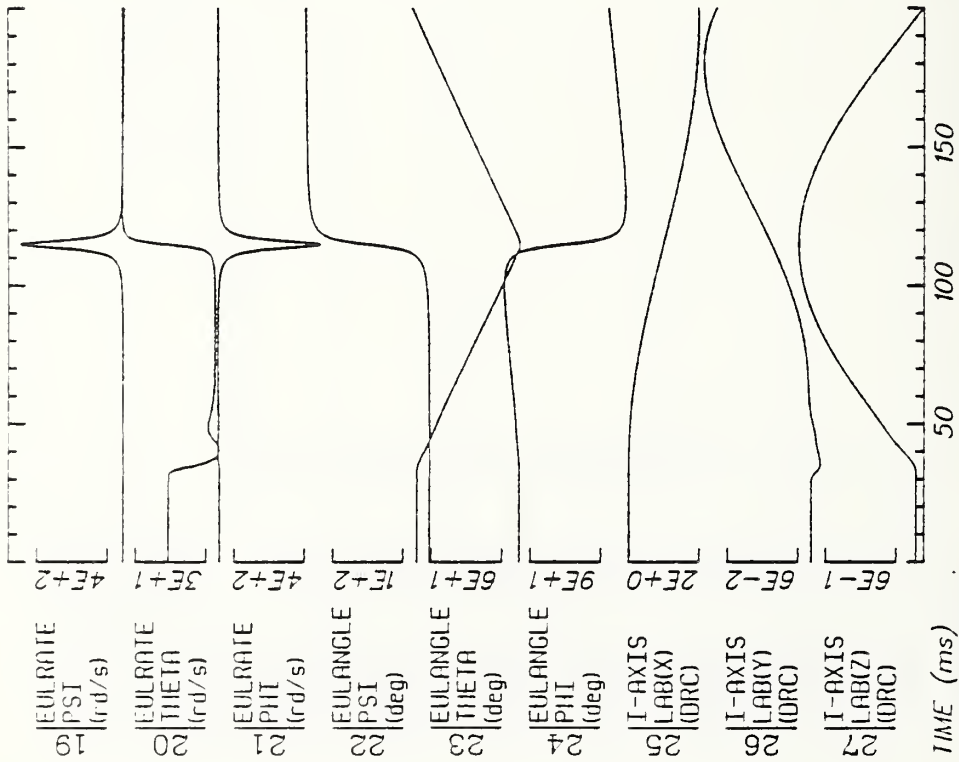
Run ID: 82E061

Disk: 82E061.3 File: 1

Date: MAR 21, 1985 Sheet: 1

Filter: 1600*4C



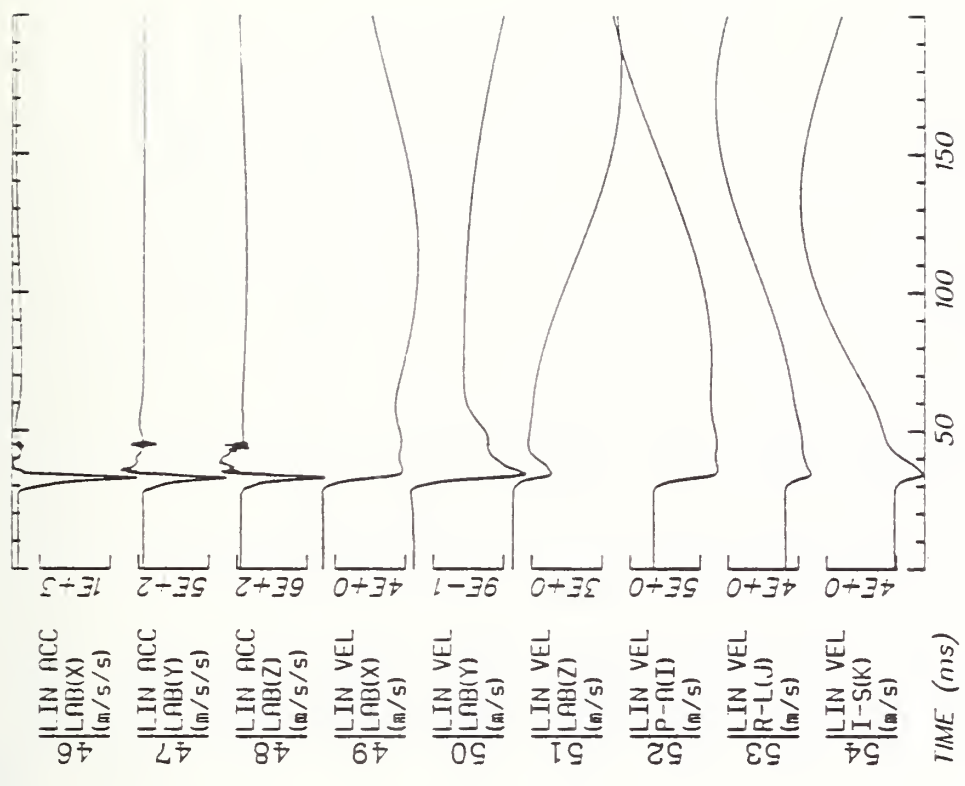
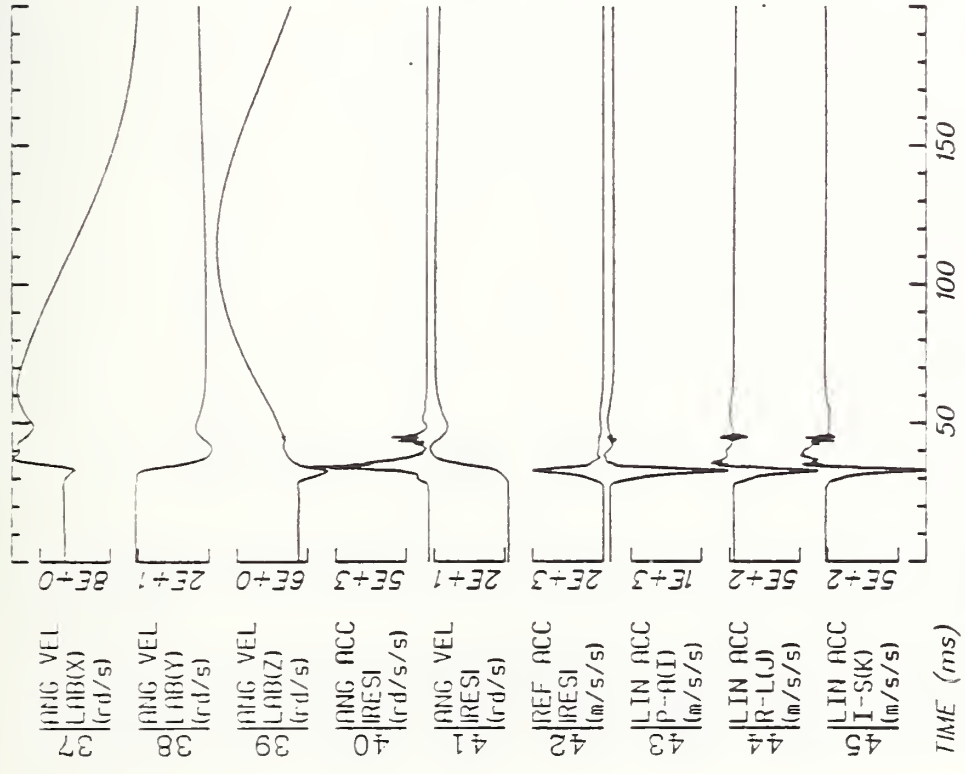


Run ID: 82E061

Disk: 82E061.3 File: 1

Date: MAR 21, 1985 Sheet: 2

Filter:1600*4C

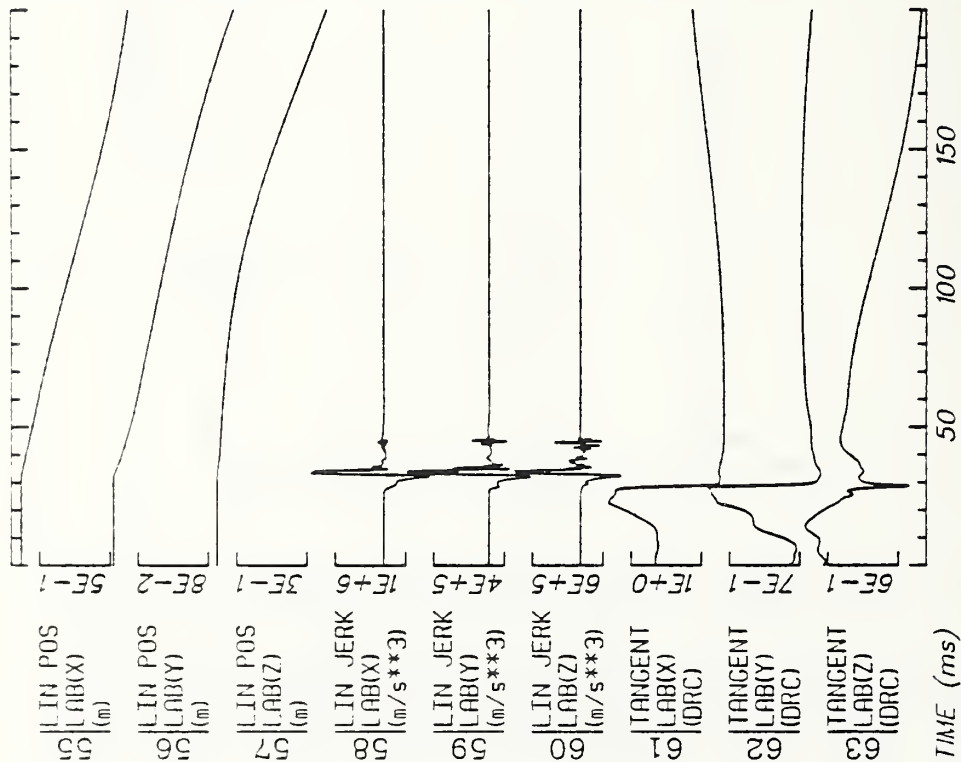
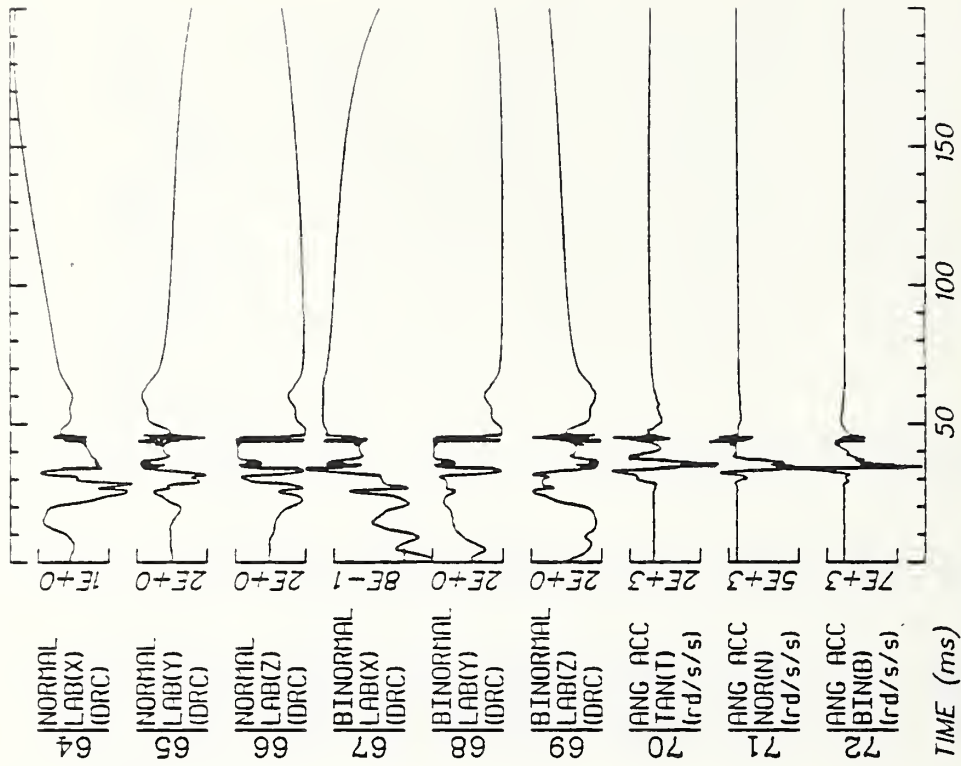


Run ID: 82E061

Disk: 82E061.3 File: 1

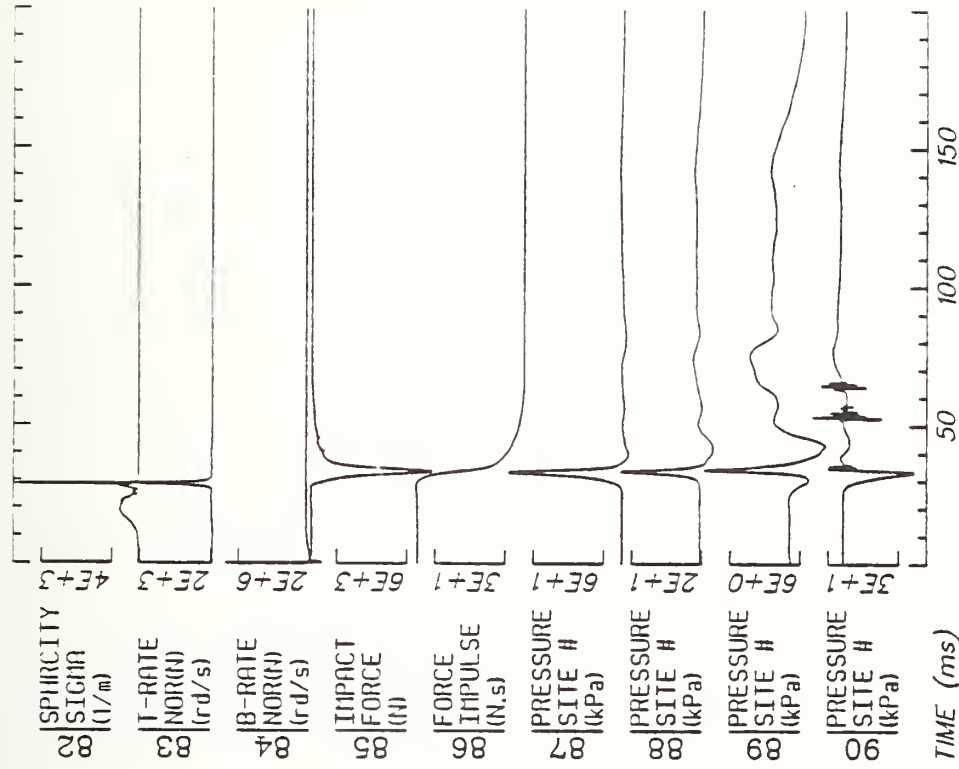
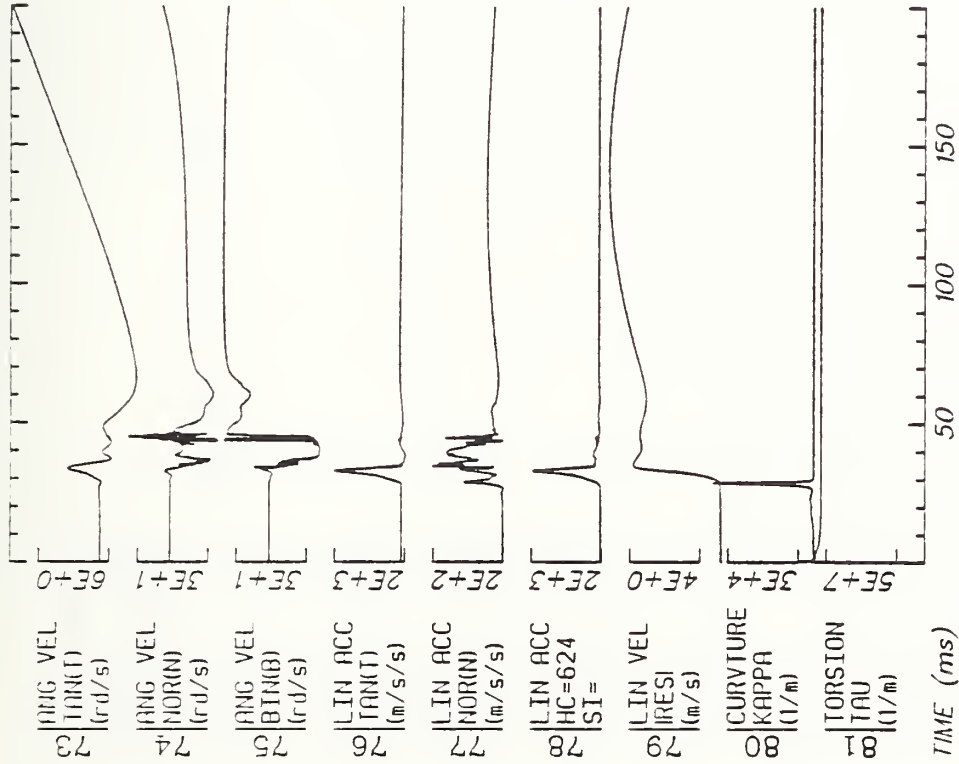
Date: MAR 21, 1985 Sheet: 3

Filter:1600*4C



Run ID: 82E061 Disk: 82E061.3 File: 1 Date: MAR 21, 1985 Sheet: 4

Filter: 1600*4C



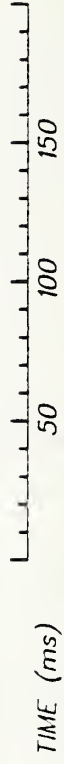
Run ID: 82E061

Disk: 82E061.3 File: 1

Date: MAR 21, 1985 Sheet: 5

Filter: f600*4C

C63



Run ID: 82E061

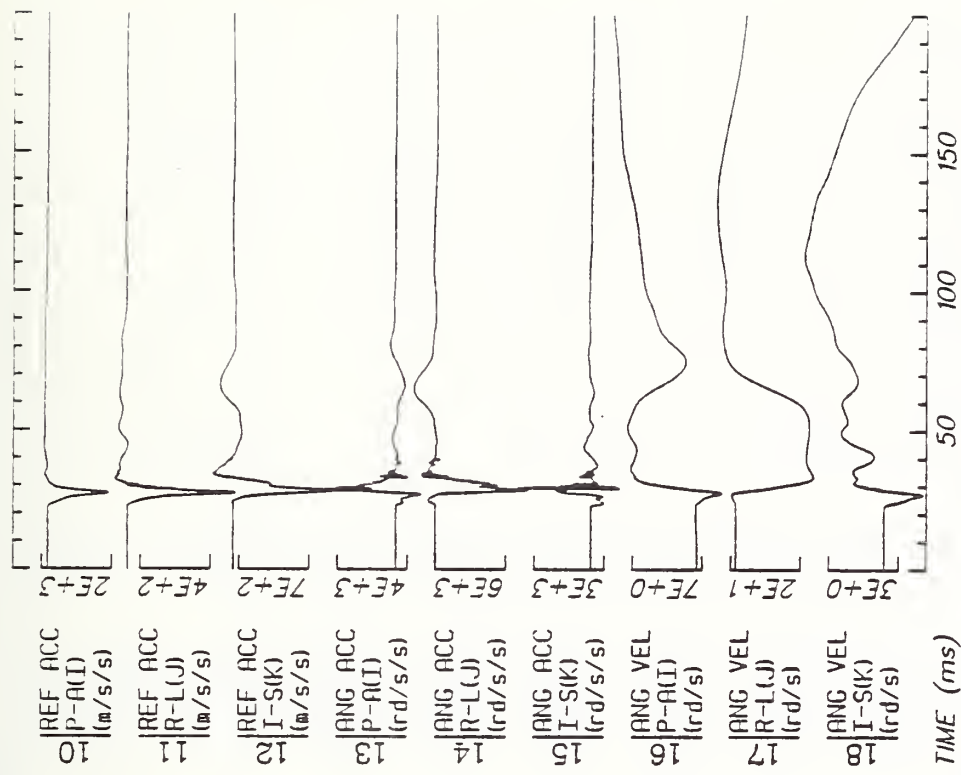
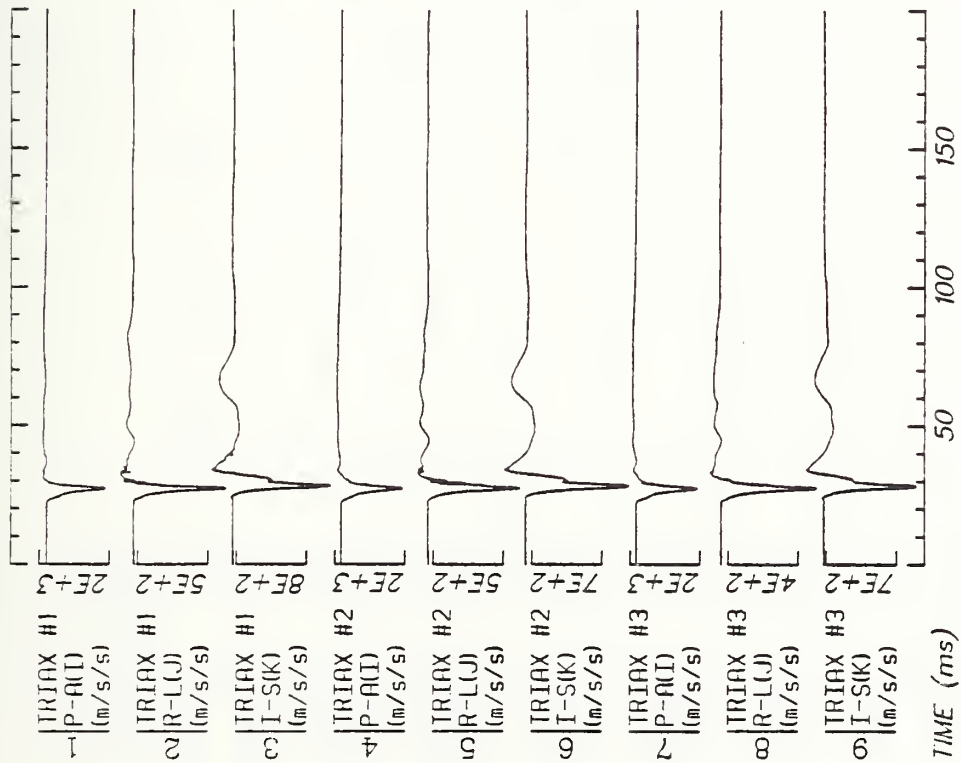
Disk: 82E061.3

File: 1

Date: MAR 21, 1985

Sheet: 6

Filter: 1600*4C

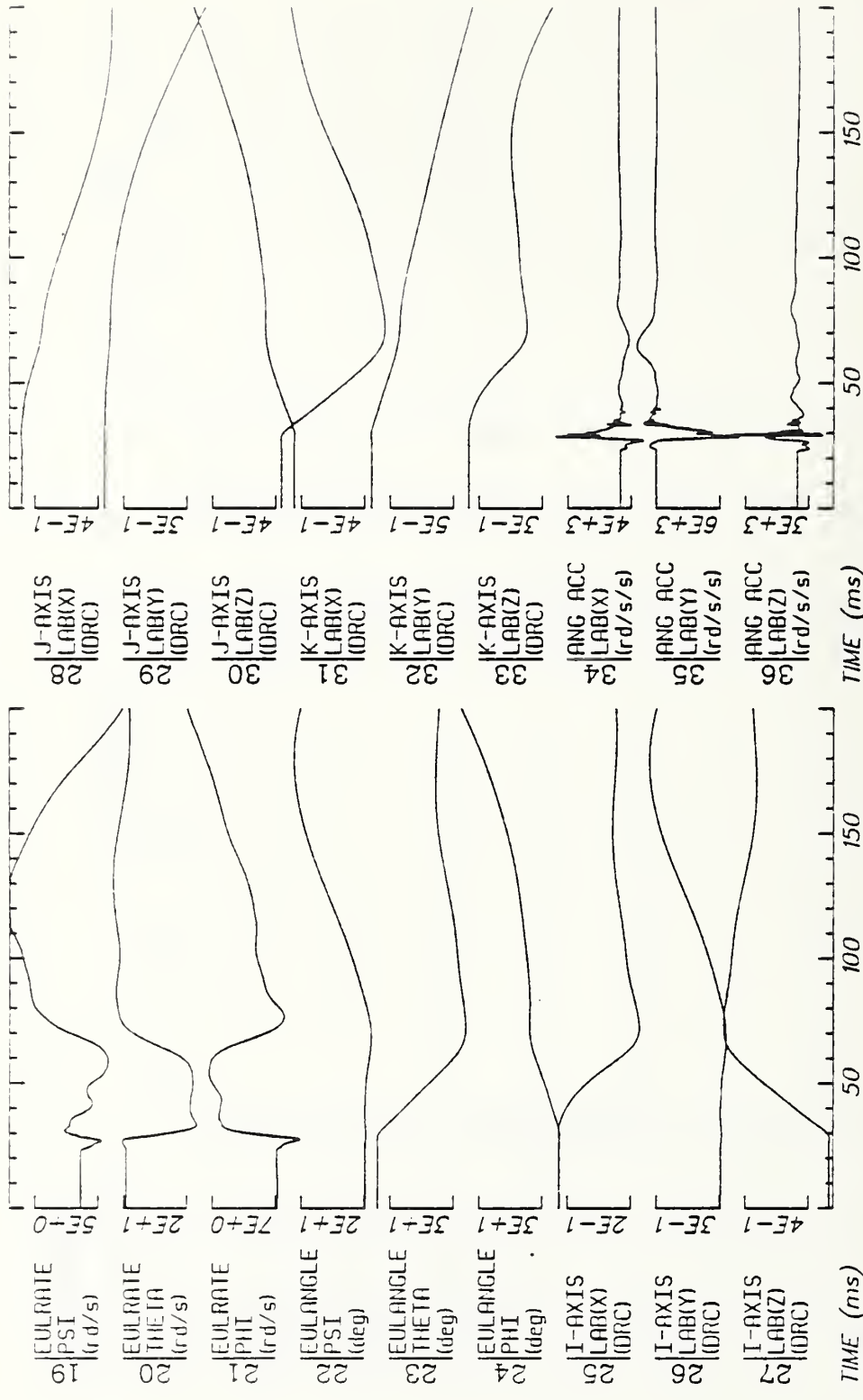


Run ID: 82E062

Disk: 82E062.3 File: 1

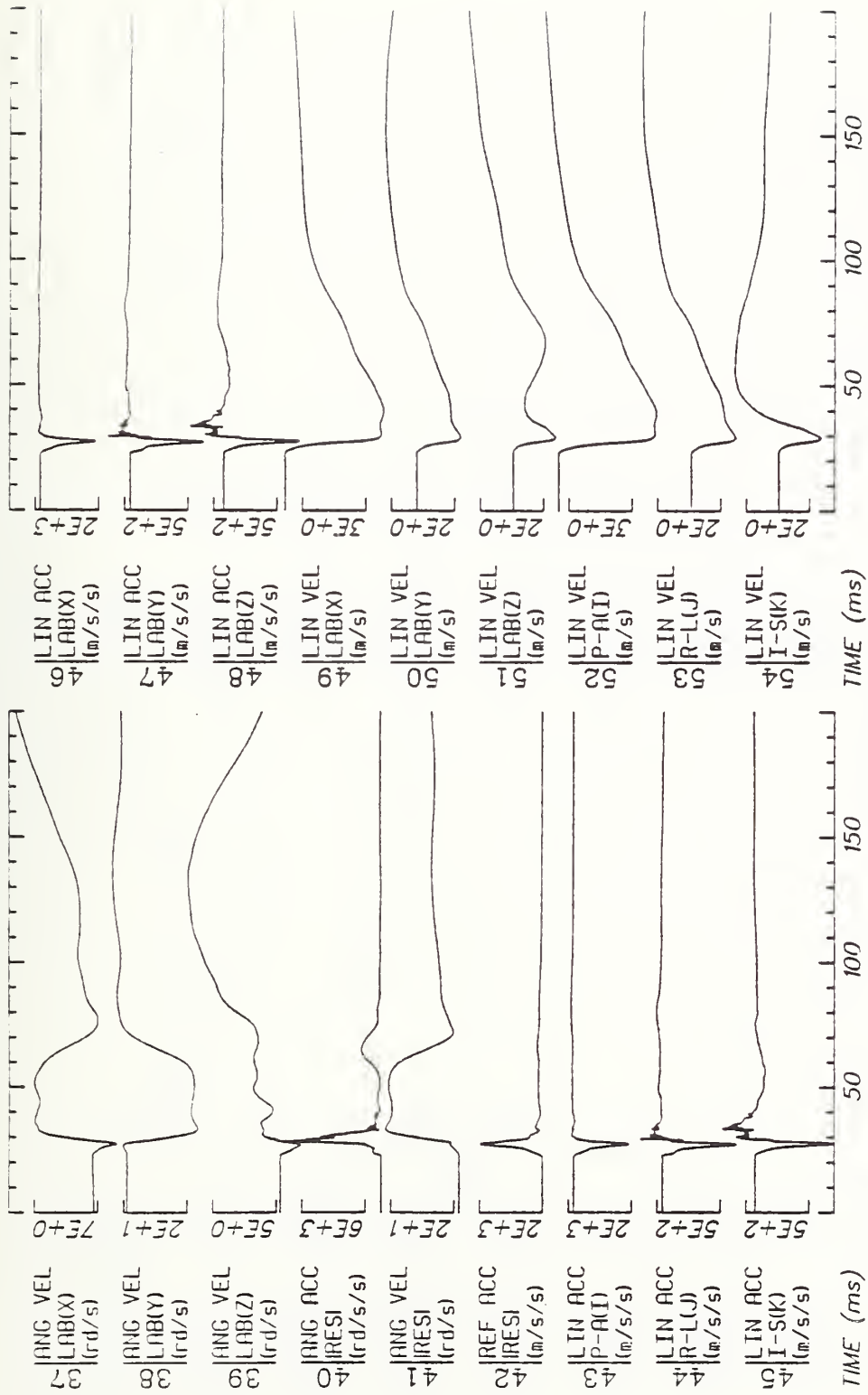
Date: APR 1, 1985 Sheet: 1

Filter: 1600*4C



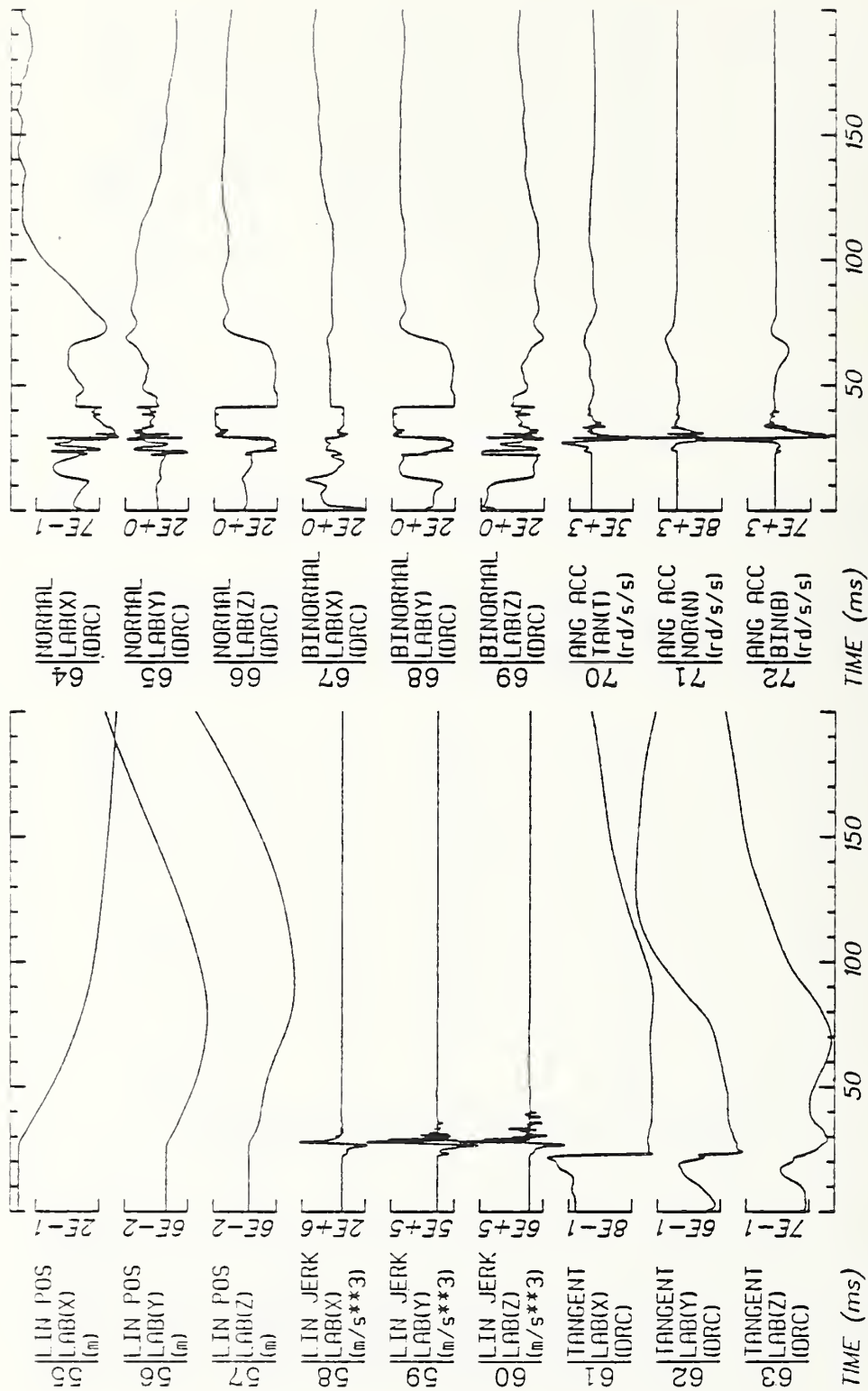
Run ID: 82E062 Disk: 82E062.3 File: 1 Date: APR 1, 1985 Sheet: 2

Filter: f600*4C



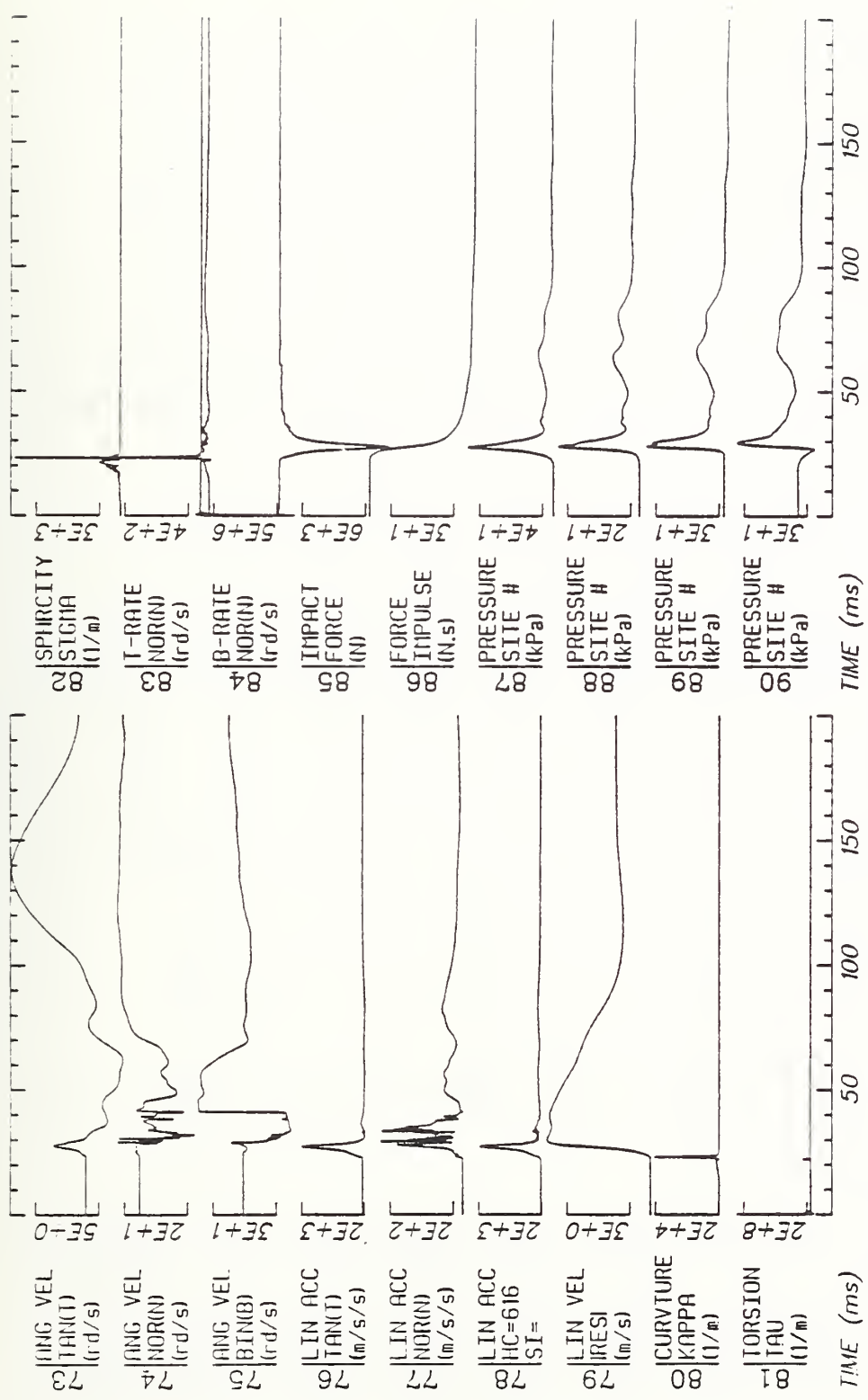
Run ID: 82E062 Disk: 82E062.3 File: 1 Date: APR 1, 1985 Sheet: 3

Filter: 1600*4C



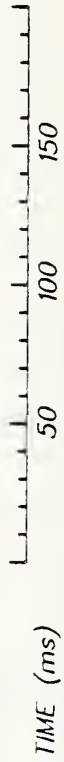
Run ID: 82E062 Disk: 82E062.3 File: 1 Date: APR 1, 1985 Sheet: 4

Filter: 1600*4C

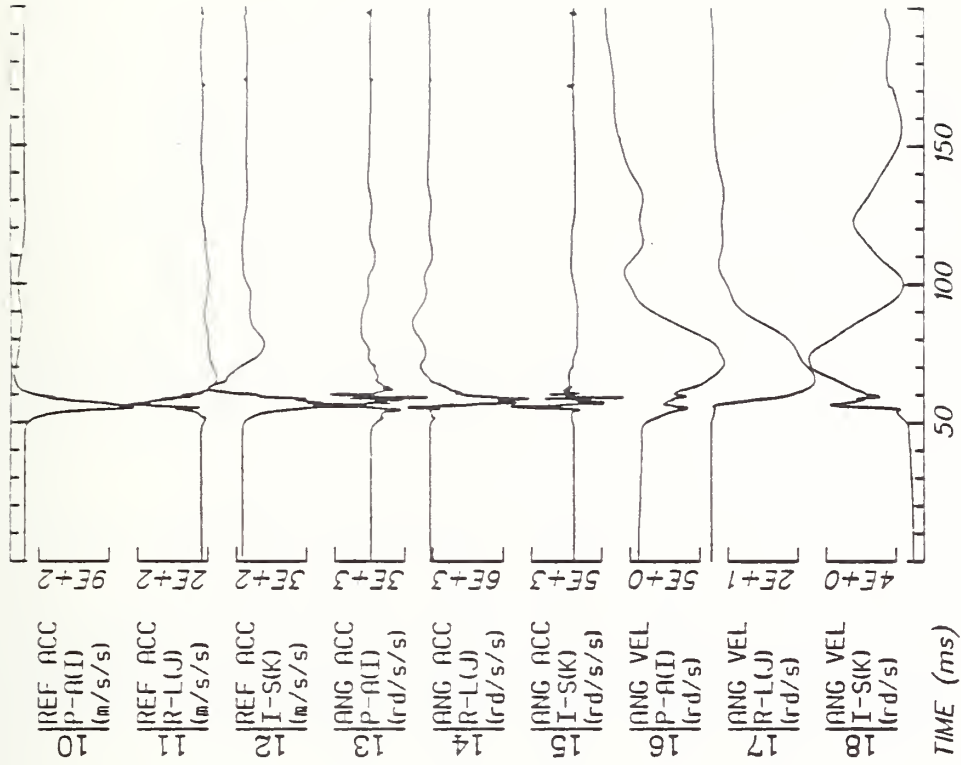
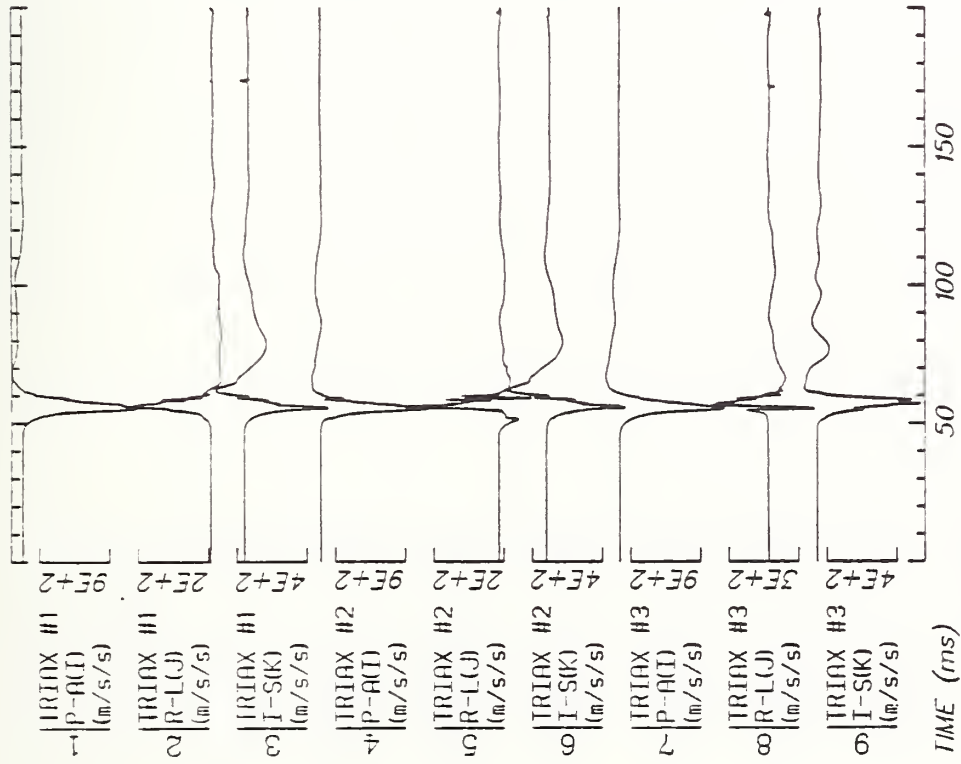


Run ID: 82E062 Disk: 82E062.3 File: 1 Date: APR 1, 1985 Sheet: 5

Filter: 1600*4C



Run ID: 82E062
 Filter: 1600*4C
 Disk: 82E062.3
 File: 1
 Date: APR 1, 1985
 Sheet: 6

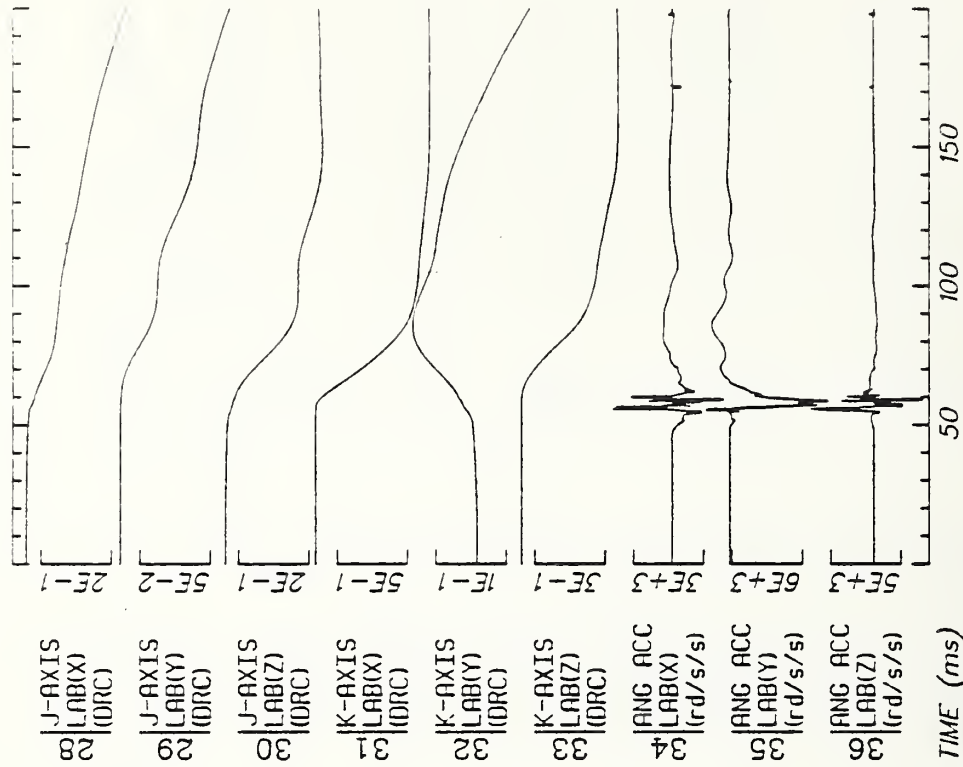
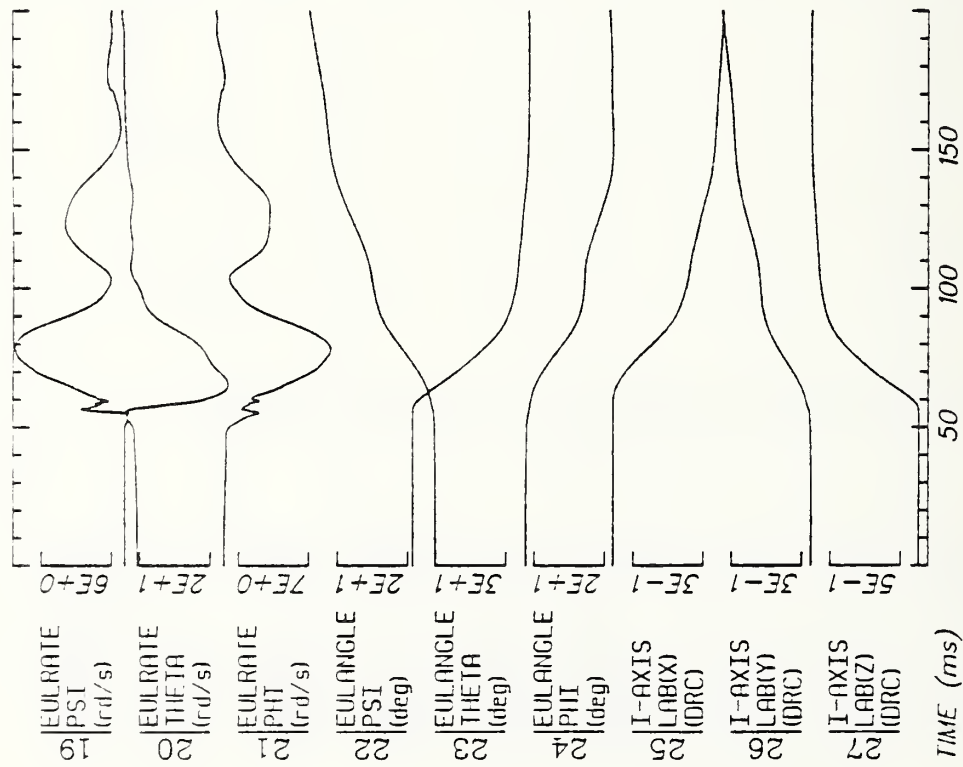


Run ID: 83E081

Disk: 83E081.3 File: 1

Date: APR 1, 1985 Sheet: 1

Filter: 1600*4C

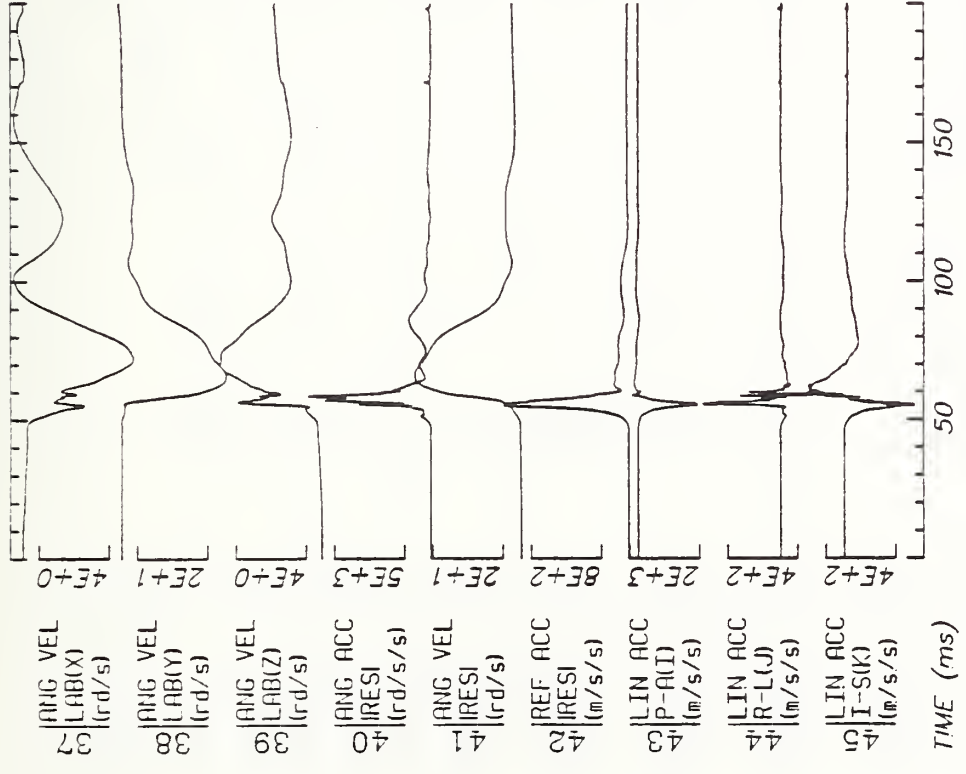
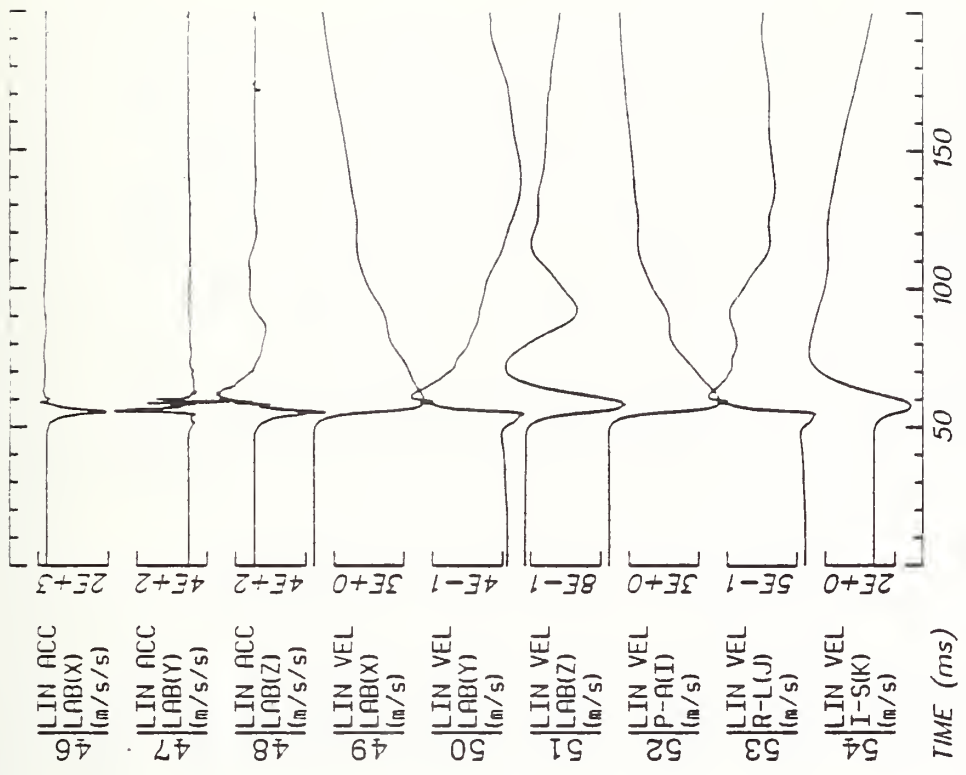


Run ID: 83E081

Disk: 83E081.3 File: 1

Date: APR 1, 1985 Sheet: 2

Filter: 1600*4C



Run ID: 83E081

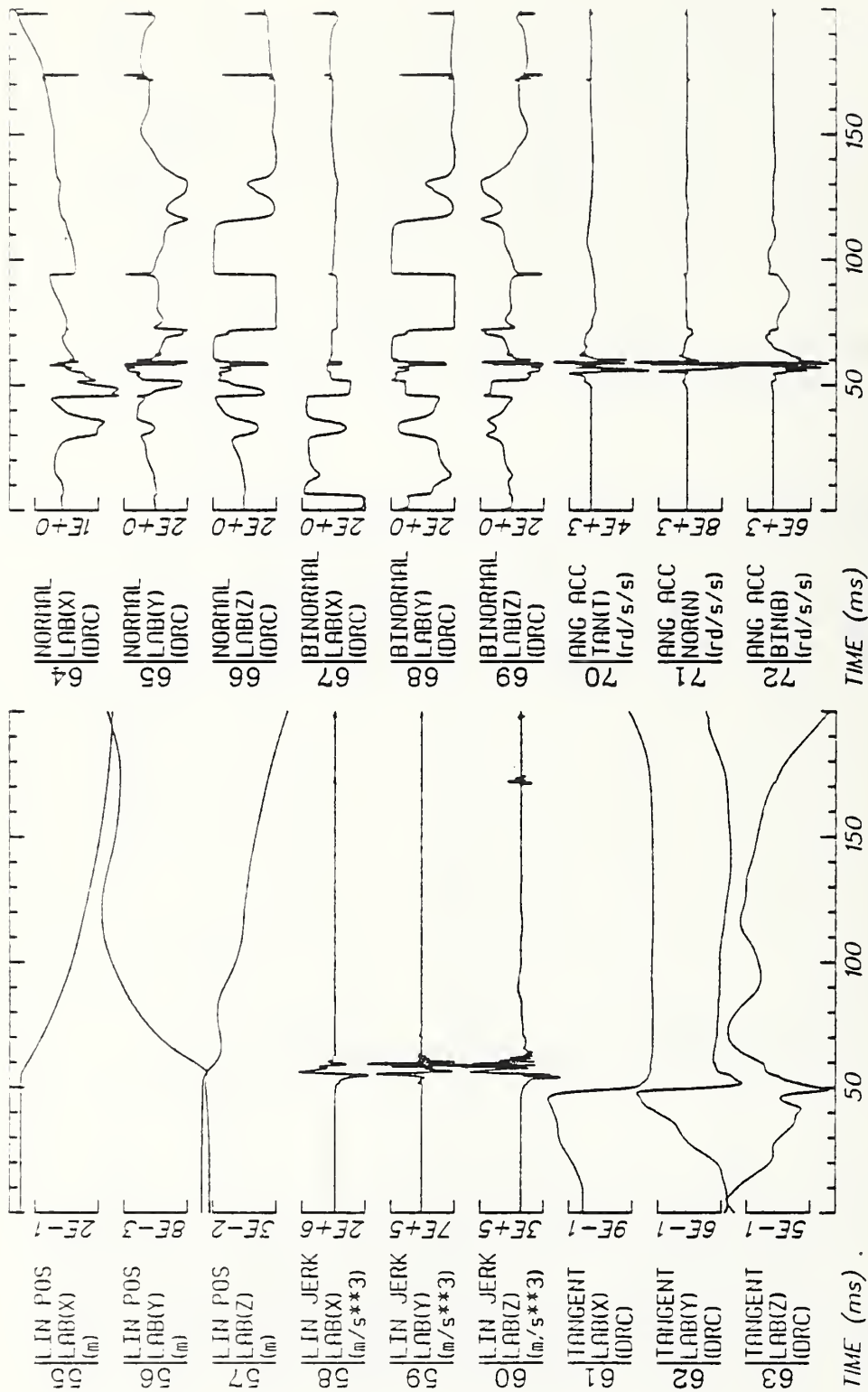
Disk: 83E081.3

File: 1

Date: APR 1, 1985

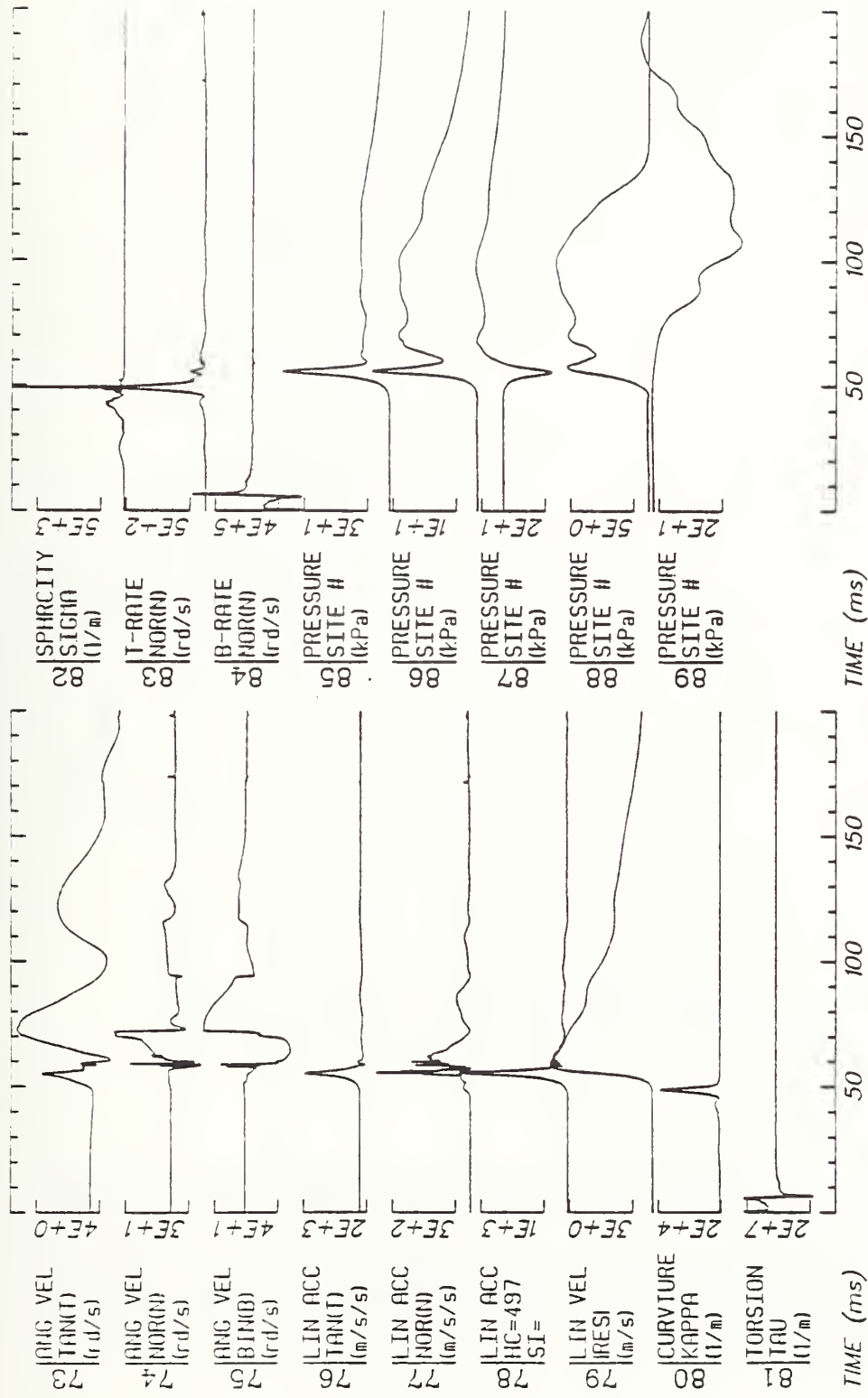
Sheet: 3

Filter: 1600*4C



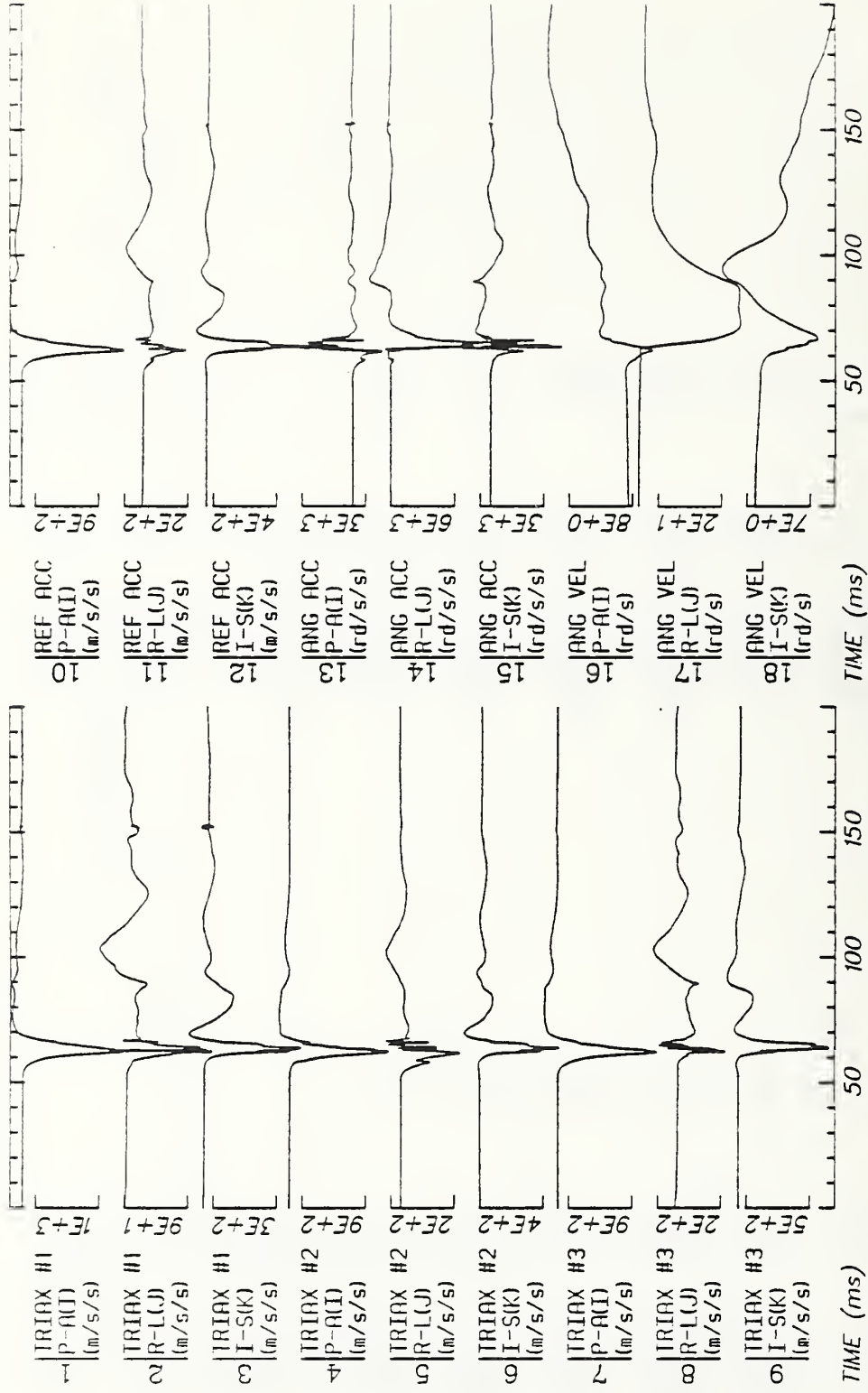
Run ID: 83E081 Disk: 83E081.3 File: 1 Date: APR 1, 1985 Sheet: 4

Filter: 1600*4C



Run ID: 83E081 Disk: 83E081.3 File: 1 Date: APR 1, 1985 Sheet: 5

Filter: 1600*4C

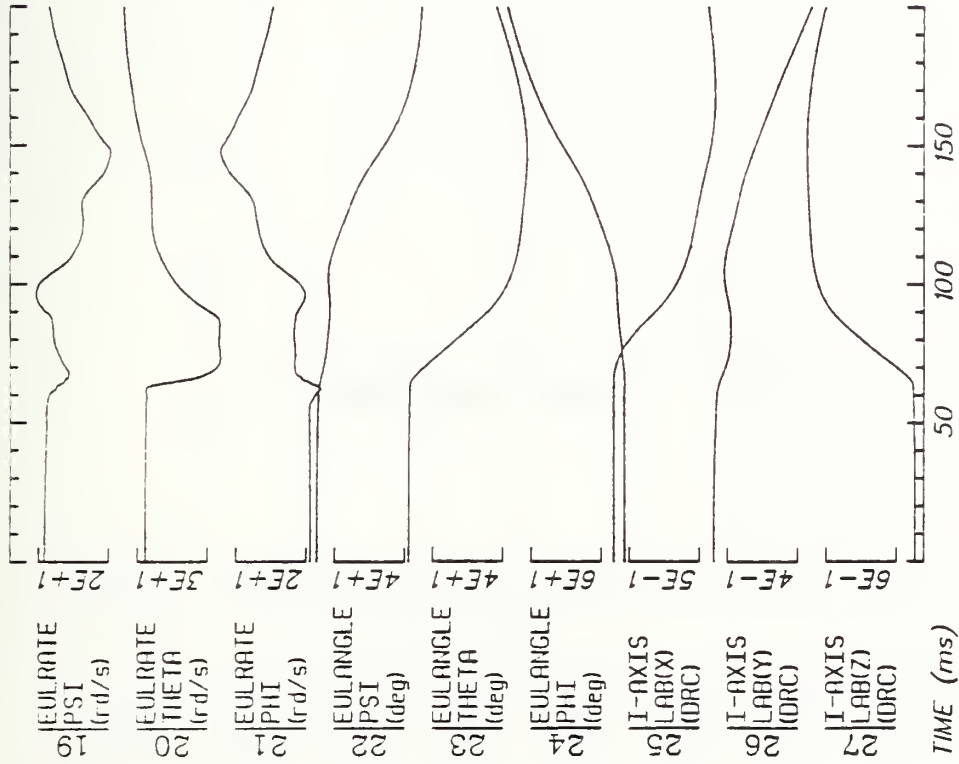
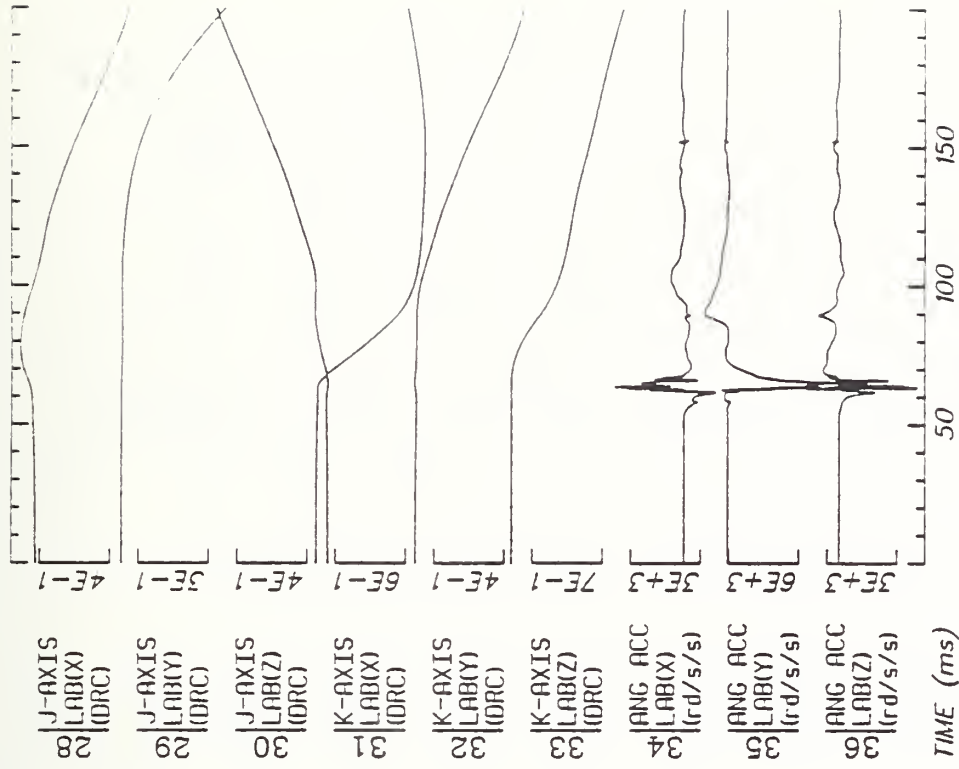


Run ID: 83E082

Disk: 83E082.3 File: 1

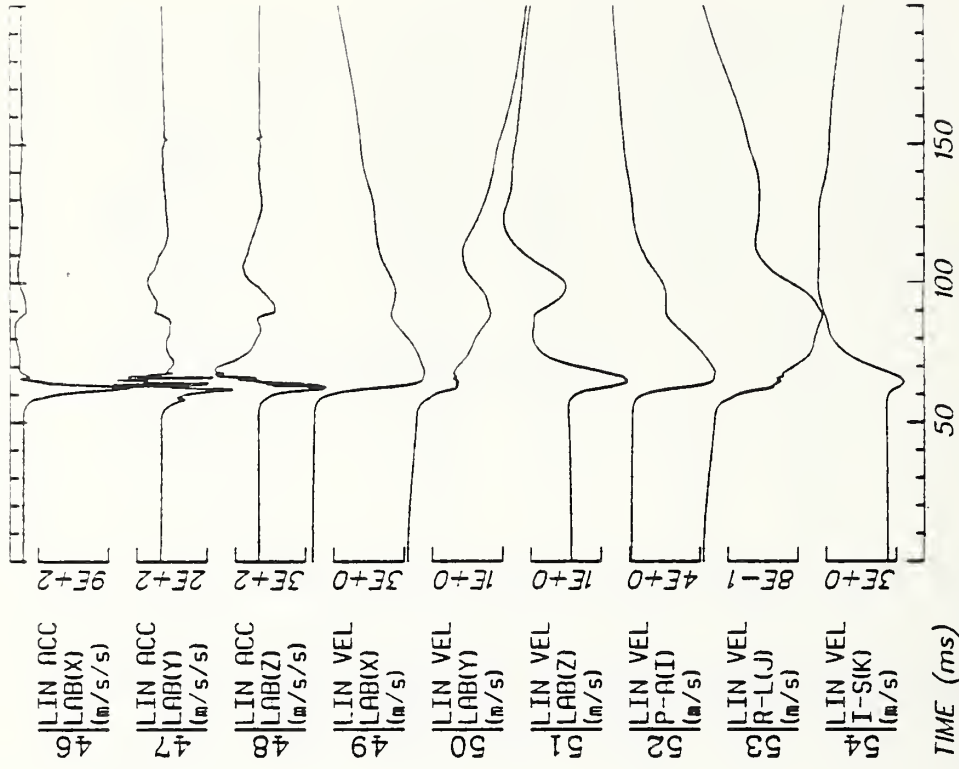
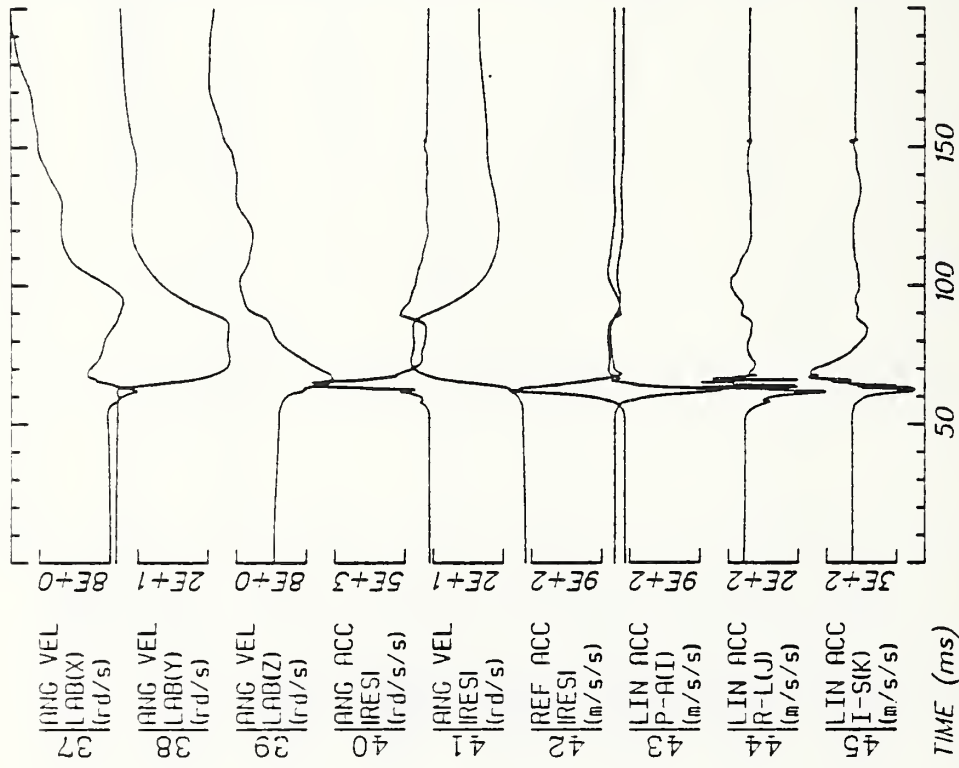
Date: APR 1, 1985 Sheet: 1

Filter: 1600*4C



Run ID: 83E082 Disk: 83E082.3 File: 1 Date: APR 1, 1985 Sheet: 2

Filter: 1600*4C

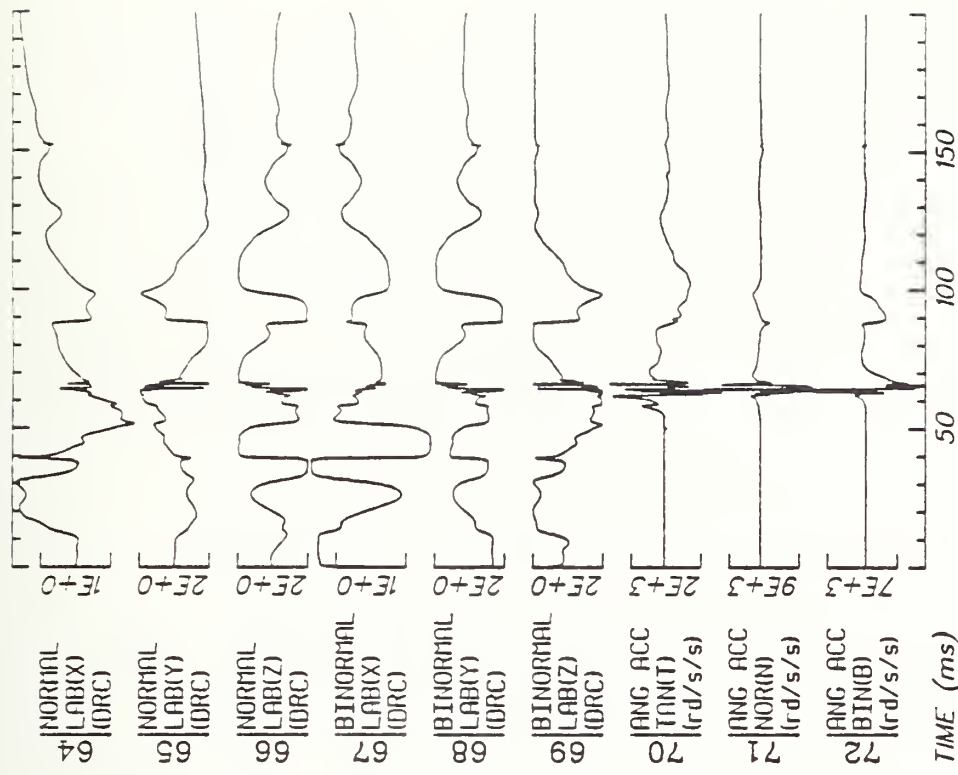
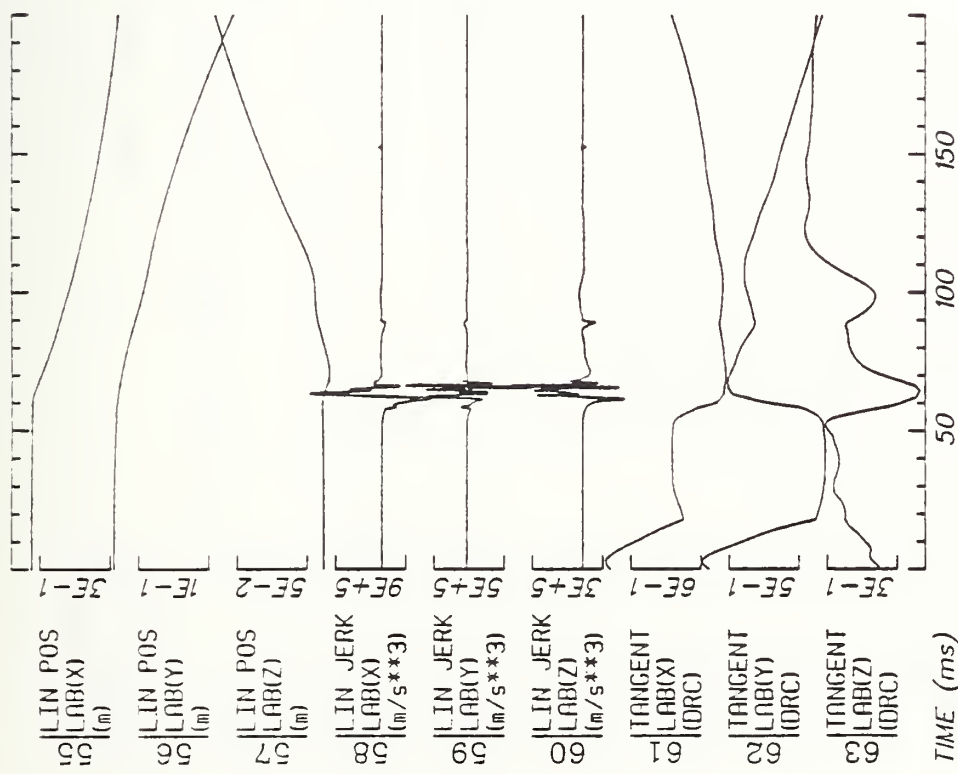


Run ID: 83E082

Disk: 83E082.3 File: 1

Date: APR 1, 1985 Sheet: 3

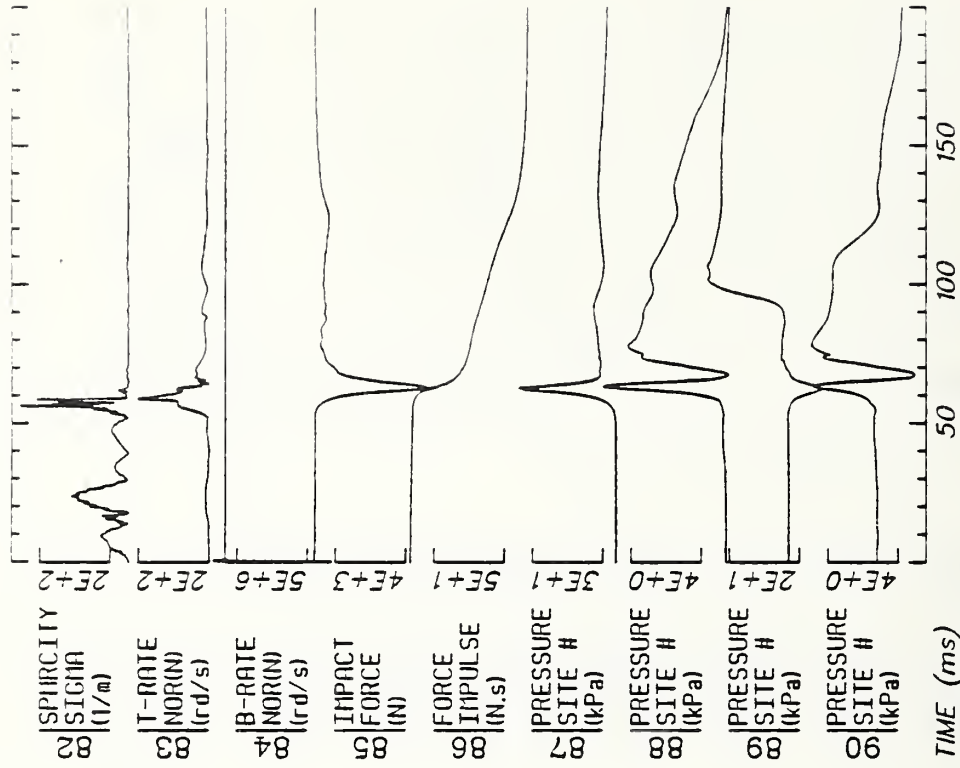
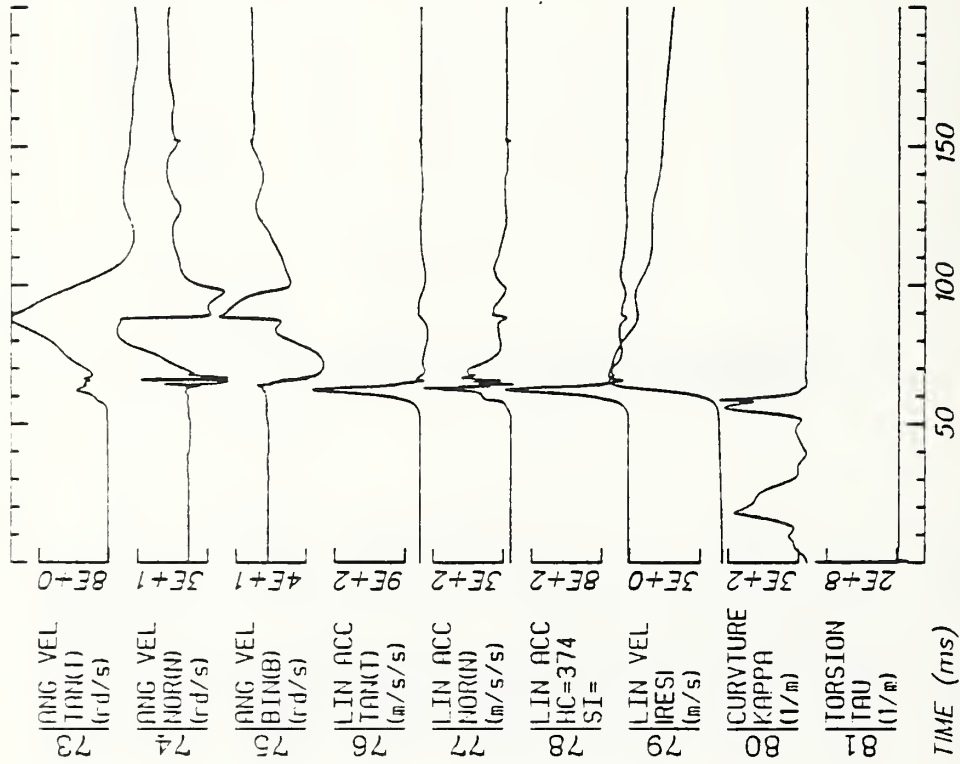
Filter: 1600*4C



Run ID: 83E082
 Filter: 1600*4C

Disk: 83E082.3 File: 1

Date: APR 1, 1985 Sheet: 4

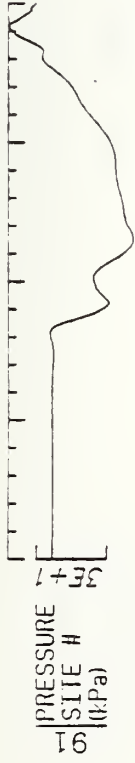


Run ID: 83E082

Disk: 83E082.3 File: 1

Date: APR 1, 1985 Sheet: 5

Filter: 1600*4C



Run ID: 83E082

Disk: 83E082.3

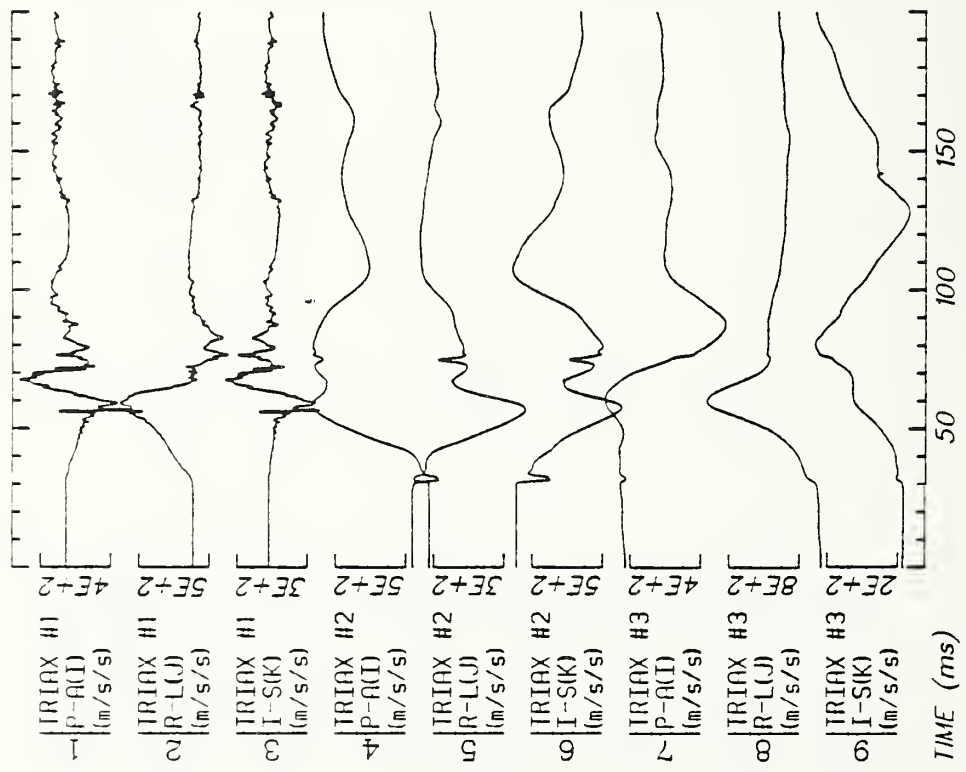
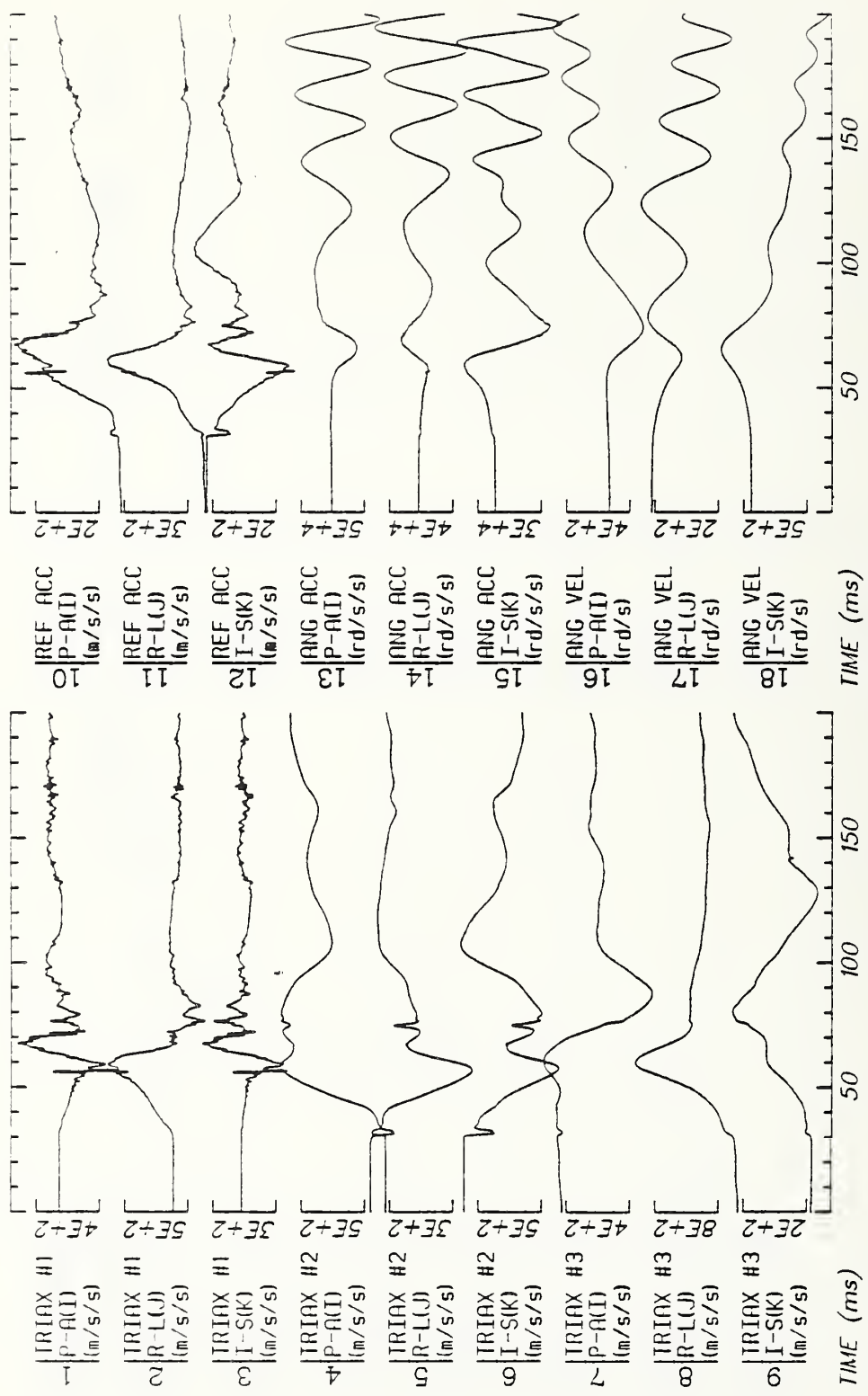
File: 1

Date: APR 1, 1985

Sheet: 6

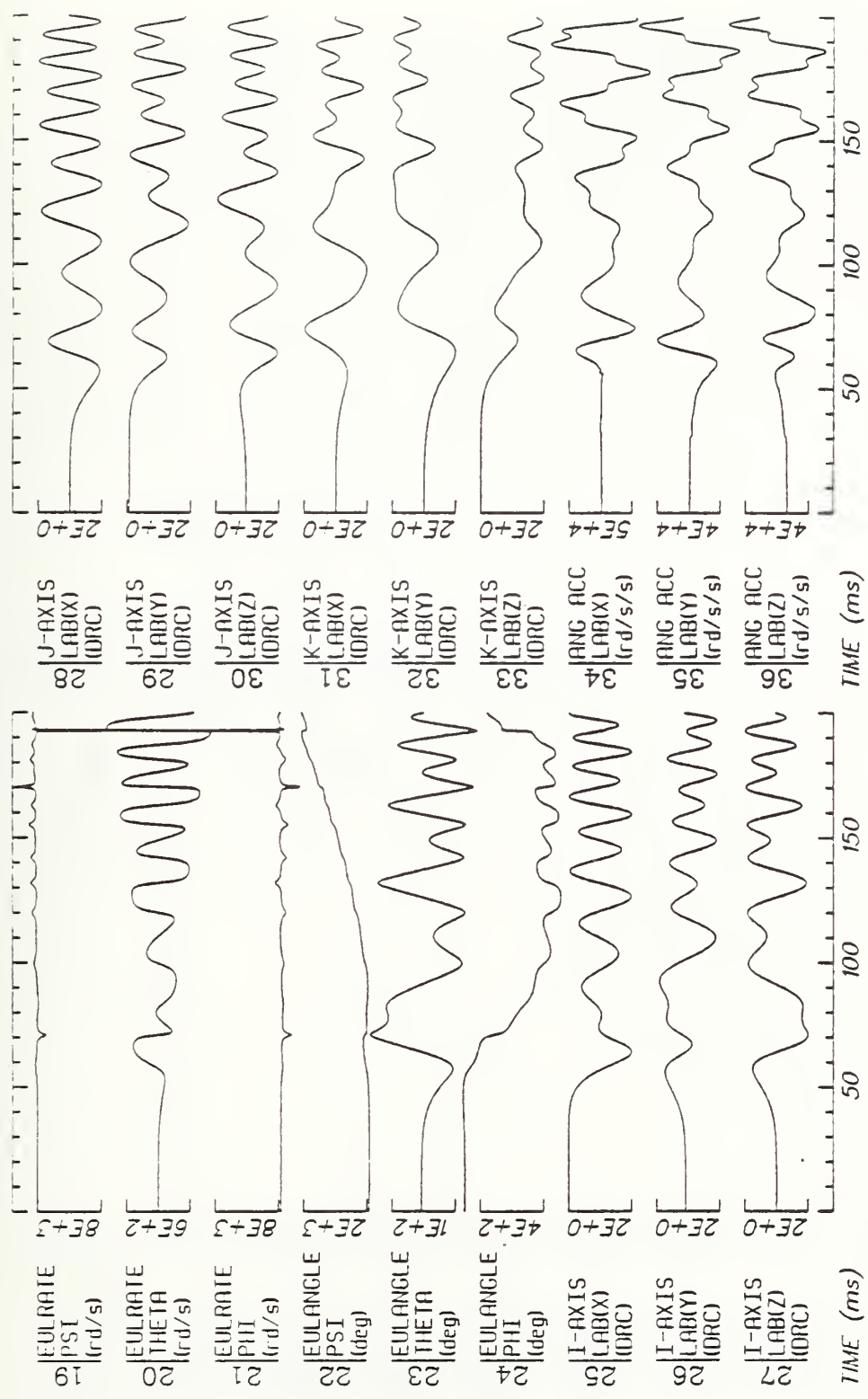
Filter: 1600*4C

C81



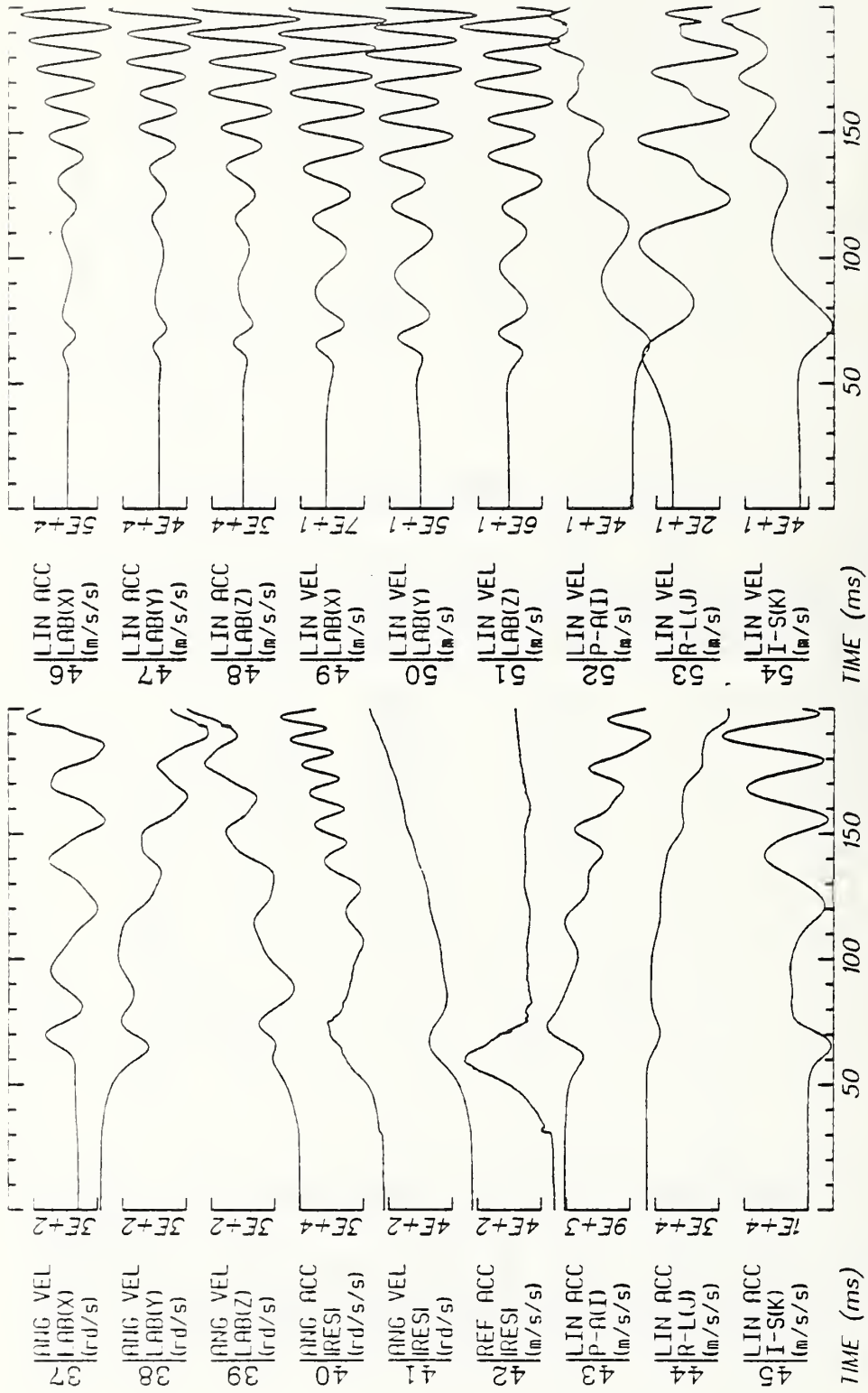
Run ID: 83E102 Disk: -HEAD File: 1 Date: MAR 12, 1985 Sheet: 1

Filter: 1600*4C



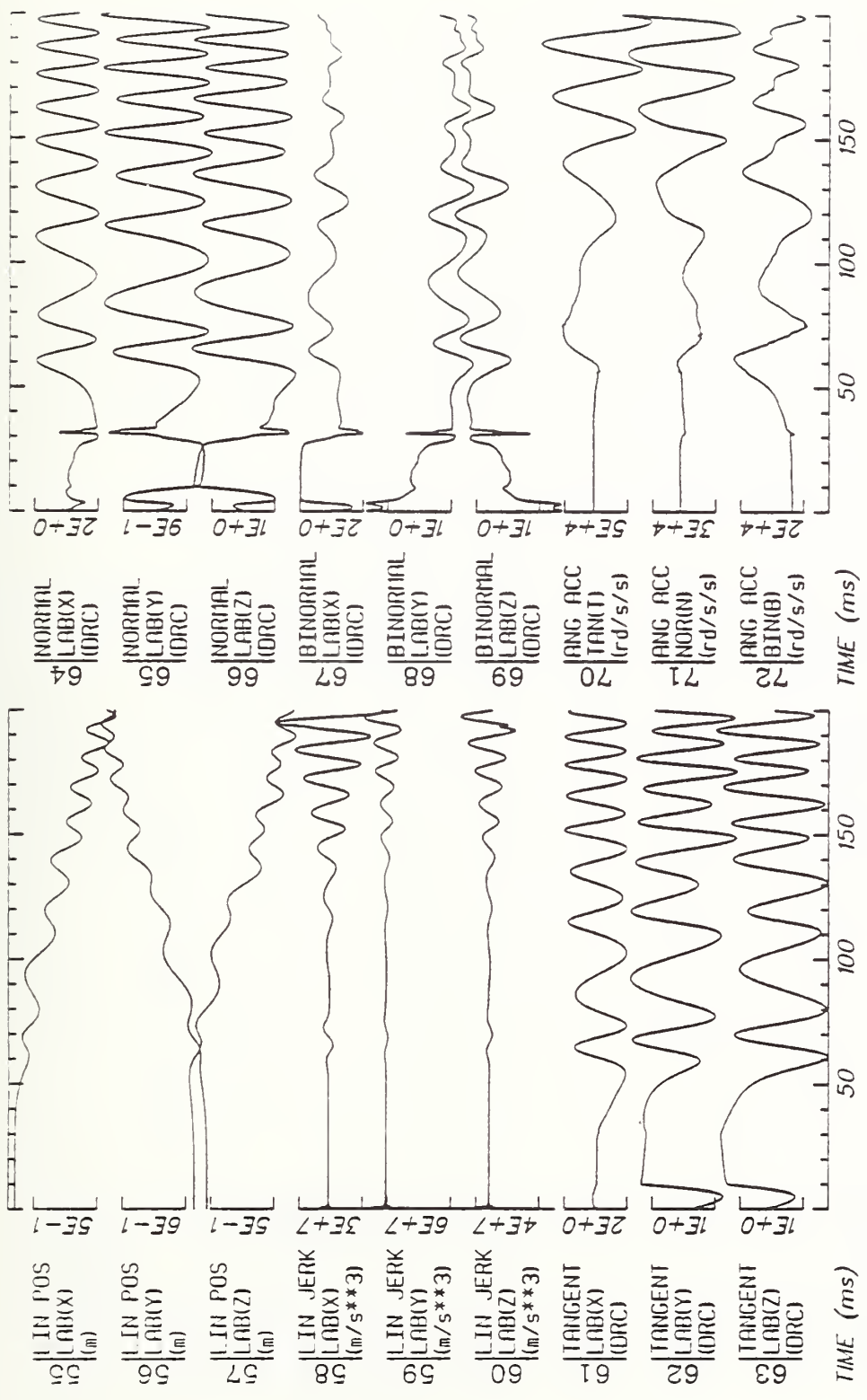
Run ID: 83E102 Disk: -HEAD File: 1 Date: MAR 12, 1985 Sheet: 2

Filter: 1600*4C



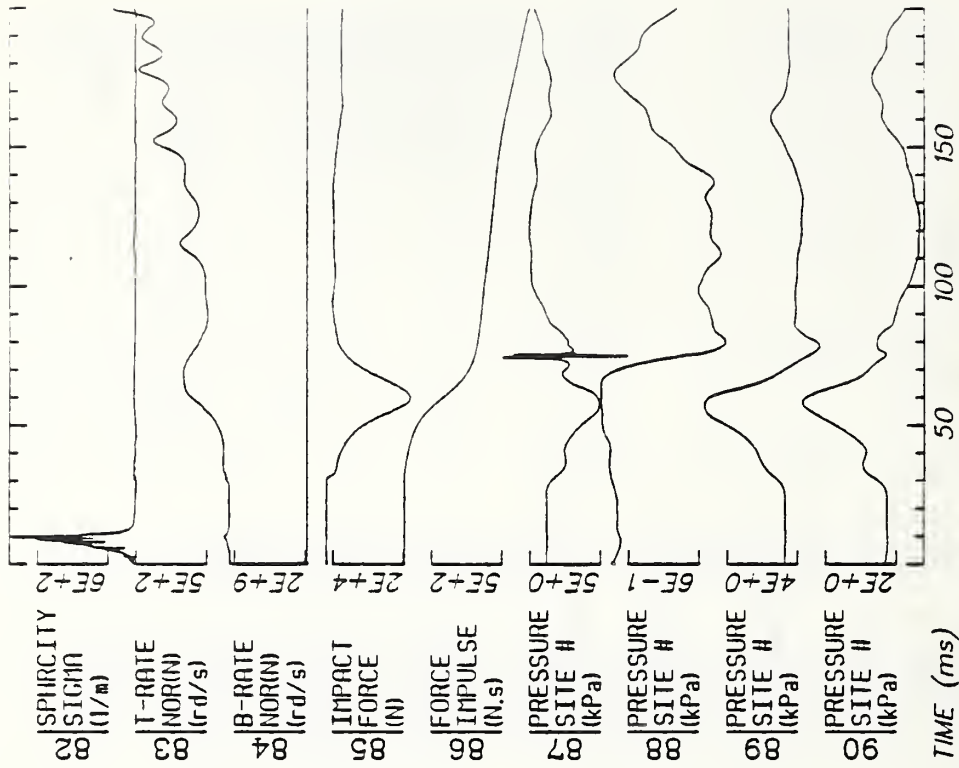
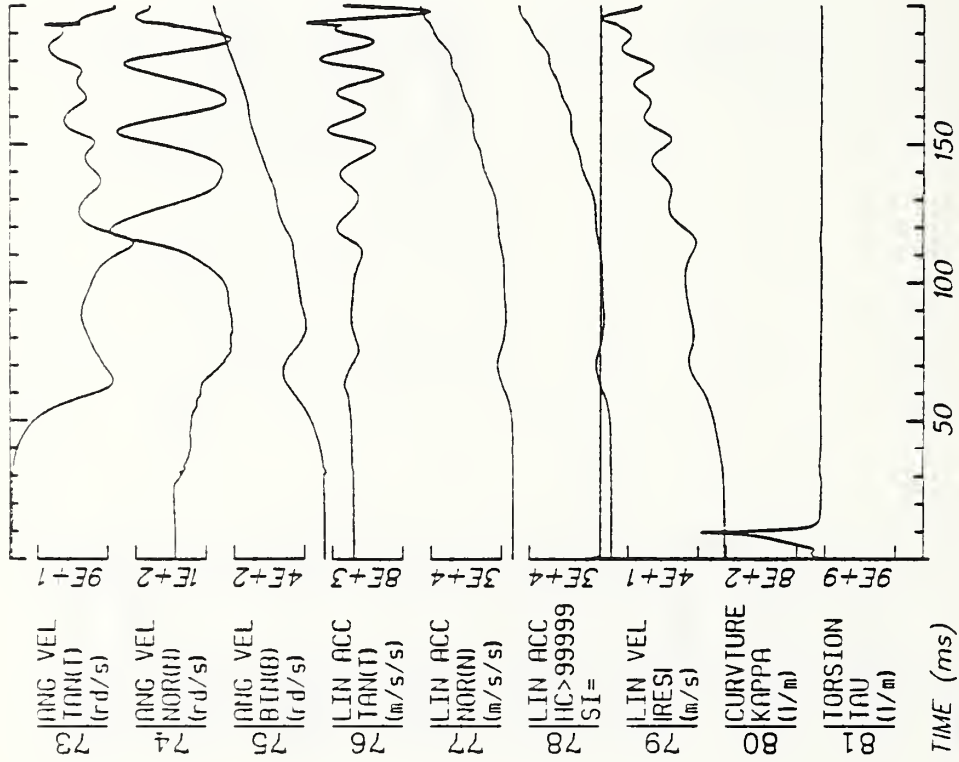
Run ID: 83E102 Disk: -HEAD File: 1 Date: MAR 12, 1985 Sheet: 3

Filter: 1600*4C



Run ID: 83E102 Disk: -HEAD File: 1 Date: MAR 12, 1985 Sheet: 4

Filter: 1600*4C



Run ID: 83E102

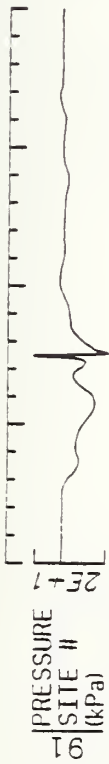
Disk: -HEAD

File: 1

Date: MAR 12, 1985

Sheet: 5

Filter: 1600*4C



Run ID: 83E102

Disk: -HEAD

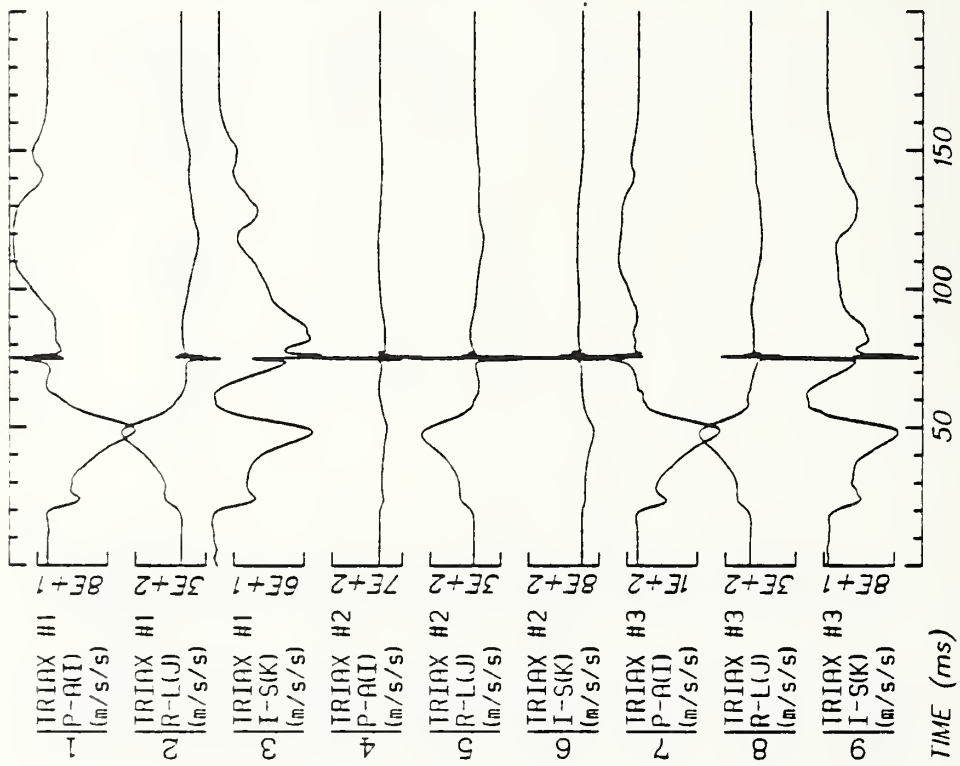
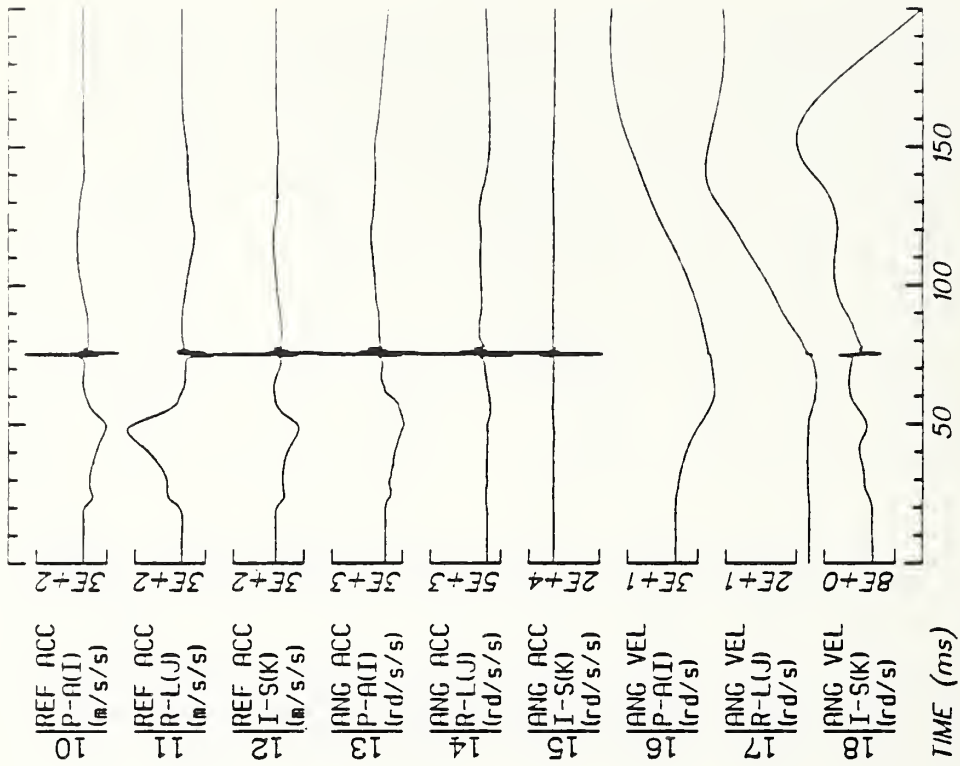
File: 1

Date: MAR 12, 1985

Sheet: 6

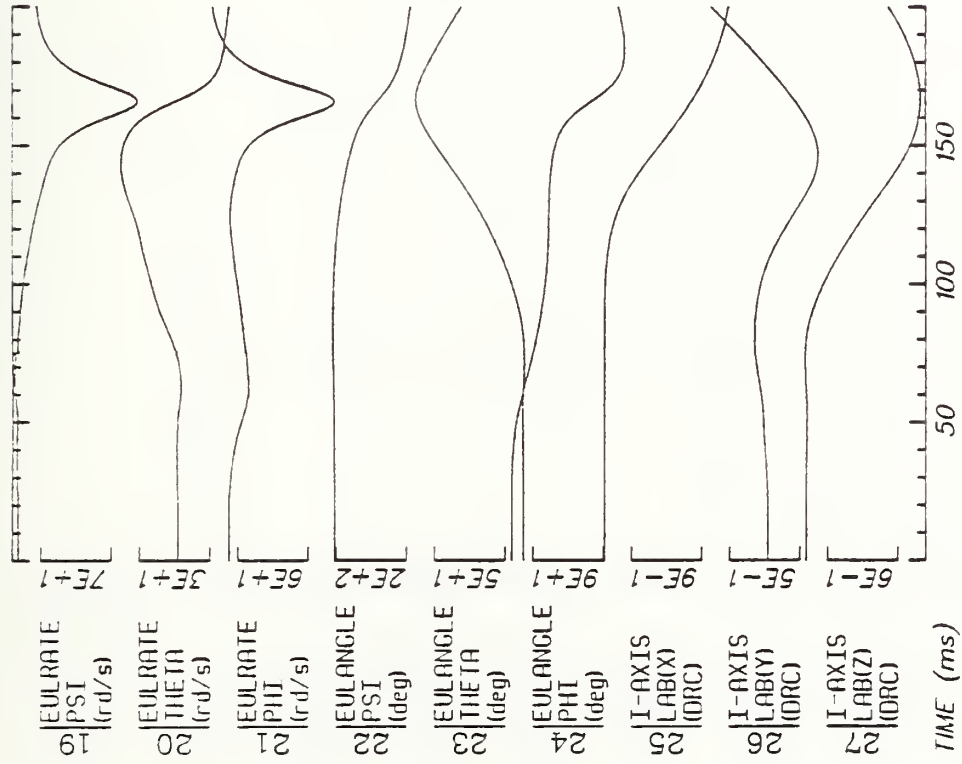
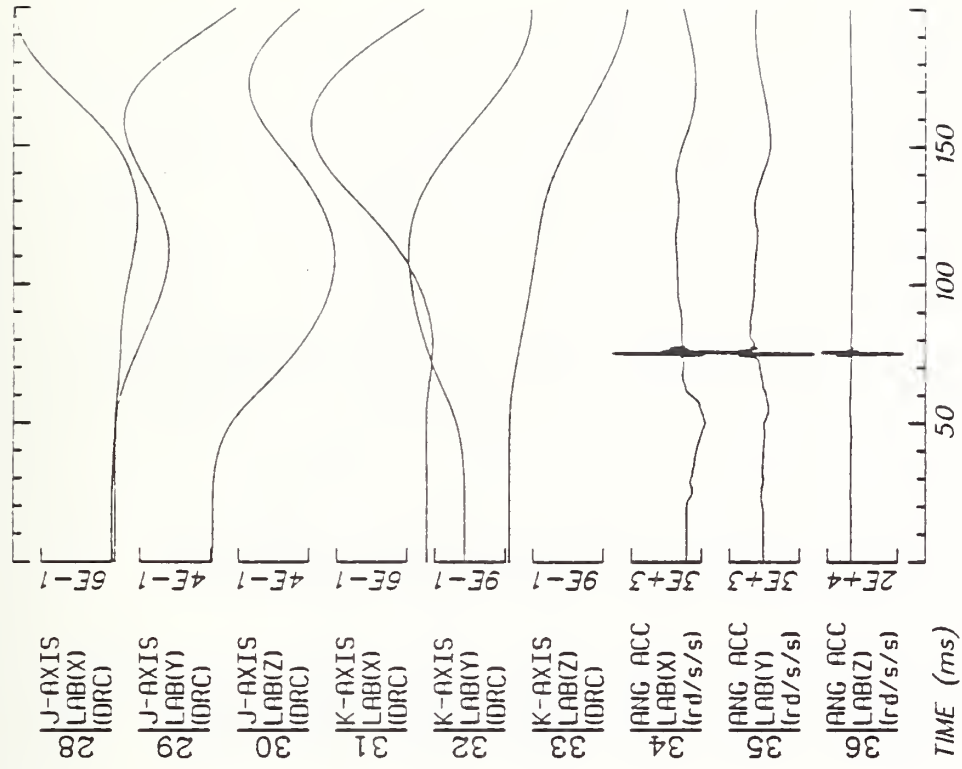
Filter: 1600*4C

C87



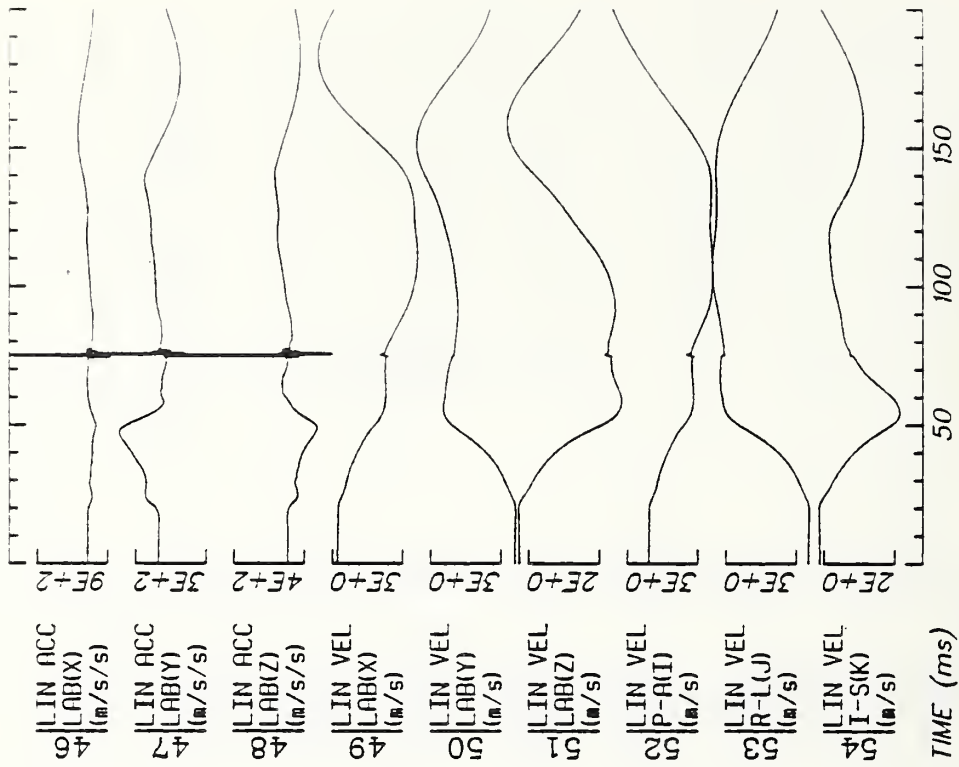
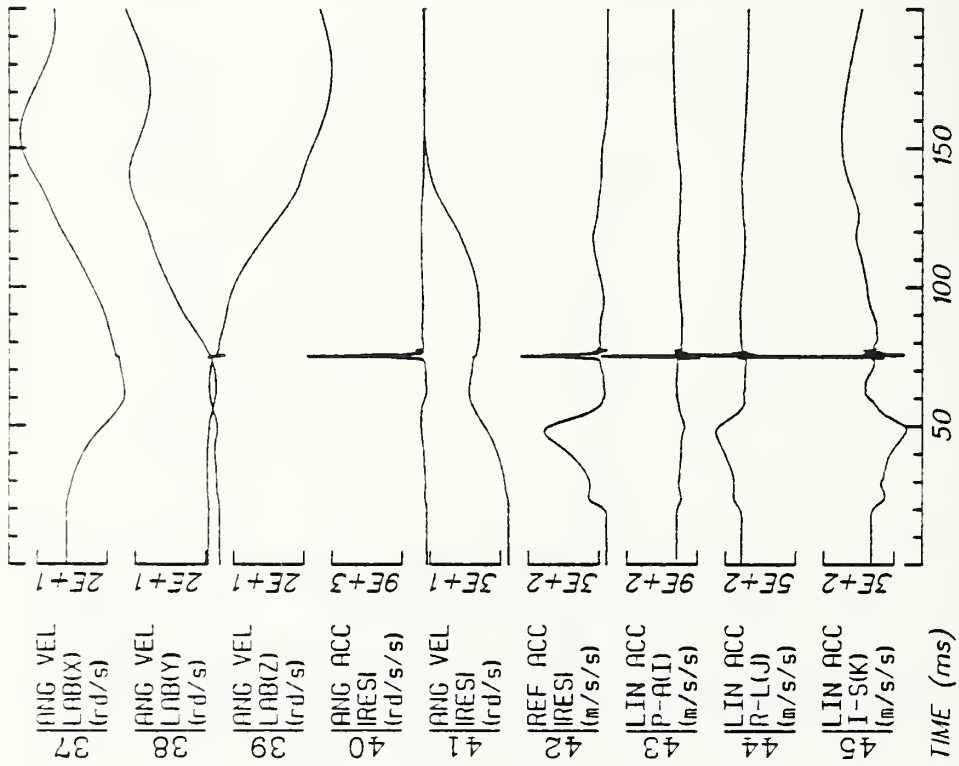
Run ID: 83E103 Disk: -HEAD File: 2 Date: MAR 12, 1985 Sheet: 1

Filter: 1600*4C



Run ID: 83E103 Disk: -HEAD File: 2 Date: MAR 12, 1985 Sheet: 2

Filter: 1600*4C



Run ID: 83E103

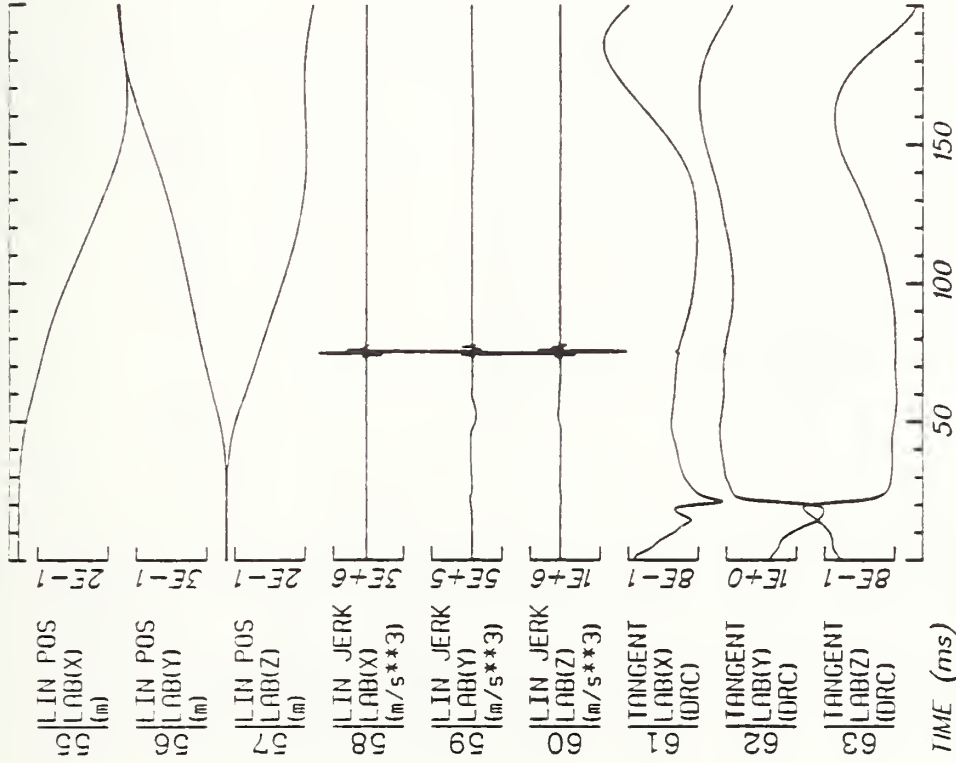
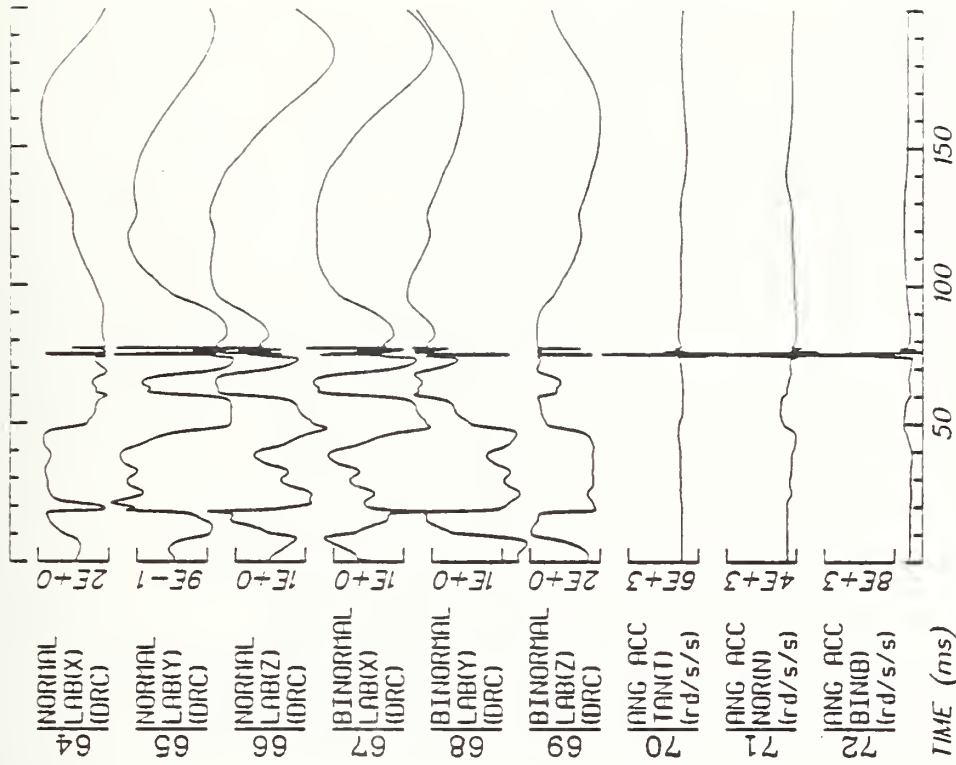
Disk: -HEAD

File: 2

Date: MAR 12, 1985

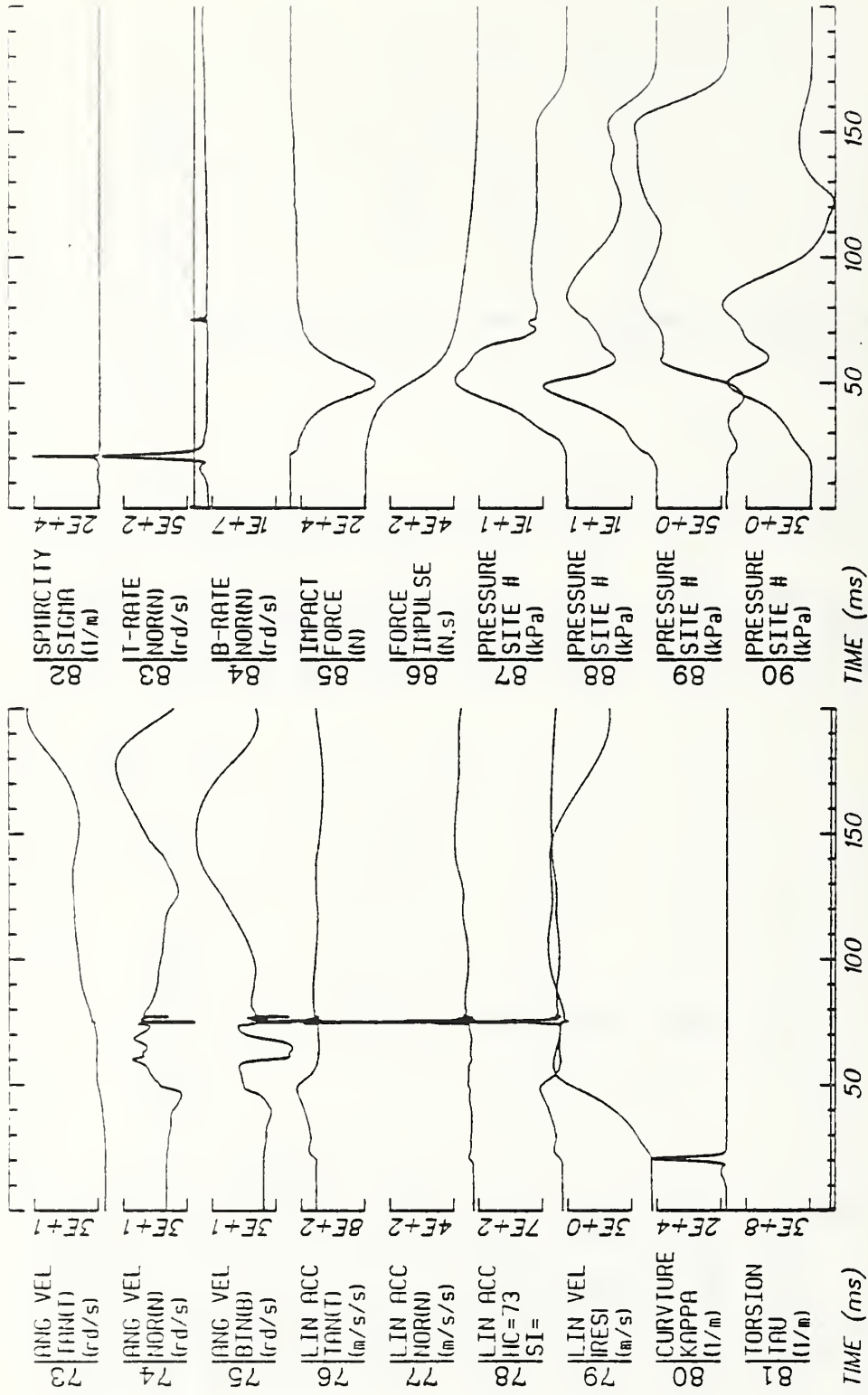
Sheet: 3

Filter: 1600*4C



Run ID: 83E103 Disk: -HEAD File: 2 Date: MAR 12, 1985 Sheet: 4

Filter: 1600*4C



Run ID: 83E103

Disk: -HEAD

File: 2

Date: MAR 12, 1985

Sheet: 5

Filter: 1600*4C



Run ID: 83E103

Disk: -HEAD

File: 2

Date: MAR 12, 1985

Sheet: 6

Filter: 1600*4C



12.0 APPENDIX D: ANTHROPOMETRY

HUMAN SUBJECT INFORMATION

CADAVER NO.: 000 DURATION OF BED CONFINEMENT Unknown

AGE: 60 SEX: M CAUSE OF DEATH: Unknown

PHYSICAL APPEARANCE: Caucasian DATE OF DEATH: 3/21/82

ANOMALY: None

ANTHROPOMETRY

0 - Weight*	52 kg	
1 - Stature**	184 cm	
2 - Shoulder (acromial) Height	159.4 cm	62.8 in
3 - Vertex to Symphision Length	91.2 cm	35.9 in
4 - Waist Height	109.8 cm	43.2 in
5 - Shoulder Breadth (Biacromial Breadth)	31.8 cm	12.5 in
6 - Chest Breadth	27.9 cm	11 in
7 - Waist Breadth	29.2 cm	11.5 in
8 - Hip Breadth	25 cm	9.8 in
9 - Shoulder to Elbow Length (Acromion-radiale .. Length)	999	999
10 - Forearm-hand Length (elbow-middle finger)....	999	999
11 - Tibiale Height	999	999
12 - Ankle Height (outside) (lateral malleous)....	999	999
13 - Foot Breadth	999	999
14 - Foot Length	999	999

Note: * weight in kilograms

** lengths in centimeters

*** measures 16 and 17 must be made in case where the subject will be used in the seated position during the tests. In all other cases enter 9999 when under these measures.

LABORATORY UMTRI

82E001-3
TEST NO. 82E004-7 82E008

15 - Top of Head to Trochanterion Length.....	88.5 cm	34.8 in
16 - Seated Height***.....	999	999
17 - Knee Height (seated)***.....	999	999
18 - Head Length.....	19.7 cm	7.8 in
19 - Head Breadth.....	15.7 cm	6.2 in
20 - Head to Chin Height (Vertex to Mentum).....	22.8 cm	9 in
21 - Biceps Circumference.....	999	999
22 - Elbow Circumference.....	999	999
23 - Forearm Circumference.....	999	999
24 - Wrist Circumference.....	999	999
25 - Thigh Circumference.....	999	999
26 - Lower Thigh Circumference.....	999	999
27 - Knee Circumference.....	999	999
28 - Calf Circumference.....	999	999
29 - Ankle Circumference.....	999	999
30 - Neck Circumference.....	32.3 cm	12.7 in
31 - Scye (armpit-shoulder) Circumference.....	999	999
32 - Chest Circumference.....	79.3 cm	31.2 in
33 - Waist Circumference.....	999	999
34 - Buttock Circumference.....	999	999
35 - Chest Depth.....	15.8 cm	6.2 in
36 - Waist Depth.....	999	999
37 - Buttock Depth.....	999	999
38 - Interscye.....	999	999

LABORATORY UMTRI TEST NO. 82E001-3
82E004-7 82E008

HUMAN SUBJECT INFORMATION

CADAVER NO.: 020 DURATION OF BED CONFINEMENT Unknown
 AGE: 67 SEX: M CAUSE OF DEATH: Unknown
 PHYSICAL APPEARANCE: Caucasian DATE OF DEATH: 3/23/82

ANOMALY: Excessive fat increased time required for spinal mounts

ANTHROPOMETRY

0 - Weight*	77 kg	
1 - Stature**	179.8 cm	
2 - Shoulder (acromial) Height	156 cm	61.4 in
3 - Vertex to Symphysis Length	88.5 cm	34.8 in
4 - Waist Height	107.3 cm	42.2 in
5 - Shoulder Breadth (Biacromial Breadth)	33.2 cm	13.1 in
6 - Chest Breadth	32.7 cm	12.9 in
7 - Waist Breadth	24 cm	9.4 in
8 - Hip Breadth	36 cm	14.2 in
9 - Shoulder to Elbow Length (Acromion-radiale .. Length)	999	999
10 - Forearm-hand Length (elbow-middle finger)....	999	999
11 - Tibiale Height	999	999
12 - Ankle Height (outside) (lateral malleous)....	999	999
13 - Foot Breadth	999	999
14 - Foot Length	999	999

Note: * weight in kilograms

** lengths in centimeters

*** measures 16 and 17 must be made in case where the subject will be used in the seated position during the tests. In all other cases enter 9999 when under these measures.

15 - Top of Head to Trochanterion Length.....	999	999
16 - Seated Height***.....	999	999
17 - Knee Height (seated)***.....	999	999
18 - Head Length.....	21 cm	8.2 in
19 - Head Breadth.....	15.8 cm	6.2 in
20 - Head to Chin Height (Vertex to Mentum).....	24.9 cm	9.8 in
21 - Biceps Circumference.....	999	999
22 - Elbow Circumference.....	999	999
23 - Forearm Circumference.....	999	999
24 - Wrist Circumference.....	999	999
25 - Thigh Circumference.....	999	999
26 - Lower Thigh Circumference.....	999	999
27 - Knee Circumference.....	999	999
28 - Calf Circumference.....	999	999
29 - Ankle Circumference.....	999	999
30 - Neck Circumference.....	42 cm	16.5 in
31 - Scye (armpit-shoulder) Circumference.....	999	999
32 - Chest Circumference.....	99 cm	39 in
33 - Waist Circumference.....	999	999
34 - Buttock Circumference.....	999	999
35 - Chest Depth.....	22.2 cm	8.7 in
36 - Waist Depth.....	999	999
37 - Buttock Depth.....	999	999
38 - Interscye.....	999	999

LABORATORY UMTRI TEST NO. 82E021-22 82E023-27 82E028

HUMAN SUBJECT INFORMATION

CADAVER NO.: 040 DURATION OF BED CONFINEMENT Unknown
 AGE: 65 SEX: M CAUSE OF DEATH: Myocardial infarction
 PHYSICAL APPEARANCE: Caucasian DATE OF DEATH: 3/27/82

ANOMALY: Upper ribs very close together and embedded in deep fat.

ANTHROPOMETRY

0 - Weight*	87 kg	
1 - Stature**	169.2 cm	
2 - Shoulder (acromial) Height	146.7 cm	57.8 in
3 - Vertex to Symphysis Length	81.8 cm	32.2 in
4 - Waist Height	102 cm	40.2 in
5 - Shoulder Breadth (Biacromial Breadth)	35.4 cm	13.9 in
6 - Chest Breadth	32.7 cm	12.9 in
7 - Waist Breadth	32 cm	12.6 in
8 - Hip Breadth	33.5 cm	13.2 in
9 - Shoulder to Elbow Length (Acromion-radiale .. Length)	999	999
10 - Forearm-hand Length (elbow-middle finger)...	999	999
11 - Tibiale Height	999	999
12 - Ankle Height (outside) (lateral malleous)...	999	999
13 - Foot Breadth	999	999
14 - Foot Length	999	999

Note: * weight in kilograms

** lengths in centimeters

*** measures 16 and 17 must be made in case where the subject will be used in the seated position during the tests. In all other cases enter 9999 when under these measures.

15 - Top of Head to Trochanterion Length.....	999	999
16 - Seated Height***.....	999	999
17 - Knee Height (seated)***.....	999	999
18 - Head Length.....	20 cm	7.9 in
19 - Head Breadth.....	16.5 cm	6.5 in
20 - Head to Chin Height (Vertex to Mentum).....	21.4 cm	8.4 in
21 - Biceps Circumference.....	999	999
22 - Elbow Circumference.....	999	999
23 - Forearm Circumference.....	999	999
24 - Wrist Circumference.....	999	999
25 - Thigh Circumference.....	999	999
26 - Lower Thigh Circumference.....	999	999
27 - Knee Circumference.....	999	999
28 - Calf Circumference.....	999	999
29 - Ankle Circumference.....	999	999
30 - Neck Circumference.....	50.4 cm	19.8 in
31 - Scye (armpit-shoulder) Circumference.....	999	999
32 - Chest Circumference.....	104.5 cm	41.1 in
33 - Waist Circumference.....	999	999
34 - Buttock Circumference.....	999	999
35 - Chest Depth.....	23.8 cm	9.4 in
36 - Waist Depth.....	999	999
37 - Buttock Depth.....	999	999
38 - Interscye.....	999	999

LABORATORY UMTRI TEST NO. 82E041-42 82E043-48 82E049

HUMAN SUBJECT INFORMATION

CADAVER NO.: 050 DURATION OF BED CONFINEMENT Unknown

AGE: 60 SEX: M CAUSE OF DEATH: Coronary thrombosis

PHYSICAL APPEARANCE: Caucasian DATE OF DEATH: 6/7/82

ANOMALY: Right and left ribs R4-R5 broken, probably from CPR.

ANTHROPOMETRY

0 - Weight*	67 kg	
1 - Stature**	180.2 cm	
2 - Shoulder (acromial) Height	155.7 cm	61.8 in
3 - Vertex to Symphision Length	999	999
4 - Waist Height	999	999
5 - Shoulder Breadth (Biacromial Breadth)	37.5 cm	14.8 in
6 - Chest Breadth	999	999
7 - Waist Breadth	999	999
8 - Hip Breadth	999	999
9 - Shoulder to Elbow Length (Acromion-radiale .. Length)	999	999
10 - Forearm-hand Length (elbow-middle finger)...	999	999
11 - Tibiale Height	999	999
12 - Ankle Height (outside) (lateral malleous)....	999	999
13 - Foot Breadth	999	999
14 - Foot Length	999	999

Note: * weight in kilograms

** lengths in centimeters

*** measures 16 and 17 must be made in case where the subject will be used in the seated position during the tests. In all other cases enter 9999 when under these measures.

15 - Top of Head to Trochanterion Length.....	999	999
16 - Seated Height***.....	999	999
17 - Knee Height (seated)***.....	999	999
18 - Head Length.....	20 cm	7.9 in
19 - Head Breadth.....	16.2 cm	6.4 in
20 - Head to Chin Height (Vertex to Mentum).....	999	999
21 - Biceps Circumference.....	999	999
22 - Elbow Circumference.....	999	999
23 - Forearm Circumference.....	999	999
24 - Wrist Circumference.....	999	999
25 - Thigh Circumference.....	999	999
26 - Lower Thigh Circumference.....	999	999
27 - Knee Circumference.....	999	999
28 - Calf Circumference.....	999	999
29 - Ankle Circumference.....	999	999
30 - Neck Circumference.....	40.5 cm	15.9 in
31 - Scye (armpit-shoulder) Circumference.....	999	999
32 - Chest Circumference.....	999	999
33 - Waist Circumference.....	999	999
34 - Buttock Circumference.....	999	999
35 - Chest Depth.....	999	999
36 - Waist Depth.....	999	999
37 - Buttock Depth.....	999	999
38 - Interscye.....	999	999

LABORATORY UMTRI TEST NO. 82E051-53

HUMAN SUBJECT INFORMATION

CADAVER NO.: 060 DURATION OF BED CONFINEMENT Unknown
 AGE: 60 SEX: M CAUSE OF DEATH: Unknown
 PHYSICAL APPEARANCE: Caucasian DATE OF DEATH: 6/1/82

ANOMALY: None

ANTHROPOMETRY

0 - Weight*	67 kg	
1 - Stature**	169.8 cm	
2 - Shoulder (acromial) Height	148.4 cm	58.4 in
3 - Vertex to Symphysis Length	86.1 cm	33.9 in
4 - Waist Height	99.8 cm	39.3 in
5 - Shoulder Breadth (Biacromial Breadth)	34.7 cm	13.7 in
6 - Chest Breadth	29.1 cm	11.5 in
7 - Waist Breadth	23 cm	9.1 in
8 - Hip Breadth	28.6 cm	11.3 in
9 - Shoulder to Elbow Length (Acromion-radiale Length)	999	999
10 - Forearm-hand Length (elbow-middle finger)	999	999
11 - Tibiale Height	999	999
12 - Ankle Height (outside) (lateral malleous)	999	999
13 - Foot Breadth	999	999
14 - Foot Length	999	999

Note: * weight in kilograms

** lengths in centimeters

*** measures 16 and 17 must be made in case where the subject will be used in the seated position during the tests. In all other cases enter 9999 when under these measures.

15 - Top of Head to Trochanterion Length.....	999	999
16 - Seated Height***.....	999	999
17 - Knee Height (seated)***.....	999	999
18 - Head Length.....	19.2 cm	7.6 in
19 - Head Breadth.....	15.5 cm	6.1 in
20 - Head to Chin Height (Vertex to Mentum).....	22.1 cm	8.7 in
21 - Biceps Circumference.....	999	999
22 - Elbow Circumference.....	999	999
23 - Forearm Circumference.....	999	999
24 - Wrist Circumference.....	999	999
25 - Thigh Circumference.....	999	999
26 - Lower Thigh Circumference.....	999	999
27 - Knee Circumference.....	999	999
28 - Calf Circumference.....	999	999
29 - Ankle Circumference.....	999	999
30 - Neck Circumference.....	44.6 cm	17.6 in
31 - Scye (armpit-shoulder) Circumference.....	999	999
32 - Chest Circumference.....	90.2 cm	35.5 in
33 - Waist Circumference.....	999	999
34 - Buttock Circumference.....	999	999
35 - Chest Depth.....	21.6 cm	8.5 in
36 - Waist Depth.....	999	999
37 - Buttock Depth.....	999	999
38 - Interscye.....	999	999

LABORATORY	UMTRI	TEST NO.	82E061-62 82E063-66	82E067
------------	-------	----------	------------------------	--------

HUMAN SUBJECT INFORMATION

CADAVER NO.: 070 DURATION OF BED CONFINEMENT unknown
 AGE: 61 SEX: M CAUSE OF DEATH: unknown
 PHYSICAL APPEARANCE: Caucasian DATE OF DEATH: 9/9/82

ANOMALY: _____

 _____ Ribs broken during CPR attached

 _____ to sternum with wire.

ANTHROPOMETRY

0 - Weight*		55 kg
1 - Stature**	181 cm	
2 - Shoulder (acromial) Height	156 cm	61.4 in
3 - Vertex to Symphysis Length	999	999
4 - Waist Height	999	999
5 - Shoulder Breadth (Biacromial Breadth)	36.2 cm	14.3 in
6 - Chest Breadth	999	999
7 - Waist Breadth	999	999
8 - Hip Breadth	999	999
9 - Shoulder to Elbow Length (Acromion-radiale Length)	999	999
10 - Forearm-hand Length (elbow-middle finger)	999	999
11 - Tibiale Height	999	999
12 - Ankle Height (outside) (lateral malleolus)	999	999
13 - Foot Breadth	999	999
14 - Foot Length	999	999

Note: * weight in kilograms

** lengths in centimeters

*** measures 16 and 17 must be made in case where the subject will be used in the seated position during the tests. In all other cases enter 9999 when under these measures.

15 - Top of Head to Trochanterion Length.....	999	999
16 - Seated Height***.....	999	999
17 - Knee Height (seated)***.....	999	999
18 - Head Length.....	20.6 cm	8.1 in
19 - Head Breadth.....	15.3 cm	6 in
20 - Head to Chin Height (Vertex to Mentum).....	999	999
21 - Biceps Circumference.....	999	999
22 - Elbow Circumference.....	999	999
23 - Forearm Circumference.....	999	999
24 - Wrist Circumference.....	999	999
25 - Thigh Circumference.....	999	999
26 - Lower Thigh Circumference.....	999	999
27 - Knee Circumference.....	999	999
28 - Calf Circumference.....	999	999
29 - Ankle Circumference.....	999	999
30 - Neck Circumference.....	32 cm	12.6 in
31 - Scye (armpit-shoulder) Circumference.....	999	999
32 - Chest Circumference.....	999	999
33 - Waist Circumference.....	999	999
34 - Buttock Circumference.....	999	999
35 - Chest Depth.....	999	999
36 - Waist Depth.....	999	999
37 - Buttock Depth.....	999	999
38 - Interscye.....	999	999

LABORATORY UMTRI TEST NO. 82E071

HUMAN SUBJECT INFORMATION

CADAVER NO.: 079 DURATION OF BED CONFINEMENT Unknown

AGE: 51 SEX: M CAUSE OF DEATH: Myocardial infarction

PHYSICAL APPEARANCE: Caucasian DATE OF DEATH: 2/26/83

ANOMALY: Structures weakened from CPR.

ANTHROPOMETRY

0 - Weight*	83 ka	
1 - Stature**	169 cm	
2 - Shoulder (acromial) Height	146.5 cm	57.7 in
3 - Vertex to Symphysis Length	999	999
4 - Waist Height	999	999
5 - Shoulder Breadth (Biacromial Breadth)	30.4 cm	12 in
6 - Chest Breadth	34.2 cm	13.5 in
7 - Waist Breadth	999	999
8 - Hip Breadth	31 cm	12.2 in
9 - Shoulder to Elbow Length (Acromion-radiale .. Length)	999	999
10 - Forearm-hand Length (elbow-middle finger)....	999	999
11 - Tibiale Height	999	999
12 - Ankle Height (outside) (lateral malleous)....	999	999
13 - Foot Breadth	999	999
14 - Foot Length	999	999

Note: * weight in kilograms

** lengths in centimeters

*** measures 16 and 17 must be made in case where the subject will be used in the seated position during the tests. In all other cases enter 9999 when under these measures.

15 - Top of Head to Trochanterion Length.....	999	999
16 - Seated Height***.....	999	999
17 - Knee Height (seated)***.....	999	999
18 - Head Length.....	20 cm	7.8 in
19 - Head Breadth.....	16 cm	6.3 in
20 - Head to Chin Height (Vertex to Mentum).....	999	999
21 - Biceps Circumference.....	999	999
22 - Elbow Circumference.....	999	999
23 - Forearm Circumference.....	999	999
24 - Wrist Circumference.....	999	999
25 - Thigh Circumference.....	999	999
26 - Lower Thigh Circumference.....	999	999
27 - Knee Circumference.....	999	999
28 - Calf Circumference.....	999	999
29 - Ankle Circumference.....	999	999
30 - Neck Circumference.....	36 cm	14.2 in
31 - Scye (armpit-shoulder) Circumference.....	999	999
32 - Chest Circumference.....	999	999
33 - Waist Circumference.....	999	999
34 - Buttock Circumference.....	999	999
35 - Chest Depth.....	999	999
36 - Waist Depth.....	999	999
37 - Buttock Depth.....	999	999
38 - Interscye.....	999	999

LABORATORY UMTRI TEST NO. 83E076

HUMAN SUBJECT INFORMATION

CADAVER NO.: 080 DURATION OF BED CONFINEMENT Unknown
 AGE: 44 SEX: M CAUSE OF DEATH: Pulmonary edema
 PHYSICAL APPEARANCE: Caucasian DATE OF DEATH: 3/6/83

ANOMALY: Left rib R4 weakened. Sternum weakened.

ANTHROPOMETRY

0 - Weight*	72 kg	
1 - Stature**	171 cm	
2 - Shoulder (acromial) Height	147.4 cm	58 in
3 - Vertex to Symphysis Length	88 cm	34.6 in
4 - Waist Height	89.5 cm	35.2 in
5 - Shoulder Breadth (Biacromial Breadth)	32.5 cm	12.8 in
6 - Chest Breadth	33.8 cm	13.3 in
7 - Waist Breadth	25 cm	9.8 in
8 - Hip Breadth	31.4 cm	12.4 in
9 - Shoulder to Elbow Length (Acromion-radiale .. Length)	999	999
10 - Forearm-hand Length (elbow-middle finger)....	999	999
11 - Tibiale Height	999	999
12 - Ankle Height (outside) (lateral malleous)....	999	999
13 - Foot Breadth	999	999
14 - Foot Length	999	999

Note: * weight in kilograms

** lengths in centimeters

*** measures 16 and 17 must be made in case where the subject will be used in the seated position during the tests. In all other cases enter 9999 when under these measures.

15 - Top of Head to Trochanterion Length.....	999	999
16 - Seated Height***.....	999	999
17 - Knee Height (seated)***.....	999	999
18 - Head Length.....	19.8 cm	7.8 in
19 - Head Breadth.....	15.5 cm	6.1 in
20 - Head to Chin Height (Vertex to Mentum).....	23 cm	9.1 in
21 - Biceps Circumference.....	999	999
22 - Elbow Circumference.....	999	999
23 - Forearm Circumference.....	999	999
24 - Wrist Circumference.....	999	999
25 - Thigh Circumference.....	999	999
26 - Lower Thigh Circumference.....	999	999
27 - Knee Circumference.....	999	999
28 - Calf Circumference.....	999	999
29 - Ankle Circumference.....	999	999
30 - Neck Circumference.....	57 cm	22.4 in
31 - Scye (armpit-shoulder) Circumference.....	999	999
32 - Chest Circumference.....	100 cm	39.4 in
33 - Waist Circumference.....	999	999
34 - Buttock Circumference.....	999	999
35 - Chest Depth.....	15.3 cm	6 in
36 - Waist Depth.....	999	999
37 - Buttock Depth.....	999	999
38 - Interscye.....	999	999

LABORATORY UJMTPT TEST NO. 83E081-82 83E083-86 83E087-88

HUMAN SUBJECT INFORMATION

CADAVER NO.: 089 DURATION OF BED CONFINEMENT Unknown

AGE: 62 SEX: M CAUSE OF DEATH: Myocardial infarction

PHYSICAL APPEARANCE: Caucasian DATE OF DEATH: 1/26/83

ANOMALY: None

ANTHROPOMETRY

0 - Weight*	76 kg	
1 - Stature**	175.8 cm	
2 - Shoulder (acromial) Height	152 cm	59.8 in
3 - Vertex to Symphysis Length	84.5 cm	33.3 in
4 - Waist Height	999	999
5 - Shoulder Breadth (Biacromial Breadth)	34.7 cm	13.7 in
6 - Chest Breadth	34 cm	13.4 in
7 - Waist Breadth	999	999
8 - Hip Breadth	31.5 cm	12.4 in
9 - Shoulder to Elbow Length (Acromion-radiale .. Length)	999	999
10 - Forearm-hand Length (elbow-middle finger)....	999	999
11 - Tibiale Height	999	999
12 - Ankle Height (outside) (lateral malleous)....	999	999
13 - Foot Breadth	999	999
14 - Foot Length	999	999

Note: * weight in kilograms

** lengths in centimeters

*** measures 16 and 17 must be made in case where the subject will be used in the seated position during the tests. In all other cases enter 9999 when under these measures.

15 - Top of Head to Trochanterion Length.....	999	999
16 - Seated Height***.....	999	999
17 - Knee Height (seated)***.....	999	999
18 - Head Length.....	19.0 cm	7.5 in
19 - Head Breadth.....	15.3 cm	6 in
20 - Head to Chin Height (Vertex to Mentum).....	999	999
21 - Biceps Circumference.....	999	999
22 - Elbow Circumference.....	999	999
23 - Forearm Circumference.....	999	999
24 - Wrist Circumference.....	999	999
25 - Thigh Circumference.....	999	999
26 - Lower Thigh Circumference.....	999	999
27 - Knee Circumference.....	999	999
28 - Calf Circumference.....	999	999
29 - Ankle Circumference.....	999	999
30 - Neck Circumference.....	37 cm	14.6 in
31 - Scye (armpit-shoulder) Circumference.....	999	999
32 - Chest Circumference.....	999	999
33 - Waist Circumference.....	999	999
34 - Buttock Circumference.....	999	999
35 - Chest Depth.....	999	999
36 - Waist Depth.....	999	999
37 - Buttock Depth.....	999	999
38 - Interscye.....	999	999

LABORATORY UMTRI TEST NO. 83E071-75 83E091

HUMAN SUBJECT INFORMATION

CADAVER NO.: 090 DURATION OF BED CONFINEMENT Unknown

AGE: 51 SEX: M CAUSE OF DEATH: Cerebral Contusion

PHYSICAL APPEARANCE: Caucasian DATE OF DEATH: _____

ANOMALY: None

ANTHROPOMETRY

0 - Weight*	68 kg	
1 - Stature**	180 cm	
2 - Shoulder (acromial) Height	155.4 cm	61.2 in
3 - Vertex to Symphysis Length	999	999
4 - Waist Height	999	999
5 - Shoulder Breadth (Biacromial Breadth)	33.3 cm	13.1 in
6 - Chest Breadth	31.9 cm	12.6 in
7 - Waist Breadth	999	999
8 - Hip Breadth	30 cm	11.8 in
9 - Shoulder to Elbow Length (Acromion-radiale .. Length)	999	999
10 - Forearm-hand Length (elbow-middle finger)....	999	999
11 - Tibiale Height	999	999
12 - Ankle Height (outside) (lateral malleous)....	999	999
13 - Foot Breadth	999	999
14 - Foot Length	999	999

Note: * weight in kilograms

** lengths in centimeters

*** measures 16 and 17 must be made in case where the subject will be used in the seated position during the tests. In all other cases enter 9999 when under these measures.

LABORATORY UMTRI D20 TEST NO. 83E092 83E093

15 - Top of Head to Trochanterion Length.....	999	999
16 - Seated Height***.....	999	999
17 - Knee Height (seated)***.....	999	999
18 - Head Length.....	19.4 cm	7.6 in
19 - Head Breadth.....	15.5 cm	6.1 in
20 - Head to Chin Height (Vertex to Mentum).....	999	999
21 - Biceps Circumference.....	999	999
22 - Elbow Circumference.....	999	999
23 - Forearm Circumference.....	999	999
24 - Wrist Circumference.....	999	999
25 - Thigh Circumference.....	999	999
26 - Lower Thigh Circumference.....	999	999
27 - Knee Circumference.....	999	999
28 - Calf Circumference.....	999	999
29 - Ankle Circumference.....	999	999
30 - Neck Circumference.....	37 cm	14.6 in
31 - Scye (armpit-shoulder) Circumference.....	999	999
32 - Chest Circumference.....	999	999
33 - Waist Circumference.....	999	999
34 - Buttock Circumference.....	999	999
35 - Chest Depth.....	999	999
36 - Waist Depth.....	999	999
37 - Buttock Depth.....	999	999
38 - Interscye.....	999	999

LABORATORY UMTRI TEST NO. 83E092 83E093

HUMAN SUBJECT INFORMATION

CADAVER NO.: 100 DURATION OF BED CONFINEMENT Unknown
 AGE: 60 SEX: M CAUSE OF DEATH: Cardiac arrest - Carcinoma of Pancreas
 PHYSICAL APPEARANCE: Caucasian DATE OF DEATH: 5/20/83

ANOMALY: Right rib R7 is abnormal.

ANTHROPOMETRY

0 - Weight*	76.5 ka	
1 - Stature**	182.3 cm	
2 - Shoulder (acromial) Height	158.5 cm	62.4 in
3 - Vertex to Symphysis Length	91.7 cm	36.1 in
4 - Waist Height	108.6 cm	42.8 in
5 - Shoulder Breadth (Biacromial Breadth)	31.4 cm	12.4 in
6 - Chest Breadth	27 cm	10.6 in
7 - Waist Breadth	31.3 cm	12.3 in
8 - Hip Breadth	33.9 cm	13.3 in
9 - Shoulder to Elbow Length (Acromion-radiale .. Length)	999	999
10 - Forearm-hand Length (elbow-middle finger)....	999	999
11 - Tibiale Height	999	999
12 - Ankle Height (outside) (lateral malleous)....	999	999
13 - Foot Breadth	999	999
14 - Foot Length	999	999

Note: * weight in kilograms

** lengths in centimeters

*** measures 16 and 17 must be made in case where the subject will be used in the seated position during the tests. In all other cases enter 9999 when under these measures.

15 - Top of Head to Trochanterion Length.....	999	999
16 - Seated Height***.....	999	999
17 - Knee Height (seated)***.....	999	999
18 - Head Length.....	19.3 cm	7.6 in
19 - Head Breadth.....	14.6 cm	5.7 in
20 - Head to Chin Height (Vertex to Mentum).....	21.8 cm	8.6 in
21 - Biceps Circumference.....	999	999
22 - Elbow Circumference.....	999	999
23 - Forearm Circumference.....	999	999
24 - Wrist Circumference.....	999	999
25 - Thigh Circumference.....	999	999
26 - Lower Thigh Circumference.....	999	999
27 - Knee Circumference.....	999	999
28 - Calf Circumference.....	999	999
29 - Ankle Circumference.....	999	999
30 - Neck Circumference.....	38.3 cm	15.1 in
31 - Scye (armpit-shoulder) Circumference.....	999	999
32 - Chest Circumference.....	91.7 cm	36.1 in
33 - Waist Circumference.....	999	999
34 - Buttock Circumference.....	999	999
35 - Chest Depth.....	22.5 cm	8.9 in
36 - Waist Depth.....	999	999
37 - Buttock Depth.....	999	999
38 - Interscye.....	999	999

LABORATORY UMTRI TEST NO. 83E101-103
83E104-108 83E109

HUMAN SUBJECT INFORMATION

CADAVER NO.: 120 DURATION OF BED CONFINEMENT Unknown
 AGE: 20 SEX: F CAUSE OF DEATH: Renal failure
 PHYSICAL APPEARANCE: Neuro DATE OF DEATH: 8/22/83

ANOMALY: Sores on skin probably from needle punctures.

ANTHROPOMETRY

0 - Weight*	46 kg	
1 - Stature**	162.7 cm	
2 - Shoulder (acromial) Height	141.6 cm	55.7 in
3 - Vertex to Symphision Length	76.3 cm	30 in
4 - Waist Height	99.2 cm	39.1 in
5 - Shoulder Breadth (Biacromial Breadth)	31 cm	12.2 in
6 - Chest Breadth	25.7 cm	10.1 in
7 - Waist Breadth	21.9 cm	8.6 in
8 - Hip Breadth	27.2 cm	10.7 in
9 - Shoulder to Elbow Length (Acromion-radiale .. Length)	999	999
10 - Forearm-hand Length (elbow-middle finger)....	999	999
11 - Tibiale Height.....	999	999
12 - Ankle Height (outside) (lateral malleous)....	999	999
13 - Foot Breadth.....	999	999
14 - Foot Length.....	999	999

Note: * weight in kilograms

** lengths in centimeters

*** measures 16 and 17 must be made in case where the subject will be used in the seated position during the tests. In all other cases enter 9999 when under these measures.

15 - Top of Head to Trochanterion Length.....	72.9 cm	28.7 in
16 - Seated Height***.....	999	999
17 - Knee Height (seated)***.....	999	999
18 - Head Length.....	18.9 cm	7.4 in
19 - Head Breadth.....	14.4 cm	5.7 in
20 - Head to Chin Height (Vertex to Mentum).....	24.5 cm	9.6 in
21 - Biceps Circumference.....	999	999
22 - Elbow Circumference.....	999	999
23 - Forearm Circumference.....	999	999
24 - Wrist Circumference.....	999	999
25 - Thigh Circumference.....	999	999
26 - Lower Thigh Circumference.....	999	999
27 - Knee Circumference.....	999	999
28 - Calf Circumference.....	999	999
29 - Ankle Circumference.....	999	999
30 - Neck Circumference.....	32 cm	12.6 in
31 - Scye (armpit-shoulder) Circumference.....	999	999
32 - Chest Circumference.....	71.4 cm	28.1 in
33 - Waist Circumference.....	999	999
34 - Buttock Circumference.....	999	999
35 - Chest Depth.....	17.6 cm	6.9 in
36 - Waist Depth.....	999	999
37 - Buttock Depth.....	999	999
38 - Interscye.....	999	999

LABORATORY UMTRI TEST NO. 83E121A-C

HUMAN SUBJECT INFORMATION

CADAVER NO.: 130 DURATION OF BED CONFINEMENT Unknown
 AGE: 57 SEX: M CAUSE OF DEATH: Acute myocardial infarction
 PHYSICAL APPEARANCE: Caucasian DATE OF DEATH: 9/11/83

ANOMALY: Autopsy revealed evidence of previous thoracic surgery. Ribs
weakened at cartilaginous junction.

ANTHROPOMETRY

0 - Weight*	72.5	kg
1 - Stature**	175.3	cm
2 - Shoulder (acromial) Height	151.4	cm 59.6 in
3 - Vertex to Symphision Length	87.5	cm 34.4 in
4 - Waist Height	104.8	cm 41.3 in
5 - Shoulder Breadth (Biacromial Breadth)	33.5	cm 13.2 in
6 - Chest Breadth	33.2	cm 13.1 in
7 - Waist Breadth	31.9	cm 12.6 in
8 - Hip Breadth	33.9	cm 13.3 in
9 - Shoulder to Elbow Length (Acromion-radiale .. Length)	999	999
10 - Forearm-hand Length (elbow-middle finger)....	999	999
11 - Tibiale Height	999	999
12 - Ankle Height (outside) (lateral malleous)....	999	999
13 - Foot Breadth	999	999
14 - Foot Length	999	999

Note: * weight in kilograms

** lengths in centimeters

*** measures 16 and 17 must be made in case where the subject will be used in the seated position during the tests. In all other cases enter 9999 when under these measures.

15 - Top of Head to Trochanterion Length.....	999	999
16 - Seated Height***.....	999	999
17 - Knee Height (seated)***.....	999	999
18 - Head Length.....	21.5 cm	8.5 in
19 - Head Breadth.....	15.4 cm	6.1 in
20 - Head to Chin Height (Vertex to Mentum).....	25.9 cm	10.2 in
21 - Biceps Circumference.....	999	999
22 - Elbow Circumference.....	999	999
23 - Forearm Circumference.....	999	999
24 - Wrist Circumference.....	999	999
25 - Thigh Circumference.....	999	999
26 - Lower Thigh Circumference.....	999	999
27 - Knee Circumference.....	999	999
28 - Calf Circumference.....	999	999
29 - Ankle Circumference.....	999	999
30 - Neck Circumference.....	42.2 cm	16.6 in
31 - Scye (armpit-shoulder) Circumference.....	999	999
32 - Chest Circumference.....	99.8 cm	39.3 in
33 - Waist Circumference.....	999	999
34 - Buttock Circumference.....	999	999
35 - Chest Depth.....	23.5 cm	9.3 in
36 - Waist Depth.....	999	999
37 - Buttock Depth.....	999	999
38 - Interscye.....	999	999

LABORATORY UMTRI TEST NO. 83E131A-C







RC
1042

~~MS7~~

1985

v.1

BORROWER

Form DOT F 172
FORMERLY FORM DC

DOT LIBRARY



00040589